Synthesis and biological evaluation of dynorphin analogs, and Caco-2 permeability of opioid macrocyclic tetrapeptides

By

C2013

Anand Anant Joshi

Submitted to the graduate degree program in department of Medicinal chemistry and the Graduate Faculty of the University of Kansas in partial fulfillment of the requirements for the degree of Doctor of Philosophy.

_____

Chairperson Dr. Jane V. Aldrich

_____

Dr. Michael Rafferty

_____

Dr. Teruna J. Siahaan

_____

Dr. Blake R. Peterson

_____

Dr. Susan M. Lunte

Date Defended: 5/17/2013

The Dissertation Committee for Anand Anant Joshi

certifies that this is the approved version of the following dissertation:

Synthesis and biological evaluation of dynorphin analogs, and Caco-2 permeability of opioid macrocyclic tetrapeptides

_____

Chairperson Dr. Jane V. Aldrich

Date approved: 6/4/2013

Abstract

We are interested in the development of potent and highly selective dynorphin (Dyn) analogs targeting kappa opioid receptors (KOR) and studying the pharmacokinetic and physicochemical properties of kappa opioid peptides.

In contrast to the extensive structure-activity relationships (SAR) studies on Dyn A, there is minimal SAR information on Dyn B. Therefore we performed an alanine scan of Dyn B amide. The results indicated that Tyr^1 and Phe^4 residues are critical, while Arg^7 is important for maintaining the KOR affinity of Dyn B amide.

There is also minimal SAR information for the selective KOR antagonist zyklophin [N^α-benzylTyr^1-*cyclo*(D-Asp^5,Dap^8)]Dyn A(1–11)NH$_2$ which is active *in vivo* after systemic administration. Hence, we synthesized linear and cyclic zyklophin analogs using solid phase peptide synthesis. To synthesize cyclic analogs the 5-11 linear fragments were selectively deprotected and cyclized, followed by extension of the peptide chain, coupling of the N-terminal *N*-alkyl amino acids and cleavage from the resin. We modified a key synthetic step to avoid potential racemization of the N-terminal residue. Pharmacological results suggested that the residue in position 5 has a greater influence on the KOR affinity of zyklophin than the residue in position 8. While Phe^4 and Arg^6 residues in zyklophin were important for maintaining KOR affinity, surprisingly Tyr^1 and Arg^7 were not important.

The natural product CJ-15,208 (*cyclo*[Phe-D-Pro-Phe-Trp]) and its D-Trp isomer exhibited KOR activity after oral administration. Therefore, we are investigating the pharmacokinetic and physicochemical properties of these lead peptides. In Caco-2 cell monolayer permeability studies the D-Trp isomer exhibited 7-fold higher permeability in the apical to basolateral direction than CJ-15,208, and the natural product appeared to be an efflux

substrate. The permeability of the D-Trp isomer was only 2-fold lower than that of the high permeability compound caffeine. We also examined various agents to solubilize these hydrophobic peptides that are compatible with *in vivo* studies. The D-Trp isomer had 5- to 40-fold higher solubility than the L-Trp isomer irrespective of the type of solubilizing enhancer used.

These studies will help guide the future design of peptidic KOR ligands.

Acknowledgements

This dissertation was possible because of the cooperation, help and valuable guidance of a number of people at and outside University of Kansas, Lawrence.

First and foremost I would like to extend my whole-hearted and sincere thank you to Dr. Jane Aldrich, my PhD advisor, for her guidance, sharing of knowledge and directing me on the right path for scientific thinking and research. This thesis would not have been possible without her efforts and guidance. I also want to extend to her my respect for instilling in me the idea of "ownership of your research" which I lacked in my initial period of PhD.

I was fortunate for having very helpful and knowledgeable committee members: Dr. Michael Rafferty, Dr. Teruna Siahaan, Dr. Susan Lunte and Dr. Blake Peterson. Their comments and suggestions helped me improve the quality of my dissertation.

I would also like to thank my lab members for their continuing support and cooperation. First and foremost I would like to thank Dr. Tatyana Yakovleva for her continuing support, love and unconditional help in research as well as non-research related activities. I would also like to thank Dr. Kshitij Patkar and Dr. Wendy Hartsock who helped and guided me during my initial PhD years and Dr Weijie Fang for providing me with control peptides and standards for biological evaluation. I cannot forget to thank Dr Tanvir Khaliq for his LC-MS/MS method development for the macrocyclic tetrapeptides and Dr Sanjeewa Senadheera for synthesizing the macrocyclic tetrapeptides. I would also like to thank other members in the Aldrich lab including Dr Dmitry Yakovlev, Dr Archana Mukhopadhyay, Solomon Gisemba and Chrstianna Reedy for their help and support during my time in the laboratory.

Table of contents

Abbreviations

Abbreviations used for amino acids follow the rules of the IUPAC-IUB Joint Commission of Biochemical Nomenclature in *Eur. J. Biochem*. **1984**, *138*, 9-37. Amino Acids are in the L-configuration except where indicated otherwise. Additional abbreviations used in this dissertation are as follows:

ABC : ATP binding cassette

AC : adenylyl cyclase

ACA : acyloxyalkoxy

ADAMB : N^{α}-amidino-Tyr-D-Arg-Phe-Meβ-Ala-OH

Aic : 2-aminoindan-2-carboxylic acid

Alloc : allyloxycarbonyl

AMEM : minimum essential medium alpha

Atc : 2-aminotetralin-2-carboxylic acid

ATP : adenosine triphosphate

AUC : area under the curve

BBB : blood-brain barrier

BBMEC : bovine brain microvessel endothelial cells

BCRP : breast cancer resistance protein

Big Dyn : big dynorphin

Boc *: tert*-butyloxycarbonyl

BSA : bovine serum albumin

CA : coumarinic acid

c-AMP : cyclic adenosine monophosphate

CE : collision energy

Cha : cyclohexylalanine

CHO : Chinese hamster ovary

CREB : cyclic adenosine monophosphate response element binding protein

DADLE : ([D-Ala^2, D-Leu^5]-enkephalin)

DALDA : Tyr-D-Arg-Phe-Lys-NH$_2$

DAMGO : ([D-Ala^2, N-MePhe^4, Gly-ol]-enkephalin)

Dap : 2,3-diaminopropionic acid

Dab : 2,3-diaminobutyric acid

DCM : dichloromethane

Dhp : 3-(2,6-dimethyl-4-hydroxyphenyl)propanoic acid

DIAD : diisopropyl diazocarboxylate

DIEA : N,N-diisopropylethylamine

DMA : N,N-dimethylacetamide

DMEM : Dulbecco's modified Eagle's medium

DMF : N,N-dimethylformamide

Dmt : 2',6'-dimethyl-Tyr

DMSO : N,N-dimethylsulfoxide

DOR : delta (δ) opioid receptor

DPDPE : $cyclo$[D-Pen^2,D-Pen^5]enkephalin

DSLET : [D-Ser^2,Leu^5,Thr^6]-enkephalin

Dyn : dynorphin

EL : extracellular loop

ERK : extracellular signal related kinases

ESI-MS : electrospray ionization mass spectroscopy

FBS : fetal bovine serum

Fmoc : 9-fluorenylmethoxycarbonyl

GDP : guanosine 5'-diphosphate

GNTI : 5'-guanidinonaltrindole

GPCR : G-protein coupled receptors

GPI : guinea pig ileum

GRK : G-protein coupled receptor kinase

GTP : guanosine 5'-triphosphate

HBSS : Hank's balanced salt solution

HOAt : 1-hydroxy-7-azabenzotriazole

HOBt : 1-hydroxy-7-benzotriazole

IAMC : immobilized artificial membrane chromatography

i.c.v : intracerebroventricular

IPC : Insulin phospholipid complex

IV : intravenous

i.t. : intrathecal

JNK : c-Jun-N-terminal kinase

KOR : kappa (κ) opioid receptor

LC-MS/MS : liquid chromatography tandem mass spectroscopy

Log P : octanol-water partition coefficient

LUVs : phospholipid large unilamellar vesicles

LY : Lucifer yellow

MAPK : mitogen activated protein kinase

MC : microcystins

MDCK : Madin Darby canine kidney

Mdp : (2S)-2-methyl-3-(2,6-dimethyl-4-hydroxyphenyl)propanoic acid

MDR : multidrug resistance

MOR : mu (μ) opioid receptor

MPCB : (-)-*cis*-*N*-(2-phenyl-2-carbomethoxy)cyclopropylmethyl-*N*-normetazocine

MRP : multidrug resistance associated protein

Mtt : 4-methyltrityl

MVD : mouse vas deferens

NMDA *: N*-methyl-D-aspartate

NMP : *N*-methylpyrrolidone

NMR : nuclear magnetic resonance

NorBNI : norbinaltorphimine

OAT : organic anion transporter

OATP : organic anion transporting polypeptides

OCT : organic cation transporter

OPip : 2-phenylisopropyl

ORL : opioid like receptor

PAL : peptide amide linker

PAMPA : parallel artificial membrane permeability

PC : polycarbonate

PET : polyethylene terapthalate

Pgp: P-glycoprotein

Pbf : 2,2,4,6,7-pentamethyldihydrobenzofuran-5-sulfonyl

PEG-PS : polyethylene glycol-polystyrene

PEPT : peptide transporter

Pip : piperidinecarboxylic acid

PPA : phenylpropionic acid

PyBOP : 7-benzotriazol-1-yl-oxytripyrrolidinophosphonium hexafluorophosphate

PyClocK : 6-chloro-7-benzotriazol-1-yl-oxytripyrrolidinophosphonium hexafluorophosphate

RCM : ring closing metathesis

RP-HPLC : reversed phase high performance liquid chromatography

RVD : rabbit vas deferens

Sar : sarcosine

SAR : structure-activity relationships

SEM : standard error of mean

SLC : solute carrier

SNEDDS : self nano-emulsifying drug delivery system

SOPT : sodium dependant oligopeptide transporters

STD : saturation transfer difference

tBu : *tert*-butyl

TEA : triethylamine

TEAP : triethylammonium phosphate

TEER : transepithelial electric resistance

TENA : triethyleneglycolnaltrexamime

TFA : trifluoroacetic acid

Tic : 1,2,3,4-tetrahydroisoquinoline 3-carboxylic acid

TIS : triisopropylsilane

TM : transmembrane

TOF : time of flight

TPP : triphenylphosphine

Trt : trityl

TW-80 : Tween-80

UPLC : ultra-performance liquid chromatography

UWL : unstirred water layer

List of figures

List of schemes

List of tables

Chapter 1 - Overview of the research projects

1.1   Introduction

Most of the peptidic ligands that target kappa opioid receptors (KOR) are analogs of the endogenous ligands for KOR the dynorphins (Dyn). Various analogs of dynorphin (Dyn) A have been synthesized earlier with activity at KOR.   In addition a few number of linear and macrocyclic opioid tetrapeptides have also been synthesized that exhibit activity at KOR. While KOR antagonists have been historically used as pharmacological tools, they have potential therapeutic uses such as anti-depressant and anxiolytic agents and for the treatment of drug abuse. The prototypical non-peptidic KOR antagonists display exceptionally long durations of action, while peptidic KOR antagonists are susceptible to metabolism by proteases and hence are expected to have a shorter duration of action.[1]

Our laboratory is interested in studying the structure-activity relationships (SAR) of peptides for KOR and develop potent KOR antagonists that can be useful for various therapeutic applications, especially for the treatment of drug abuse. We are also interested in studying the pharmacokinetic and physicochemical properties of the orally active macrocyclic tetrapeptides.

The present thesis is divided into three research projects (chapters 3, 4 and 6). Project 1 (chapter 3) and project 2 (chapter 4) focused on studies of the SAR of the two Dyn related peptides, Dyn B amide and the selective KOR antagonist zyklophin ([N^{α}-benzylTyr^1-*cyclo*(D-Asp^5,Dap^8)]Dyn A(1−11)NH$_2$),[2] respectively. Project 3 (chapter 6) focused on evaluation of the permeability of the opioid macrocyclic tetrapeptide CJ 15,208 and its D-Trp isomer through the Caco-2 monolayer intestinal cell model and their solubility analysis in the presence of various solubilizing enhancers.

Project 1: Synthesis and biological evaluation of alanine substituted analogs of Dyn B amide (chapter 3).

The endogenous opioid peptides Dyn A and Dyn B (Figure 1.1) are obtained from the proteolytic cleavage of the precursor protein prodynorphin.[3] To date studies involving SAR of dynorphins have focused almost exclusively on Dyn A with minimal SAR studies related to Dyn B. While both Dyn A and Dyn B have identical N-terminal sequences, their C-terminal sequences differ. Although Dyn B exhibits lower opioid affinity and potency than Dyn A,[4-7] it appears to be devoid of the cytotoxic non-opioid effects exhibited by Dyn A.[8] Hence, the differences in their C-terminal sequences result in differences in their pharmacological actions.

Tyr-Gly-Gly-Phe-Leu-Arg-Arg-Ile-Arg-Pro-Lys-Leu-Lys

Dyn A(1-13)

Tyr-Gly-Gly-Phe-Leu-Arg-Arg-Gln-Phe-Lys-Val-Val-Thr

Dyn B

Figure 1.1 Dyn A(1-13) and Dyn B

It was hypothesized that unique residue(s) in the C-terminus of Dyn B interact with the receptor and contribute to its activity at KOR. To determine which residues are important for KOR interaction alanine substituted analogs of Dyn B amide were synthesized. All of the non-glycine residues up through residue 11 were substituted with Ala in order to explore the role of their side chains to the activity of Dyn B. The analogs were synthesized by solid phase peptide synthesis using fluorenylmethyloxycarbonyl (Fmoc) protection strategy and evaluated for their opioid receptor affinities in radioligand binding assays[9] and for their efficacy and potency at KOR in the GTPγS assay.[10]

Project 2: Structure-activity relationships of the KOR selective antagonist zyklophin (chapter 4).

We are exploring analogs of the endogenous opioid peptide Dyn A as ligands for KOR. In our earlier studies of Dyn A analogs, zyklophin (Figure 1.2) was synthesized; this peptide is a selective KOR antagonist *in vitro*[2] and is active *in vivo* after systemic administration.[11] Zyklophin was the first reported selective KOR antagonist to display finite duration of action (less than 12 h) *in vivo*.[11] However, there was minimal SAR information available for zyklophin.[2, 11, 12]

$$\text{NBenzyl-Tyr-Gly-Gly-Phe-D-Asp-Arg-Arg-Dap-Arg-Pro-Lys-NH}_2$$
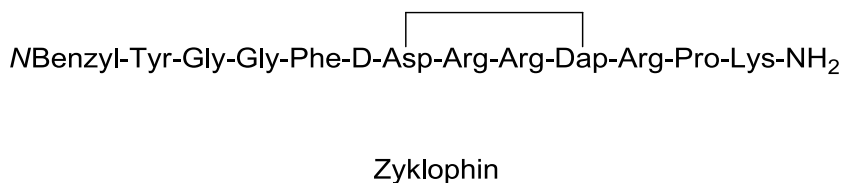
Zyklophin

Figure 1.2 Structure of zyklophin

The objective of this project was to study the SAR of zyklophin and identify structural features responsible for its KOR selectivity and antagonist activity and to enhance its potency. It was hypothesized that the N-terminal alkyl group of zyklophin might affect the interactions of the rest of the peptide with KOR, resulting in the ability of zyklophin to bind to the receptor without activating it. Hence, to test this hypothesis we synthesized zyklophin analogs with different *N*-alkyl substitutents on the N-terminal Tyr. It was also hypothesized that as the residue in position 5 is in proximity to the postulated "message" sequence (see chapter 2, section 2.7.1 for a discussion of the "message-address" concept),[13] this residue could play a significant role in the antagonist activity of zyklophin. To test this hypothesis the linear analogs [*N*-benzylTyr[1],D-Asn[5]]Dyn A(1-11)NH$_2$ and [*N*-benzylTyr[1],Dap(Ac)[8]]Dyn A(1-11)NH$_2$ with substitutions in positions 5 and 8, respectively, were also synthesized. In addition, in order to explore the role of

ring size and residues involved in the cyclic constraint on the KOR interaction and antagonist activity of zyklophin, we synthesized several cyclic analogs containing ring size variants analogs and an analog with the opposite configuration of residue 5. We also wanted to investigate the importance of different residue side chains to the activity of zyklophin. Hence, we performed an Ala scan of the non-glycine residues of zyklophin, excluding residues 5 and 8, up through the residue in position 9. In addition, to explore the importance of the phenolic group of Tyr[1] on the activity of zyklophin we also synthesized the Phe[1] analog of zyklophin.

The synthesis of zyklophin involved solid phase synthesis of the (2-11) peptide fragment on resin using the Fmoc protection strategy followed by coupling of the *N*-alkyl N-terminal amino acid to the peptide fragment on the resin.[2] The coupling reaction involved dissolution of the *N*-alkyl amino acid in DMF at elevated temperature followed by cooling and coupling to the (2-11) peptide fragment. This could lead to potential racemization of the N-terminal residue. An HPLC system containing a linear gradient of MeCN over aqueous triethyl ammonium phosphate that could resolve the diastereomeric mixture of zyklophin was identified. A modified synthetic strategy was used for some of the zyklophin analogs that contained N-terminal residues with minimal solubility in DMF or that were prone to racemization.

The synthesis of the zyklophin analogs and their subsequent evaluation for opioid affinity in radioligand assays and efficacy and potency in the GTPγS assay are discussed in chapter 4.

Project 3: Caco-2 cell monolayer permeability and solubility analysis of opioid macrocyclic tetrapeptides (chapter 6)

The macrocyclic tetrapeptide natural product CJ 15,208 (*cyclo*[Phe-D-Pro-Phe-Trp]), was reported to exhibit KOR antagonism *in vitro*.[14] The syntheses of the L- and D-Trp isomers of CJ-15,208 (Figure 1.3) were performed to establish the stereochemistry of the Trp residue in the

natural product (the L-Trp peptide appears to be the natural product).[15] The L- and D-Trp isomers of this peptide display opioid activity, but exhibit different pharmacological profiles *in vivo* after intracerebroventricular administration to mice;[10] and both exhibit activity following oral administration.[16, 17] Therefore, both isomers can serve as lead compounds for further structural modifications.

CJ 15,208   D-Trp isomer of CJ 15,208
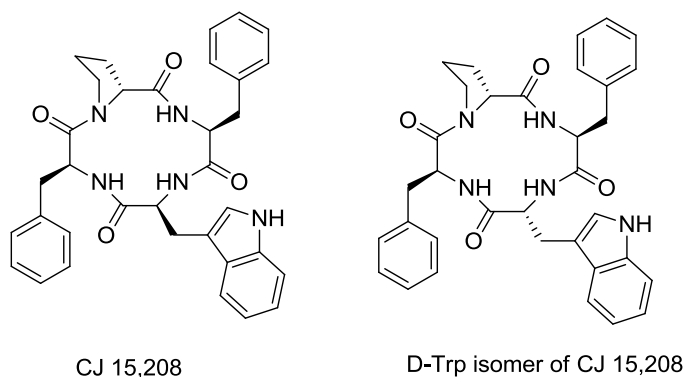
Figure 1.3 L- and D-Trp isomers of CJ-15,208

In order to enhance the oral activity of these macrocyclic peptides, we are exploring the pharmacokinetic and physicochemical properties of these two lead compounds. Because of their hydrophobicity, we have examined various solubilizing agents, including organic cosolvents, the β-cyclodextrin derivative Captisol and the surfactants Solutol HS 15 and Tween-80 that are compatible with *in vivo* studies, to solubilize these compounds. We have also evaluated the bidirectional permeability of these compounds in the Caco-2 cell monolayer model for intestinal absorption using liquid chromatography-tandem mass spectrometry (LC-MS/MS) for quantification.

The results obtained from the Caco-2 permeability assay and solubility analysis of the L- and D-Trp isomers of CJ 15,208 are discussed in chapter 6.

1.2   References

1.   Aldrich, J. V.; McLaughlin, J. P. Peptide kappa opioid receptor ligands: potential for drug development. *AAPS J* **2009,** *11*, 312-322.

2.   Patkar, K. A.; Yan, X.; Murray, T. F.; Aldrich, J. V. [N^{α}-benzylTyr^1,cyclo(D-Asp^5,Dap^8)]- dynorphin A-(1-11)NH$_2$ cyclized in the "address" domain is a novel kappa-opioid receptor antagonist. *J Med Chem* **2005,** *48*, 4500-4503.

3.   Hollt, V. Opioid peptide processing and receptor selectivity. *Annu Rev Pharmacol Toxicol* **1986,** *26*, 59-77.

4.   Rezvani, A.; Hollt, V.; Way, E. L. K receptor activities of the three opioid peptide families. *Life Sci* **1983,** *33 Suppl 1*, 271-274.

5.   James, I. F.; Fischli, W.; Goldstein, A. Opioid receptor selectivity of dynorphin gene products. *J Pharmacol Exp Ther* **1984,** *228*, 88-93.

6.   Merg, F.; Filliol, D.; Usynin, I.; Bazov, I.; Bark, N.; Hurd, Y. L.; Yakovleva, T.; Kieffer, B. L.; Bakalkin, G. Big dynorphin as a putative endogenous ligand for the kappa-opioid receptor. *J Neurochem* **2006,** *97*, 292-301.

7.   Garzon, J.; Sanchez-Blazquez, P.; Hollt, V.; Lee, N. M.; Loh, H. H. Endogenous opioid peptides: comparative evaluation of their receptor affinities in the mouse brain. *Life Sci* **1983,** *33 Suppl 1*, 291-294.

8.   Tan-No, K.; Cebers, G.; Yakovleva, T.; Hoon Goh, B.; Gileva, I.; Reznikov, K.; Aguilar-Santelises, M.; Hauser, K. F.; Terenius, L.; Bakalkin, G. Cytotoxic effects of dynorphins through nonopioid intracellular mechanisms. *Exp Cell Res* **2001,** *269*, 54-63.

9.   Arttamangkul, S.; Ishmael, J. E.; Murray, T. F.; Grandy, D. K.; DeLander, G. E.; Kieffer, B. L.; Aldrich, J. V. Synthesis and opioid activity of conformationally constrained dynorphin A

analogues. 2. Conformational constraint in the "address" sequence. *J Med Chem* **1997,** *40*, 1211-1218.

10.   Ross, N. C.; Reilley, K. J.; Murray, T. F.; Aldrich, J. V.; McLaughlin, J. P. Novel opioid cyclic tetrapeptides: Trp isomers of CJ-15,208 exhibit distinct opioid receptor agonism and short-acting kappa opioid receptor antagonism. *Br J Pharmacol* **2012,** *165*, 1097-1108.

11.   Aldrich, J. V.; Patkar, K. A.; McLaughlin, J. P. Zyklophin, a systemically active selective kappa opioid receptor peptide antagonist with short duration of action. *Proc Natl Acad Sci U S A* **2009,** *106*, 18396-18401.

12.   Patkar, K. A.; Murray, T. F.; Aldrich, J. V. The effects of C-terminal modifications on the opioid activity of [N-benzylTyr(1)]dynorphin A-(1-11) analogues. *J Med Chem* **2009,** *52*, 6814-6821.

13.   Chavkin, C.; Goldstein, A. Specific receptor for the opioid peptide dynorphin: structure--activity relationships. *Proc Natl Acad Sci U S A* **1981,** *78*, 6543-6547.

14.   Saito, T.; Hirai, H.; Kim, Y. J.; Kojima, Y.; Matsunaga, Y.; Nishida, H.; Sakakibara, T.; Suga, O.; Sujaku, T.; Kojima, N. CJ-15,208, a novel kappa opioid receptor antagonist from a fungus, Ctenomyces serratus ATCC15502. *J Antibiot (Tokyo)* **2002,** *55*, 847-854.

15.   Ross, N. C.; Kulkarni, S. S.; McLaughlin, J. P.; Aldrich, J. V. Synthesis of CJ-15,208, a novel kappa-opioid receptor antagonist. *Tetrahedron Lett* **2010,** *51*, 5020-5023.

16.   Aldrich, J. V.; Senadheera, S. N.; Ross, N. C.; Ganno, M. L.; Eans, S. O.; McLaughlin, J. P. The Macrocyclic Peptide Natural Product CJ-15,208 Is Orally Active and Prevents Reinstatement of Extinguished Cocaine-Seeking Behavior. *J Nat Prod* **2013,** *76*, 433-438.

17.   Eans, S. O.; Ganno, M. L.; Reilley, K. J.; Patkar, K. A.; Senadheera, S. N.; Aldrich, J. V.; McLaughlin, J. P. The macrocyclic tetrapeptide [D-Trp]CJ-15,208 produces short-acting kappa

opioid receptor antagonism in the CNS after oral administration. *Br J Pharmacol* **2013,** *169*, 426-436.

Chapter 2 - Literature review – Kappa opioid receptor ligands

2.1 Introduction

While treatment of mild to moderate pain can be accomplished by non-narcotic analgesics such as acetaminophen or aspirin, treatment of severe pain requires use of opioid analgesics such as morphine. These analgesics, however, suffer from serious side effects including addiction liability and respiratory depression which limit their clinical utility.[1]

Beckett and Casy in 1954 proposed that the effects of opioid analgesics were receptor mediated,[2] but it wasn't until 1970 that the stereospecific binding of opioid ligands to specific receptors was shown in mammalian brain tissue preparations.[3-5] Later, Martin and coworkers in the mid-1970's characterized and classified the opioid receptors into three different types,[6, 7] revolutionizing the field of opioid pharmacology. Concurrently, the search for endogenous ligands for opioid receptors with opioid-like activity was ongoing. The pentapeptides leucine and methionine enkephalin[8] were the first to be identified, followed by dynorphin (Dyn) A,[9] β-endorphin[10] and more recently the endomorphins[11] (see Tables 2.1 for the peptide sequences and 2.2 for opioid receptor affinities and activity). Another major advancement in the field of opioid pharmacology came with the cloning of the delta (δ) opioid receptor (DOR)[12, 13] and the mu (μ) opioid receptor (MOR),[14] and followed by the kappa (κ) opioid receptor (KOR).[15]

Table 2.1 Mammalian opioid peptides and orphanin FQ/nociceptin,[1] grouped based on their precursor proteins

Proenkephalin peptides	
Leu-enkephalin	Tyr-Gly-Gly-Phe-Leu
Met-enkephalin	Tyr-Gly-Gly-Phe-Met
Met-enkephalin-Arg[6]-Phe[7]	Tyr-Gly-Gly-Phe-Met-Arg-Phe
Met-enkephalin-Arg[6]-Gly[7]-Leu[8]	Tyr-Gly-Gly-Phe-Met-Arg-Gly-Leu
Prodynorphin peptides	
Dynorphin A	Tyr-Gly-Gly-Phe-Leu-Arg-Arg-Ile-Arg-Pro-Lys-Leu-Lys-Trp-Asp-Asn-Gln
Dynorphin B	Tyr-Gly-Gly-Phe-Leu-Arg-Arg-Gln-Phe-Lys-Val-Val-Thr
α-Neoendorphin	Tyr-Gly-Gly-Phe-Leu-Arg-Lys-Tyr-Arg-Pro-Lys
β-Neoendorphin	Tyr-Gly-Gly-Phe-Leu-Arg-Lys-Tyr-Arg-Pro
Pro-opiomelanocortin peptides	
β-endorphin (human)	Tyr-Gly-Gly-Phe-Met-Thr-Ser-Glu-Lys-Ser-Gln-Thr-Pro-Leu-Val-Thr-Leu-Phe-Lys-Asn-Ala-Ile-Ile-Lys-Asn-Ala-Tyr-Lys-Lys-Gly-Glu
Endomorphins[a]	
Endomorphin-1	Tyr-Pro-Trp-Phe-NH_2
Endomorphin-2	Tyr-Pro-Phe-Phe-NH_2
Orphanin FQ/nociceptin and related peptides	
Orphanin FQ/	
Nociceptin	Phe-Gly-Gly-Phe-Thr-Gly-Ala-Arg-Lys-Ser-Ala-Arg-Lys-Leu-Ala-Asn-Gln
Orphanin FQ 2	Phe-Ser-Glu-Phe-Met-Arg-Gln-Tyr-Leu-Val-Leu-Ser-Met-Gln-Ser-Ser-Gln
Nocistatin (human)	Pro-Glu-Pro-Gly-Met-Glu-Glu-Ala-Gly-Glu-Met-Glu-Gln-Lys-Gln-Leu-Gln

[a]Precursor protein not know

2.2   Opioid Receptors

In the mid 1970's Martin and coworkers proposed three types of opioid receptors[6, 7] MOR, KOR and sigma (σ) receptors, with morphine, ketocyclazocine and SKF-10,047, respectively, as the prototypical ligands (Figure 2.1). The discovery of the enkephalins led to the proposal of another opioid receptor type, namely DOR.[16] Sigma receptors, however, are not considered to be opioid receptors as the effects associated with these receptors are not reversed

by opioid antagonists such as naloxone.[17] Later Mollereau *et al.* discovered the opioid-like receptor (ORL-1);[18] orphanin FQ/nociceptin[19, 20] is the endogenous ligand for this receptor.
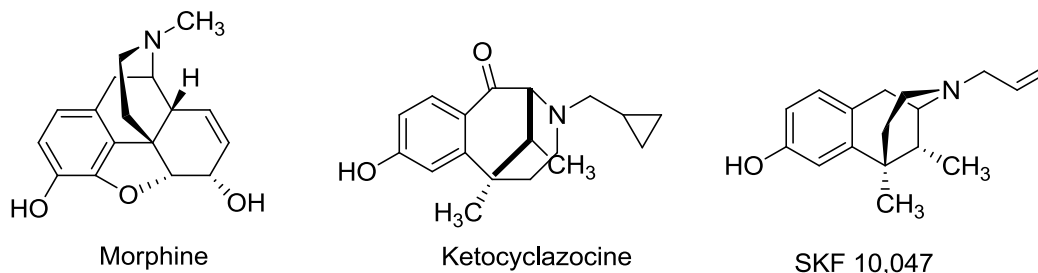
Figure 2.1 Prototypical ligands for opioid and sigma receptors

Table 2.2 Opioid receptor affinities and opioid activity of endogenous opioid peptides in the guinea pig ileum (GPI).[1]

	K_i (nM)			K_i Ratio	IC_{50} (nM)
Peptide	MOR	DOR	KOR	MOR/DOR/KOR	GPI
Proenkephalin peptides					
Leu-enkephalin	19	1.2	8210	16/1/6840	36
Met-enkephalin	9.5	0.91	4440	10/1/4880	6.7
Met-enkephalin-Arg⁶-Phe⁷	3.7	9.4	93	1/2.5/25	10
Met-enkephalin-Arg⁶-Phe⁷-Leu⁸	6.6	4.8	79	1.4/1/16	35
Prodynorphin peptides					
Dynorphin A	0.73	2.4	0.12	6.1/20/1	0.29
Dynorphin A-(1-8)	3.8	5	1.3	2.9/17/1	4.9
Dynorphin B	0.68	2.9	0.12	5.7/1.8/1	0.25
Neoendorphin	6.9	2.1	1.2	5.7/1.8/1	3.3
Neoendorphin	1.2	0.57	0.2	6/2.8/1	3.0
POMC peptide					
β-Endorphin	2.1	2.4	96	1/1.1/46	62
Endomorphins					
Endomorphins-1	0.36	1510	5430	1/4180/15100	3.6
Endomorphins-2	0.69	9230	5240	1/13400/7590	4.0

2.2.1 Opioid receptor structure

The opioid receptors belong to the superfamily of G-protein coupled receptors (GPCRs). These receptors contain an extracellular N-terminal region, extracellular loops, seven putative transmembrane (TM) regions, intracellular loops and an intracellular C-terminus.[1] The highest sequence homology between the three receptors appeared to be in the TM2, TM3 and TM7 regions (Figure 2.2). The conserved Asp residue in TM3 was proposed to interact with the positively charged protonated amine on the opioid ligands.[21] The third intracellular loop was proposed to interact with G-proteins. While the second and third extracellular loops (EL), TM1 and TM4 to TM6 were less conserved, the largest structural diversity occurred in the extracellular N-terminus. Several potential sites for possible post-translational modifications in the N-terminal and C-terminal regions of the receptors were also identified.[22]
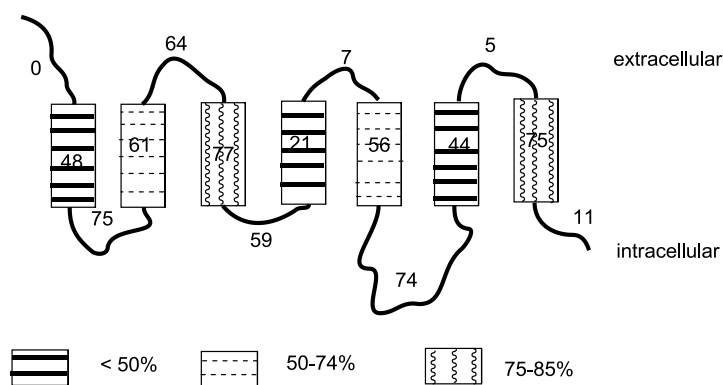
Figure 2.2 Schematic diagram of the protein structure of the three opioid receptors.[1] Rectangles indicate transmembrane helices and numbers indicate the percentage of identical residues among the three opioid receptors in that segment.

The cloning of all three types of human opioid receptors has been reported.[23-25] The human MOR, KOR and DOR exhibit 90-95% homology to the corresponding type of receptor from other species such as rat or mouse.[26] The ORL-1 receptor also exhibits high sequence

homology with the three opioid receptors, with 60-62% identity for the entire transmembrane domains and higher homology for TM2, TM3 and TM7.[27]

Several chimeric receptor studies have attempted to identify the regions of the receptors involved in ligand recognition and receptor type selectivity. MOR/KOR chimeric receptors suggested that EL3 may be responsible for the low affinity binding of the MOR agonist DAMGO ([D-Ala^2,N-MePhe^4,Gly-ol]-enkephalin) for KOR.[28, 29] Subsequent site directed mutagenesis studies identified Glu 297, Ser 310, Tyr 312 and Tyr 313 as the responsible residues in the KOR.[30] In contrast the study of MOR/DOR chimeric receptors suggested that the exchange of EL1 causes the loss of high affinity binding of DAMGO to DOR,[31, 32] and further site directed mutagenesis studies suggested that Lys 108 in EL1 of DOR was the responsible residue.[33] It was hypothesized that there are acidic residues in EL2 of KOR that could contribute directly to the affinity of the opioid peptides Dyn A and Dyn B through ionic interactions with the positively charged basic residues in the C-terminus of the peptides. Studies of KOR/MOR[34, 35] and KOR/DOR[36] chimeric receptors support the importance of EL2 in KOR for the high affinity of Dyn A. However, even after the replacement of half of the acidic residues in EL2 with the corresponding neutral amides, Dyn A still displayed high KOR affinity suggesting that the charge interactions may not be primarily important for maintaining the binding affinity and selectivity of Dyn A.[37] In contrast the KOR/MOR and KOR/DOR chimeric receptor studies indicated that the KOR-selective non-peptide agonists U50,488 and U69,593 appear to require the whole KOR except EL2 for binding. These results suggested that different portions of the receptors might be involved in interactions with different (peptide and non-peptide) ligands.[34, 35] There is also some evidence indicating that agonists and antagonists might differ in their interactions with KOR.[38]

15

Very recently, the crystal structures of MOR, KOR, DOR and nociception/orphanin FQ receptor complexed with β-funaltrexamine,[39] JDTic[40], naltrindole,[41] and a peptide mimetic[42] respectively, have been reported. All four crystal structures reveal conserved ligand-receptor binding interactions in the TM region binding pocket of the receptors.[43] For example, several conserved amino acids (for example Asp 138$^{3.32}$ (the positions of residues in the receptors are indicated using Ballesteros-Weinstein numbering[44] as a superscript) which forms a salt bridge and Tyr 139$^{3.33}$ which is involved in hydrogen bonding with the ligand) in TM3, TM6 and TM7 interact with the "message" region (see section 2.7.1 for discussion of the "message-address" concept) of the ligand and are responsible for opioid efficacy. The chemical moieties present in the "address" region of ligands can interact with different regions in the binding pocket depending on the ligand. For example, the classical morphinan opioids interact with TM6 and/or TM7 (for example, the second basic moiety of morphinans (amine in the case of norbinaltorphimine (norBNI, Figure 2.8) and guanidine in the case of 5'-guanidinonaltrindole (GNTI, Figure 2.8) interact with Glu 297$^{6.58}$) while the phenylpiperidine KOR antagonist JDTic interacts with TM2 and TM3 and also with TM7 of KOR. The structure of EL2 appears to be very similar in the opioid receptors. The common β-hairpin loop structure of EL2 in the opioid receptors allows unobstructed access of the ligands to the binding pocket which also might explain the reason for the opioid drugs being potent and reversible.[43]

The crystal structure of KOR[40] shows that JDTic tightly fits into the binding cleft and forms ionic, polar and extensive hydrophobic interactions with the receptor (Figures 2.3 and 2.4) and also shows electron density for structured water molecules that mediate polar interactions between the receptor and hydroxyl groups. The human KOR consists of a narrow deep binding pocket which is partially capped by the EL2 β-hairpin.[40] In the crystal structure JDTic reaches

deep in the binding pocket where the protonated amines of the piperidine and isoquionoline moieties form salt bridges to the Asp $138^{3.32}$ side chain, anchoring the ligand in a characteristic V-shape. JDTic interacts with four residues, Val $108^{2.53}$, Val $118^{2.63}$, Ile $294^{6.55}$ and Tyr $312^{7.35}$, in the binding pocket that are unique to KOR. The differences in these residues in MOR and DOR are thought to contribute to the KOR selectivity of JDTic. The isopropyl group of JDTic reaches deep inside the binding pocket to form hydrophobic interactions with the Trp $287^{6.48}$ side chain, which could possibly have a critical role in the activation of the receptor.
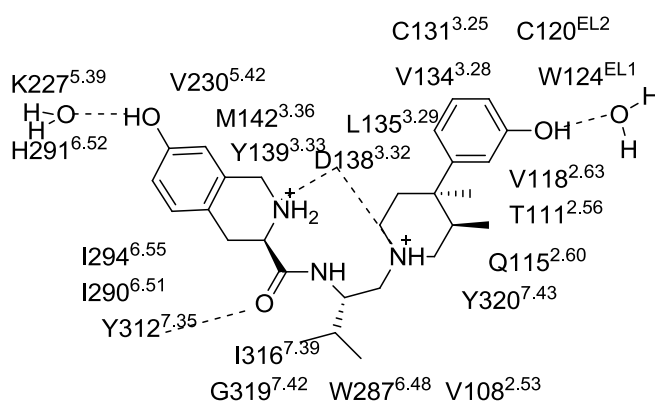
Figure 2.3 Interactions of JDTic in the binding pocket of human KOR.[40]
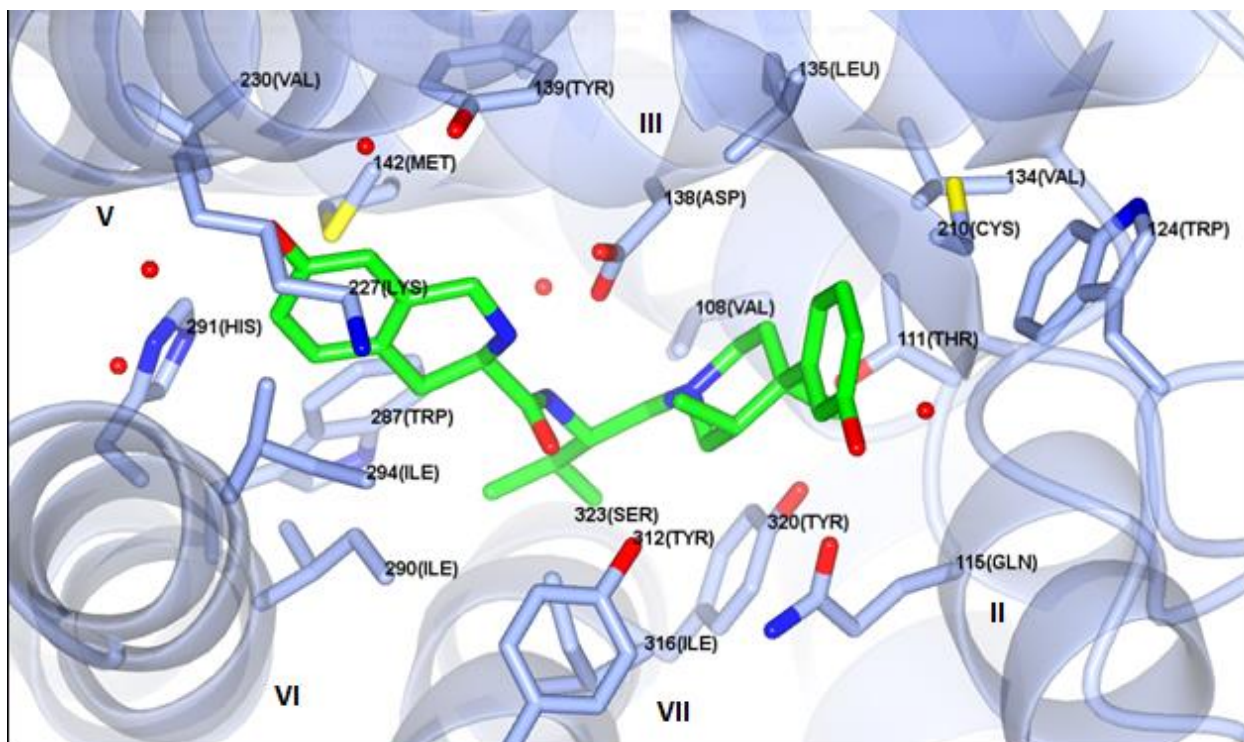
Figure 2.4 Crystal structure of KOR complexed with JDTic. The nitrogen atoms are shown in cyan, the oxygen atoms are red and the carbon atoms are green. The water molecules are indicated by red dots. TM domains are indicated by roman numbers.

The opioid receptors are coupled to G proteins and produce effects through these proteins. G-proteins are heterotrimers consisting of α, β and γ subunits.[45] Following binding by an agonist, the opioid receptor undergoes a conformational change. This causes the release of guanosine 5'-diphosphate (GDP) from the α subunit followed by the binding of guanosine 5'-diphosphate (GTP). The GTP-α subunit then dissociates from the β and γ subunits. Subsequently, both the GTP-α subunit and the β and γ subunits can interact with a variety of downstream signaling pathways including the cyclic adenosine monophosphate (c-AMP) pathway and ion channels.[46, 47] The response is terminated when the GTP bound to the α subunit is hydrolyzed to GDP, subsequently leading to reformation of the G-protein heterotrimer. The binding of an agonist to opioid receptors results in inhibition of the activity of adenylyl cyclase

(AC) and thereby decreases the amount of intracellular c-AMP. Consequently, the activity of c-AMP-dependent protein kinases is reduced. These events can produce pharmacological effects including analgesia.[48] The opioid receptors also interact with ion channels through G_i or G_o type G-proteins.[49, 50] Activation of opioid receptors can result in inactivation of voltage- dependant Ca^{++} channels and activation of K^+ channels. While inactivation of Ca^{++} channels causes reduced neurotransmitter release, activation of K^+ channels causes cell hyperpolarization.[49]

Opioid ligands can also display signal transduction through arrestin-dependent pathways. Among the various subtypes of arrestins, β-arrestins can act as signal transducers and connect the activated receptor to various signaling pathways within the cells.[51] Recent evidence has shown that phosphorylated arrestin-bound GPCRs can elicit responses through mitogen activated protein kinase (MAPK) signaling.[51] The MAPK is a family of genes; and the most characterized forms are extracellular signal related kinases 1 and 2 (ERK 1/2), c-Jun-N-terminal kinase (JNK 1-3) and p38 (α, β, γ, δ) stress kinases. While KOR induced activation of p38 requires G-protein coupled receptor kinase (GRK) 3/arrestin3 (also called β-arrestin2), KOR mediated ERK 1/2 activation has both β-arrestin2 dependent and β-arrestin independent components.[52]

2.3   Opioids with clinical applications

2.3.1   Clinically used opioids

Clinically used opioids are mainly MOR agonists such as morphine and its analogs which have been used as analgesics for a considerable period of time. Other opioids, especially fentanyl and other 4-anilinopiperidines have been extensively used as adjuvants to anesthesia, while methadone (Figure 2.5) is used as a maintenance agent for individuals who are addicted to narcotics. Other uses of opioid agonists are as antitussive (for example, codeine), and antidiarrheal agents (for example, loperamide). Nalfurafine hydrochloride (TRK-820) is a

clinically successful KOR agonist that was approved in Japan in 2009 for the treatment of severe itching related to hemodialysis.[53, 54] It was found to be 78-fold selective for KOR over MOR in the GPI assay (evaluated using selective opioid receptor antagonists to block specific receptor types).[55] While KOR agonists produce analgesia and generally lack the reinforcing effects, however, they have limited utility because of side effects including dysphoria and sedation.[56]

The mixed agonist/antagonists pentazocine and nalbuphine appear to be KOR agonists and MOR antagonists, and butorphanol which exhibits partial MOR agonist and antagonist activity and partial KOR agonism are used as analgesics.[1, 57] Buprenorphine which is a partial MOR agonist and KOR antagonist[58, 59] that also activates ORL-1 receptors,[60] has been clinically approved for the treatment of opioid dependence.[61] To counteract its potential misuse, buprenorphine has been formulated in combination with naloxone for the treatment of opioid dependence.[62] The combination of buprenorphine and naltrexone has been tested in humans as a "functional KOR antagonist"[63] and shown to be effective in the treatment of opioid dependence.[63, 64] (The same combination was recently been shown to decrease compulsive cocaine self-administration in rodents with minimal liability to produce opioid dependence [65] and to attenuate drug primed reinstatement to cocaine and morphine in rats in a conditioned place preference paradigm.[66]

The opioid antagonist naloxone is used in the treatment of opioid overdose and post-operative sedation, while naltrexone is used for the treatment of opioid dependence and alcohol abuse.[1, 57] Recently, the peripheral MOR antagonist methylnaltrexone bromide[67] and alvimopan[68] (Figure 2.5) have been clinically approved for their use against constipation and recovery of normal gastrointestinal function after surgery, respectively.
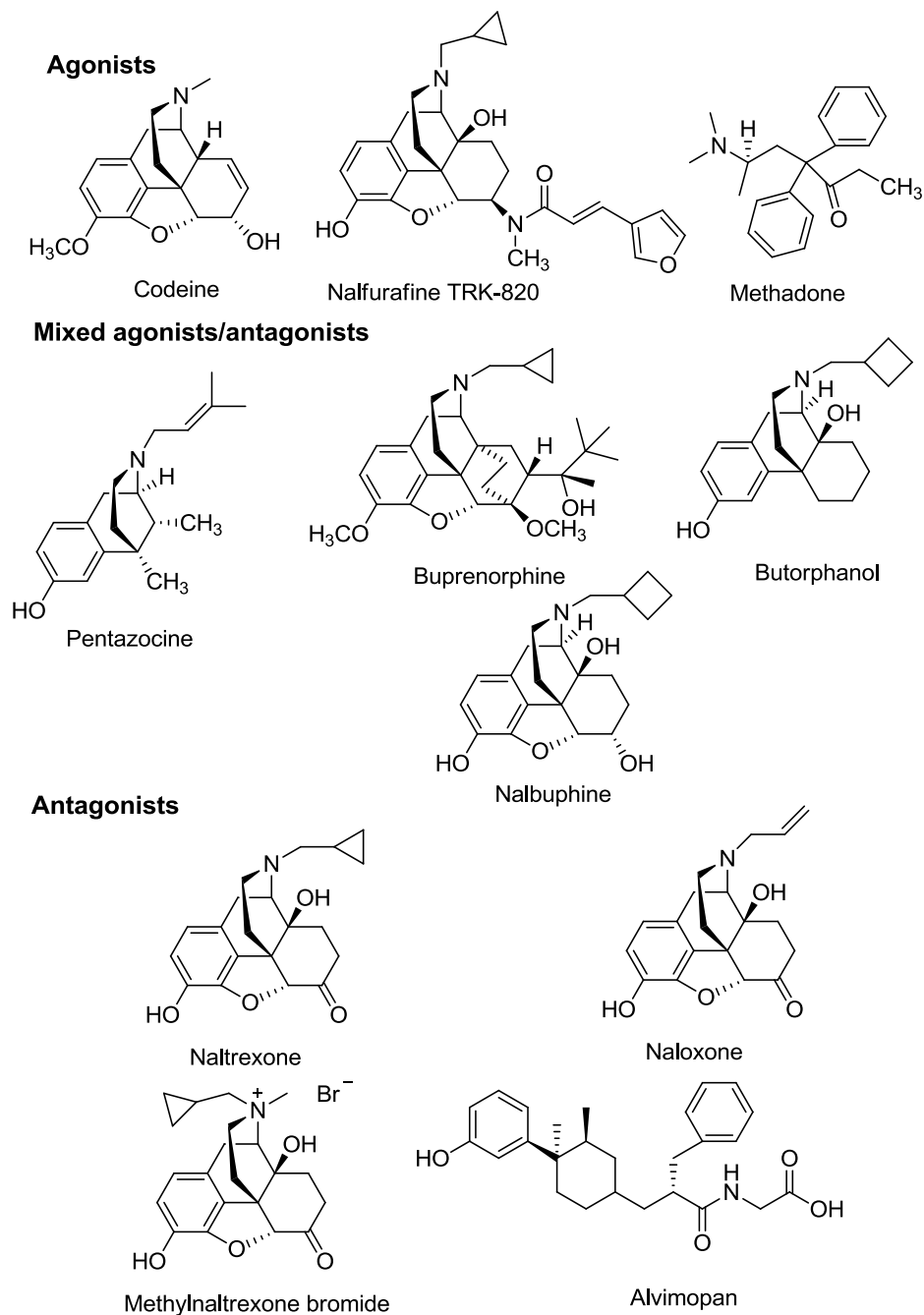
Figure 2.5 Clinically used opioids and opioid antagonists

2.3.2　Opioids in clinical trials or under clinical development

A variety of peptidic entities targeting opioid receptors have been tested in clinical trials (see Figure 2.6 for opioids under clinical development). Recently, a novel dynorphin A(1-13)

derivative CJC-1008 (structure undisclosed) was in Phase II clinical trials for postherpetic neuralgia.[69] It contains a maleimidopropionyl group covalently attaching the peptide to serum albumin and thereby extending the peptide's duration of action. Following intravenous (i.v.) infusion it exhibited analgesic activity for at least 8 h, but less than 24 h.[69, 70] FE200665 (now known as CR665), a peripheral KOR agonist,[71] has completed phase Ia clinical trials and exhibited selectivity against visceral pain.[70, 72] A second generation orally available peptide CR 845 (structure not disclosed) has been reported to have successfully completed a Phase I trial in an oral formulation[73] and is currently in Phase II clinical trials in an i.v. formulation.[74] This peptide is being clinically developed for the treatment of postoperative pain. Met^5-enkephalin (referred to as opioid growth factor or OGF)[75] has been examined in Phase I and II clinical trials for the treatment of advanced pancreatic cancer.[75] It was reported to provide clinical benefit to 53% of the patients who had failed standard chemotherapy and also to increase survival time by three fold.[70, 75] It is also currently in Phase II clinical trials in head and neck cancers and in Phase I clinical trials for hepatocellular cancer.[76] Recently, a clinical trial of gene therapy with the replication defective herpes simplex virus-based NP2 vector that expressed human proenkephalin was conducted. The therapy has shown promising results in terms of pain relief and safety.[70, 77]

Along with peptidic drug candidates, several small molecules targeting opioid receptors are also in clinical trials or have the potential for clinical development. The peripherally selective KOR agonist asimadoline is currently undergoing clinical trials for the treatment of diarrhea predominant irritable bowel syndrome.[78] Small molecule DOR agonists in clinical trials include PF-04856880[79] (Adolor, Pfizer) for relieving pain related with rheumatoid arthritis and PF-0465881[80] (Adolor, Pfizer) for postherpetic neuralgia. A selective DOR antagonist TRK-851 (Toray) which is an antitussive agent is in clinical development.[81]

Peptidic ligands

D-Phe-D-Phe-D-Nle-D-Arg-N(H)—CH₂—[pyridine]
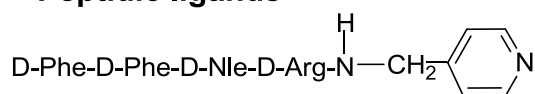
Tyr-Gly-Gly-Phe-Met

FE200665

Met-enkephalin

Non-peptidic ligands
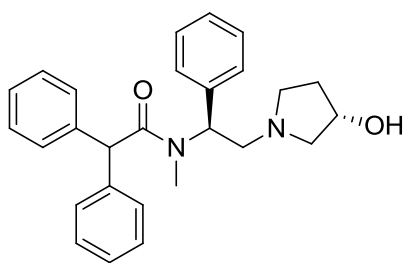
Asimadoline
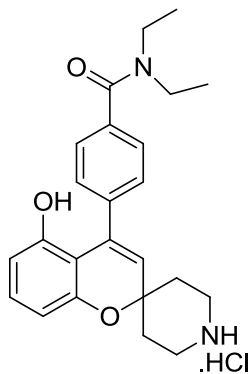
PF-04856880
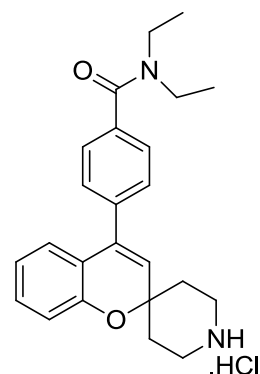
PF-04856881
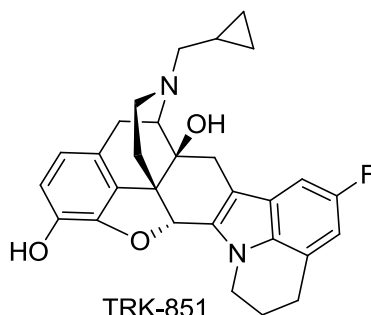
TRK-851

Figure 2.6 Structures of opioids in clinical trials or under clinical development

2.4 Significance of KOR

KOR agonists, unlike MOR agonists, are devoid of respiratory depression and dependence liability. Hence, they have been recently recognized for several potential therapeutic applications (see below), sparking renewed interest in ligands for this receptor. The effectiveness of KOR agonists in antinociceptive assays varies significantly with the type of noxious stimuli.[82] KOR agonists are less effective against thermal antinociception, compared to their effectiveness

against mechanical and chemical induced pain.[56] KOR agonists produce antinociception at both, receptors in the CNS and the peripheral KOR that are responsible for mediating inflammatory pain.[83, 84] In addition, KOR agonists have been reported to display anti-arthritic[85] and anti-inflammatory activity.[84, 85] While MOR agonists reinforce the effects of cocaine, KOR agonists alone do not produce reinforcing effects and following acute administration have been shown to block acute cocaine self-administration.[86-88] However, it appears that under chronic treatment they may paradoxically contribute to cocaine seeking behavior.[89-91] In addition KOR agonists also display other activities that include antipruritic activity,[92] diuretic effects,[83, 93] neuroprotective effects,[94] suppression of HIV-1 expression[95-97] and modulation of immune responses.[98] KOR agonists have also been reported to decrease tolerance to morphine,[56] and dynorphins have been reported to inhibit opiate withdrawal symptoms in opiate dependent animals.[56, 99, 100]

The endogenous KOR system is involved in multiple behavioral responses to stress which can impact responses to drugs of abuse and other disease states.[56] KOR activation also contributes to stress induced analgesia.[89, 101, 102] When exposed to inescapable physical or psychological stress, rodents demonstrate stress-induced analgesia that is blocked by disruption of the prodynorphin gene[102] or by KOR antagonists.[56] Activation of KOR results in decreasing dopamine levels, while activation of MOR results in increasing dopamine levels.[103] Cocaine exerts its effects by elevating levels of dopamine. Stressors such as repeated forced swim stress dramatically increase the rewarding effects of cocaine[89, 102] and cause reinstatement of extinguished cocaine seeking behavior through a mechanism involving KOR.[104, 105] This has led to the demonstration that KOR selective antagonists can block stress-induced reinstatement of cocaine seeking behavior.[106-109] Further, exposure to forced swim stress also potentiates the

immobility response of rodents which appears to be mediated through activation of the endogenous KOR system.[110] The cyclic adenosine monophosphate response element binding protein (CREB)-mediated increase in immobility behavior in rodents in forced swim stress was blocked by the KOR selective antagonist norBNI, suggesting involvement of KOR.[110] Increased immobility in response to a stressor is also an animal model of depression, and hence KOR antagonists may have potential antidepressant activity[111-115] and anti-anxiety properties.[115-118]

2.5   Non-Peptidic KOR ligands

2.5.1   KOR agonists

A variety of non-peptidic kappa agonists (Figure 2.7) have been developed as potential analgesics. Some of the early KOR agonists were benzomorphan derivatives that included ligands such as cyclazocine, ethylketocyclazocine and bremazocine. These ligands were used as pharmacological tools to study KOR, but they display low selectivity for KOR.[1, 119] The first KOR selective agonist was the benzacetamide U50,488.[120] Introduction of a spiro ether group on the cyclohexane ring of U50,488 resulted U69,593 which had improved selectivity compared U50,488.[121] Replacement of the phenyl ring in U69593 with a benzofuran yielded enandoline (CI-977) which is one of the most potent and selective kappa agonists.[122, 123] Radiolabeled derivatives of U69593 and enanadoline have been extensively used as pharmacological tools for KOR radioligand binding assays.

Several novel classes of KOR agonists have emerged recently. Octahydroisoquinoline carboxamides, a novel class of KOR agonists that does not contain a basic nitrogen, have been disclosed.[124] The novel KOR agonist, SA14867, was found to be an antinociceptive and antipruritic agent in preclinical studies and potently inhibited substance P-induced scratching behavior to a similar extent as nalfurafine after oral administration.[125] Some other structural

classes that have been recently described as KOR agonists are the pyrromorphinans[126] and 6,8-diazabicyclononane derivatives.[127] In order to avoid centrally mediated side effects, peripherally selective KOR agonists such as asimadoline[128] were also developed. Asimadoline is currently in clinical trials for the treatment of diarrhea-predominant irritable bowel syndrome.[78]

Non-peptidic agonists

U 50,488

U 69, 593

Ethylketocyclazocine

Bremazocine

Enandoline (CI-977)

N-alkyl octahydroisoquinoline carboxamide scaffold

SA14867

Pyrromorphinan scaffold

6,8-diazabicyclononane derivatives

Asimadoline
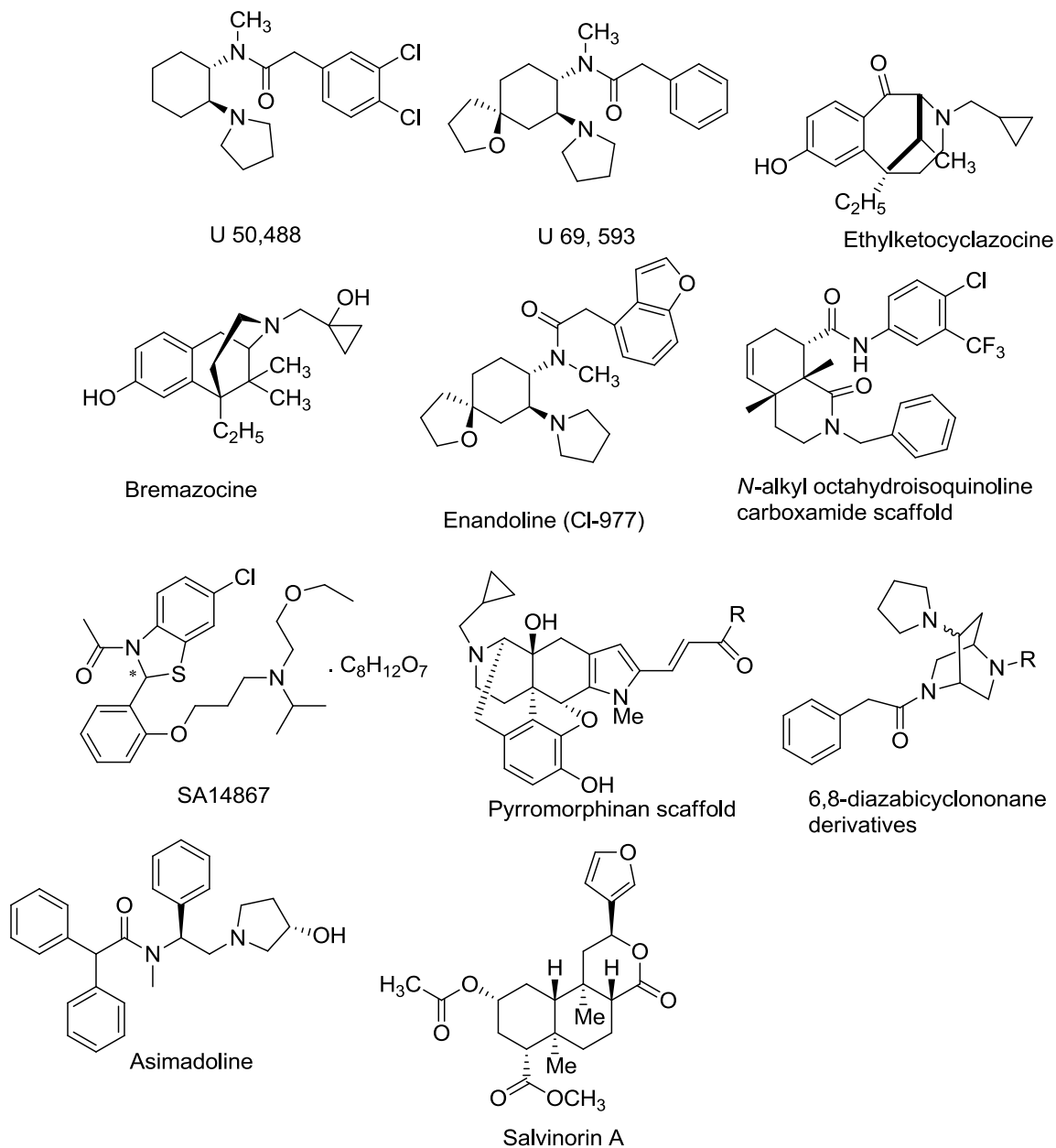
Salvinorin A

Figure 2.7 Non-peptidic KOR agonists

In addition, the non-nitrogenous natural product salvinorin A[129] displayed potent and selectiveKOR agonist activity. Several analogs of salvinorin A have been synthesized to study its structure-activity relationships (SAR) and as potentially therapeutically useful analogs for the treatment of pain, mood, personality disorder, substance abuse and gastrointestinal disorders.[130, 131]

2.5.2 KOR antagonists

While the early KOR antagonists developed were not very selective for KOR, the antagonists developed subsequently displayed much greater selectivity for KOR. The first selective non-peptide KOR antagonist described was triethyleneglycolnaltrexamime (TENA, Figure 2.8)[132] which displayed modest selectivity for KOR. Subsequently, the KOR antagonist norBNI (Figure 2.8) displayed improved selectivity for KOR.[133, 134] Later, the delta antagonist naltrindole when guanidylated at position 5, produced GNTI[135] (Figure 2.8) a KOR antagonist with increased affinity, selectivity and potency over norBNI. Surprisingly, the guanidylation of naltrindole at position 6' afforded a KOR agonist.[136]

Among the various 4-phenylpiperidine *N*-substituted derivatives, none of them were selective KOR antagonists[137, 138] until the discovery of JDTic[139] (Figure 2.8). JDTic and norBNI not only displayed selective KOR antagonism in various antinociceptive assays, but also suppressed KOR agonist induced diuresis in rats.[140] JDTic[106] and norBNI[102] have been shown to inhibit stress induced reinstatement of cocaine and also displayed antidepressant-like activity in the forced swim stress,[111] prompting the examination of these compounds for potential use in the treatment of depression[113, 114] and anxiety.[116, 117]

These prototypical non-peptide KOR antagonists exhibited delayed onset of activity and long durations of action.[140] The long duration of action extended from weeks to more than a

month depending on the species.[140] Several mechanisms for this unusual long duration of action have been proposed including partitioning into the cell membranes, thereby forming a depot from which drug is slowly released, and/or due to their resistance to metabolism.[141] Another hypothesis for the slow and persistent antagonism of these selective KOR antagonists may be due to an inactive conformation of the receptor which is induced by the compound.[141] It has been proposed that the delay in the onset of norBNI may be due to the large size of the compound and/or poor permeability across the blood-brain barrier which in turn causes slow diffusion to the site of action.[142] Recently, it was reported that norBNI, GNTI and JDTic caused activation of JNK1 which in turn caused prolonged inhibition of the KOR signaling pathways.[143, 144] Very recently, it was reported that KOR antagonists that exhibit low efficacy for the activation of JNK1 pathway have shorter durations of action.[145]

Recently several analogs of JDTic have been investigated in order to make more potent shorter acting derivatives. One of the analogs (compound W, see Figure 2.8), where the -NH-group in the tetrahydroisoquinoline ring of JDTic is replaced by a methylene antagonized selective kappa agonist-induced diuresis and displayed a duration of action of less than a week.[146] However, it was 9-fold less potent at KOR and 30-fold less selective for KOR over MOR than JDTic.[146] Another analog of JDTic, RTI-194, although not as efficacious as JDTic in inhibiting relapse to cocaine due to stress, is one of the very few orally bioavailable KOR antagonists[109] along with JDTic.[147]
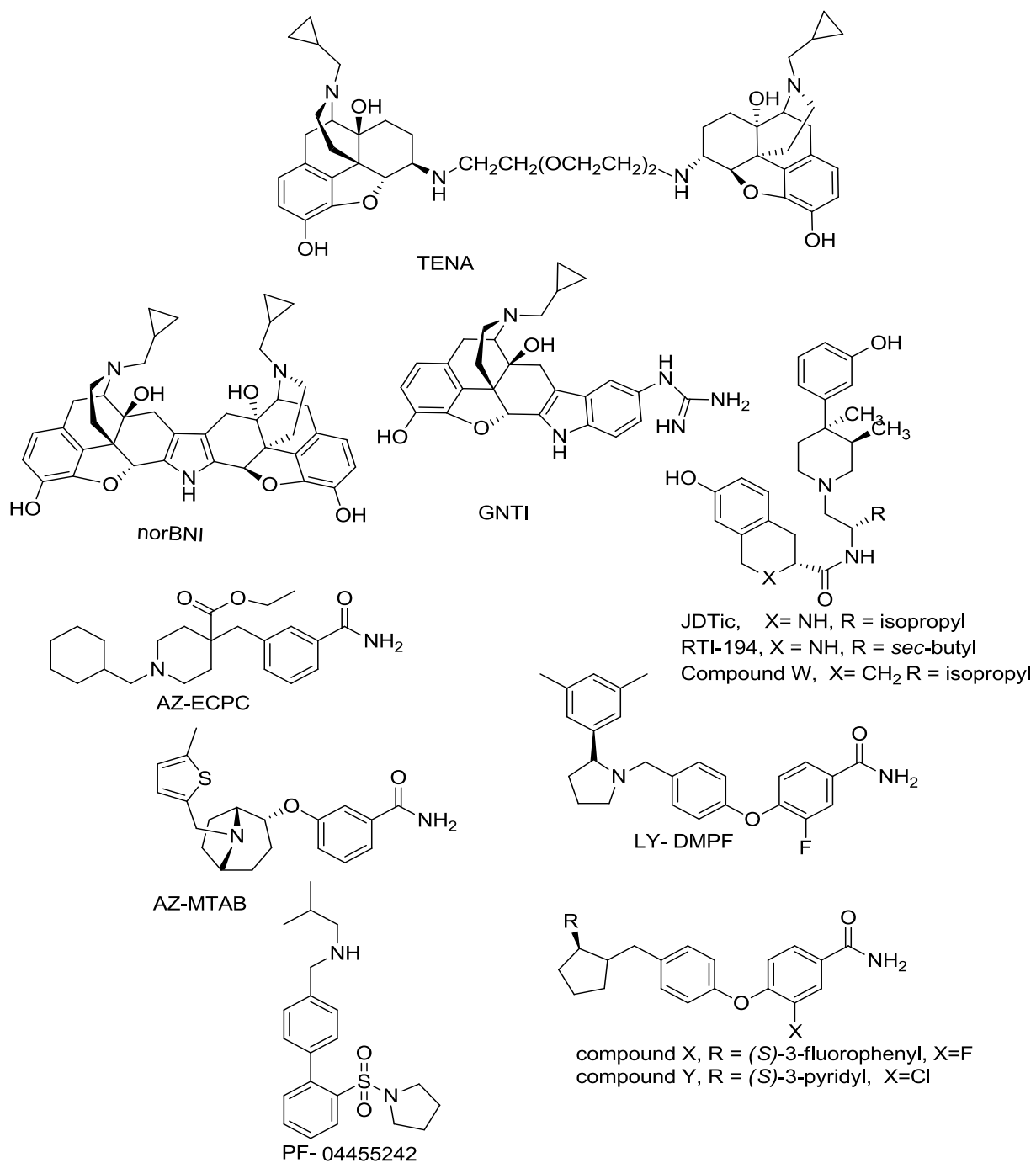
Figure 2.8 Non-peptidic KOR antagonists

Three antagonists, AZ-ECPC, AZ-MTAB and LY-DMPF (Figure 2.8), that belong to three different chemical classes lacked the long lasting inhibition (less than 1 week vs. 4 weeks exhibited by norBNI) of kappa agonist-induced diuresis.[118] In the elevated plus maze model for

mood disorders, AZ-MTAB and LY-DMPF were able to reverse prenatal stress-induced behavioral deficits.[118] AZ-ECPC, AZ-MTAB and LY-DMPF displayed KOR affinities (K_i) values of 53 nM, 35 nM and 1.8 nM, respectively, in the radioligand binding assays and KOR antagonist potencies (IC_{50} for antagonism of 15 nM Dyn A(1-13)) with values of 83 nM, 19 nM and 1.3 nM in the GTPγS assay.[118] AZ-ECPC, AZ-MTAB and LY-DMPF displayed 5-, 37- and 40-fold selectivity, respectively, for KOR vs MOR in the GTPγS assay as compared to 102-fold selectivity obtained for norBNI.[118] In addition, while KOR antagonists such as norBNI,[105] JDTic[106] and zyklophin[108] must be administered prior to induction of stress to prevent stress-induced reinstatement of cocaine seeking behaviour, recently developed KOR antagonists such as AZ-MTAB and LY-DMPF have been effective post-stress in a model of anxiety.[118]

PF-04455242 (Figure 2.8) is a selective KOR antagonist developed by Pfizer that has been studied extensively *in vivo* as well as *in vitro*. Receptor occupancy studies of PF-04455242[148] showed that this compound was bound to central KOR for not more than 8 h, suggesting that it had a short duration of action[149] which was later confirmed by the results from the warm water tail withdrawal antinociception assay.[145] PF-04455242 displayed a K_i value of 3 nM for KOR, and a 20-fold selectivity for KOR over MOR and a KOR antagonist potency of 1.23 nM in the GTPγS assay.[149] PF-04455242 was also shown to have excellent brain penetration and is not a P-glycoprotein substrate.[148] Although it is highly bound to plasma proteins, its free concentrations in the brain strongly correlated with its K_i value for KOR.[148] PF-04455242 displayed antidepressant-like behavior, inhibited stress-induced reinstatement of cocaine and also inhibited spirolidine-induced increases in rat plasma prolactin levels.[149]

One of compounds belonging to the class of aminobenzloxyarylamides was an orally active selective KOR antagonist (compound X, Figure 2.8)[150] and another was used as a KOR

occupancy tracer (compound Y, Figure 2.8).[150] Unlike the previously developed tracer that is a KOR agonist,[151] compound Y is a KOR antagonist.[150] It (compound Y) displays favorable specific vs. nonspecific binding, had good brain uptake and could be blocked by pretreatment with the orally active KOR antagonist compound X in a dose-dependent manner, demonstrating its utility as a tracer for determining the KOR occupancy levels of other KOR ligands. The orally active antagonist (compound X), unlike the prototypical KOR antagonists that exhibit a delayed onset of action showed potent *in vivo* antagonism within 30 min of oral dosing and was 63- and 373-fold selective for KOR over MOR and over DOR, respectively, in radioligand binding assays.

2.6   Overview of peptidic KOR ligands

Peptidic ligands targeting KOR include both agonists and antagonists. These ligands mainly include analogs of the endogenous KOR ligand the dynorphins, however, peptides structurally unrelated to dynorphins such as linear and macrocyclic tetrapeptides also exhibit activity at KOR. We are interested in developing Dyn analogs as pharmacological tools to study the structure and function of KOR and for therapeutic *in vivo* applications. Hence, the SAR of Dyn A analogs will be discussed extensively in section 2.7.

2.6.1   Peptide agonists

Several Dyn A analogs with modifications in the "message" and "address" sequence (The "message-address" concept will be discussed below in section 2.7.1) have been reported and evaluated in both *in vitro* and *in vivo* studies. Dyn A analogs with agonist activity and high selectivity at KOR include [D-Pro[10]]Dyn A(1-11) analogs with N-terminal monoalkylation[152] and analogs with substitution of either Ala or D-Ala in position 3 of Dyn A(1-11)NH$_2$[153] (Figure 2.9 for peptide KOR agonists).

Peptidic agonists

Dyn A   Tyr-Gly-Gly-Phe-Leu-Arg-Arg-Ile-Arg-Pro-Lys-Leu-Lys^{13}-Trp-Asp-Asn-Gln

N-alkyl[D-Pro^{10}]Dyn A(1-11)   R-Tyr-Gly-Gly-Phe-Leu-Arg-Arg-Ile-Arg-D-Pro-Lys
(R= allyl, cyclopropylmethyl,
or benzyl)

[L/D-Ala^3]Dyn A(1-11)NH$_2$ Tyr-Gly-L/D-Ala-Phe-Leu-Arg-Arg-Ile-Arg-Pro-LysNH$_2$

[NMeTyr^1]Dyn A(1-13)NH$_2$ Tyr-Gly-Gly-Phe-Leu-Arg-Arg-Ile-Arg-Pro-Lys-Leu-LysNH$_2$

E2078   NMe-Tyr-Gly-Gly-Phe-Leu-Arg-NMeArg-DLeu-NEt$_2$

SK-9707   NMe-Tyr-DAla-Gly-Phe-Leu-Arg-ψ(CH$_2$NH)-Arg-Ile-NH$_2$

                         D-Phe-D-Phe-D-Nle-D-Arg-NH─R
                                    ─R─
FE200041   H

FE200665
(CR665)

FE200666   D-Phe-D-Phe-D-Leu-D-Orn-N⟨   ⟩O
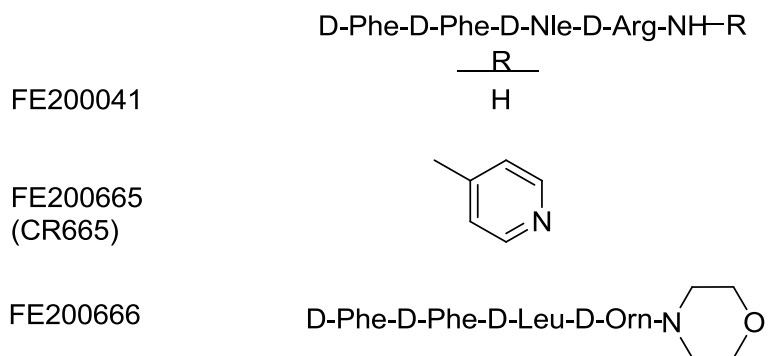
Figure 2.9 Peptidic KOR agonists

A number of modifications have been made to Dyn A to increase its metabolic stability
so that the peptides can be studied *in vivo*. Dyn A(1-13) is a potent fragment of Dyn A.[154]
[*N*MeTyr^1]Dyn A(1-13)NH$_2$ was one of the very early Dyn A analogs with KOR agonist activity
and improved metabolic stability.[154] This peptide produced antinociception and enhanced
morphine analgesia in morphine tolerant rats *in vivo* after intravenous, subcutaneous and
pulmonary administration.[155, 156] The Dyn A-(1-8) derivative E-2078 ([*N*MeTyr^1,*N*MeArg^7,D-

Leu[8]]Dyn A(1-8)NEt$_2$,[157] (Figure 2.9), contains several modifications to impart metabolic stability. This peptide has been extensively studied in rodents,[158-161] monkeys[162-165] and humans.[166, 167] In humans it exhibited analgesic activity comparable to pentazocine.[166] Radioiodinated E-2078 was detected in rat brain parenchyma following brain perfusion studies,[158] and E-2078 was also detected in the cerebrospinal fluid of monkeys by mass spectrometry.[163] [I^{125}-Tyr]E2078 was shown to cross bovine brain microvessel endothelial cell (BBMEC) monolayers, which is a model of blood-brain barrier (BBB), by absorptive-mediated endocytosis.[168] While this peptide has been shown to cross the BBB, the elevation of serum prolactin levels by E-2078 suggested that this peptide is a potent peripherally selective KOR agonist.[162] SK-9709 ([D-Ala^2,Arg^{6}ψ(CH$_2$NH)Arg^7]Dyn A-(1-8) amide, Figure 2.9) is another metabolically stable Dyn A(1-8) analog. SK-9709 is 15-fold selective for KOR over MOR which is comparable to that of Dyn A(1-13).[169] It exhibits antinociceptive activity which appears to be mediated by both KOR and MOR. Similar to E-2078, SK-9709 exhibited long lasting antinociception (maximal effect at 120 min after systemic (s.c.) administration) in the acetic acid writhing and the hot plate tests, although it was less potent than E-2078.[169]

Peptidic KOR agonists unrelated to Dyn includes several all-D tetrapeptides. A combinatorial library of these tetrapeptides was screened to identify peptides with affinity for each of the opioid receptors.[170] The tetrapeptides with affinity for KOR included those consisting of all D-amino acids include FE20041 (Figure 2.9) which exhibited 30,000- and 68,000-fold selectivity for KOR over MOR and DOR, respectively;[171] this peptide was approximately 10-fold selective for peripheral over central KOR.[171] C-terminal modifications of this peptide resulted in FE200665 and FE20066 (Figure 2.9) that were 548- and 182-fold selective, respectively, for peripheral KOR over the central KOR.[71, 172] FE200665 has completed phase Ia

clinical trial and exhibited peripheral KOR selectivity,[72] and a second generation peptide CR 845 (structure undisclosed) has successfully completed Phase I trial in an oral formulation[73] and is currently in Phase II clinical trials as an i.v. formulation.[74] The candidate is being clinically developed for the treatment of postoperative pain.

2.6.2 Peptide antagonists

Most of the peptide based KOR antagonists that have been developed are modified Dyn A(1-11) derivatives (see Figure 2.10). These include analogs without a basic N-terminus,[173-176] [Pro^3]Dyn A(1-11)NH$_2$ derivatives[177-179] and also [*N,N*-diallyl-Tyr^1,D-Pro^{10}]Dyn A(1-11).[152, 180, 181] Arodyn (Ac[Phe^{1,2,3},Arg^4,D-Ala^8]Dyn A(1-11)NH$_2$), a selective KOR antagonist, synthesized in the Aldrich laboratory,[174] when administered centrally antagonized the antinociceptive effects of the centrally administered KOR agonist U50488 in the warm water tail withdrawal assay and was able to inhibit stress induced reinstatement of cocaine seeking behavior in the cocaine conditioned place preference assay.[107] While arodyn was metabolized when tested in whole rat blood *in vitro*, zyklophin ([*N*^{α}-benzylTyr^1-*cyclo*(D-Asp^5,Dap^8)]Dyn A(1–11)NH$_2$), a cyclic selective KOR antagonist, displayed greater metabolic stability than arodyn *in vitro*[182] and was effective when administered both centrally and peripherally.[108] The ability of peripherally administered zyklophin to antagonize centrally administered U50,488 strongly suggested that zyklophin was able to cross the blood brain barrier.[108] Zyklophin when systemically administered (3 mg/kg s.c.) prevented stress- induced reinstatement of cocaine seeking behavior in conditioned place preference assay. In the antinociceptive assay, unlike the small molecule KOR antagonists, zyklophin inhibited the antinociceptive effect of U50,488 for a shorter duration (12-18 h) after s.c administration. [108]

N,N-diallyl-Tyr-Gly-Gly-Phe-Leu-Arg-Arg-Ile-Arg-D-Pro-Lys

[N,N-diallyl-Tyr^1,D-Pro^{10}]Dyn A(1-11)

Ac-Tyr-Lys-Trp-Trp-Leu-Arg-Arg-DAla-Arg-Pro-Lys-NH$_2$

JVA 901 (Venorphin)

Tyr-Gly-D-Pro-Phe-Leu-Arg-Arg-Ile-Arg-Pro-Lys-NH$_2$

[D-Pro^3]Dyn A(1-11)NH$_2$

Ac-Phe-Phe-Phe-Arg-Leu-Arg-Arg-DAla-Arg-Pro-Lys-NH$_2$

Arodyn

Tyr-Gly-Trp-Trp-Glu-Arg-Arg-Ile-Arg-Pro-Lys-NH$_2$

Cyclodyn

Bz-Tyr-Gly-Gly-Phe-DAsp-Arg-Arg-Dap-Arg-Pro-LysNH$_2$

Zyklophin
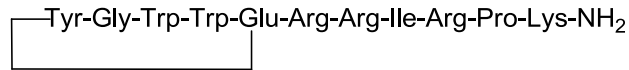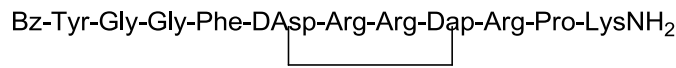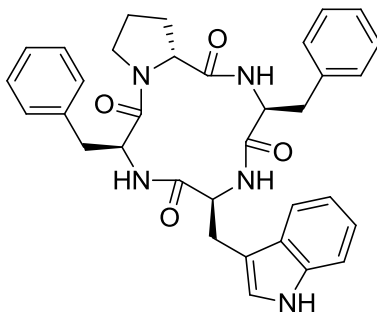
CJ 15,208*   D-Trp isomer of CJ 15,208

* Mixed agonist/antagonist
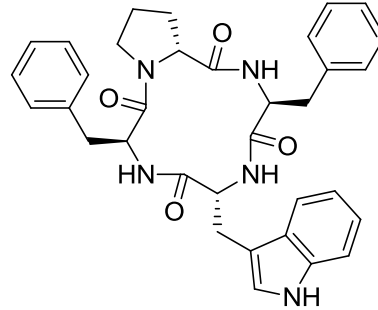
Figure 2.10 Peptidic KOR antagonists

Other peptides unrelated to Dyn A have also exhibited KOR antagonism. The natural product macrocyclic tetrapeptide CJ-15,208 (*cyclo*[Phe-D-Pro-Phe-Trp], Figure 2.10) exhibited KOR antagonism in a smooth muscle assay *in vitro*.[183] *In vivo*, the parent peptide with L-Trp exhibited mixed agonist/antagonist activity.[184] Orally administered L-Trp isomer displayed dose dependent and time dependent inhibition of both cocaine-induced and stress-induced reinstatement of cocaine, making it a promising lead for the treatment of drug abuse, especially

relapse.[185] Following intracerebroventricular administration the D-Trp isomer of CJ-15,208 displayed minimal agonist activity and exhibited KOR selective antagonism that lasted less than 18 h.[184] The D-Trp isomer also inhibited stress- but not cocaine-induced reinstatement of extinguished cocaine seeking behavior. The relatively short duration of action produced by the D-Trp isomer makes it a promising lead compound for maintaining abstinence from substance abuse.[184] Following oral administration the D-Trp isomer exhibited weak KOR agonism, displayed KOR antagonism, and prevented stress-, but not cocaine-, induced extinguished cocaine seeking behavior in a dose-dependent manner.[186]

2.7   Dynorphin A analogs

2.7.1   Introduction

Dyn A has the N-terminal tetrapeptide sequence Tyr-Gly-Gly-Phe, common to most other endogenous mammalian opioid peptides; however, the C-terminal sequence differs from other opioid peptides. Chavkin and Goldstein proposed the "message-address" hypothesis wherein the N-terminal "message" sequence imparts opioid receptor affinity and activity, while the C-terminal "address" sequence imparts affinity for KOR.[154] Dyn A(1-13) and Dyn A(1-11) account for most of the parent peptide's opioid activity.[154] Therefore these two shorter peptides are generally used as the parent peptides for incorporating structural modifications.[154] Most of the SAR studies have been focused on Dyn A, and very few Dyn B analogs[187] have been synthesized.

Several linear and cyclic Dyn A analogs with modifications in the "message" and "address" sequences have been synthesized. Some of the early Dyn A analogs include the mono- and dialkylated analogs of [D-Pro^{10}]Dyn A(1-11).[152, 180, 181, 188] In addition several cyclic analogs

with conformational constraint through a lactam[189-191] or disulfide bridge[192-194] have also synthesized. Detailed reviews that discuss the early SAR of Dyn A were published earlier.[195, 196]

2.7.2 Analogs with modifications in the *N*-terminal "message" sequence

2.7.2.1 Dyn A analogs with modifications at position 1

Several analogs containing modifications in position 1 of the "message" sequence have been synthesized to explore the SAR of Dyn A (see Table 2.3 for opioid receptor binding affinities, and Tables 2.4 and 2.5 for opioid agonist and antagonist potencies, respectively).

[D-Pro^{10}]Dyn A(1-11) was one of the early Dyn A analogs that was synthesized.[197] N-Alkylation of Tyr^1 in this peptide resulted in analogs with increased KOR selectivity, while dialkylation resulted in lower KOR affinity and selectivity than the parent peptide.[152, 181, 188] In the earlier studies *N,N*-diallyl analog was found to be a KOR antagonist.[180] Subsequent studies of the monoalkylated [D-Pro^{10}]Dyn A(1-11) showed that the *N*-benzyl analog has high KOR affinity, but, displayed weak agonist activity in the GPI assay[152, 181] and displayed partial agonism (~70% efficacy compared to full agonist Dyn A(1-13)NH$_2$) in the AC assay.[188] The *N*-allyl and the *N*-cyclopropylmethyl (CPM) analogs also showed high KOR affinity and displayed potent agonist activity in GPI assay.[152] The N-CPM analog also displayed full agonist activity (94% efficacy compared to full agonist Dyn A(1-13)NH2) in the AC assay.[188]

Schiller *et al.* showed that substitution of the Tyr^1 residue of opioid agonist peptides with residues in which the positively charged N-terminal amino group was replaced with hydrogen or methyl group produced opioid antagonists.[175, 198] The Tyr^1 residue in Dyn A(1-11)NH$_2$ was replaced with Dhp (Dhp = 3-(2,6-dimethyl-4-hydroxyphenyl)propanoic acid, Figure 2.11) or with Mdp (Mdp = (2*S*)-2-methyl-3-(2,6-dimethyl-4-hydroxyphenyl)propanoic acid, Figure 2.11). In the GPI assay the Dhp^1 analog was a potent KOR antagonist with a K_e value of 17.4 nM,

while the Mdp[1] analog (called dynantin) was found to be even more potent with a K_e value of 0.63 nM against the agonist Dyn A(1-11)NH$_2$. Dynantin also displayed subnanomolar KOR affinity (K_i = 0.82 nM) and high KOR binding selectivity (K_i (KOR/MOR/DOR = 1/259/198)). The D-Ala[3] analogs of [Dhp[1]]Dyn A(1-11)NH$_2$ and [Mdp[1]]Dyn A(1-11)NH$_2$ were prepared, but none of them showed significant improvements in selectivities or antagonist potencies as compared to their parent analogs.[175] The Mdp analog of the KOR agonist E2078 was also synthesized, although it was less potent and selective than dynantin.[187] Schiller and coworkers desribed the Mdp[1] analog of Dyn B, the first Dyn B based KOR antagonist. However, it was less potent and less selective than dynantin (see Table 2.3 and 2.5).[187]
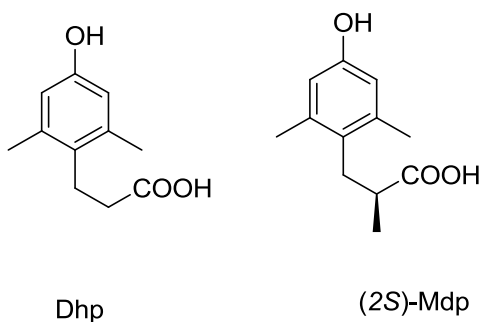
Figure 2.11 Tyrosine analogs incorporated into Dyn A analogs

Table 2.3 Opioid receptor binding affinities of Dyn A and Dyn B analogs modified at position 1.

| Compound | K_i (nM ± SEM) | | | K_i ratio | Ref |
	KOR	MOR	DOR	KOR/MOR/DOR	
[D-Pro[10]]Dyn A(1-11)[a]	0.030 ± 0.001	0.24 ± 0.002	2.1 ± 0.4	1/8/70	152
[N-Allyl-Tyr[1],D-Pro[10]]Dyn A(1-11)[a]	0.049 ± 0.001	10.9 ± 0.5	499 ± 15	1/222/9160	152
[N-CPM-Tyr[1],D-Pro[10]]Dyn A(1-11)[a]	0.020 ± 0.001	9.6 ± 0.6	558 ± 8.9	1/480/27900	152
[N-Benzyl-Tyr[1],D-Pro[10]]Dyn A(1-11)[a]	0.029 ± 0.001	31.1 ± 0.2	176 ± 17	1/1070/6080	152
[N,N-Diallyl-Tyr[1],D-Pro[10]]Dyn A(1-11)[a]	3.60 ± 0.50	31.7 ± 3.8	149 ± 58	1/8.8/41	152
[N,N-DiCPM-Tyr[1],D-Pro[10]]Dyn A(1-11)[a]	0.19 ± 0.002	3.9 ± 0.1	166 ± 14	1/21/880	152
[Dhp[1]]Dyn A(1–11)NH$_2$[b]	3.49 ± 0.12	27.9 ± 3.3	122 ± 24	1/8/35	175
[(2S)-Mdp[1]]Dyn A(1–11)NH$_2$ (Dynantin)[b]	0.823 ± 0.162	213 ± 50	163 ± 15	1/259/198	175
[Dhp[1],D-Ala[3]]Dyn A(1–11)NH$_2$[b]	3.84 ± 0.90	73.0 ± 1.1	419 ± 57	1/19/109	175
[(2S)-Mdp[1],D-Ala[3]]Dyn A(1–11)NH$_2$[b]	2.47 ± 0.38	167 ± 17	364 ± 101	1/68/147	175
[(2S)-Mdp[1],MeArg[7],D-Leu[8]]Dyn A(1–8)NH$_2$[b,c]	4.07	154	118	1/38/29	187
[(2S)-Mdp[1],MeArg[7],D-Leu[8]]Dyn A(1–8)NHEt$_2$[b,c]	15.2	51.2	13.5	1/3/1	187
[(2S)-Mdp[1]]Dyn B[b,c]	9.12	21.3	43.6	1/2/5	187

[a] Affinity for KOR was determined by measuring the inhibition of [^{3}H]bremazocine binding to guinea pig cerebellar membranes. Affinities for MOR and DOR were measured in rat forebrain using [^{3}H]DAMGO and [^{3}H]DPDPE, respectively.
[b] Determined by displacement of [^{3}H]U69,593 from guinea pig brain membrane binding sites and of [^{3}H]DAMGO and [^{3}H]DSLET from rat brain membrane binding sites.
[c] SEM not reported

Table 2.4 Opioid agonist potencies of N-terminally modified [D-Pro[10]]Dyn A(1-11) analogs

Compound	IC$_{50}$ (nM)[a]	Ref
[D-Pro[10]]Dyn A(1-11)	0.22 (0.11-0.49)	152
[N-Allyl-Tyr[1],D-Pro[10]]Dyn A(1-11)	18.3 (13.2-22.4)	152
[N-CPM-Tyr[1],D-Pro[10]]Dyn A(1-11)	2.16 (1.6-2.8)	152
[N-Benzyl-Tyr[1],D-Pro[10]]Dyn A(1-11)	990 (657-1500)	152

[a] IC$_{50}$ values obtained in the GPI assay. 95% confidence intervals are given in parentheses.

Table 2.5 Antagonist potencies of Dyn A and Dyn B analogs modified at position 1.

Compound	K_e (nM ± SEM)	Ref
[N,N-Diallyl-Tyr[1],D-Pro[10]]Dyn A(1-11)[a]	188 ± 32	180
[Dhp[1]]Dyn A(1–11)-NH$_2$[b]	17.4 ± 2.7	175
[(2S)-Mdp[1]]Dyn A(1–11)-NH$_2$ (Dynantin)[b]	0.632 ± 0.136	175
[Dhp[1],D-Ala[3]]Dyn A(1–11)NH$_2$[b]	11.6 ± 1.4	175
[(2S)-Mdp[1],D-Ala[3]]Dyn A(1–11)NH$_2$[b]	3.31 ± 0.24	175
[(2S)-Mdp[1],MeArg[7],D-Leu[8]]Dyn A(1–8)-NH$_2$[b,c]	8.29	187
[(2S)-Mdp[1],MeArg[7],D-Leu[8]]Dyn A(1–8)-NHEt$_2$[b,c]	39.1	187
[(2S)-Mdp[1]]Dyn B[b,c]	114	187

[a] Antagonist potency in the GPI assay against [D-Pro[10]]Dyn A(1-11).
[b] Antagonist potency in the GPI assay against Dyn A(1-13).
[c] SEM not reported

2.7.2.2 Dyn A analogs modified at position 2 and/or 3

Schlectingen *et al.* synthesized Dyn A(1-11)NH$_2$ analogs with Pro-substituted at positions 2 and 3[177, 179] (see Table 2.6 for opioid receptor affinities and Table 2.7 for antagonist potencies). The Pro[2] and D-Pro[2] analogs showed similar KOR affinity and selectivity (~30-fold selective for KOR vs. MOR), but their affinities were substantially lower (1000-fold) than Dyn A(1-11)NH$_2$. Substitution of Sar (Sar = sarcosine, i.e N-Me Gly) at position 2 yielded an analog that exhibited higher KOR affinity (K_i = 1.5 nM) than the Pro[2] and D-Pro[3] analogs and was a full agonist (IC$_{50}$ = 280 nM)   in the GTPγS assay. Although substitution of Pro at position 3 reduced the affinity for all three opioid receptors relative to the parent peptide Dyn A(1-11)NH$_2$, it retained reasonably high KOR affinity (K_i = 2.7 nM) and is one of the most selective KOR ligands (2200-fold selective for KOR vs MOR). In contrast, the D-Pro[3] analog had very low KOR affinity (K_i = 160 nM) without any gain in selectivity. While the configuration of Pro at position 3 had a significant effect on the KOR affinity and selectivity, all of the Pro analogs with substitution in positions 2 or 3 were found to be weak KOR antagonists in the [^{35}S]GTPγS assay, with the Pro[3]

analog being the most potent (IC_{50} = 380 nM), (see Table 2.7). These analogs were also found to be weak antagonists in the GPI assay.[177] The analog with the larger ring size homolog of Pro, piperidinecarboxylic acid (Pip) exhibited decreased KOR affinity (K_i (KOR) = 210 nM) and KOR selectivity (60-fold selective for KOR vs MOR) compared to the Pro[3] analog suggesting that increasing the ring size of Pro[3] residue resulted in decreased KOR affinity and selectivity. This suggested that the ϕ dihedral angle and backbone geometry of residue 3 were important for maintaining affinity and selectivity for KOR. The disubstituted analog [Sar[2],Pro[3]]Dyn A(1-11)NH$_2$ displayed high KOR affinity (K_i = 3.2 nM) and retained selectivity for KOR (see Table 2.6). While the Sar[2],Pro[3] analog displayed comparable KOR affinities to the Pro[3] analog, it was 8-fold less potent as an antagonist relative to Pro[3] analog (see Table 2.7).[178]

Table 2.6 Opioid receptor binding affinities of Dyn A analogs modified in positions 2 and 3.

Compound	K_i (nM ± SEM)[a]			K_i ratio KOR/MOR/DOR	Ref
	KOR	MOR	DOR		
[Pro[2]]Dyn A(1-11)NH$_2$	94 ± 18	3200 ± 290	6800 ± 350	1/34/72	177
[D-Pro[2]]Dyn A(1-11)NH$_2$	65 ± 8.7	1700 ± 160	3900 ± 300	1/26/1960	177
[Sar[2]]Dyn A(1-11)NH$_2$	1.5 ± 0.15	390 ± 120	390 ± 62	1/260/260	178
[Pro[3]]Dyn A(1-11)NH$_2$	2.7 ± 0.33	5700 ± 860	8800 ± 2100	1/2110/3260	177
[D-Pro[3]]Dyn A(1-11)NH$_2$	160 ± 28	8300 ± 1500	7100 ± 200	1/52/44	177
[Pip[3]]Dyn A(1-11)NH$_2$	210 ± 19	12600 ± 2400	4700 ± 180	1/60/22	178
[Sar[2], Pro[3]]Dyn A(1-11)NH$_2$	3.2 ± 0.3	1490 ± 350	>10,000	1/460/>3000	178
Dyn A(1-11)NH$_2$	0.059 ± 0.015	5.6 ± 1.6	3.2 ± 0.83	1/95/55	178

[a] K_i values were obtained using Chinese hamster ovary (CHO) cell membranes stably expressing opioid receptors with [^{3}H]diprenorphine as the radiolabeled ligand

Table 2.7 Antagonist potencies of Dyn A analogs substituted at position 2 and 3.

Compound	IC$_{50}$ (nM ± SEM)^a	Ref
[Pro^2]Dyn A(1-11)NH$_2$	760 ± 220	177
[D-Pro^2]Dyn A(1-11)NH$_2$	940 ± 470	177
[Pro^3]Dyn A(1-11)NH$_2$^{b}	380 ± 54	177
[D-Pro^3]Dyn A(1-11)NH$_2$	2200 ± 1300	177
[Sar^2, Pro^3]Dyn A(1-11)NH$_2$	2790 ± 1050	178

^{a}Antagonist activity determined against 50 nM U50,488 in GTPγS assay.
^{b}Antagonist activity (K_e = 244 ± 51 nM) determined against U50,488 in GPI assay.

2.7.2.3 Dyn A analogs modified at position 4

Vig *et al*. synthesized various Dyn A analogs with substitutions in position 4 of the peptide [D-Ala^8]Dyn A(1-11)NH$_2$[199] in an effort to understand the spatial orientation of the aromatic ring of Phe^4 required for interaction with KOR (see Table 2.8 for opioid receptor binding affinities and Table 2.9 for agonist potencies and efficacies). Substitution of D-Phe at position 4 caused a 78-fold decrease in KOR affinity as compared to the parent peptide, demonstrating that the backbone stereochemistry at position 4 is important for maintaining KOR affinity.[200] The analog with L-Homophe (homophenylalanine, Figure 2.12) in position 4 showed subnanomolar affinity for KOR (K_i = 0.66 nM) and retained selectivity for KOR over MOR comparable to the parent peptide. The D-Homophe^4 substitution, however, resulted in a 3-fold decrease in KOR affinity as compared to the L-Homophe^4 analog.[199] When the isomers of the conformationally constrained residue Atc (Atc = 2-aminotetralin-2-carboxylic acid, Figure 2.12) were incorporated in position 4 of [D-Ala^8]Dyn A(1-11)NH$_2$ the *(R)*-Atc analog, which corresponds to a constrained analog of the D-Phe^4 peptide, displayed 10-fold higher KOR affinity (K_i = 0.89 nM) compared to the *(S)*-Atc analog. Hence, substitution of Atc at position 4 of [D-Ala^8]Dyn A(1-11)NH$_2$ demonstrated a reversal of the preferred stereochemistry for KOR.[200] This also suggested that Atc behaved more as a constrained Homophe rather than as a

Phe analog at position 4 in this peptide. Other conformationally constrained Phe analogs i.e. the Aic (2-aminoindan-2-carboxylic acid, Figure 2.12, K_i = 26.5 nM) and Tic (1,2,3,4-tetrahydroisoquinoline 3-carboxylic acid, Figure 2.12, K_i = 4.69 nM) analogs displayed lower KOR affinities as compared to the *(R)*-Atc analog. Therefore among the various conformationally constrained residues at position 4, (*R*)-Atc displayed the most compatible spatial orientation for interaction with KOR. These results suggested that the side chain of the Phe^4 residue of Dyn A(1-11)NH$_2$ preferred either the gauche (-), with χ^1 of approximately -60°, or trans. These findings are consistent with the computational model of Dyn A interacting with KOR that was proposed by Paterlini *et al.*[201] Other substitutions at position 4 that could influence the backbone conformation of the peptide also affected receptor affinities and selectivities, for example, the α-MePhe^4 analog displayed a decrease in KOR affinity while MOR affinity was maintained, hence causing a decrease in KOR vs. MOR selectivity compared to the parent peptide. The *N*-MePhe^4 analog maintained the KOR affinity but displayed an increase in MOR affinity causing a decrease in KOR vs. MOR selectivity. While KOR and MOR were able to tolerate various substitutions at position 4, these peptides displayed very low affinity for DOR. The analogs also differed in their potencies for KOR in the AC assay. While the parent Phe^4 analog showed 500-fold higher potency compared to the D-Phe^4 analog, the *(R)*-Atc analog showed only 8-fold higher potency than the *(S)*-Atc analog and the Homophe^4 analog was only 9-fold more potent at KOR than its D-isomer. These results demonstrated that the affinity, potency and selectivity of [D-Ala^8]Dyn A(1-11)NH$_2$ analogs were influenced by the spatial orientation, stereochemistry and backbone conformation of residue 4. However, modifications at position 4 had minimal effect on efficacy at KOR, and all of these analogs were KOR agonists.[199]
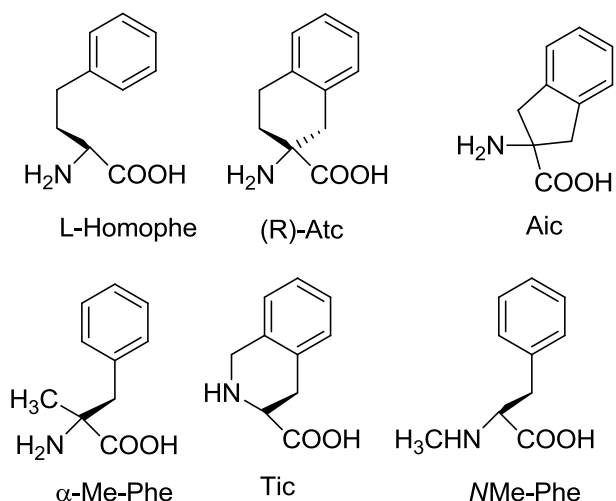
Figure 2.12 Phenylalanine derivatives

Table 2.8 Opioid receptor binding affinities of Dyn A analogs modified in position 4.

Compound	K_i (nM ± SEM)[a]			K_i ratio	Ref
	KOR	MOR	DOR	KOR/MOR/DOR	
[(R)-Atc^4,D-Ala^8]Dyn A(1-11)NH$_2$	0.89 ± 0.14	32.9 ± 4.7	>10,000	1/37/>10,000	199
[(S)-Atc^4,D-Ala^8]Dyn A(1-11)NH$_2$	9.54 ± 2.77	88.3 ± 5.9	>10,000	1/9.3/>10,000	199
[HomoPhe^4,D-Ala^8]Dyn A(1-11)NH$_2$	0.66 ± 0.03	13.7 ± 0.3	190 ± 58	1/21/288	199
[D-HomoPhe^4,D-Ala^8]Dyn A(1-11)NH$_2$	1.73 ± 0.51	47.0 ± 3.0	5570 ± 1620	1/27/3220	199
[D-Phe^4,D-Ala^8]Dyn A(1-11)NH$_2$	8.91 ± 0.07	123 ± 37	>10,000	1/14/>1120	200
[Aic^4,D-Ala^8]Dyn A(1-11)NH$_2$	26.5 ± 12.7	364 ± 52	>10,000	1/14/>377	199
[Tic^4,D-Ala^8]Dyn A(1-11)NH$_2$	4.69 ± 0.75	206 ± 36	3590 ± 580	1/44/765	199
[α-MePhe,D-Ala^8]Dyn A(1-11)NH$_2$	3.20 ± 0.79	3.24 ± 0.87	157 ± 46	1/1/49	199
[NMePhe^4,D-Ala^8]Dyn A(1-11)NH$_2$	0.62 ± 0.19	1.03 ± 0.4	56.1 ± 7.1	1/1.7/90	199
[D-Ala^8]Dyn A(1-11)NH$_2$	0.11 ± 0.05	4.20 ± 1.9	6.57 ± 0.23	1/10.4/64.2	200

[a] K_i values were obtained using CHO cell membranes stably expressing opioid receptors with [^{3}H]diprenorphine, [^{3}H]DAMGO and [^{3}H]DPDPE as the radiolabeled ligands for KOR, MOR and DOR, respectively

Table 2.9 Agonist potencies and efficacies at KOR in AC assay of Dyn A analogs modified at position 4.

Compound	IC$_{50}$ (nM ± SEM)	% max inhibition[a]	Ref
[(R)-Atc^4,D-Ala^8]Dyn A(1-11)NH$_2$	72.4 ± 28.1	96 ± 3	199
[(S)-Atc^4,D-Ala^8]Dyn A(1-11)NH$_2$	573 ± 220	74 ± 1	199
[HomoPhe^4,D-Ala^8]Dyn A(1-11)NH$_2$	5.20 ± 1.99	95 ± 5	199
[D-HomoPhe^4,D-Ala^8]Dyn A(1-11)NH$_2$	46.9 ± 7.1	100	199
[D-Phe^4,D-Ala^8]Dyn A(1-11)NH$_2$	515 ± 330	73 ± 10	199
[Aic^4,D-Ala^8]Dyn A(1-11)NH$_2$	-	39 ± 8	199
[Tic^4,D-Ala^8]Dyn A(1-11)NH$_2$	29.4 ± 10.3	91 ± 5	199
[α-MePhe,D-Ala^8]Dyn A(1-11)NH$_2$	36.5 ± 6.4	100	199
[NMePhe^4,D-Ala^8]Dyn A(1-11)NH$_2$	3.56 ± 0.64	99 ± 1	199
[D-Ala^8]Dyn A(1-11)NH$_2$	1.24 ± 0.43	100	199

[a] Maximum percent inhibition of adenylyl cyclase at a concentration of 10 μM relative to the inhibition produced by 100 nM Dyn A(1-13)NH$_2$ (100% inhibition).

2.7.2.4 Dyn A analogs modified at multiple positions in the N-terminal "message" sequence

Several linear analogs of Dyn A with modifications in multiple positions of the N-terminal tetrapeptide have been synthesized (see Table 2.10 for receptor binding affinities and Table 2.11 for efficacies).

Wan *et al*. reported the chimeric peptide Ac[Lys^2,Trp^{3,4},D-Ala^8]Dyn A-(1-11)NH$_2$ (initially called JVA901 and more recently called venorphin, see Figure 2.10) which combined the N-terminal acetylated derivative of the tetrapeptide Boc-Tyr-Lys-Trp-Trp-NH$_2$,[202] which displayed weak KOR antagonism in the GPI assay, with the "address" sequence (residues 5-11) of [D-Ala^8]Dyn A-(1-11)NH$_2$.[173] Venorphin displayed KOR selectivity comparable to [D-Ala^8]Dyn A-(1-11)NH$_2$, but had 100-fold lower KOR affinity (K_i = 19.8 nM, see Table 2.10). In the AC assay, venorphin was found to be a low efficacy partial agonist at KOR (efficacy = 28% of the maximum inhibition of c-AMP formation by Dyn A(1-13)NH$_2$) and was able to

completely reverse the agonistic effects of 1 nM Dyn A(1-13)NH$_2$ at KOR in a concentration-dependent manner.[173]

In another study, the N-terminal sequence of [D-Ala^8]Dyn A(1-11)NH$_2$ was replaced by [Arg^6]acetalin (Ac-Arg-Phe-Met-Trp-Met-Arg-NH$_2$), a potent MOR peptide antagonist to yield a peptide with a 65-fold increase in affinity for KOR (K_i = 6.6 nM) and retained high MOR affinity (K_i = 1.12 nM) which the authors labeled extacet.[203] Exploration of the SAR of extacet through a mixture based combinatorial library[204] led to the identification of Ac[Phe^{1,2,3},Arg^4,D-Ala^8]Dyn A-(1–11)NH$_2$ (called arodyn, Figure 2.9) that had KOR affinity (K_i = 10 nM) comparable to extacet and was 174-fold selective for KOR vs. MOR.[174]

Initial analogs of arodyn included an alanine scan and other analogs with substitutions in position 1. The Ala scan of arodyn suggested that while the basic residues in position 6 and 7 are important for maintaining the KOR binding affinity, the basic residues in position 4, 9 and 11 and residue in position 1 also contributed to the KOR affinity of arodyn.[205] Replacement of the Phe^1 residue in arodyn with Tyr caused a 7-fold decrease in KOR affinity, suggesting that the binding mode of arodyn at KOR differs from that of Dyn A. The Dmt^1 analog of arodyn displayed comparable KOR affinity for arodyn, and hence showed 7-fold higher KOR affinity as compared to the Tyr^1 analog of arodyn.[205] All of these arodyn analogs exhibited low efficacy at KOR in the AC assay ($\leq$ 32% inhibition of AC compared to the full agonist Dyn A(1-13)NH$_2$) except for the Tyr^1 analog of arodyn which was found to be an inverse agonist resulting in a dose dependent increase in c-AMP levels over forskolin controls.[205]

Additional analogs of arodyn involved introducing an NMe group on Phe^1 and other amino acid substitutions in position 3. The NMePhe^1 analog of arodyn exhibited the highest KOR affinity (K_i = 4.56 nM) and 6-fold higher selectivity for KOR vs. MOR as compared to

arodyn (see Table 2.10). The NMePhe[1] analog was also found to completely reverse the agonist effects of 10 nM Dyn A(1-13)NH$_2$ in a concentration-dependant manner.[205] The NMePhe[1] analog was unstable, however, and prone to deletion of the Ac-NMe-Phe moiety under acidic conditions.[206] By replacing the acetyl groups with a heteroatom containing group such as CH$_3$OCO produced an acid stable analog that had similar KOR affinity and retained KOR selectivity (see Table 2.10).[207] In the AC assay the CH$_3$OCO-NMe-Phe[1] analog was found to be a potent KOR antagonist (K_B = 8.5 nM).[207] The Tyr[3] and Cha[3] (Cha = cyclohexylalanine) analogs of CH$_3$OCO-NMe-Phe[1] arodyn retained similar affinity for KOR indicating that replacing Phe[3] with a Tyr[3] or with a non-aromatic residue like Cha[3] is tolerated by KOR (see Table 2.10).[207] These analogs also displayed 4-fold higher efficacy in the AC assay compared to arodyn and exhibited partial agonism at KOR (see Table 2.11).[207]

Table 2.10 Opioid receptor binding affinities of Dyn A analogs modified in multiple positions in the N-terminus.

Compound	K_i (nM± SEM)[a]			K_i ratio KOR/MOR/ DOR	Ref
	KOR	MOR	DOR		
JVA-901 (Venorphin)	19.8 ± 5.2	251 ± 22	5320 ± 1130	1/12.6/268	173
Arodyn	10.0 ± 3.0	1740 ± 130	5830 ± 1960	1/174/583	174
[Ala^1]arodyn	35.4 ± 3.0	3510 ± 340	>10,000	1/100/>280	205
[Ala^4]arodyn	54.2 ± 7.4	1390 ± 70	>10,000	1/30/>185	205
[Ala^6]arodyn	71.2 ± 10.8	5370 ± 220	>10,000	1/75/>140	205
[Ala^7]arodyn	75.5 ± 2.8	6860 ± 1820	>10,000	1/90/>130	205
[Ala^{11}]arodyn	44.1 ± 13.6	4500 ± 780	>10,000	1/100/>230	205
[Tyr^1]arodyn	71.6 ± 10.9	2010 ± 200	>10,000	1/30/>140	205
[Dmt^1]arodyn	13.4 ± 0.9	1610 ± 340	>10,000	1/120/>740	205
[NMePhe^1]arodyn	4.56 ± 0.45	5060 ± 790	>10,000	1/1100/>2170	205
[CH$_3$OCO-NMe-Phe^1]arodyn	4.93 ± 0.15	1750 ± 100	ND	1/355	207
[C$_6$H$_5$OCH$_2$CO-NMe-Phe^1]arodyn	7.34 ± 1.37	1450 ± 190	ND	1/198	207
[CH$_3$OCO-NMe-Phe^1, Tyr^3]arodyn	5.8 ± 1.27	1300 ± 340	ND	1/224	207
[CH$_3$OCO-NMe-Phe^1, Cha^3]arodyn	3.60 ± 0.21	818 ± 253	ND	1/227	207

[a] K_i values were obtained using CHO cell membranes stably expressing opioid receptors with [^{3}H] diprenorphine, [^{3}H] DAMGO and [^{3}H] DPDPE as the radiolabeled ligands for KOR, MOR and DOR, respectively
ND-not determined

Table 2.11 KOR efficacies of arodyn analogs in the AC assay

Compound	AC % inhibition at 10 μM[a]	Ref
Arodyn	12 ± 8	207
[NMePhe^1]	14 ± 1	207
[CH$_3$OCO-NMe-Phe^1]	26 ± 13	207
[C$_6$H$_5$OCH$_2$CO-NMe-Phe^1]	2 ± 21	207
[CH$_3$CO-Gly-NMe-Phe^1]	18 ± 17	207
[CH$_3$OCO-NMe-Phe^1, Tyr^3]	42 ± 10	207
[CH$_3$OCO-NMe-Phe^1, Cha^3]	45 ± 18	207

[a] relative to the full agonist Dyn A(1-13)NH$_2$ (100% inhibition, 0% control)

2.7.2.5 Dyn A analogs cyclized in the N-terminal "message" sequence

Several Dyn A analogs with a cyclic constraint in the N-terminal "message" sequence including cyclizations from the N-terminus to a side chain and side chain to side chain, have

been synthesized (see Table 2.12 for binding affinities and Table 2.13 for potencies and efficacies).

The N-terminal to side chain cyclic analog of venorphin, $cyclo^{N,5}$[Trp^3,Trp^4,Glu^5]Dyn A(1-11)NH$_2$ (called cyclodyn, Figure 2.10), displayed KOR affinity and selectivity comparable to venorphin, exhibited negligible efficacy (maximum inhibition of 8 ± 8% relative to Dyn A(1-13)NH$_2$) at KOR in the AC assay and was able to completely reverse the agonist activity of 10 nM Dyn A(1-13)NH$_2$ in a concentration-dependent manner.[176]

Table 2.12 Opioid receptor binding affinities of Dyn A analogs cyclized in the N-terminal "message" sequence

Compound	K_i (nM ± SEM)[a]			K_i ratio KOR/MOR/ DOR	Ref
	KOR	MOR	DOR		
Cyclodyn ($cyclo^{N,5}$[Trp^3,Trp^4,Glu^5] Dyn A(1-11)NH$_2$)	26.8 ± 2.8	331 ± 29	>8900	1/12>330	176
Analogs of *cyclo* [D-Asp^2, Dap^5]Dyn A(1-11)NH$_2$					
[D-Asp^2, Dap^5]	1.59 ± 0.44	0.22 ± 0.04	11.6 ± 2.0	7.2/1/53	208
cyclo[D-Asp^2, Dap^5]	0.46 ± 0.14	0.52 ± 0.06	5.10 ± 0.50	1/1.1/11	208
cyclo[Ala^3]	1.10 ± 0.20	2.52 ± 0.13	30.8 ± 3.7	1/2.3/28	208
cyclo[D-Ala^3]	0.21 ± 0.05	3.89 ± 0.52	139 ± 11	1/18/662	208
cyclo[Trp^3]	1.33 ± 0.26	2.09 ± 0.64	7070 ± 1920	1/1.6/5320	208
cyclo[D-Trp^3]	2.25 ± 0.37	7.27 ± 2.01	949 ± 49	1/3.2/422	208
cyclo[Pro^3]	9.03 ± 2.26	125 ± 11	>10000	1/14/>1000	208
RCM analogs of Dyn A(1-11)NH$_2$					
cyclo[Ala^2(-CH=CH-)Ala^5]Dyn A(1-11)NH$_2$, *cis*	87.2 ± 6.9	763 ± 35	7670 ± 1030	1/8.8/88	209
cyclo[Ala^2(-CH=CH-)Ala^5]Dyn A(1-11)NH$_2$, *trans*	9.46 ± 1.80	180 ± 10	1130 ± 98	1/19/119	209
cyclo[D-Ala^2(-CH=CH-)Ala^5]Dyn A(1-11)NH$_2$ *cis*	0.84 ± 0.10	2.33 ± 0.20	9.30 ± 1.00	1/2.8/11	209
cyclo[D-Ala^2(-CH=CH-)Ala^5]Dyn A(1-11)NH$_2$, *trans*	1.38 ± 0.31	2.33 ± 0.22	7.17 ± 0.55	1/1.7/5.2	209
Dyn A(1-11)NH$_2$	0.57 ± 0.01	1.85 ± 0.52	6.81 ± 1.01	1/3/11	210

[a] K_i values were obtained using CHO cell membranes stably expressing opioid receptors with [^{3}H]diprenorphine, [^{3}H]DAMGO and [^{3}H]DPDPE as the radiolabeled ligands for KOR, MOR and DOR, respectively.

Several analogs of *cyclo*[D-Asp^2,Dap^5]Dyn A(1-11)NH$_2$, a potent high affinity KOR agonist,[190] were synthesized in our laboratory to explore the structure- and conformation-activity relationships of the residues within the cyclic region of this peptide.[208] While the substitutions of

Gly^3 by Ala, D-Ala, Trp and D-Trp in the linear counterpart [D-Asp^2,Dap^5]Dyn A(1-11)NH$_2$ and in the lead cyclic peptide *cyclo*[D-Asp^2,Dap^5]Dyn A(1-11)NH$_2$ were well tolerated by KOR and MOR, these substitutions resulted in large decreases in DOR affinity.[208] These results suggested that there is limited space around residue 3 of Dyn A in the DOR binding pocket compared to that of KOR and MOR. In the case of the cyclic analogs, for smaller amino acids such as Ala the stereochemistry of residue 3 had a more pronounced effect on the affinity and selectivity as compared to the bulkier amino acids such as Trp (see Table 2.12). The effect of bulkier substituents on the potency of the cyclic peptides in the AC assay was pronounced (10-30 fold decrease in potency) compared to the lead cyclic peptide. All of the cyclic peptides with substitutions at position 3 except the Pro^3 analog were full agonists in AC assay. The Pro^3 substitution caused a decrease in efficacy and potency and resulted in a weak partial KOR agonist.[208]

Table 2.13 KOR agonist potencies and efficacies of Dyn A analogs cyclized in the "message" sequence.

Compound	IC$_{50}$ (nM ± SEM)	% max inhibition[a]	Ref
Analogs of *cyclo*[D-Asp^2, Dap^5]Dyn A(1-11)NH$_2$			
cyclo[D-Asp^2,Dap^5]	0.39 ± 0.07	100	208
cyclo[Ala^3]	0.65 ± 0.10	100	208
cyclo[D-Ala^3]	0.54 ± 0.15	100	208
cyclo[Trp^3]	4.19 ± 0.55	100	208
cyclo[D-Trp^3]	12.0 ± 2.8	100	208
cyclo[Pro^3]	153 ± 86	37 ± 7	208
RCM analogs of Dyn A(1-11)NH$_2$			
cyclo[Ala^2(-CH=CH-)Ala^5]Dyn A(1-11)NH$_2$, *cis*	190 ± 19	90 ± 2	209
cyclo[Ala^2(-CH=CH-)Ala^5]Dyn A(1-11)NH$_2$, *trans*	27 ± 1	104 ± 4	209
cyclo[D-Ala^2(-CH=CH-)Ala^5]Dyn A(1-11)NH2, *cis*	0.80 ± 0.34	111 ± 6	209
cyclo[D-Ala^2(-CH=CH-)Ala^5]Dyn A(1-11)NH2, *trans*	0.47 ± 0.11	107 ± 4	209

[a] Maximum percent inhibition of AC at a concentration of 10 μM, relative to the full agonist Dyn A(1-13)NH$_2$ (100% inhibition).

Fang *et al.* synthesized cyclic analogs of Dyn A(1-11)NH$_2$ utilizing ring closing metathesis (RCM) of the side chains of allylgylcine residues incorporated in positions 2 and 5.[209] Both *cis* and *trans* isomers of the peptide were obtained. The isomers with the L-amino acid in position 2 showed several fold lower opioid receptor affinities compared to Dyn A(1-11)NH$_2$. This indicated that, similar to the earlier reported linear Dyn A analogs,[211] an L-amino acid in position 2 of these cyclic peptides is not well tolerated by opioid receptors. However, MOR and DOR were less tolerant to an L-amino acid in position 2 compared to KOR, making these peptides more selective for KOR over MOR and DOR. Both the *cis* and *trans* isomers of *cyclo*[D-Ala^2(-CH=CH-)Ala^5]Dyn A(1-11)NH$_2$ exhibited high KOR affinities ($K_i = 0.84$ nM and 1.38 nM, respectively, see Table 2.12) that were comparable to that of Dyn A(1-11)NH$_2$. This suggested that, as was also observed in the case of earlier reported Dyn A analogs,[190] a D-amino acid in position 2 of these peptides is well tolerated by the opioid receptors. These peptides also exhibited high affinity for MOR and DOR, making them less selective for KOR over MOR and DOR than Dyn A(1-11)NH$_2$. All of the analogs exhibited concentration-dependent agonist activity in the AC assay and efficacies ($\geq 90\%$) comparable to Dyn A(1-13)NH$_2$. The *cis* and *trans* isomers of *cyclo*[D-Ala^2(-CH=CH-)Ala^5]Dyn A(1-11)NH$_2$ displayed the highest potencies (EC$_{50} = 0.80$ and 0.47 nM, respectively), while analogs with the L-configuration in position 2 were less potent than Dyn A(1-11)NH$_2$ (see Table 2.13).[209]

2.7.3 Analogs with modifications in the C-terminus

Both linear and cyclic modifications in the C-terminal sequence of Dyn A have been reported.

Based on the Ala scan of [Pro^3]Dyn A(1-11)NH$_2$ the Ile^8 and Pro^{10} residues made minor contributions to the activity of the parent peptide. Hence, two analogs with Arg substitution in

either position 8 or 10 were synthesized.[179] [Pro³,Arg⁸]Dyn A(1-11)NH₂ was one of the most potent analogs with a subnanomolar KOR affinity (K_i = 0.44 nM) and several thousand-fold KOR selectivity (see Table 2.14 for opioid receptor affinities and Table 2.15 for antagonist potencies) and both the Arg⁸ and Arg¹⁰ analogs were found to be KOR antagonists in the GTPγS assay. The parent Pro³ peptide and its Arg⁸ analog were also found to be KOR antagonists in GPI assay. At higher doses they were partial agonists in the [³⁵S]GTPγS assay (16-22% response compared to U50,488).[179]

Table 2.14 Opioid receptor binding affinities of [Pro³]Dyn A(1-11)NH₂ analogs substituted in the "address" sequence.

Compound	K_i (nM ± SEM)[a]				Ref
	KOR	MOR	DOR	KOR/MOR/DOR	
[Pro³,Arg⁸]Dyn A(1-11)NH₂	0.44 ± 0.10	2750 ± 770	6760 ± 620	1/6300/15000	179
[Pro³,Arg¹⁰]Dyn A(1-11)NH₂	1.20 ± 0.14	1660 ± 76	3230 ± 1460	1/1400/2700	179
[Pro³]Dyn A(1-11)NH₂	2.40 ± 0.22	5250 ± 730	8900 ± 2300	1/2200/3700	179

[a]K_i values were obtained using CHO cell membranes stably expressing opioid receptors using [³H]diprenorphine as radioligand.

Table 2.15 Antagonist potencies of [Pro³]Dyn A(1-11)NH₂ analogs substituted in the "address" sequence.

Compound	IC₅₀ (nM ± SEM)[a]	K_e (nM ± SEM)[b]	Ref
[Pro³, Arg⁸]Dyn A(1-11)NH₂	340 ± 60	280 ± 53	179
[Pro³, Arg¹⁰]Dyn A(1-11)NH₂	410 ± 200		179
[Pro³]Dyn A(1-11)NH₂	440 ± 60	494 ± 74	179

[a]Antagonist activity determined against 50 nM U50,488 in the GTPγS assay.
[b]Antagonist activity determined against [D-Ala³]Dyn A(1-11)NH₂ in the GPI assay.

In order to examine the role of the C-terminus residues in the efficacy of a Dyn A analog, Patkar *et al.* synthesized several analogs of the partial agonist [*N*-benzyl-Tyr¹]Dyn A(1-11)NH₂[212] (see Table 2.16 for receptor binding affinities). Analogs of [*N*-benzyl-Tyr¹]Dyn A(1-11)NH₂ (K_i (KOR) = 8.17 nM) containing substitutions in positions 7, 8 and/or 10 were

synthesized. In position 7, *N*Me-Arg was the substituent, while the substitutions in positions 8 and 10 were D-Ala and D-Pro, respectively. All of the peptides showed 2- to 4-fold higher KOR affinities and 2-fold higher KOR selectivities over MOR as compared to [*N*-benzyl-Tyr[1]]Dyn A(1-11)NH$_2$. The selectivity for KOR over DOR was dependent on the individual substitutions, with the results indicating that the D-Ala[8] substitution was important for maintaining high selectivity for KOR over DOR.[212] [*N*-benzyl-Tyr[1]]Dyn A(1-11)OH was also synthesized and interestingly, it displayed 2-fold lower KOR affinity and 3-fold lower KOR selectivity over DOR as compared to the C-terminal amide derivative.

Some of the early examples of Dyn A analogs cyclized in the "address" sequence include cyclic disulfide analogs[192-194] and cyclic lactam analogs.[189, 191] In the case of cyclic disulfide analogs, especially the cyclic (5,11) analogs with an L-amino acid in position 5 displayed high binding affinities for KOR (K_i = 0.5-3.1 nM) in guinea pig brain, but displayed low KOR vs. MOR selectivities. However, these analogs displayed relatively low potencies in the GPI assay (IC$_{50}$ > 90 nM), i.e. at peripheral opioid receptors. Those analogs with a D-amino acid in position 5 displayed low KOR affinities, while either configuration was tolerated for the residue in position 11.[194] Among the cyclic lactam analogs, the cyclic (5,8) (K_i (KOR) = 8-12 nM) and cyclic (6,9) Dyn A(1-13)NH$_2$ (K_i (KOR) = 1.5-2.6 nM) analogs showed relatively high KOR affinities, but low KOR vs. MOR selectivities. While the cyclic (6,9) analogs displayed high KOR potency (IC$_{50}$ = 6-46 nM), the cyclic (5,8) analogs displayed surprisingly low KOR potencies (IC$_{50}$ > 500 nM) in the GPI assay.[191]

Two cyclic analogs of [*N*-benzyl-Tyr[1]]Dyn A(1-11)NH$_2$ were also synthesized. The [5,8] cyclic analog [*N*$^\square$-benzylTyr[1],*cyclo*(D-Asp[5],Dap[8])]Dyn A(1-11)NH$_2$ (now called zyklophin, Figure 2.10)[210] and [*N*$^\square$-benzylTyr[1],*cyclo*(D-Asp[6],Dap[9])]Dyn A(1-11)NH$_2$[212] were also

synthesized. While zyklophin exhibited 4-fold lower KOR affinity (K_i = 30.3 nM) compared to [N-benzyl-Tyr^1]Dyn A(1-11)NH$_2$, it was 194-fold selective for KOR over MOR (see Table 2.16). It completely reversed the agonist activity of 10 nM Dyn A-(1-13)NH$_2$ in a concentration-dependent manner in the AC assay and in Schild analysis for antagonism exhibited a K_B value of 84 nM.[210] In comparison, the linear counterparts of both cyclic analogs displayed lower affinities and selectivities. In the AC assay, the linear analogs with modifications in positions 7, 8 and/or 10 displayed 70-90% efficacy,[212] whereas zyklophin and its linear counterpart displayed negligible efficacy.[210]

Table 2.16 Opioid binding affinities of C-terminal substituted analogs of [N-benzyl-Tyr^1]Dyn A(1-11)NH$_2$

Compound	K_i (nM± SEM)[a]				Ref
	KOR	MOR	DOR	KOR/MOR/DOR	
[N^α-benzyl-Tyr^1]Dyn A(1-11)NH$_2$	8.17 ± 2.16	84.9 ± 16.9	474 ± 47	1/10/58	212
[N^a-MeArg^7]	3.99 ± 1.09	49.9 ± 9.7	345 ± 31	1/13/86	212
[D-Ala^8]	4.64 ± 0.91	51.2 ± 3.0	372 ± 25	1/11/80	212
[D-Pro^{10}]	4.56 ± 0.42	45.1 ± 4.9	148 ± 5	1/10/32	212
[N^a-MeArg^7, D-Ala^8]	3.11 ± 0.64	44.8 ± 7.3	458 ± 130	1/14/147	212
[N^a-MeArg^7, D-Pro^{10}]	2.17 ± 0.22	36.5 ± 3.6	120 ± 24	1/17/55	212
[D-Ala^8, D-Pro^{10}]	3.10 ± 0.98	46.1 ± 8.6	337 ± 54	1/15/109	212
[N^a-MeArg^7, D-Ala^8, D-Pro^{10}]	4.40 ± 0.75	69.8 ± 0.7	665 ± 174	1/16/151	212
$cyclo$[D-Asp^5, Dap^8] (zyklophin)	30.3 ± 1.9	5880 ± 1420	>10,000	1/194/>330	210
[D-Asn^5, Dap(Ac)^8]	66.9 ± 5.9	1660 ± 440	>10,000	1/25/149	210

[a]K_i values were obtained using CHO cell membranes stably expressing opioid receptors with [^{3}H]diprenorphine, [^{3}H]DAMGO and [^{3}H]DPDPE as the radiolabeled ligands for KOR, MOR and DOR, respectively.

In vivo zyklophin was devoid of antinociceptive activity and antagonized the antinociceptive effects of the KOR selective agonist U50,488 in the mouse warm water tail withdrawal assay.[108] Zyklophin (3 mg/kg, s.c) was also found to be selective for KOR over MOR and DOR *in vivo*. Moreover, peripheral pretreatment with zyklophin (3 mg/kg, s.c.) antagonized the antinociceptive effects of centrally administered U50,488 (40 nmol, i.c.v), strongly

suggesting that zyklophin crossed the blood-brain barrier (BBB) to act on central KOR. Zyklophin (3 mg/kg, s.c.) antagonized the antinociceptive effects of U50,488 for at least 8 h, but for less than 12 h. This is in contrast to the prototypical selective KOR antagonists that exhibit their antagonist effects ranging from weeks to more than a month depending on the species.[56] Zyklophin (3 mg/kg s.c.) inhibited stress- induced reinstatement of cocaine seeking behavior in a conditioned place preference assay which was another strong indication that zyklophin was able to cross the BBB to exert its effect in the CNS. However, zyklophin did not inhibit cocaine induced reinstatement of cocaine seeking in a conditioned place preference assay, consistent with results for the other KOR antagonists.[108]

Fang *et al.* synthesized Dyn A(1-11)NH$_2$ cyclized by RCM involving allylglycine in positions 5 and 8 (see Table 2.17 for receptor binding affinities and Table 2.18 for efficacies). The *trans* isomer of *cyclo*[Ala^5(-CH=CH-)Ala^8]Dyn A(1-11)NH$_2$ exhibited 4-fold lower KOR affinity (K_i = 2.46 nM), while the *cis* isomer exhibited 20-fold lower affinity for KOR, compared to Dyn A(1-11)NH$_2$. They both also exhibited several fold lower affinities for MOR and DOR, making them more KOR selective than Dyn A(1-11)NH$_2$. While both isomers displayed ≥90% efficacies in the AC assay compared to Dyn A(1-13)NH$_2$, they showed several fold lower potencies as compared to Dyn A(1-11)NH$_2$ (see Table 2.18 for efficacies) . Consistent with their affinities the *trans* isomer (EC$_{50}$ = 8.3 nM) was 3-fold more potent than the *cis* isomer.[209]

Table 2.17 Opioid receptor binding affinities of *cyclo*(5,8) Dyn A(1-11) NH$_2$ analogs cyclized by RCM

Compound	K_i (nM± SEM)[a]				Ref
	KOR	MOR	DOR	KOR/MOR/DOR	
cyclo[Ala^5(-CH=CH-)Ala^8]Dyn A(1-11)NH$_2$, *cis*	10.9 ± 1.8	93.0 ± 6.0	1210 ± 90	1/8.5/111	209
cyclo[Ala^5(-CH=CH-)Ala^8]Dyn A(1-11)NH$_2$, *trans*	2.46 ± 0.57	36.0 ± 2.1	460 ± 51	1/15/187	209
Dyn A(1-11)NH$_2$	0.57 ± 0.01	1.85 ± 0.52	6.81 ± 1.01	1/3/11	210

[a]K_i values were obtained using CHO cell membranes stably expressing opioid receptors with [^{3}H]diprenorphine, [^{3}H]DAMGO and [^{3}H]DPDPE as the radiolabeled ligands for KOR, MOR and DOR, respectively.

Table 2.18 Agonist potencies and efficacies of *cyclo*(5,8) Dyn A(1-11) NH$_2$ analogs cyclized by RCM

Compound	IC$_{50}$ (nM ± SEM)	% max response[a]	Ref
cyclo[Ala^5(-CH=CH-)Ala^8]Dyn A-(1-11)NH$_2$, *cis*	23 ± 11	110 ± 10	209
cyclo[Ala^5(-CH=CH-)Ala^8]Dyn A-(1-11)NH$_2$, *trans*	8.3 ± 3.7	106 ± 6	209
Dyn A(1-11)NH$_2$	0.39 ± 0.02	100	209

[a] % response in AC assay relative to full agonist Dyn A(1-13)NH$_2$ (100%)

2.7.4 Non-peptide hybrid analogs of Dyn A

Ronsisvalle *et al.* synthesized a series of hybrid analogs in which the heterocyclic nucleus MPCB ((-)-*cis*-*N*-(2-phenyl-2-carbomethoxy)cyclopropylmethyl-*N*-normetazocine) was linked to the C-terminal residues Dyn A(6-8)[213] (Figure 2.13). The MPCB-GRRI and MPCB-RRI hybrid analogs displayed comparable KOR affinities (K_i = 54.3 ± 8.5 and 78.4 ± 6.4 nM, respectively) and 4- and 5-fold higher selectivities for KOR over MOR, respectively, compared to Dyn A(1-8) (K_i = 123.8 ± 6.2 nM), suggesting that the heterocyclic moiety mimicked the *N*-terminal fragment of dynorphin A.[214] Various analogs of these hybrid compounds involving non-peptide replacements of the C-terminal fragment were also described (Figure 2.11). Two analogs containing the dipeptide Gly-Leu, a 5-6 carbon atom diamine linker and a butylamidino substitution on the C-terminal nitrogen of the diamine linker exhibited high KOR affinities (K_i range = 5-7 nM) and KOR over MOR selectivities which were 6- to10-fold higher than those of

the parent hybrid analogs MPCB-RRI and MPCB-GRRI. The two butylamidino analogs showed potent antinociceptive effects (ED_{50} = 0.88-1.1 mg/kg, s.c.) in the mouse abdominal constriction assay comparable to U50,488 (ED_{50} = 0.76 mg/kg, s.c.) that was fully prevented by norBNI. [213]

MPCB-RRI	X = Arg-Arg-Ile	R = H
MPCB-GRRI	X = Gly-Arg-Arg-Ile	R = H

n = 5 or 6
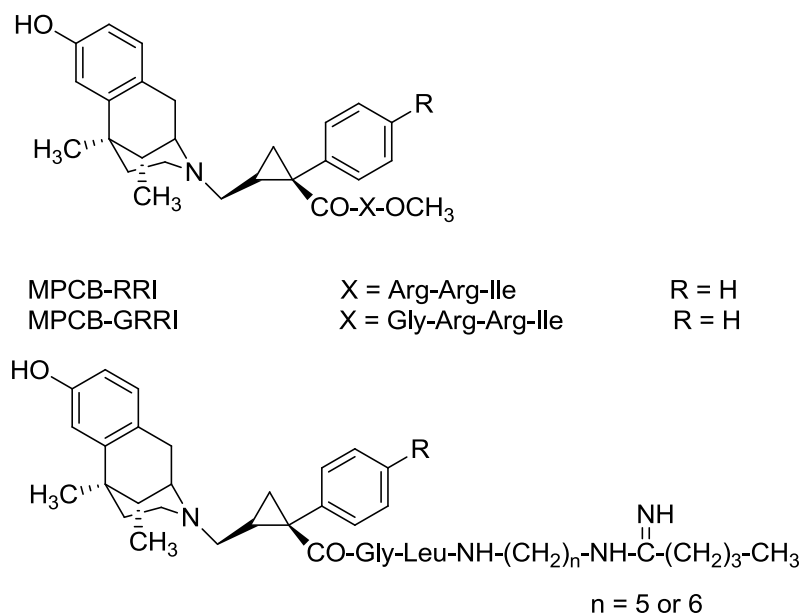
Figure 2.13 Non- peptide analogs of Dyn A

2.8   Conclusions

Dyn A, the endogenous peptidic ligand for KOR, has been studied extensively and various analogs including both agonists and antagonists have been identified. KOR ligands have several potential therapeutic applications in addition to pain. Some ligands with mixed activity involving KOR are used clinically, and some KOR ligands are in clinical development. While a number of non-peptidic KOR antagonists have recently been reported, peptide-based KOR antagonists are also being developed and are gaining importance because of their finite duration of action. Peptides can have several advantages as potential drugs including their high specificity and potency and low toxicity.[215] However, the delivery of peptides for therapeutic applications

still remains a challenge due in part to their metabolism by peptidases. In addition to several Dyn A analogs, other metabolically stable peptides including the cyclic tetrapeptides and all D-amino acids linear tetrapeptides are gaining importance for therapeutic applications.

2.9   References

1.   Aldrich, J. V.; Vigil-Cruz, S. C., Narcotic Analgesics. In *Burger's Medicinal Chemistry & Drug Discovery*, Abraham, D. J., Ed. John Wiley & Sons, New York, 2003; Vol.6, pp 329-481.

2.   Beckett, A. H.; Casy, A. F. Synthetic analgesics: stereochemical considerations. *J Pharm Pharmacol* **1954,** *6*, 986-1001.

3.   Pert, C. B.; Snyder, S. H. Opiate receptor: demonstration in nervous tissue. *Science* **1973,** *179*, 1011-1014.

4.   Simon, E. J.; Hiller, J. M.; Edelman, I. Stereospecific binding of the potent narcotic analgesic (3H) Etorphine to rat-brain homogenate. *Proc Natl Acad Sci U S A* **1973,** *70*, 1947-1949.

5.   Terenius, L. Stereospecific interaction between narcotic analgesics and a synaptic plasm a membrane fraction of rat cerebral cortex. *Acta Pharmacol Toxicol (Copenh)* **1973,** *32*, 317-320.

6.   Martin, W. R.; Eades, C. G.; Thompson, J. A.; Huppler, R. E.; Gilbert, P. E. The effects of morphine- and nalorphine- like drugs in the nondependent and morphine-dependent chronic spinal dog. *J Pharmacol Exp Ther* **1976,** *197*, 517-532.

7.   Gilbert, P. E.; Martin, W. R. The effects of morphine and nalorphine-like drugs in the nondependent, morphine-dependent and cyclazocine-dependent chronic spinal dog. *J Pharmacol Exp Ther* **1976,** *198*, 66-82.

8.   Hughes, J.; Smith, T. W.; Kosterlitz, H. W.; Fothergill, L. A.; Morgan, B. A.; Morris, H. R. Identification of two related pentapeptides from the brain with potent opiate agonist activity. *Nature* **1975,** *258*, 577-580.

9.   Cox, B. M.; Opheim, K. E.; Teschemacher, H.; Goldstein, A. A peptide-like substance from pituitary that acts like morphine. 2. Purification and properties. *Life Sci* **1975,** *16*, 1777-1782.

10.   Loh, H. H.; Tseng, L. F.; Wei, E.; Li, C. H. beta-endorphin is a potent analgesic agent. *Proc Natl Acad Sci U S A* **1976,** *73*, 2895-2898.

11.   Zadina, J. E.; Hackler, L.; Ge, L. J.; Kastin, A. J. A potent and selective endogenous agonist for the mu-opiate receptor. *Nature* **1997,** *386*, 499-502.

12.   Evans, C. J.; Keith, D. E., Jr.; Morrison, H.; Magendzo, K.; Edwards, R. H. Cloning of a delta opioid receptor by functional expression. *Science* **1992,** *258*, 1952-1955.

13.   Kieffer, B. L.; Befort, K.; Gaveriaux-Ruff, C.; Hirth, C. G. The delta-opioid receptor: isolation of a cDNA by expression cloning and pharmacological characterization. *Proc Natl Acad Sci U S A* **1992,** *89*, 12048-12052.

14.   Chen, Y.; Mestek, A.; Liu, J.; Hurley, J. A.; Yu, L. Molecular cloning and functional expression of a mu-opioid receptor from rat brain. *Mol Pharmacol* **1993,** *44*, 8-12.

15.   Yasuda, K.; Raynor, K.; Kong, H.; Breder, C. D.; Takeda, J.; Reisine, T.; Bell, G. I. Cloning and functional comparison of kappa and delta opioid receptors from mouse brain. *Proc Natl Acad Sci U S A* **1993,** *90*, 6736-6740.

16.   Lord, J. A.; Waterfield, A. A.; Hughes, J.; Kosterlitz, H. W. Endogenous opioid peptides: multiple agonists and receptors. *Nature* **1977,** *267*, 495-499.

17.   Quirion, R., Chicheportiche, R., Contreras, P. C., Johnson, K. M., Lodge, D., Tam, S.W., Woods, J. H., Zukin, S. R. . *Trends in Neurosciences* **1987,** *10*, 444-446.

18.   Mollereau, C.; Parmentier, M.; Mailleux, P.; Butour, J. L.; Moisand, C.; Chalon, P.; Caput, D.; Vassart, G.; Meunier, J. C. ORL1, a novel member of the opioid receptor family. Cloning, functional expression and localization. *FEBS Lett* **1994,** *341*, 33-38.

19.   Reinscheid, R. K.; Nothacker, H. P.; Bourson, A.; Ardati, A.; Henningsen, R. A.; Bunzow, J. R.; Grandy, D. K.; Langen, H.; Monsma, F. J., Jr.; Civelli, O. Orphanin FQ: a neuropeptide that activates an opioidlike G protein-coupled receptor. *Science* **1995,** *270*, 792-794.

20.   Meunier, J. C.; Mollereau, C.; Toll, L.; Suaudeau, C.; Moisand, C.; Alvinerie, P.; Butour, J. L.; Guillemot, J. C.; Ferrara, P.; Monsarrat, B.; et al. Isolation and structure of the endogenous agonist of opioid receptor-like ORL1 receptor. *Nature* **1995,** *377*, 532-535.

21.   Subramanian, G.; Paterlini, M. G.; Larson, D. L.; Portoghese, P. S.; Ferguson, D. M. Conformational analysis and automated receptor docking of selective arylacetamide-based kappa-opioid agonists. *J Med Chem* **1998,** *41*, 4777-4789.

22.   Chen, Y.; Mestek, A.; Liu, J.; Yu, L. Molecular cloning of a rat kappa opioid receptor reveals sequence similarities to the mu and delta opioid receptors. *Biochem J* **1993,** *295 (Pt 3)*, 625-628.

23.   Befort, K.; Mattei, M. G.; Roeckel, N.; Kieffer, B. Chromosomal localization of the delta opioid receptor gene to human 1p34.3-p36.1 and mouse 4D bands by in situ hybridization. *Genomics* **1994,** *20*, 143-145.

24.   Wang, J. B.; Johnson, P. S.; Persico, A. M.; Hawkins, A. L.; Griffin, C. A.; Uhl, G. R. Human mu opiate receptor. cDNA and genomic clones, pharmacologic characterization and chromosomal assignment. *FEBS Lett* **1994,** *338*, 217-222.

25.   Yasuda, K.; Espinosa, R., 3rd; Takeda, J.; Le Beau, M. M.; Bell, G. I. Localization of the kappa opioid receptor gene to human chromosome band 8q11.2. *Genomics* **1994,** *19*, 596-597.

26.   Knapp, R. J.; Malatynska, E.; Collins, N.; Fang, L.; Wang, J. Y.; Hruby, V. J.; Roeske, W. R.; Yamamura, H. I. Molecular biology and pharmacology of cloned opioid receptors. *FASEB J* **1995,** *9*, 516-525.

27.   Meunier, J.; Mouledous, L.; Topham, C. M. The nociceptin (ORL1) receptor: molecular cloning and functional architecture. *Peptides* **2000,** *21*, 893-900.

28.   Minami, M.; Onogi, T.; Nakagawa, T.; Katao, Y.; Aoki, Y.; Katsumata, S.; Satoh, M. DAMGO, a mu-opioid receptor selective ligand, distinguishes between mu-and kappa-opioid receptors at a different region from that for the distinction between mu- and delta-opioid receptors. *FEBS Lett* **1995,** *364*, 23-27.

29.   Xue, J. C.; Chen, C.; Zhu, J.; Kunapuli, S. P.; de Riel, J. K.; Yu, L.; Liu-Chen, L. Y. The third extracellular loop of the mu opioid receptor is important for agonist selectivity. *J Biol Chem* **1995,** *270*, 12977-12979.

30.   Seki, T.; Minami, M.; Nakagawa, T.; Ienaga, Y.; Morisada, A.; Satoh, M. DAMGO recognizes four residues in the third extracellular loop to discriminate between mu- and kappa-opioid receptors. *Eur J Pharmacol* **1998,** *350*, 301-310.

31.   Onogi, T.; Minami, M.; Katao, Y.; Nakagawa, T.; Aoki, Y.; Toya, T.; Katsumata, S.; Satoh, M. DAMGO, a mu-opioid receptor selective agonist, distinguishes between mu- and delta-opioid receptors around their first extracellular loops. *FEBS Lett* **1995,** *357*, 93-97.

32.   Fukuda, K.; Kato, S.; Mori, K. Location of regions of the opioid receptor involved in selective agonist binding. *J Biol Chem* **1995,** *270*, 6702-6709.

33.   Minami, M.; Nakagawa, T.; Seki, T.; Onogi, T.; Aoki, Y.; Katao, Y.; Katsumata, S.; Satoh, M. A single residue, Lys 108, of the delta-opioid receptor prevents the mu-opioid-selective ligand [D-Ala^2,*N*-MePhe^4,Gly-ol^5]enkephalin from binding to the delta-opioid receptor. *Mol Pharmacol* **1996,** *50*, 1413-1422.

34.   Wang, J. B.; Johnson, P. S.; Wu, J. M.; Wang, W. F.; Uhl, G. R. Human kappa opiate receptor second extracellular loop elevates dynorphin's affinity for human mu/kappa chimeras. *J Biol Chem* **1994,** *269*, 25966-25969.

35.   Xue, J. C.; Chen, C.; Zhu, J.; Kunapuli, S.; DeRiel, J. K.; Yu, L.; Liu-Chen, L. Y. Differential binding domains of peptide and non-peptide ligands in the cloned rat kappa opioid receptor. *J Biol Chem* **1994,** *269*, 30195-30199.

36.   Meng, F.; Hoversten, M. T.; Thompson, R. C.; Taylor, L.; Watson, S. J.; Akil, H. A chimeric study of the molecular basis of affinity and selectivity of the kappa and the delta opioid receptors. Potential role of extracellular domains. *J Biol Chem* **1995,** *270*, 12730-12736.

37.   Ferguson, D. M.; Kramer, S.; Metzger, T. G.; Law, P. Y.; Portoghese, P. S. Isosteric replacement of acidic with neutral residues in extracellular loop-2 of the kappa-opioid receptor does not affect dynorphin A(1-13) affinity and function. *J Med Chem* **2000,** *43*, 1251-1252.

38.   Kong, H.; Raynor, K.; Yano, H.; Takeda, J.; Bell, G. I.; Reisine, T. Agonists and antagonists bind to different domains of the cloned kappa opioid receptor. *Proc Natl Acad Sci U S A* **1994,** *91*, 8042-8046.

39.   Manglik, A.; Kruse, A. C.; Kobilka, T. S.; Thian, F. S.; Mathiesen, J. M.; Sunahara, R. K.; Pardo, L.; Weis, W. I.; Kobilka, B. K.; Granier, S. Crystal structure of the micro-opioid receptor bound to a morphinan antagonist. *Nature* **2012,** *485*, 321-326.

40.   Wu, H.; Wacker, D.; Mileni, M.; Katritch, V.; Han, G. W.; Vardy, E.; Liu, W.; Thompson, A. A.; Huang, X. P.; Carroll, F. I.; Mascarella, S. W.; Westkaemper, R. B.; Mosier, P. D.; Roth, B. L.; Cherezov, V.; Stevens, R. C. Structure of the human kappa-opioid receptor in complex with JDTic. *Nature* **2012,** *485*, 327-332.

41.   Granier, S.; Manglik, A.; Kruse, A. C.; Kobilka, T. S.; Thian, F. S.; Weis, W. I.; Kobilka, B. K. Structure of the delta-opioid receptor bound to naltrindole. *Nature* **2012,** *485*, 400-404.

42.   Thompson, A. A.; Liu, W.; Chun, E.; Katritch, V.; Wu, H.; Vardy, E.; Huang, X. P.; Trapella, C.; Guerrini, R.; Calo, G.; Roth, B. L.; Cherezov, V.; Stevens, R. C. Structure of the nociceptin/orphanin FQ receptor in complex with a peptide mimetic. *Nature* **2012,** *485*, 395-399.

43.   Filizola, M.; Devi, L. A. Structural biology: How opioid drugs bind to receptors. *Nature* **2012,** *485*, 314-317.

44.   Ballesteros JA, W. H. Integrated methods for the construction of three-dimensional models and computational probing of structure-function relations in G protein-coupled receptors. *Methods in Neurosciences* **1995,** *25*, 366-428.

45.   Gether, U. Uncovering molecular mechanisms involved in activation of G protein-coupled receptors. *Endocr Rev* **2000,** *21*, 90-113.

46.   Bourne, H. R.; Sanders, D. A.; McCormick, F. The GTPase superfamily: conserved structure and molecular mechanism. *Nature* **1991,** *349*, 117-127.

47.   Hamm, H. E. The many faces of G protein signaling. *J Biol Chem* **1998,** *273*, 669-672.

48.   Harrison, C.; Smart, D.; Lambert, D. G. Stimulatory effects of opioids. *Br J Anaesth* **1998,** *81*, 20-28.

49.   McFadzean, I. The ionic mechanisms underlying opioid actions. *Neuropeptides* **1988,** *11*, 173-180.

50.   Loh, H. H.; Smith, A. P. Molecular characterization of opioid receptors. *Annu Rev Pharmacol Toxicol* **1990,** *30*, 123-147.

51.   Lefkowitz, R. J.; Shenoy, S. K. Transduction of receptor signals by beta-arrestins. *Science* **2005,** *308*, 512-517.

52.   Bruchas, M. R.; Chavkin, C. Kinase cascades and ligand-directed signaling at the kappa opioid receptor. *Psychopharmacology (Berl)* **2010,** *210*, 137-147.

53.   Nagase, H.; Fujii, H. Opioids in preclinical and clinical trials. *Top Curr Chem* **2011,** *299*, 29-62.

54.   Inui, S. Nalfurafine hydrochloride for the treatment of pruritus. *Expert Opin Pharmacother* **2012,** *13*, 1507-1513.

55.   Kawai, K.; Hayakawa, J.; Miyamoto, T.; Imamura, Y.; Yamane, S.; Wakita, H.; Fujii, H.; Kawamura, K.; Matsuura, H.; Izumimoto, N.; Kobayashi, R.; Endo, T.; Nagase, H. Design, synthesis, and structure-activity relationship of novel opioid kappa-agonists. *Bioorg Med Chem* **2008,** *16*, 9188-9201.

56.   Aldrich, J. V.; McLaughlin, J. P. Peptide kappa opioid receptor ligands: potential for drug development. *AAPS J* **2009,** *11*, 312-322.

57.   Gutstein H. B. Akil, H., In *Goodman and Gilman's The Pharmacological Basis of Therapeutics*, 10th ed.; Hardman, J.; Limbird, L and Gilman, A., Eds. New York, 2001; pp 569-619.

58.   Dum, J. E.; Herz, A. In vivo receptor binding of the opiate partial agonist, buprenorphine, correlated with its agonistic and antagonistic actions. *Br J Pharmacol* **1981,** *74*, 627-633.

59.   Romero, D. V.; Partilla, J. S.; Zheng, Q. X.; Heyliger, S. O.; Ni, Q.; Rice, K. C.; Lai, J.; Rothman, R. B. Opioid peptide receptor studies. 12. Buprenorphine is a potent and selective mu/kappa antagonist in the [^{35}S]-GTP-gamma-S functional binding assay. *Synapse* **1999,** *34*, 83-94.

60.   Lutfy, K.; Eitan, S.; Bryant, C. D.; Yang, Y. C.; Saliminejad, N.; Walwyn, W.; Kieffer, B. L.; Takeshima, H.; Carroll, F. I.; Maidment, N. T.; Evans, C. J. Buprenorphine-induced antinociception is mediated by mu-opioid receptors and compromised by concomitant activation of opioid receptor-like receptors. *J Neurosci* **2003,** *23*, 10331-10337.

61.   Kraus, M. L.; Alford, D. P.; Kotz, M. M.; Levounis, P.; Mandell, T. W.; Meyer, M.; Salsitz, E. A.; Wetterau, N.; Wyatt, S. A. Statement of the american society of addiction medicine consensus panel on the use of buprenorphine in office-based treatment of opioid addiction. *J Addict Med* **2011,** *5*, 254-263.

62.   Ducharme, S.; Fraser, R.; Gill, K. Update on the clinical use of buprenorphine: in opioid-related disorders. *Can Fam Physician* **2012,** *58*, 37-41.

63.   Rothman, R. B.; Gorelick, D. A.; Heishman, S. J.; Eichmiller, P. R.; Hill, B. H.; Norbeck, J.; Liberto, J. G. An open-label study of a functional opioid kappa antagonist in the treatment of opioid dependence. *J Subst Abuse Treat* **2000,** *18*, 277-281.

64.   Gerra, G.; Fantoma, A.; Zaimovic, A. Naltrexone and buprenorphine combination in the treatment of opioid dependence. *J Psychopharmacol* **2006,** *20*, 806-814.

65.   Wee, S.; Vendruscolo, L. F.; Misra, K. K.; Schlosburg, J. E.; Koob, G. F. A combination of buprenorphine and naltrexone blocks compulsive cocaine intake in rodents without producing dependence. *Sci Transl Med* **2012,** *4*, 146ra110.

66.   Cordery, S. F.; Taverner, A.; Ridzwan, I. E.; Guy, R. H.; Delgado-Charro, M. B.; Husbands, S. M.; Bailey, C. P. A non-rewarding, non-aversive buprenorphine/naltrexone combination attenuates drug-primed reinstatement to cocaine and morphine in rats in a conditioned place preference paradigm. *Addict Biol* **2012**, *In press.*

67.   Diego, L.; Atayee, R.; Helmons, P.; von Gunten, C. F. Methylnaltrexone: a novel approach for the management of opioid-induced constipation in patients with advanced illness. *Expert Rev Gastroenterol Hepatol* **2009,** *3*, 473-485.

68.   Bream-Rouwenhorst, H. R.; Cantrell, M. A. Alvimopan for postoperative ileus. *Am J Health Syst Pharm* **2009,** *66*, 1267-1277.

69.   Wallace, M. S.; Moulin, D.; Clark, A. J.; Wasserman, R.; Neale, A.; Morley-Forster, P.; Castaigne, J. P.; Teichman, S. A Phase II, multicenter, randomized, double-blind, placebo-controlled crossover study of CJC-1008--a long-acting, parenteral opioid analgesic--in the treatment of postherpetic neuralgia. *J Opioid Manag* **2006,** *2*, 167-173.

70.   Aldrich, J. V.; McLaughlin, J. P. Opioid Peptides: Potential for Drug Development. *Drug Discov Today Technol* **2012,** *9*, e23-e31.

71.   Vanderah, T. W.; Largent-Milnes, T.; Lai, J.; Porreca, F.; Houghten, R. A.; Menzaghi, F.; Wisniewski, K.; Stalewski, J.; Sueiras-Diaz, J.; Galyean, R.; Schteingart, C.; Junien, J. L.; Trojnar, J.; Riviere, P. J. Novel D-amino acid tetrapeptides produce potent antinociception by selectively acting at peripheral kappa-opioid receptors. *Eur J Pharmacol* **2008,** *583*, 62-72.

72. Arendt-Nielsen, L.; Olesen, A. E.; Staahl, C.; Menzaghi, F.; Kell, S.; Wong, G. Y.; Drewes, A. M. Analgesic efficacy of peripheral kappa-opioid receptor agonist CR665 compared to oxycodone in a multi-modal, multi-tissue experimental human pain model: selective effect on visceral pain. *Anesthesiology* **2009,** *111*, 616-624.

73. (http://www.caratherapeutics.com/cr845-phase1-complete-release.shtml)

74. (http://www.caratherapeutics.com/post-operative-release12.shtml)

75. Smith, J. P.; Bingaman, S. I.; Mauger, D. T.; Harvey, H. H.; Demers, L. M.; Zagon, I. S. Opioid growth factor improves clinical benefit and survival in patients with advanced pancreatic cancer. *Open Access J Clin Trials* **2010,** *2010*, 37-48.

76. http://clinicaltrials.gov; NCT00905099; NCT00982696; NCT00706576.

77. Fink, D. J.; Wechuck, J.; Mata, M.; Glorioso, J. C.; Goss, J.; Krisky, D.; Wolfe, D. Gene therapy for pain: results of a phase I clinical trial. *Ann Neurol* **2011,** *70*, 207-212.

78. Mangel, A. W.; Hicks, G. A. Asimadoline and its potential for the treatment of diarrhea-predominant irritable bowel syndrome: a review. *Clin Exp Gastroenterol* **2012,** *5*, 1-10.

79. http://clinicaltrials.gov; NCT00626275.

80. http://clinicaltrials.gov; NCT01058642.

81. Sakami, S.; Kawai, K.; Maeda, M.; Aoki, T.; Fujii, H.; Ohno, H.; Ito, T.; Saitoh, A.; Nakao, K.; Izumimoto, N.; Matsuura, H.; Endo, T.; Ueno, S.; Natsume, K.; Nagase, H. Design and synthesis of a metabolically stable and potent antitussive agent, a novel delta opioid receptor antagonist, TRK-851. *Bioorg Med Chem* **2008,** *16*, 7956-7967.

82. Millan, M. J. Kappa-opioid receptors and analgesia. *Trends Pharmacol Sci* **1990,** *11*, 70-76.

83.   DeHaven-Hudkins, D. L.; Dolle, R. E. Peripherally restricted opioid agonists as novel analgesic agents. *Curr Pharm Des* **2004,** *10*, 743-757.

84.   Walker, J. S. Anti-inflammatory effects of opioids. *Adv Exp Med Biol* **2003,** *521*, 148-160.

85.   Bileviciute-Ljungar, I.; Saxne, T.; Spetea, M. Anti-inflammatory effects of contralateral administration of the kappa-opioid agonist U-50,488H in rats with unilaterally induced adjuvant arthritis. *Rheumatology (Oxford)* **2006,** *45*, 295-302.

86.   Glick, S. D.; Maisonneuve, I. M.; Raucci, J.; Archer, S. Kappa opioid inhibition of morphine and cocaine self-administration in rats. *Brain Res* **1995,** *681*, 147-152.

87.   Negus, S. S.; Mello, N. K. Effects of kappa opioid agonists on the discriminative stimulus effects of cocaine in rhesus monkeys. *Exp Clin Psychopharmacol* **1999,** *7*, 307-317.

88.   Mori, T.; Nomura, M.; Nagase, H.; Narita, M.; Suzuki, T. Effects of a newly synthesized kappa-opioid receptor agonist, TRK-820, on the discriminative stimulus and rewarding effects of cocaine in rats. *Psychopharmacology (Berl)* **2002,** *161*, 17-22.

89.   McLaughlin, J. P.; Land, B. B.; Li, S.; Pintar, J. E.; Chavkin, C. Prior activation of kappa opioid receptors by U50,488 mimics repeated forced swim stress to potentiate cocaine place preference conditioning. *Neuropsychopharmacology* **2006,** *31*, 787-794.

90.   Kuzmin, A. V.; Semenova, S.; Gerrits, M. A.; Zvartau, E. E.; Van Ree, J. M. Kappa-opioid receptor agonist U50,488H modulates cocaine and morphine self-administration in drug-naive rats and mice. *Eur J Pharmacol* **1997,** *321*, 265-271.

91.   Negus, S. S. Effects of the kappa opioid agonist U50,488 and the kappa opioid antagonist nor-binaltorphimine on choice between cocaine and food in rhesus monkeys. *Psychopharmacology (Berl)* **2004,** *176*, 204-213.

92.   Inan, S.; Cowan, A. Kappa opioid agonists suppress chloroquine-induced scratching in mice. *Eur J Pharmacol* **2004,** *502*, 233-237.

93.   Barber, A.; Gottschlich, R. Novel developments with selective, non-peptidic kappa-opioid receptor agonists. *Expert Opin Investig Drugs* **1997,** *6*, 1351-1368.

94.   Tortella, F. C.; DeCoster, M. A. Kappa opioids: therapeutic considerations in epilepsy and CNS injury. *Clin Neuropharmacol* **1994,** *17*, 403-416.

95.   Peterson, P. K.; Gekker, G.; Lokensgard, J. R.; Bidlack, J. M.; Chang, A. C.; Fang, X.; Portoghese, P. S. Kappa-opioid receptor agonist suppression of HIV-1 expression in CD4+ lymphocytes. *Biochem Pharmacol* **2001,** *61*, 1145-1151.

96.   Chao, C. C.; Gekker, G.; Hu, S.; Sheng, W. S.; Shark, K. B.; Bu, D. F.; Archer, S.; Bidlack, J. M.; Peterson, P. K. kappa opioid receptors in human microglia downregulate human immunodeficiency virus 1 expression. *Proc Natl Acad Sci U S A* **1996,** *93*, 8051-8056.

97.   Lokensgard, J. R.; Gekker, G.; Peterson, P. K. Kappa-opioid receptor agonist inhibition of HIV-1 envelope glycoprotein-mediated membrane fusion and CXCR4 expression on CD4(+) lymphocytes. *Biochem Pharmacol* **2002,** *63*, 1037-1041.

98.   McCarthy, L.; Wetzel, M.; Sliker, J. K.; Eisenstein, T. K.; Rogers, T. J. Opioids, opioid receptors, and the immune response. *Drug Alcohol Depend* **2001,** *62*, 111-123.

99.   Greenwald, M. K.; Stitzer, M. L.; Haberny, K. A. Human pharmacology of the opioid neuropeptide dynorphin A(1-13). *J Pharmacol Exp Ther* **1997,** *281*, 1154-1163.

100.   Specker, S.; Wananukul, W.; Hatsukami, D.; Nolin, K.; Hooke, L.; Kreek, M. J.; Pentel, P. R. Effects of dynorphin A(1-13) on opiate withdrawal in humans. *Psychopharmacology (Berl)* **1998,** *137*, 326-332.

101.   Takahashi M, S. T., Tokuyama S, Kaneto H. Further evidence for the implication of a kappa-opioid receptor mechanism in the production of psychological stress-induced analgesia. *Jpn J Pharmacol* **1990,** *53*, 487-494.

102.   McLaughlin, J. P.; Marton-Popovici, M.; Chavkin, C. Kappa opioid receptor antagonism and prodynorphin gene disruption block stress-induced behavioral responses. *J Neurosci* **2003,** *23*, 5674-5683.

103.   Spanagel, R.; Herz, A.; Shippenberg, T. S. Opposing tonically active endogenous opioid systems modulate the mesolimbic dopaminergic pathway. *Proc Natl Acad Sci U S A* **1992,** *89*, 2046-2050.

104.   Valdez, G. R.; Platt, D. M.; Rowlett, J. K.; Ruedi-Bettschen, D.; Spealman, R. D. Kappa agonist-induced reinstatement of cocaine seeking in squirrel monkeys: a role for opioid and stress-related mechanisms. *J Pharmacol Exp Ther* **2007,** *323*, 525-533.

105.   Redila, V. A.; Chavkin, C. Stress-induced reinstatement of cocaine seeking is mediated by the kappa opioid system. *Psychopharmacology (Berl)* **2008,** *200*, 59-70.

106.   Beardsley, P. M.; Howard, J. L.; Shelton, K. L.; Carroll, F. I. Differential effects of the novel kappa opioid receptor antagonist, JDTic, on reinstatement of cocaine-seeking induced by footshock stressors vs cocaine primes and its antidepressant-like effects in rats. *Psychopharmacology (Berl)* **2005,** *183*, 118-126.

107.   Carey, A. N.; Borozny, K.; Aldrich, J. V.; McLaughlin, J. P. Reinstatement of cocaine place-conditioning prevented by the peptide kappa-opioid receptor antagonist arodyn. *Eur J Pharmacol* **2007,** *569*, 84-89.

108.   Aldrich, J. V.; Patkar, K. A.; McLaughlin, J. P. Zyklophin, a systemically active selective kappa opioid receptor peptide antagonist with short duration of action. *Proc Natl Acad Sci U S A* **2009,** *106*, 18396-18401.

109.   Beardsley, P. M.; Pollard, G. T.; Howard, J. L.; Carroll, F. I. Effectiveness of analogs of the kappa opioid receptor antagonist (3R)-7-hydroxy-N-((1S)-1-{[(3R,4R)-4-(3-hydroxyphenyl)-3,4-dimethyl-1-piperidinyl]methyl}-2-methylpropyl)-1,2,3,4-tetrahydro-3isoquinolinecarboxamide (JDTic) to reduce U50,488-induced diuresis and stress-induced cocaine reinstatement in rats. *Psychopharmacology (Berl)* **2010,** *210*, 189-198.

110.   Pliakas, A. M.; Carlson, R. R.; Neve, R. L.; Konradi, C.; Nestler, E. J.; Carlezon, W. A., Jr. Altered responsiveness to cocaine and increased immobility in the forced swim test associated with elevated cAMP response element-binding protein expression in nucleus accumbens. *J Neurosci* **2001,** *21*, 7397-7403.

111.   Mague, S. D.; Pliakas, A. M.; Todtenkopf, M. S.; Tomasiewicz, H. C.; Zhang, Y.; Stevens, W. C., Jr.; Jones, R. M.; Portoghese, P. S.; Carlezon, W. A., Jr. Antidepressant-like effects of kappa-opioid receptor antagonists in the forced swim test in rats. *J Pharmacol Exp Ther* **2003,** *305*, 323-330.

112.   Newton, S. S.; Thome, J.; Wallace, T. L.; Shirayama, Y.; Schlesinger, L.; Sakai, N.; Chen, J.; Neve, R.; Nestler, E. J.; Duman, R. S. Inhibition of cAMP response element-binding protein or dynorphin in the nucleus accumbens produces an antidepressant-like effect. *J Neurosci* **2002,** *22*, 10883-10890.

113.   Shirayama, Y.; Ishida, H.; Iwata, M.; Hazama, G. I.; Kawahara, R.; Duman, R. S. Stress increases dynorphin immunoreactivity in limbic brain regions and dynorphin antagonism produces antidepressant-like effects. *J Neurochem* **2004,** *90*, 1258-1268.

114. Carr, G. V.; Bangasser, D. A.; Bethea, T.; Young, M.; Valentino, R. J.; Lucki, I. Antidepressant-like effects of kappa-opioid receptor antagonists in Wistar Kyoto rats. *Neuropsychopharmacology* **2010,** *35*, 752-763.

115. Casal-Dominguez, J. J.; Clark, M.; Traynor, J. R.; Husbands, S. M.; Bailey, S. J. In vivo and in vitro characterization of naltrindole-derived ligands at the kappa-opioid receptor. *J Psychopharmacol* **2013,** *27*, 192-202.

116. Knoll, A. T.; Meloni, E. G.; Thomas, J. B.; Carroll, F. I.; Carlezon, W. A., Jr. Anxiolytic-like effects of kappa-opioid receptor antagonists in models of unlearned and learned fear in rats. *J Pharmacol Exp Ther* **2007,** *323*, 838-845.

117. Rogala, B.; Li, Y.; Li, S.; Chen, X.; Kirouac, G. J. Effects of a post-shock injection of the kappa opioid receptor antagonist norbinaltorphimine (norBNI) on fear and anxiety in rats. *PLoS One* **2012,** *7*, e49669.

118. Peters, M. F.; Zacco, A.; Gordon, J.; Maciag, C. M.; Litwin, L. C.; Thompson, C.; Schroeder, P.; Sygowski, L. A.; Piser, T. M.; Brugel, T. A. Identification of short-acting kappa-opioid receptor antagonists with anxiolytic-like activity. *Eur J Pharmacol* **2011,** *661*, 27-34.

119. Prisinzano, T. E.; Tidgewell, K.; Harding, W. W. Kappa opioids as potential treatments for stimulant dependence. *AAPS J* **2005,** *7*, E592-599.

120. Szmuszkovicz, J.; Von Voigtlander, P. F. Benzeneacetamide amines: structurally novel non-m mu opioids. *J Med Chem* **1982,** *25*, 1125-1126.

121. Lahti, R. A.; Mickelson, M. M.; McCall, J. M.; Von Voigtlander, P. F. [^{3}H]U-69593 a highly selective ligand for the opioid kappa receptor. *Eur J Pharmacol* **1985,** *109*, 281-284.

122. Halfpenny, P. R.; Horwell, D. C.; Hughes, J.; Hunter, J. C.; Rees, D. C. Highly selective kappa-opioid analgesics. 3. Synthesis and structure-activity relationships of novel N-[2-(1-

pyrrolidinyl)-4- or -5-substituted-cyclohexyl]arylacetamide derivatives. *J Med Chem* **1990,** *33*, 286-291.

123.   Hunter, J. C.; Leighton, G. E.; Meecham, K. G.; Boyle, S. J.; Horwell, D. C.; Rees, D. C.; Hughes, J. CI-977, a novel and selective agonist for the kappa-opioid receptor. *Br J Pharmacol* **1990,** *101*, 183-189.

124.   Frankowski, K. J.; Ghosh, P.; Setola, V.; Tran, T. B.; Roth, B. L.; Aube, J. N-Alkyl-octahydroisoquinolin-1-one-8-carboxamides: a Novel Class of Selective, Nonbasic, Nitrogen-Containing kappa-Opioid Receptor Ligands. *ACS Med Chem Lett* **2010,** *1*, 189-193.

125.   Tsukahara-Ohsumi, Y.; Tsuji, F.; Niwa, M.; Nakamura, M.; Mizutani, K.; Inagaki, N.; Sasano, M.; Aono, H. SA14867, a newly synthesized kappa-opioid receptor agonist with antinociceptive and antipruritic effects. *Eur J Pharmacol* **2010,** *647*, 62-67.

126.   Fujii, H.; Ida, Y.; Hanamura, S.; Osa, Y.; Nemoto, T.; Nakajima, M.; Hasebe, K.; Nakao, K.; Mochizuki, H.; Nagase, H. Synthesis of pyrrolomorphinan derivatives as kappa opioid agonists. *Bioorg Med Chem Lett* **2010,** *20*, 5035-5038.

127.   Geiger, C.; Zelenka, C.; Lehmkuhl, K.; Schepmann, D.; Englberger, W.; Wunsch, B. Conformationally constrained kappa receptor agonists: stereoselective synthesis and pharmacological evaluation of 6,8-diazabicyclo[3.2.2]nonane derivatives. *J Med Chem* **2010,** *53*, 4212-4222.

128.   Barber, A.; Bartoszyk, G. D.; Bender, H. M.; Gottschlich, R.; Greiner, H. E.; Harting, J.; Mauler, F.; Minck, K. O.; Murray, R. D.; Simon, M.; et al. A pharmacological profile of the novel, peripherally-selective kappa-opioid receptor agonist, EMD 61753. *Br J Pharmacol* **1994,** *113*, 1317-1327.

129.   Roth, B. L.; Baner, K.; Westkaemper, R.; Siebert, D.; Rice, K. C.; Steinberg, S.; Ernsberger, P.; Rothman, R. B. Salvinorin A: a potent naturally occurring nonnitrogenous kappa opioid selective agonist. *Proc Natl Acad Sci U S A* **2002,** *99*, 11934-11939.

130.   Cunningham, C. W.; Rothman, R. B.; Prisinzano, T. E. Neuropharmacology of the naturally occurring kappa-opioid hallucinogen salvinorin A. *Pharmacol Rev* **2011,** *63*, 316-347.

131.   Lovell, K. M.; Prevatt-Smith, K. M.; Lozama, A.; Prisinzano, T. E. Synthesis of neoclerodane diterpenes and their pharmacological effects. *Top Curr Chem* **2011,** *299*, 141-185.

132.   Erez, M.; Takemori, A. E.; Portoghese, P. S. Narcotic antagonistic potency of bivalent ligands which contain beta-naltrexamine. Evidence for bridging between proximal recognition sites. *J Med Chem* **1982,** *25*, 847-849.

133.   Portoghese, A. S.; Lipkowski, A. W.; Takemori, A. E. Bimorphinans as highly selective, potent kappa opioid receptor antagonists. *J Med Chem* **1987,** *30*, 238-239.

134.   Portoghese, P. S.; Lipkowski, A. W.; Takemori, A. E. Binaltorphimine and nor-binaltorphimine, potent and selective kappa-opioid receptor antagonists. *Life Sci* **1987,** *40*, 1287-1292.

135.   Jones, R. M.; Hjorth, S. A.; Schwartz, T. W.; Portoghese, P. S. Mutational evidence for a common kappa antagonist binding pocket in the wild-type kappa and mutant mu[K303E] opioid receptors. *J Med Chem* **1998,** *41*, 4911-4914.

136.   Sharma, S. K.; Jones, R. M.; Metzger, T. G.; Ferguson, D. M.; Portoghese, P. S. Transformation of a kappa-opioid receptor antagonist to a kappa-agonist by transfer of a guanidinium group from the 5'- to 6'-position of naltrindole. *J Med Chem* **2001,** *44*, 2073-2079.

137.   Zimmerman, D. M.; Leander, J. D.; Cantrell, B. E.; Reel, J. K.; Snoddy, J.; Mendelsohn, L. G.; Johnson, B. G.; Mitch, C. H. Structure-activity relationships of trans-3,4-dimethyl-4-(3-

hydroxyphenyl)piperidine antagonists for mu- and kappa-opioid receptors. *J Med Chem* **1993,** *36*, 2833-2841.

138.   Thomas, J. B.; Fall, M. J.; Cooper, J. B.; Rothman, R. B.; Mascarella, S. W.; Xu, H.; Partilla, J. S.; Dersch, C. M.; McCullough, K. B.; Cantrell, B. E.; Zimmerman, D. M.; Carroll, F. I. Identification of an opioid kappa receptor subtype-selective N-substituent for (+)-(3R,4R)-dimethyl-4-(3-hydroxyphenyl)piperidine. *J Med Chem* **1998,** *41*, 5188-5197.

139.   Thomas, J. B.; Atkinson, R. N.; Rothman, R. B.; Fix, S. E.; Mascarella, S. W.; Vinson, N. A.; Xu, H.; Dersch, C. M.; Lu, Y.; Cantrell, B. E.; Zimmerman, D. M.; Carroll, F. I. Identification of the first trans-(3R,4R)- dimethyl-4-(3-hydroxyphenyl)piperidine derivative to possess highly potent and selective opioid kappa receptor antagonist activity. *J Med Chem* **2001,** *44*, 2687-2690.

140.   Metcalf, M. D.; Coop, A. Kappa opioid antagonists: past successes and future prospects. *AAPS J* **2005,** *7*, E704-722.

141.   Horan, P.; Taylor, J.; Yamamura, H. I.; Porreca, F. Extremely long-lasting antagonistic actions of nor-binaltorphimine (nor-BNI) in the mouse tail-flick test. *J Pharmacol Exp Ther* **1992,** *260*, 1237-1243.

142.   Takemori, A. E.; Ho, B. Y.; Naeseth, J. S.; Portoghese, P. S. Nor-binaltorphimine, a highly selective kappa-opioid antagonist in analgesic and receptor binding assays. *J Pharmacol Exp Ther* **1988,** *246*, 255-258.

143.   Bruchas, M. R.; Yang, T.; Schreiber, S.; Defino, M.; Kwan, S. C.; Li, S.; Chavkin, C. Long-acting kappa opioid antagonists disrupt receptor signaling and produce noncompetitive effects by activating c-Jun N-terminal kinase. *J Biol Chem* **2007,** *282*, 29803-29811.

144.   Melief, E. J.; Miyatake, M.; Bruchas, M. R.; Chavkin, C. Ligand-directed c-Jun N-terminal kinase activation disrupts opioid receptor signaling. *Proc Natl Acad Sci U S A* **2010,** *107*, 11608-11613.

145.   Melief, E. J.; Miyatake, M.; Carroll, F. I.; Beguin, C.; Carlezon, W. A., Jr.; Cohen, B. M.; Grimwood, S.; Mitch, C. H.; Rorick-Kehn, L.; Chavkin, C. Duration of action of a broad range of selective kappa-opioid receptor antagonists is positively correlated with c-Jun N-terminal kinase-1 activation. *Mol Pharmacol* **2011,** *80*, 920-929.

146.   Runyon, S. P.; Brieaddy, L. E.; Mascarella, S. W.; Thomas, J. B.; Navarro, H. A.; Howard, J. L.; Pollard, G. T.; Carroll, F. I. Analogues of (3R)-7-hydroxy-N-[(1S)-1-{[(3R,4R)-4-(3-hydroxyphenyl)-3,4-dimethyl-1-pipe ridinyl]methyl}-2-methylpropyl)-1,2,3,4-tetrahydro-3-isoquinolinecarboxami de (JDTic). Synthesis and in vitro and in vivo opioid receptor antagonist activity. *J Med Chem* **2010,** *53*, 5290-5301.

147.   Carroll, I.; Thomas, J. B.; Dykstra, L. A.; Granger, A. L.; Allen, R. M.; Howard, J. L.; Pollard, G. T.; Aceto, M. D.; Harris, L. S. Pharmacological properties of JDTic: a novel kappa-opioid receptor antagonist. *Eur J Pharmacol* **2004,** *501*, 111-119.

148.   Verhoest, P. R.; Basak, A. S.; Parikh, V.; Hayward, M.; Kauffman, G. W.; Paradis, V.; McHardy, S. F.; McLean, S.; Grimwood, S.; Schmidt, A. W.; Vanase-Frawley, M.; Freeman, J.; Van Deusen, J.; Cox, L.; Wong, D.; Liras, S. Design and discovery of a selective small molecule kappa opioid antagonist (2-methyl-N-((2'-(pyrrolidin-1-ylsulfonyl)biphenyl-4-yl)methyl)propan-1-amine, PF-4455242). *J Med Chem* **2011,** *54*, 5868-5877.

149.   Grimwood, S.; Lu, Y.; Schmidt, A. W.; Vanase-Frawley, M. A.; Sawant-Basak, A.; Miller, E.; McLean, S.; Freeman, J.; Wong, S.; McLaughlin, J. P.; Verhoest, P. R. Pharmacological   characterization   of   2-methyl-N-((2'-(pyrrolidin-1-ylsulfonyl)biphenyl-4-

yl)methyl)propan-1-amine (PF-04455242), a high-affinity antagonist selective for kappa-opioid receptors. *J Pharmacol Exp Ther* **2011,** *339*, 555-566.

150.   Mitch, C. H.; Quimby, S. J.; Diaz, N.; Pedregal, C.; de la Torre, M. G.; Jimenez, A.; Shi, Q.; Canada, E. J.; Kahl, S. D.; Statnick, M. A.; McKinzie, D. L.; Benesh, D. R.; Rash, K. S.; Barth, V. N. Discovery of aminobenzyloxyarylamides as kappa opioid receptor selective antagonists: application to preclinical development of a kappa opioid receptor antagonist receptor occupancy tracer. *J Med Chem* **2011,** *54*, 8000-8012.

151.   Talbot, P. S.; Narendran, R.; Butelman, E. R.; Huang, Y.; Ngo, K.; Slifstein, M.; Martinez, D.; Laruelle, M.; Hwang, D. R. 11C-GR103545, a radiotracer for imaging kappa-opioid receptors in vivo with PET: synthesis and evaluation in baboons. *J Nucl Med* **2005,** *46*, 484-494.

152.   Choi, H.; Murray, T. F.; DeLander, G. E.; Schmidt, W. K.; Aldrich, J. V. Synthesis and opioid activity of [D-Pro[10]]dynorphin A-(1-11) analogues with N-terminal alkyl substitution. *J Med Chem* **1997,** *40*, 2733-2739.

153.   Lung, F. D.; Meyer, J. P.; Lou, B. S.; Xiang, L.; Li, G.; Davis, P.; DeLeon, I. A.; Yamamura, H. I.; Porreca, F.; Hruby, V. J. Effects of modifications of residues in position 3 of dynorphin A(1-11)-NH$_2$ on kappa receptor selectivity and potency. *J Med Chem* **1996,** *39*, 2456-2460.

154.   Chavkin, C.; Goldstein, A. Specific receptor for the opioid peptide dynorphin: structure--activity relationships. *Proc Natl Acad Sci U S A* **1981,** *78*, 6543-6547.

155.   Al-Fayoumi, S. I.; Brugos, B.; Arya, V.; Mulder, E.; Eppler, B.; Mauderli, A. P.; Hochhaus, G. Identification of stabilized dynorphin derivatives for suppressing tolerance in morphine-dependent rats. *Pharm Res* **2004,** *21*, 1450-1456.

156.   Brugos, B.; Arya, V.; Hochhaus, G. Stabilized dynorphin derivatives for modulating antinociceptive activity in morphine tolerant rats: effect of different routes of administration. *AAPS J* **2004,** *6*, e36.

157.   Yoshino, H.; Nakazawa, T.; Arakawa, Y.; Kaneko, T.; Tsuchiya, Y.; Matsunaga, M.; Araki, S.; Ikeda, M.; Yamatsu, K.; Tachibana, S. Synthesis and structure-activity relationships of dynorphin A-(1-8) amide analogues. *J Med Chem* **1990,** *33*, 206-212.

158.   Terasaki, T.; Deguchi, Y.; Sato, H.; Hirai, K.; Tsuji, A. In vivo transport of a dynorphin-like analgesic peptide, E-2078, through the blood-brain barrier: an application of brain microdialysis. *Pharm Res* **1991,** *8*, 815-820.

159.   Nakazawa, T.; Furuya, Y.; Kaneko, T.; Yamatsu, K. Spinal kappa receptor-mediated analgesia of E-2078, a systemically active dynorphin analog, in mice. *J Pharmacol Exp Ther* **1991,** *256*, 76-81.

160.   Nakazawa, T.; Kaneko, T.; Yoshino, H.; Tachibana, S.; Goto, M.; Taki, T.; Yamatsu, K. Physical dependence liability of dynorphin A analogs in rodents. *Eur J Pharmacol* **1991,** *201*, 185-189.

161.   Salas, S. P.; Roblero, J. S.; Lopez, L. F.; Tachibana, S.; Huidobro-Toro, J. P. [*N*-methyl-Tyr[1],*N*-methyl-Arg[7]-D-Leu[8]]-dynorphin-A-(1-8)ethylamide, a stable dynorphin analog, produces diuresis by kappa-opiate receptor activation in the rat. *J Pharmacol Exp Ther* **1992,** *262*, 979-986.

162.   Butelman, E. R.; Ball, J. W.; Kreek, M. J. Peripheral selectivity and apparent efficacy of dynorphins: comparison to non-peptidic kappa-opioid agonists in rhesus monkeys. *Psychoneuroendocrinology* **2004,** *29*, 307-326.

163.   Yu, J.; Butelman, E. R.; Woods, J. H.; Chait, B. T.; Kreek, M. J. Dynorphin A (1-8) analog, E-2078, crosses the blood-brain barrier in rhesus monkeys. *J Pharmacol Exp Ther* **1997,** *282*, 633-638.

164.   Butelman, E. R.; Vivian, J. A.; Yu, J.; Kreek, M. J.; Woods, J. H. Systemic effects of E-2078, a stabilized dynorphin A(1-8) analog, in rhesus monkeys. *Psychopharmacology (Berl)* **1999,** *143*, 190-196.

165.   Butelman, E. R.; Harris, T. J.; Kreek, M. J. Effects of E-2078, a stable dynorphin A(1-8) analog, on sedation and serum prolactin levels in rhesus monkeys. *Psychopharmacology (Berl)* **1999,** *147*, 73-80.

166.   Fujimoto, K.; Momose, T. [Analgesic efficacy of E2078 (dynorphin analog) in patients following abdominal surgery]. *Masui* **1995,** *44*, 1233-1237.

167.   Ohnishi, A.; Mihara, M.; Yasuda, S.; Tomono, Y.; Hasegawa, J.; Tanaka, T. Aquaretic effect of the stable dynorphin-A analog E2078 in the human. *J Pharmacol Exp Ther* **1994,** *270*, 342-347.

168.   Terasaki, T.; Hirai, K.; Sato, H.; Kang, Y. S.; Tsuji, A. Absorptive-mediated endocytosis of a dynorphin-like analgesic peptide, E-2078 into the blood-brain barrier. *J Pharmacol Exp Ther* **1989,** *251*, 351-357.

169.   Hiramatsu, M.; Inoue, K.; Ambo, A.; Sasaki, Y.; Kameyama, T. Long-lasting antinociceptive effects of a novel dynorphin analogue, Tyr-D-Ala-Phe-Leu-Arg psi (CH(2)NH) Arg-NH(2), in mice. *Br J Pharmacol* **2001,** *132*, 1948-1956.

170.   Dooley, C. T.; Ny, P.; Bidlack, J. M.; Houghten, R. A. Selective ligands for the mu, delta, and kappa opioid receptors identified from a single mixture based tetrapeptide positional scanning combinatorial library. *J Biol Chem* **1998,** *273*, 18848-18856.

171.   Vanderah, T. W.; Schteingart, C. D.; Trojnar, J.; Junien, J. L.; Lai, J.; Riviere, P. J. FE200041 (D-Phe-D-Phe-D-Nle-D-Arg-NH$_2$): A peripheral efficacious kappa opioid agonist with unprecedented selectivity. *J Pharmacol Exp Ther* **2004,** *310*, 326-333.

172.   Binder, W.; Machelska, H.; Mousa, S.; Schmitt, T.; Riviere, P. J.; Junien, J. L.; Stein, C.; Schafer, M. Analgesic and antiinflammatory effects of two novel kappa-opioid peptides. *Anesthesiology* **2001,** *94*, 1034-1044.

173.   Wan, Q.; Murray, T. F.; Aldrich, J. V. A novel acetylated analogue of dynorphin A-(1-11) amide as a kappa-opioid receptor antagonist. *J Med Chem* **1999,** *42*, 3011-3013.

174.   Bennett, M. A.; Murray, T. F.; Aldrich, J. V. Identification of arodyn, a novel acetylated dynorphin A-(1-11) analogue, as a kappa opioid receptor antagonist. *J Med Chem* **2002,** *45*, 5617-5619.

175.   Lu, Y.; Nguyen, T. M.; Weltrowska, G.; Berezowska, I.; Lemieux, C.; Chung, N. N.; Schiller, P. W. [2',6'-Dimethyltyrosine]dynorphin A(1-11)-NH$_2$ analogues lacking an N-terminal amino group: potent and selective kappa opioid antagonists. *J Med Chem* **2001,** *44*, 3048-3053.

176.   Vig, B. S.; Murray, T. F.; Aldrich, J. V. A novel N-terminal cyclic dynorphin A analogue cyclo(N,5)[Trp(3),Trp(4),Glu(5)] dynorphin A-(1-11)NH(2) that lacks the basic N-terminus. *J Med Chem* **2003,** *46*, 1279-1282.

177.   Schlechtingen, G.; Zhang, L.; Maycock, A.; DeHaven, R. N.; Daubert, J. D.; Cassel, J.; Chung, N. N.; Schiller, P. W.; Goodman, M. [Pro(3)]Dyn A(1-11)-NH(2): a dynorphin analogue with high selectivity for the kappa opioid receptor. *J Med Chem* **2000,** *43*, 2698-2702.

178.   Schlechtingen, G.; DeHaven, R. N.; Daubert, J. D.; Cassel, J.; Goodman, M. Structure-activity relationships of dynorphin analogs substituted in positions 2 and 3. *Biopolymers* **2003,** *71*, 71-76.

179.   Schlechtingen, G.; DeHaven, R. N.; Daubert, J. D.; Cassel, J. A.; Chung, N. N.; Schiller, P. W.; Taulane, J. P.; Goodman, M. Structure-activity relationships of dynorphin a analogues modified in the address sequence. *J Med Chem* **2003,** *46*, 2104-2109.

180.   Gairin, J. E.; Mazarguil, H.; Alvinerie, P.; Botanch, C.; Cros, J.; Meunier, J. C. N,N-diallyl-tyrosyl substitution confers antagonist properties on the kappa-selective opioid peptide [D-Pro[10]]dynorphin A(1-11). *Br J Pharmacol* **1988,** *95*, 1023-1030.

181.   Choi, H.; Murray, T. F.; DeLander, G. E.; Caldwell, V.; Aldrich, J. V. N-terminal alkylated derivatives of [D-Pro[10]]dynorphin A-(1-11) are highly selective for kappa-opioid receptors. *J Med Chem* **1992,** *35*, 4638-4639.

182.   Aldrich, J. V. Patkar, K. A. Chappa, A. K. Fang, W, Audus, K. L. Lunte, S. M. Carey, A. N. McLaughlin, J. P. Development of centrally acting peptide analogs: structure-transport studies and pharmacological evaluation of analogs of the opioid peptide dynorphin A, *Proceedings of the 4th International Peptide Symposium,* 2008; Wilce, J., Ed. 2008; pp M 64.

183.   Saito, T.; Hirai, H.; Kim, Y. J.; Kojima, Y.; Matsunaga, Y.; Nishida, H.; Sakakibara, T.; Suga, O.; Sujaku, T.; Kojima, N. CJ-15,208, a novel kappa opioid receptor antagonist from a fungus, Ctenomyces serratus ATCC15502. *J Antibiot (Tokyo)* **2002,** *55*, 847-854.

184.   Ross, N. C.; Reilley, K. J.; Murray, T. F.; Aldrich, J. V.; McLaughlin, J. P. Novel opioid cyclic tetrapeptides: Trp isomers of CJ-15,208 exhibit distinct opioid receptor agonism and short-acting kappa opioid receptor antagonism. *Br J Pharmacol* **2012,** *165*, 1097-1108.

185.   Aldrich, J. V.; Senadheera, S. N.; Ross, N. C.; Ganno, M. L.; Eans, S. O.; McLaughlin, J. P. The Macrocyclic Peptide Natural Product CJ-15,208 Is Orally Active and Prevents Reinstatement of Extinguished Cocaine-Seeking Behavior. *J Nat Prod* **2013,** *76*, 433-438.

186.   Eans, S. O. Ganno, M. L.; Reilley, K. J.; Patkar, K.J.; Senadheera, S.N.; Aldrich, J. V.; McLaughlin, J. P. The macrocyclic tetrapeptide [D-Trp]CJ-15,208 produces short acting κ opioid receptor antagonism in the CNS after oral administration. *Br. J. Pharmacol* **2013,** *169*, 426-436.

187.   Schiller, P. W.; Weltrowska, G.; Nguyen, T. M.; Lemieux, C.; Chung, N. N.; Lu, Y. Conversion of delta-, kappa- and mu-receptor selective opioid peptide agonists into delta-, kappa- and mu-selective antagonists. *Life Sci* **2003,** *73*, 691-698.

188.   Soderstrom, K.; Choi, H.; Berman, F. W.; Aldrich, J. V.; Murray, T. F. N-alkylated derivatives of [D-Pro[10]]dynorphin A-(1-11) are high affinity partial agonists at the cloned rat kappa-opioid receptor. *Eur J Pharmacol* **1997,** *338*, 191-197.

189.   Lung, F. D.; Collins, N.; Stropova, D.; Davis, P.; Yamamura, H. I.; Porreca, F.; Hruby, V. J. Design, synthesis, and biological activities of cyclic lactam peptide analogues of dynorphine A(1-11)-NH$_2$. *J Med Chem* **1996,** *39*, 1136-1141.

190.   Arttamangkul, S.; Murray, T. F.; DeLander, G. E.; Aldrich, J. V. Synthesis and opioid activity of conformationally constrained dynorphin A analogues. 1. Conformational constraint in the "message" sequence. *J Med Chem* **1995,** *38*, 2410-2417.

191.   Arttamangkul, S.; Ishmael, J. E.; Murray, T. F.; Grandy, D. K.; DeLander, G. E.; Kieffer, B. L.; Aldrich, J. V. Synthesis and opioid activity of conformationally constrained dynorphin A analogues. 2. Conformational constraint in the "address" sequence. *J Med Chem* **1997,** *40*, 1211-1218.

192.   Kawasaki, A. M.; Knapp, R. J.; Kramer, T. H.; Wire, W. S.; Vasquez, O. S.; Yamamura, H. I.; Burks, T. F.; Hruby, V. J. Design and synthesis of highly potent and selective cyclic dynorphin A analogues. *J Med Chem* **1990,** *33*, 1874-1879.

193.   Kawasaki, A. M.; Knapp, R. J.; Kramer, T. H.; Walton, A.; Wire, W. S.; Hashimoto, S.; Yamamura, H. I.; Porreca, F.; Burks, T. F.; Hruby, V. J. Design and synthesis of highly potent and selective cyclic dynorphin A analogs. 2. New analogs. *J Med Chem* **1993,** *36*, 750-757.

194.   Meyer, J. P.; Collins, N.; Lung, F. D.; Davis, P.; Zalewska, T.; Porreca, F.; Yamamura, H. I.; Hruby, V. J. Design, synthesis, and biological properties of highly potent cyclic dynorphin A analogues. Analogues cyclized between positions 5 and 11. *J Med Chem* **1994,** *37*, 3910-3917.

195.   Naqvi, T.; Haq, W.; Mathur, K. B. Structure-activity relationship studies of dynorphin A and related peptides. *Peptides* **1998,** *19*, 1277-1292.

196.   Hruby, V. J.; Agnes, R. S. Conformation-activity relationships of opioid peptides with selective activities at opioid receptors. *Biopolymers* **1999,** *51*, 391-410.

197.   Gairin, J. E.; Gouarderes, C.; Mazarguil, H.; Alvinerie, P.; Cros, J. [D-Pro[10]]Dynorphin-(1-11) is a highly potent and selective ligand for kappa opioid receptors. *Eur J Pharmacol* **1984,** *106*, 457-458.

198.   Lu, Y.; Weltrowska, G.; Lemieux, C.; Chung, N. N.; Schiller, P. W. Stereospecific synthesis of (2S)-2-methyl-3-(2',6'-dimethyl-4'-hydroxyphenyl)-propionic acid (Mdp) and its incorporation into an opioid peptide. *Bioorg Med Chem Lett* **2001,** *11*, 323-325.

199.   Vig, B. S.; Zheng, M. Q.; Murray, T. F.; Aldrich, J. V. Effects of the substitution of Phe[4] in the opioid peptide [D-Ala[8]]dynorphin A-(1-11)NH$_2$. *J Med Chem* **2003,** *46*, 4002-4008.

200.   Aldrich, J. V.; Zheng, Q. I.; Murray, T. F. Dynorphin A analogs containing a conformationally constrained phenylalanine derivative in position 4: reversal of preferred stereochemistry for opioid receptor affinity and discrimination of kappa vs. delta receptors. *Chirality* **2001,** *13*, 125-129.

201.   Paterlini, G.; Portoghese, P. S.; Ferguson, D. M. Molecular simulation of dynorphin A-(1-10) binding to extracellular loop 2 of the kappa-opioid receptor. A model for receptor activation. *J Med Chem* **1997,** *40*, 3254-3262.

202.   Orosz, G.; Ronai, A. Z.; Bajusz, S.; Medzihradszky, K. N-terminally protected penta- and tetrapeptide opioid antagonists based on a pentapeptide sequence found in the venom of Philippine cobra. *Biochem Biophys Res Commun* **1994,** *202*, 1285-1290.

203.   Kulkarni, S. S. Choi, H. Murray, T. F. DeLander, G. E. Aldrich, J. V. The use of the message-address concept in the design of potential antagonists based on dynorphin A. In *Peptides: Chemistry, Structure and Biology*, Kaumaya, T. P. Hodges, R. S. Eds. Mayflower Scientific Ltd.: Weat Midlands England, 1996; pp 655-656.

204.   Aldrich, J. V. Wan, Q. Murray, T. F. Identification of novel kappa opioid receptor selective peptides from a combinatorial library. *Pacifichem* 2000, Honolulu, Hawaii.

205.   Bennett, M. A.; Murray, T. F.; Aldrich, J. V. Structure-activity relationships of arodyn, a novel acetylated kappa opioid receptor antagonist. *J Pept Res* **2005,** *65*, 322-332.

206.   Fang, W. J.; Bennett, M. A.; Aldrich, J. V. Deletion of Ac-NMePhe(1) from [NMePhe(1)]arodyn under acidic conditions, part 1: effects of cleavage conditions and N-terminal functionality. *Biopolymers* **2011,** *96*, 97-102.

207.   Fang, W. J.; Bennett, M. A.; Murray, T. F.; Aldrich, J. V. Deletion of Ac-NMePhe(1) from [NMePhe(1)]arodyn under acidic conditions, part 2: effects of substitutions on pharmacological activity. *Biopolymers* **2011,** *96*, 103-110.

208.   Vig, B. S.; Murray, T. F.; Aldrich, J. V. Synthesis and opioid activity of side-chain-to-side-chain cyclic dynorphin A-(1-11) amide analogues cyclized between positions 2 and 5. 1. Substitutions in position 3. *J Med Chem* **2004,** *47*, 446-455.

209.   Fang, W. J.; Cui, Y.; Murray, T. F.; Aldrich, J. V. Design, synthesis, and pharmacological activities of dynorphin A analogues cyclized by ring-closing metathesis. *J Med Chem* **2009,** *52*, 5619-5625.

210.   Patkar, K. A.; Yan, X.; Murray, T. F.; Aldrich, J. V. [N^{α}-benzylTyr^1,cyclo(D-Asp^5,Dap^8)]- dynorphin A-(1-11)NH$_2$ cyclized in the "address" domain is a novel kappa-opioid receptor antagonist. *J Med Chem* **2005,** *48*, 4500-4503.

211.   Story, S. C.; Murray, T. F.; Delander, G. E.; Aldrich, J. V. Synthesis and opioid activity of 2-substituted dynorphin A-(1-13) amide analogues. *Int J Pept Protein Res* **1992,** *40*, 89-96.

212.   Patkar, K. A.; Murray, T. F.; Aldrich, J. V. The effects of C-terminal modifications on the opioid activity of [N-benzylTyr(1)]dynorphin A-(1-11) analogues. *J Med Chem* **2009,** *52*, 6814-6821.

213.   Ronsisvalle, G.; Pasquinucci, L.; Pittala, V.; Marrazzo, A.; Prezzavento, O.; Di Toro, R.; Falcucci, B.; Spampinato, S. Nonpeptide analogues of dynorphin A(1-8): design, synthesis, and pharmacological evaluation of kappa-selective agonists. *J Med Chem* **2000,** *43*, 2992-3004.

214.   Ronsisvalle, G. P., M. S. Carboni, L. Vittorio, F. Pasquinucci, L. Marrazzo, A. Caccaguerra, S. Spampinato, S. Peptidomimetics of kappa opioid receptor. A hybrid MPCB/peptide ligand (MPCB-RRI) binds kappa cloned receptor in namolar affinity. *Analgesia* **1996,** *2*, 283-286.

215.   Marx, M. Watching peptide drugs grow up. *Chem Eng News* **2005,** *83*, 17-24.

Chapter 3 - Structure-activity relationships of Dynorphin B amide

*Compound numbers in this chapter are applicable only to this chapter

3.1 Introduction

3.1.1 Dynorphins and their precursor protein

Prodynorphin is the precursor peptide for the dynorphins. Prodynorphin is primarily cleaved into four larger opioid peptides, dynorphin (Dyn) A, leumorphin, and α and β-neoendorphin.[1] Dyn A undergoes cleavage to yield dynorphin (1-8) (Figure 3.1). Leumorphin is cleaved between the Thr-Arg residues to yield Dyn B. Along with the smaller peptides, larger peptides such as Dyn 32 (big Dyn) that contains Dyn A at the N-terminus and Dyn B at the C-terminus and Dyn 24 are also produced.[1] These prodynorphin-derived peptides are most abundant in the neural lobe of the rat pituitary and in the posterior pituitary. However, they are differentially processed in various parts of the brain.[1]

Fischli and Goldstein initially isolated the 17-amino acid peptide Dyn A from porcine pituitary.[2, 3] Subsequently, the same group also isolated big Dyn[4, 5] and Dyn B[4] from the same porcine preparation. The porcine preparation was subjected to a series of purification steps involving extraction, gel filtration chromatography, and high performance liquid chromatography (HPLC) to obtain Dyn A, big Dyn and Dyn B.

α-neoendorphin Dyn A Dyn B
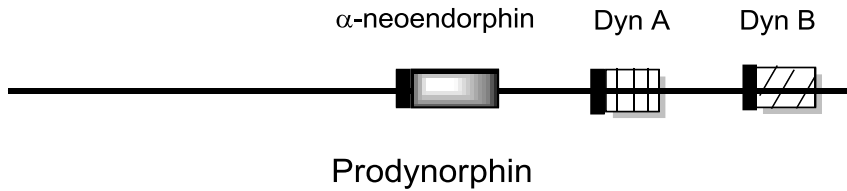
Prodynorphin

Major fragments from prodynorphin

Dyn A: Tyr-Gly-Gly-Phe-Leu-Arg-Arg-Ile-Arg-Pro-Lys-Leu-Lys-Trp-Asp-Asn-Gln

Leumorphin: Tyr-Gly-Gly-Phe-Leu-Arg-Arg-Gln-Phe-Lys-Val-Val-Thr-Ser-Gln-Glu
-Asp-Pro-Asn-Ala-Tyr-Ser-Gly-Glu-Leu-Phe-Asp-Ala

α-Neoendorphin- Tyr-Gly-Gly-Phe-Leu-Arg-Lys-Tyr-Pro-Lys

Smaller fragments from major peptides

Dyn A(1-8): Tyr-Gly-Gly-Phe-Leu-Arg-Arg-Ile

Dyn B: Tyr-Gly-Gly-Phe-Leu-Arg-Arg-Gln-Phe-Lys-Val-Val-Thr

Other larger fragments

Big Dyn: Tyr-Gly-Gly-Phe-Leu-Arg-Arg-Ile-Arg-Pro-Lys-Leu-Lys-Trp-Asp-Asn-Gln
Lys-Arg-Tyr-Gly-Gly-Phe-Leu-Arg-Arg-Gln-Phe-Lys-Val-Val-Thr

Dyn 24 : Tyr-Gly-Gly-Phe-Leu-Arg-Arg-Ile-Arg-Pro-Lys-Leu-Lys-Trp-Asp-Asn-Gln-
Lys-Arg-Tyr-Gly-Gly-Phe-Leu

Blue - Dyn A or its fragments
Red - Dyn B
Green - α-Neoendorphin

Figure 3.1 Dynorphins and related peptides derived from the precursor protein prodynorphin[6]

3.2   Pharmacological profile of the dynorphins

Following their isolation, Dyn A, big Dyn and Dyn B were tested for their opioid receptor potencies in the rabbit vas deferens (RVD)[7] and in the guinea pig ileum (GPI) bioassay.[8] While the RVD is known to exclusively contain kappa opioid receptors (KOR),[9] the GPI contains multiple opioid receptors.[10] In the RVD bioassay, Dyn A displayed an IC_{50} value of

88

0.30 ± 0.07 μM while big Dyn and Dyn B displayed values of 3.95 ± 1.91 μM and 1.57 ± 0.360 μM, respectively.[7] Another group also tested Dyn B in the RVD bioassay and obtained a relatively potent IC_{50} value of 41.3 ± 8.8 nM.[11] In the GPI bioassay, the IC_{50} values (99% confidence intervals) for Dyn A, big Dyn and Dyn B were 0.19 (0.16-0.22) nM, 1.4 (0.77-2.7) nM and 3.3 (1.9-5.8) nM, respectively. Another group also tested Dyn B in the GPI assay and obtained an IC_{50} value of 3.23 ± 0.35 nM.[11] Along with the preparations containing peripheral opioid receptors, Dyn A, big Dyn and Dyn B were also evaluated for opioid receptor affinities in mouse brain preparations (Table 3.1).[12]

The three peptides Dyn A, Dyn B and big Dyn were tested at cloned human opioid receptors in radioligand binding assays for affinity and in the GTPγS assay for potency and efficacy[13] (see Table 3.2 for affinities and Table 3.3 for potencies and efficacies). The peptides showed varying selectivity for human kappa opioid receptors (h-KOR) over human mu opioid receptors (h-MOR) and human delta opioid receptors (h-DOR). In the binding assays, Dyn A showed the highest affinity and selectivity for h-KOR over h-MOR and h-DOR. In the GTPγS assay, big Dyn was the most potent for h-KOR followed by Dyn A and then by Dyn B. The selectivity in the GTPγS assay was highest for big Dyn followed by Dyn A and Dyn B.[13] Species differences (rodents vs. human) could contribute to the differences in results from different assays.

Table 3.1 Binding affinities of dynorphins in mouse brain preparation.[12]

Peptide	K_i (nM ± SEM)[a]			
	KOR	MOR	DOR	KOR/MOR/DOR
Dyn A	0.3 ± 0.09	2.6 ± 0.9	6.3 ± 0.9	1/9/21
Dyn B	1.4 ± 0.32	12.6 ± 1.2	20.5 ± 2.5	1/9/15

[a]K_i values were obtained from competition binding experiments performed using mouse brain preparation and [³H]ethylketocyclazocine, [³H]dihydromorphine and [³H]DPDPE as the radioligands for KOR, MOR and DOR, respectively.

Table 3.2 Binding affinities of dynorphins in radioligand binding assays using human cloned receptors.[13]

Peptide	K_i (nM ± SEM)[a]			
	h-KOR	h-MOR	h-DOR	KOR/MOR/DOR
Dyn A	0.082 ± 0.036	21.4 ± 5.8	111.9 ± 3.8	1/261/1366
Dyn B	3.80 ± 1.58	13.0 ± 2.40	12.8 ± 2.8	1/3/3
Big Dyn	0.198 ± 0.080	14.1 ± 0.5	43.0 ± 14.4	1/71/217

[a]K_i values were obtained from competition binding experiments performed using membranes prepared from receptor-expressing cell lines (Chinese hamster ovary (CHO) cells expressing h-KOR and human embryonic kidney (HEK) cells expressing h-MOR and h-DOR) and [³H]diprenorphine as the radioligand.

Table 3.3 Efficacy and potency of dynorphins in the GTPγS assay.[13]

Peptide	EC_{50} (nM ± SEM) (%efficacy[a])			EC_{50} ratio
	h KOR	h MOR	h DOR	KOR/MOR/DOR
Dyn A	10.7 ± 4.4 (100%)	150.0 ± 42.1 (100%)	254.0 ± 39.8 (100%)	1/14/24
Dyn B	23.5 ± 10.7 (131%)	105.1 ± 52.6 (88%)	122.7 ± 6.0 (86%)	1/4/5
Big dynorphin	0.741 ± 0.048 (159%)	87.0 ± 9.9 (115%)	119.2 ± 65.1 (100%)	1/117/161

[a] Shown as percentage relative to Dyn A (100%). Experiments were performed using membranes prepared from the receptor-expressing cell lines as in Table 3.2.

3.3 Non-opioid effects of dynorphins

Although Dyn A is an endogenous ligand for KOR[14] it not only displays opioid effects but also produces non-opioid effects.[15-17] Dyn A (5 or 20 nmol)[18] produced hind limb paralysis when injected intrathecally (i.t.) into rats[18, 19] and caused depletion of cell bodies of inter-sensory and motor neurons in the lumbosacral cord associated with loss of motor activity.[20] Lower (1 nmol) intrathecal doses of Dyn A(1-13) produced no analgesia in rats,[21] while higher doses (25 nmol, i.t.) caused irreversible loss of thermally evoked tail flick reflex as a result of hind limb paralysis.[22] This loss of tail flick reflex was resistant to naloxone, but it was blocked by preadministration of the *N*-methyl-D-aspartate (NMDA) antagonist dizoclipine.[22] Big Dyn (1-10 fmol, i.t) and Dyn A (0.1-3 pmol, i.t) produced a characteristic nociceptive behavior in rats involving hind paw and tail biting. This nociceptive effect was shown to be resistant to naloxone but was blocked by dizoclipine, an NMDA antagonist.[23] Additionally a long lasting state of allodynia was caused by single i.t. injections of 3 nmol[24] and 15 nmol[25] of Dyn A. Dyn A (5 and 10 nmol) and Big Dyn (2.5 and 5 nmol) also induced hypothermia in rats after intracerebroventricular (i.c.v.) administration. Induction of hypothermia is considered to be a mixture of the opioid and non-opioid effects of dynorphins.[26] The non-opioid effects were also displayed by the des Tyr fragment Dyn A(2-17) which does not bind to opioid receptors.[17]

Dyn A levels are elevated under certain pathophysiological conditions, for example Dyn A levels are increased at sites of spinal cord injury.[27, 28] It was reported in two studies that the increase in concentration of Dyn A was proportional to the severity of trauma.[27, 29] For example, Dyn A levels increased 40% following moderate spinal injury by the end of two weeks, while the levels increased 150% following severe spinal injury.[27] In another study it was shown that the

Dyn A levels were elevated approximately 2-fold in rats subjected to nerve injury that subsequently caused neuropathic pain.[30]

The Dyn A fragment Dyn A(1-13) can have dual neurotoxic[31, 32] and neuroprotective[33, 34] actions in spinal cord neurons. At nanomolar concentrations Dyn A(1-13) activates KOR and can be neuroprotective, while at micromolar concentrations it exerts excitotoxic effects causing neuronal death through NMDA receptors.[33, 34] In addition, it was also shown subsequently that Dyn A and big Dyn caused cytotoxicity in non-neuronal cells as well as neuronal cells through a mechanism resistant to naloxone.[31, 32]

Dyn B has not been studied as extensively for its non-opioid effects as Dyn A. Dyn B at higher concentrations (50-100 nmol coinjected with peptidase inhibitors) produced hind limb paralysis similar to Dyn A (12.5-25 nmol without peptidase inhibitors) when injected into the lumbar space in rats.[35] In contrast to Dyn A, Dyn B (1000 pmol) administered i.t. did not produce characteristic nociceptive behavior in rats involving hind paw and tail biting.[23] Also Dyn B (up to 50 nmol) did not induce hypothermia after i.c.v. administration in rats.[26] Unlike Dyn A, Dyn B did not produce the cytotoxic effects (see above) in neuronal and non-neuronal cells *in vitro.*[31]

3.4   Membrane interactions of dynorphins

Membrane interactions of dynorphins have been studied in membrane model systems such as phospholipid large unilamellar vesicles (LUVs).[36] Big Dyn and Dyn A produced membrane perturbations of phospholipid LUVs and induced calcein leakage in phospholipid LUVs probably by causing a transient pore formation. In contrast, Dyn B did not cause membrane perturbation and calcein leakage.[36]

Studies of the membrane interactions of dynorphins were also performed with phospholipid bicelles and the results analyzed by NMR and saturation transfer difference (STD) experiments.[37] These studies showed that the N-terminus of Dyn A was inserted in the hydrophobic lipid bilayer region while the C-terminal residues were loosely attached to the bicelle surface. The N-terminus of Dyn A displayed changes in its NMR due to insertion into the phospholipid membrane.[37] In contrast, Dyn B was bound to the bilayer but did not insert into the lipid bilayer, and the NMR of the N-terminus did not change in the presence of the bicelles.[37]

The above results (sections 3.3 and 3.4) suggest a possible connection between the non-opioid cytotoxic actions and membrane perturbations of the phospholipid bilayer induced by the dynorphins. Although there is a difference in the number of charged residues for the two peptides Dyn A and Dyn B, the net charge difference is minimal and the charges do not seem to be the driving force for the difference in membrane interactions. Thus, the non-opioid cytotoxic effects produced by Dyn A but not by Dyn B (section 3.3) may be due in part to either transient pore formation and/or membrane perturbations.

It is worthwhile to note that although Dyn B exhibits lower affinity, potency and selectivity for KOR, it does not exhibit the cytotoxic non-opioid effects exhibited by Dyn A and big Dyn. While Dyn A and Dyn B have identical N-terminal sequences, their C-terminal sequences differ. Hence, the differences in their interaction with lipid membranes and non-opioid cytotoxic effects must be due to their differences in the C-terminal sequences. To date studies involving structure-activity relationships (SAR) of dynorphins have focused almost exclusively on Dyn A, with minimal SAR studies related to Dyn B. Schiller and coworkers synthesized the Mdp[1] (Mdp = (2S)-2-methyl-3-(2,6-dimethyl-4-hydroxyphenyl)propanoic acid) analog of Dyn A

(also called dynantin) and Dyn B.[38] The Dyn A analog was a 180-fold more potent KOR antagonist than the Dyn B analog in the GPI assay.

3.5 Alanine scan of Dyn B amide

3.5.1 Rationale

It is hypothesized that unique residue(s) in the C-terminus of Dyn B interact with the receptor and contribute to its activity at KOR. To test the above hypothesis, alanine substituted analogs of Dyn B were synthesized. All of the non-glycine residues up through residue 11 were substituted with Ala in order to explore the roles of their side chains to the activity of Dyn B (Figure 3.2).

N-Terminal analogs

Ala^1-Gly-Gly-Phe-Leu-Arg-Arg-Gln-Phe-Lys-Val-Val-Thr-NH_2 **(1)**

Tyr-Gly-Gly-Ala^4-Leu-Arg-Arg-Gln-Phe-Lys-Val-Val-Thr-NH_2 **(2)**

C-Terminal analogs

Tyr-Gly-Gly-Phe-Ala^5-Arg-Arg-Gln-Phe-Lys-Val-Val-Thr-NH_2 **(3)**

Tyr-Gly-Gly-Phe-Leu-Ala^6-Arg-Gln-Phe-Lys-Val-Val-Thr-NH_2 **(4)**

Tyr-Gly-Gly-Phe-Leu-Arg-Ala^7-Gln-Phe-Lys-Val-Val-Thr-NH_2 **(5)**

Tyr-Gly-Gly-Phe-Leu-Arg-Arg-Ala^8-Phe-Lys-Val-Val-Thr-NH_2 **(6)**

Tyr-Gly-Gly-Phe-Leu-Arg-Arg-Gln-Ala^9-Lys-Val-Val-Thr-NH_2 **(7)**

Tyr-Gly-Gly-Phe-Leu-Arg-Arg-Gln-Phe-Ala^{10}-Val-Val-Thr-NH_2 **(8)**

Tyr-Gly-Gly-Phe-Leu-Arg-Arg-Gln-Phe-Lys-Ala^{11}-Val-Thr-NH_2 **(9)**

Figure 3.2 Alanine analogs of Dyn B amide

3.6   Results and discussion

3.6.1   Chemistry

The peptides were synthesized by the Fmoc (9-fluorenylmethoxycarbonyl) solid phase synthetic strategy (Scheme 3.1). The Dyn B amide sequences were assembled on a polyethylene glycol-polystyrene (PEG-PS) resin containing the PAL [peptide amide linker, 5-(4-Fmoc-aminomethyl-3,5-dimethoxyphenoxy)valeric acid] linker using 7-benzotriazol-1-yl-oxytripyrrolidinophosphonium hexafluorophosphate (PyBOP) and 1-hydroxy-7-benzotriazole (HOBt) as the coupling agents and *N*,*N*-diisopropylethylamine (DIEA) as the base. The side chains of Lys, Gln, Arg and Tyr were protected with *tert*-butyloxycarbonyl (Boc), trityl (Trt), 2,2,4,6,7-pentamethyldihydrobenzofuran-5-sulfonyl (Pbf) and *tert*-butyl (*t*Bu) groups, respectively. The peptides were assembled using cycles consisting of Fmoc deprotection and Fmoc-amino acid coupling. The crude peptides were cleaved from the resin using Reagent B[39] (trifluoroacetic acid (TFA) in the presence of scavengers).

Fmoc--NH-PAL-PEG-PS-⬤

|
Piperidine:DMF (1:4)
↓

NH$_2$-PAL-PEG-PS-⬤

| Fmoc-amino
| acid, PyBOP,
| HOBt (4 equiv each)
↓ DIEA (10 equiv)
   DCM:DMF (1:1)

FmocHN⟍ ⟍C(=O)⟍NHPAL-PEG-PS-⬤
          |
         OtBu

Piperidine:DMF (1:4)
↓

H$_2$N⟍ ⟍C(=O)⟍NH-PAL-PEG-PS-⬤
          |
         OtBu

Repeat above steps
for n amino acids,
n = 12
↓

H$_2$N-Tyr-Gly-Gly-Phe-Leu-Ala-Arg-Gln-Phe-Lys-Val-Val-Thr-NH-PAL-PEG-PS-⬤
      | | | | |
     tBu   Pbf Trt   Boc   tBu

Reagent B
(88% TFA, 5% H$_2$O,
5% phenol, 2% TIPS)
↓

Tyr-Gly-Gly-Phe-Leu-Ala-Arg-Gln-Phe-Lys-Val-Val-Thr-NH$_2$

Scheme 3.1 Synthesis of [Ala[6]]Dyn B amide

Table 3.4 Analytical data for the Dyn B amide analogs

Compound	HPLC system t_R (min)		ESI-MS (*m/z*)	
	System 1[a] (% Purity)	System 2[b] (% Purity)	Calculated	Observed
1	19.1 (100)	29.1 (100)	739.4 $(M + 2H)^{2+}$	739.4 $(M + 2H)^{2+}$
2	20.7 (100)	24.6 (100)	747.4$(M + 2H)^{2+}$	747.4$(M + 2H)^{2+}$
3	21.7 (97.9)	23.9 (100)[c]	764.4 $(M + 2H)^{2+}$	764.4 $(M + 2H)^{2+}$
4	22.2 (99.6)	34.5 (100)	742.9 $(M + 2H)^{2+}$	742.9 $(M + 2H)^{2+}$
5	23.8 (100)	33.3 (100)	742.9 $(M + 2H)^{2+}$	742.9 $(M + 2H)^{2+}$
6	29.9 (99.7)	39.8 (100)	756.9 $(M + 2H)^{2+}$	756.9 $(M + 2H)^{2+}$
7	16.6 (100)	23.2 (100)	747.4 $(M + 2H)^{2+}$	747.4 $(M + 2H)^{2+}$
8	20.3 (95.5)	31.1 (100)	756.9 $(M + 2H)^{2+}$	756.9 $(M + 2H)^{2+}$
9	20.1 (99.8)	30.0 (100)	771.4 $(M + 2H)^{2+}$	771.4 $(M + 2H)^{2+}$
Dyn B amide	18.6 (100)	31.9 (100)	785.4 $(M + 2H)^{2+}$	785.4 $(M + 2H)^{2+}$

[a]Aqueous MeCN containing 0.1% TFA. [b]Aqueous MeOH containing 0.1% TFA. [c]Peptide **3** displayed a $t_R = 18.4$ min and purity of 96.2% on a 25-45% aqueous MeOH containing 0.1% TFA over 40 min. See the Experimental Section for gradient details.

The peptides were isolated and purified according to the standard procedures described under the Experimental section. Following TFA cleavage of the peptides,[39] the crude peptide residues were diluted with water and lyophilized. The Dyn B amide analogs were hydrophobic and required organic solvent for solubilization of the peptide prior to purification by reversed phase high performance liquid chromatography (RP-HPLC). MeOH which is a weaker solvent for RP-HPLC than MeCN, was used to assist in peptide dissolution while minimizing impact on the chromatography.

3.6.2 Pharmacological activity

Opioid binding affinities of the alanine substituted analogs of Dyn B amide were determined in Chinese hamster ovary (CHO) cell membranes expressing cloned rat MOR and KOR and mouse DOR (Table 3.5). The aromatic residues in positions 1 and 4 of the N-terminal

sequence of Dyn B amide are critical for its opioid receptor binding affinity. Substitution of Ala in position 1 caused a 121-fold decrease while substitution in position 4 caused a 204-fold decrease in the KOR binding affinity compared to Dyn B amide. Ala[1] and Ala[4] analogs exhibited 24- and 38-fold decreases, respectively, in MOR binding affinity and showed minimal affinity for DOR, suggesting that these two residues are critical for binding to MOR and DOR as well.

Table 3.5 Opioid binding affinities of Dyn B amide alanine analogs.

$\text{Tyr}^1\text{-Gly-Gly-Phe}^4\text{-Leu}^5\text{-Arg}^6\text{-Arg}^7\text{-Gln}^8\text{-Phe}^9\text{-Lys}^{10}\text{-Val}^{11}\text{-Val-Thr-NH}_2$
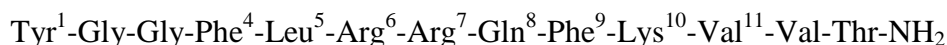
Compound	K_i (nM ± SEM)[a]			
	KOR	MOR	DOR	KOR/MOR/DOR
N-Terminal alanine substituted analogs				
1 [Ala[1]]	885 ± 219	651 ± 70	>10,000	1/0.7/11
2 [Ala[4]]	1500 ± 320	1040 ± 100	>10,000	1/0.7/7
C-Terminal alanine substituted analogs				
3 [Ala[5]]				
4 [Ala[6]]	43.1 ± 3.8	14.1 ± 3.0	25.5 ± 1.5	1/0.3/0.6
5 [Ala[7]]	82.4 ± 19.0	16.7 ± 5.1	67.4 ± 8.3	1/0.2/0.8
6 [Ala[8]]	13.3 ± 1.9	4.31 ± 0.09	53.9 ± 6.8	1/0.3/4
7 [Ala[9]]	11.3 ± 3.4	3.76 ± 0.22	42.1 ± 2.5	1/0.3/4
8 [Ala[10]]	31.6 ± 6.0	40.5 ± 3.9	119 ± 16	1/1/4
9 [Ala[11]]	12.4 ± 0.7	7.45 ± 2.7	58.8 ± 3.4	1/0.6/5
Dyn B amide	7.3 ± 2.0	27.3 ± 14.0	43.2 ± 1.6	1/4/6

[a] values are mean ± SEM for n ≥ 3.

The basic residues in position 6 and 7, i.e. Arg[6] and Arg[7], appear to contribute to the KOR binding affinity of Dyn B amide. Substitutions of Ala in positions 6 and 7 caused 6- and 11-fold decreases in KOR binding affinity, respectively. Substitution of the basic Lys residue in position 10 by Ala caused a 4-fold decrease, suggesting that Lys[10] also contributed to KOR binding affinity. Substitution of Ala in positions 8, 9 and 11 caused less than a 2-fold decrease in

98

KOR affinity, indicating that these non-charged residues do not contribute significantly to the KOR affinity of Dyn B amide.

None of the residues in the C-terminus appear to be important for MOR binding affinity. In contrast it was observed that Ala substitutions in the C-terminus, except for the Ala[10] analog, increased the MOR affinity of most of the analogs while the KOR affinity remained unaltered or decreased. Consequently, this shifted the selectivity of these Dyn B analogs from KOR-preferring to MOR preferring. Similarly, most of the residues did not appear to contribute to DOR affinity, with only residue 10 appearing to make minor contributions to the DOR affinity of Dyn B(1-13) amide.

Turcotte *et al.* performed the Ala scan of Dyn A(1-13)[40] (Table 3.6). Within the N-terminal sequence of this peptide Ala[1] and Ala[4] substitutions caused dramatic decreases in the opioid receptor binding affinity, indicating that the Tyr[1] and Phe[4] residues were critical for opioid receptor binding.[40] Outside the N-terminal tetrapeptide sequence the Ala[5] analog displayed a 15-fold decrease in opioid receptor binding affinity while the Ala[6] and Ala[7] analogs showed 3- to 7-fold decreases in the opioid receptor binding affinities suggesting that Leu[5], Arg[6] and Arg[7] also contributed to opioid receptor interactions in the C-terminus. Ala[9] and Ala[11] analogs also showed small decreases (2- to 3-fold) in opioid receptor binding affinities, suggesting that these residues may be minor contributions to opioid receptor interactions. The agonist potencies of the analogs containing Ala substitutions in positions 1 and 4 showed a similar trend in the GPI assay as found in the radioligand binding assay. Similarly, among the C-terminal residues 5, 6 and 7 contributed the most, while residues 9 and 11 also contributed to maintaining the agonist potency of Dyn A (1-13) at opioid receptors in the GPI assay.[40]

Table 3.6 Alanine scan of Dyn A(1-13)[40]

Tyr^1-Gly^2-Gly^3-Phe^4-Leu^5-Arg^6-Arg^7-Ile^8-Arg^9-Pro^{10}-Lys^{11}-Leu-Lys

Peptide	Agonist potency		Affinity	
	IC_{50} (nM)[a]	Fold decrease[c]	IC_{50} (nM)[b]	Fold decrease[c]
[Ala^1] Dyn A(1-13)	750 ± 30	1070	1400 ± 210	519
[Ala^2]- "	104 ± 32	149	13.5 ± 0.4	5
[Ala^3]- "	2.0 ± 0.3	3	21.5 ± 3.7	8
[Ala^4]- "	700 ± 20	1000	750 ± 35	278
[Ala^5]- "	14 ± 4	20	45.0 ± 1.1	17
[Ala^6]- "	23 ± 6	33	19.2 ± 0.8	7
[Ala^7]- "	19 ± 5	27	10.0 ± 1.2	4
[Ala^8]- "	1.4 ± 0.1	2	0.3 ± 0.0	-
[Ala^9]- "	5.5 ± 0.8	8	7.4 ± 0.8	3
[Ala^{10}]- "	3.3 ± 0.7	5	3.8 ± 0.5	1.5
[Ala^{11}]- "	7.6 ± 0.4	11	8.7 ± 0.9	3
Dyn A(1-13)	0.7 ± 0.1	-	2.7 ± 0.3	-

[a]IC_{50} obtained from the GPI assay. [b]IC_{50} obtained from radioligand binding assays using [^{3}H]etorphine in rat brain homogenates. [c]As compared to Dyn A(1-13).

A comparison of the results obtained from the alanine substituted analogs of Dyn A(1-13) and Dyn B amide suggests that the as expected aromatic residues in positions 1 and 4 of both Dyn A(1-13) and Dyn B amide are critical for opioid receptor binding. The residues in position 6 and 7 appear to contribute to the opioid receptor binding of Dyn A(1-13) and KOR binding of Dyn B amide. Basic residues 9 and 11 appear to contribute to opioid receptor binding affinity in the case of Dyn A(1-13), and Lys^{10} appears to contribute to KOR binding in the case of Dyn B(1-13) amide. Hence, it appears likely that in addition to the basic residues in position 6 and 7, a basic residue in the 8-11 sequence of the C-terminus sequences of both peptides contributes to the peptides' receptor binding affinities. Arg^6 and Arg^7 residues do not appear to be important for

the MOR and DOR affinities of Dyn B amide. While Lys^{10} is not important for MOR affinity, it appears to makes minor contributions to DOR affinity. The difference in relative positions of the basic residues may be one reason for the differences in the pharmacological profiles exhibited by the two peptides. Nonetheless, there could be other reasons for the different pharmacological activities exhibited by the two peptides.

It should be noted that there exists several differences in the radioligand binding assays used to evaluate the Ala analogs of the two peptides. In the early studies of Dyn A analogs the results represent a weighted average of the affinities at multiple opioid receptors in rat brain (which have relatively low expression of KOR)[41] because a non-selective radiolabeled opioid agonist was used. In the case of the Dyn B amide analogs, the opioid affinities were determined using cell membranes expressing individual cloned opioid receptors and a radiolabeled antagonist that permitted the displayed different effects of substitution of C-terminal residues on KOR affinity vs. MOR and DOR affinity to be assessed. Hence, the comparisons of the Ala substituted analogs from the two peptides should be made with some caution.

Table 3.7 Potencies and efficacies of the Dyn B amide alanine analogs at KOR in GTPγS assay

Peptide	EC$_{50}$ (nM ± SEM)[a]	Efficacy (%)[b]
C-Terminal alanine substituted analogs		
3 [Ala^5]		
4 [Ala^6]	115 ± 17	92 ± 9
5 [Ala^7]	300 ± 96	100
6 [Ala^8]	51.9 (n=1)	89
7 [Ala^9]	17.3 (n=1)	96
8 [Ala^{10}]		
9 [Ala^{11}]		
Dyn B amide		
Dyn A(1-13)NH$_2$	30.3 ± 15 (n=4)	100

[a] Values are for n=2 unless otherwise noted. [b] As compared to Dyn A(1-13)NH$_2$ (efficacy = 100%). The efficacy of peptides **1** and **2** was not determined given their low affinity in the radioligand binding assays.

The potencies and the efficacies of the Ala substituted analogs of Dyn B amide were determined using the GTPγS assay (see Table 3.7). The analogs with Ala substitutions in positions 6 to 9 displayed efficacies from 89 to 100% compared to the reference agonist Dyn A(1-13)NH$_2$. The remaining analogs will be evaluated in this assay shortly.

3.7   Conclusions

The differences in the C-terminal sequences of Dyn A (1-13) and Dyn B are responsible for the differences in their pharmacological profiles. An alanine scan of Dyn B amide and Dyn A(1-13) revealed that residues 1 and 4 in the N-terminal regions of both peptides are critical for their opioid receptor binding. The Ala^4 analog of Dyn B amide displayed 1.5- to 2-fold larger decreases in KOR and MOR affinities as compared to the Ala^1 analog. This suggested that in the case of Dyn B amide, Phe^4 may contribute more to KOR and MOR binding than Tyr^1. Residues

in positions 1 and 4 also contribute to the KOR vs. MOR selectivity of Dyn B amide. While the basic residue Arg^7 appears to be important, Arg^6 and Lys^{10} also contribute to KOR binding affinity of Dyn B amide. While the Arg residues in position 6 and 7 are important for the KOR selectivity by both increasing KOR affinity and decreasing MOR affinity, the Lys^{10} residue contributes to KOR selectivity primarily by increasing KOR affinity. In the case of Dyn A(1-13), along with Arg residues 6 and 7, basic residues 9 and 11 also make minor contributions to opioid receptor binding affinity. Thus it is clear that the basic residues in the C-terminus of both peptides contribute to their opioid receptor affinities; however, their relative positions in residues 8-11 in the peptide could be one of the reasons contributing to their different pharmacological profiles.

3.8   Experimental section

Materials

The PAL-PEG-PS resin was purchased from Applied Biosystems (Foster City, CA, USA). The Fmoc-protected amino acids were purchased from Novabiochem Corp. (San Diego, CA, USA) or Peptides International, Inc. (Louisville, KY, USA). PyBOP and HOBt were purchased from Novabiochem and Peptide International, Inc., respectively and DIEA was obtained from Fischer Scientific (Fair Lawn, NJ). Piperidine was purchased from Sigma Aldrich (Milwaukee, WI, USA). All HPLC grade solvents [MeCN, *N,N*-dimethylformamide (DMF), dichloromethane (DCM), and MeOH] used for peptide synthesis or HPLC analysis were obtained from Fischer Scientific. TFA for HPLC purification and analysis was purchased from Pierce (Rockville, IL, USA). Triisopropylsilane (TIS) were from Acros Organics (Fairlawn, NJ)

Peptide synthesis

The peptides were prepared by solid phase peptide synthesis performed on an automated CS Bio 336 peptide synthesizer. The peptides were assembled on the PAL-PEG-PS resin (0.19 mmol/g, 200 mg) using standard Fmoc synthetic strategy. The resin was swollen with 5 mL of DMF (2 X 10 min). The Fmoc group on the resin was removed using 20% piperidine in DMF (5 mL, 2 X 10 min), and the resin was washed with DCM/DMF (1:1, 10 X 30 sec). The desired Fmoc-protected amino acids (4 equiv) were coupled to the resin with PyBOP, HOBt (4 equiv each) and DIEA (10 equiv) in DMF (2 mL) for 2 h. The side chains of Lys, Gln, Arg and Tyr were protected with Boc, trityl (Trt), Pbf and *tert*-butyl, respectively. The Fmoc deprotection of the amino acid on the resin was repeated followed by the next coupling cycle. The deprotection-coupling cycle was repeated until the desired peptide was assembled on the resin.

Cleavage of the peptide from the resin

The peptide resins were treated with Reagent B[39] (88% TFA, 5% phenol, 5% water, and 2% TIS, 5 mL) for 2 h with occasional shaking. Subsequently, the resins were filtered and the TFA was evaporated *in vacuo*. Water (20 mL) was added to the residues, and the solutions lyophilized to give the crude peptides.

Purification and analysis of the peptides

The crude peptides were purified by preparative reversed phase HPLC using an LC-AD liquid chromatograph (Shimadzu) equipped with a SPD-10A VP system controller and SPD-10A VP UV-Vis detector and a Vydac C18 column (10 μ, 300 Å, 22 mm x 250 mm) equipped with a Vydac C18 guard cartridge. For purification, the crude peptides (20-30 mg) were dissolved in 75-85% MeOH in water (total volume ~1.5 mL). A linear gradient of 15-50% aqueous MeCN containing 0.1% TFA over 45 min, at a flow rate of 18 mL/min, was used. The purification was

monitored at 214 nm. Peptide **3** was purified using a linear gradient of 30-50% aqueous MeOH containing 0.1% TFA over 40 min. Peptide **8** was purified using a linear gradient of 5-40% aqueous MeCN containing 0.1% TFA over 70 min with a flow rate of 15 mL/min. The purity of the final peptides was verified on a Vydac 218-TP column (5 μ, 300 Å, 4.6 mm x 50 mm) equipped with a Vydac guard cartridge on a LC-10AT VP analytical HPLC (Shimadzu) equipped with a SCL-10A VP system controller and SPD-10A VP UV-visible detector or on an Agilent 1200 series liquid chromatograph system equipped with a multiple wavelength UV-visible detector. Two systems, a linear gradient of 5-50% solvent B (solvent A = aqueous 0.1% TFA and solvent B = MeCN containing 0.1% TFA) over 45 min, at a flow rate of 1 mL/min (system 1), and a linear gradient of 15-60% solvent B (solvent A = aqueous 0.1% TFA and solvent B = MeOH containing 0.1% TFA) over 45 min, also at a flow rate of 1.0 mL/min (system 2), were used for the analyses. The final purity of all peptides by both analytical systems was ≥ 98%, except for peptides **3** and **8** that displayed purity of > 95%. Peptide **3** displayed a purity of 96.2% on 25-45% of MeOH with 0.1% TFA in water containing 0.1% TFA over 40 min, while peptide **8** displayed a purity of 95.5% in system 1. Molecular weights of the compounds were determined by ESI-MS using a Waters-time of flight (TOF) mass spectrometer (LCT premier, Waters, Milford, MA).

Pharmacological assays

Radioligand binding assays

Radioligand binding assays were performed as previously described[42] using cloned rat KOR and MOR, and mouse DOR stably expressed separately on CHO cells. [^{3}H]Diprenorphine, [^{3}H]DAMGO ([D-Ala^2,*N*-MePhe^4,Gly-ol]enkephalin) and [^{3}H]DPDPE (*cyclo*[D-Pen^2,D-Pen^5]enkephalin) were used as radioligands in the binding assays for KOR, MOR and DOR,

respectively. Incubations were carried out in triplicate with varying concentrations of peptides (0.1-10,000 nM) for 90 min at RT in the presence of peptidase inhibitors (10 μM bestatin, 30 μM captopril, and 50 μM L-leucyl-L-leucine) and 3 mM Mg^{2+}. Nonspecific binding was determined in the presence of 10 μM unlabeled Dyn A-(1-13)NH_2, DAMGO and DPDPE for KOR, MOR and DOR, respectively. IC_{50} values were determined by nonlinear regression analysis fit to a logistic equation for the competition data using Prism software (GraphPad Software Co., San Diego, CA). K_i values were calculated from the IC_{50} values by the Cheng and Prusoff equation[43] using K_D values of 0.45, 0.49, and 1.76 nM for [^{3}H]diprenorphine, [^{3}H]DAMGO, and [^{3}H]DPDPE, respectively.

GTPγS assay

The binding of the GTP analog [^{35}S]GTPγS to CHO cell membranes expressing cloned KOR was assayed as described previously.[44] Binding of the test compound was determined in a volume of 500 μL. The assay mixtures contained 50 mM HEPES, pH 7.4; 1 mM EDTA; 5 mM magnesium acetate; 1 μM GDP; 1 mM dithiothreitol; 100 mM NaCl, 10 μM bestatin, 30 μM captopril, 50 μM Leu-Leu, 1 mg bovine serum albumin per mL; and approximately 100,000 disintegrations per min (dpm) [^{35}S]GTPγS (0.08-0.15 nM). Approximately 10 μg of KOR expressing CHO cell membrane protein was used per tube. Following 90 min incubation at 22 ^{o}C, the assay was terminated by filtration under vacuum on a Brandel (Gaithersburg, MD) model M-48R cell harvester using Schleicher and Schuell Inc. (Keene, NH) number 32 glass fiber filters. The filters were rinsed five times (4 mL for each wash) with ice-cold 50 mM Tris HCl, pH 7.4, containing 5 mM MgCl, at 5 ^{o}C to remove unbound [^{35}S]GTPγS. Filter disks were then placed into counting vials to which 8 mL of Biocount scintillation fluid (Research Products International Corp., Mount Prospect, IL) was added. Filter-bound radioactivity was determined

by liquid scintillation spectrometry (Beckman Instruments, Fullerton, CA) following overnight extraction at room temperature. The amount of radioligand bound was less than 10% of the total added in all experiments. Specific binding was defined as total binding minus non-specific binding occurring in the presence of 3 μM unlabeled GTPγS. Nonspecific binding was approximately 1% of the total binding at 0.1 nM [^{35}S]GTPγS.

3.9   References

1.   Hollt, V. Opioid peptide processing and receptor selectivity. *Annu Rev Pharmacol Toxicol* **1986,** *26*, 59-77.

2.   Goldstein, A.; Tachibana, S.; Lowney, L. I.; Hunkapiller, M.; Hood, L. Dynorphin-(1-13), an extraordinarily potent opioid peptide. *Proc Natl Acad Sci U S A* **1979,** *76*, 6666-6670.

3.   Goldstein, A.; Fischli, W.; Lowney, L. I.; Hunkapiller, M.; Hood, L. Porcine pituitary dynorphin: complete amino acid sequence of the biologically active heptadecapeptide. *Proc Natl Acad Sci U S A* **1981,** *78*, 7219-7223.

4.   Fischli, W.; Goldstein, A.; Hunkapiller, M. W.; Hood, L. E. Isolation and amino acid sequence analysis of a 4,000-dalton dynorphin from porcine pituitary. *Proc Natl Acad Sci U S A* **1982,** *79*, 5435-5437.

5.   Fischli, W.; Goldstein, A.; Hunkapiller, M. W.; Hood, L. E. Two "big" dynorphins from porcine pituitary. *Life Sci* **1982,** *31*, 1769-1772.

6.   Aldrich, J. V.; Vigil-Cruz, S. C., Narcotic Analgesics. In *Burger's Medicinal Chemistry & Drug Discovery*, Abraham, D. J., Ed. John Wiley and Sons: New York, 2003; Vol. 6, pp 329-481.

7.   Rezvani, A.; Hollt, V.; Way, E. L. K receptor activities of the three opioid peptide families. *Life Sci* **1983,** *33 Suppl 1*, 271-274.

8.   James, I. F.; Fischli, W.; Goldstein, A. Opioid receptor selectivity of dynorphin gene products. *J Pharmacol Exp Ther* **1984,** *228*, 88-93.

9.   Oka, T.; Negishi, K.; Suda, M.; Matsumiya, T.; Inazu, T.; Ueki, M. Rabbit vas deferens: a specific bioassay for opioid kappa-receptor agonists. *Eur J Pharmacol* **1981,** *73*, 235-236.

10.   Gintzler, A. R.; Hyde, D. Multiple opiate receptors in the guinea pig enteric nervous system: unmasking the copresence of receptor subtypes. *Proc Natl Acad Sci U S A* **1984,** *81*, 2252-2254.

11.   Suda, M.; Nakao, K.; Yoshimasa, T.; Ikeda, Y.; Sakamoto, M.; Yanaihara, C.; Yanaihara, N.; Numa, S.; Imura, H. Comparison of the action of putative endogenous kappa-agonists, leumorphin and rimorphin in vitro. *Life Sci* **1983,** *33 Suppl 1*, 275-278.

12.   Garzon, J.; Sanchez-Blazquez, P.; Hollt, V.; Lee, N. M.; Loh, H. H. Endogenous opioid peptides: comparative evaluation of their receptor affinities in the mouse brain. *Life Sci* **1983,** *33 Suppl 1*, 291-294.

13.   Merg, F.; Filliol, D.; Usynin, I.; Bazov, I.; Bark, N.; Hurd, Y. L.; Yakovleva, T.; Kieffer, B. L.; Bakalkin, G. Big dynorphin as a putative endogenous ligand for the kappa-opioid receptor. *J Neurochem* **2006,** *97*, 292-301.

14.   Chavkin, C.; James, I. F.; Goldstein, A. Dynorphin is a specific endogenous ligand of the kappa opioid receptor. *Science* **1982,** *215*, 413-415.

15.   Faden, A. I. Opioid and nonopioid mechanisms may contribute to dynorphin's pathophysiological actions in spinal cord injury. *Ann Neurol* **1990,** *27*, 67-74.

16.   Shukla, V. K.; Lemaire, S. Non-opioid effects of dynorphins: possible role of the NMDA receptor. *Trends Pharmacol Sci* **1994,** *15*, 420-424.

17.   Walker, J. M.; Moises, H. C.; Coy, D. H.; Baldrighi, G.; Akil, H. Nonopiate effects of dynorphin and des-Tyr-dynorphin. *Science* **1982,** *218*, 1136-1138.

18.   Long, J. B.; Rigamonti, D. D.; de Costa, B.; Rice, K. C.; Martinez-Arizala, A. Dynorphin A-induced rat hindlimb paralysis and spinal cord injury are not altered by the kappa opioid antagonist nor-binaltorphimine. *Brain Res* **1989,** *497*, 155-162.

19.   Herman, B. H.; Goldstein, A. Antinociception and paralysis induced by intrathecal dynorphin A. *J Pharmacol Exp Ther* **1985,** *232*, 27-32.

20.   Long, J. B.; Petras, J. M.; Mobley, W. C.; Holaday, J. W. Neurological dysfunction after intrathecal injection of dynorphin A (1-13) in the rat. II. Nonopioid mechanisms mediate loss of motor, sensory and autonomic function. *J Pharmacol Exp Ther* **1988,** *246*, 1167-1174.

21.   Stevens, C. W.; Yaksh, T. L. Dynorphin A and related peptides administered intrathecally in the rat: a search for putative kappa opiate receptor activity. *J Pharmacol Exp Ther* **1986,** *238*, 833-838.

22.   Isaac, L.; Van Zandt O'Malley, T.; Ristic, H.; Stewart, P. MK-801 blocks dynorphin A (1-13)-induced loss of the tail-flick reflex in the rat. *Brain Res* **1990,** *531*, 83-87.

23.   Tan-No, K.; Esashi, A.; Nakagawasai, O.; Niijima, F.; Tadano, T.; Sakurada, C.; Sakurada, T.; Bakalkin, G.; Terenius, L.; Kisara, K. Intrathecally administered big dynorphin, a prodynorphin-derived peptide, produces nociceptive behavior through an *N*-methyl-D-aspartate receptor mechanism. *Brain Res* **2002,** *952*, 7-14.

24.   Laughlin, T. M.; Vanderah, T. W.; Lashbrook, J.; Nichols, M. L.; Ossipov, M.; Porreca, F.; Wilcox, G. L. Spinally administered dynorphin A produces long-lasting allodynia: involvement of NMDA but not opioid receptors. *Pain* **1997,** *72*, 253-260.

25.   Vanderah, T. W.; Laughlin, T.; Lashbrook, J. M.; Nichols, M. L.; Wilcox, G. L.; Ossipov, M. H.; Malan, T. P., Jr.; Porreca, F. Single intrathecal injections of dynorphin A or des-Tyr-dynorphins produce long-lasting allodynia in rats: blockade by MK-801 but not naloxone. *Pain* **1996,** *68*, 275-281.

26.   Cavicchini, E.; Candeletti, S.; Spampinato, S.; Ferri, S. Hypothermia elicited by some prodynorphin-derived peptides: opioid and non-opioid actions. *Neuropeptides* **1989,** *14*, 45-50.

27.   Faden, A. I.; Molineaux, C. J.; Rosenberger, J. G.; Jacobs, T. P.; Cox, B. M. Endogenous opioid immunoreactivity in rat spinal cord following traumatic injury. *Ann Neurol* **1985,** *17*, 386-390.

28.   Faden, A. I.; Molineaux, C. J.; Rosenberger, J. G.; Jacobs, T. P.; Cox, B. M. Increased dynorphin immunoreactivity in spinal cord after traumatic injury. *Regul Pept* **1985,** *11*, 35-41.

29.   Cox, B. M.; Molineaux, C. J.; Jacobs, T. P.; Rosenberger, J. G.; Faden, A. I. Effects of traumatic injury on dynorphin immunoreactivity in spinal cord. *Neuropeptides* **1985,** *5*, 571-574.

30.   Malan, T. P.; Ossipov, M. H.; Gardell, L. R.; Ibrahim, M.; Bian, D.; Lai, J.; Porreca, F. Extraterritorial neuropathic pain correlates with multisegmental elevation of spinal dynorphin in nerve-injured rats. *Pain* **2000,** *86*, 185-194.

31.   Tan-No, K.; Cebers, G.; Yakovleva, T.; Hoon Goh, B.; Gileva, I.; Reznikov, K.; Aguilar-Santelises, M.; Hauser, K. F.; Terenius, L.; Bakalkin, G. Cytotoxic effects of dynorphins through nonopioid intracellular mechanisms. *Exp Cell Res* **2001,** *269*, 54-63.

32.   Hauser, K. F.; Knapp, P. E.; Turbek, C. S. Structure-activity analysis of dynorphin A toxicity in spinal cord neurons: intrinsic neurotoxicity of dynorphin A and its carboxyl-terminal, nonopioid metabolites. *Exp Neurol* **2001,** *168*, 78-87.

33.   Faden, A. I. Neurotoxic versus neuroprotective actions of endogenous opioid peptides: Implications for treatment of CNS injury. *NIDA Res. Mongr.* **1996,** *163*, 318-330.

34.   Hauser, K. F.; Foldes, J. K.; Turbek, C. S. Dynorphin A (1-13) neurotoxicity in vitro: opioid and non-opioid mechanisms in mouse spinal cord neurons. *Exp Neurol* **1999,** *160*, 361-375.

35.   Long, J. B.; Martinez-Arizala, A.; Echevarria, E. E.; Tidwell, R. E.; Holaday, J. W. Hindlimb paralytic effects of prodynorphin-derived peptides following spinal subarachnoid injection in rats. *Eur J Pharmacol* **1988,** *153*, 45-54.

36.   Hugonin, L.; Vukojevic, V.; Bakalkin, G.; Graslund, A. Membrane leakage induced by dynorphins. *FEBS Lett* **2006,** *580*, 3201-3205.

37.   Lind, J.; Graslund, A.; Maler, L. Membrane interactions of dynorphins. *Biochemistry* **2006,** *45*, 15931-15940.

38.   Schiller, P. W.; Weltrowska, G.; Nguyen, T. M.; Lemieux, C.; Chung, N. N.; Lu, Y. Conversion of delta-, kappa- and mu-receptor selective opioid peptide agonists into delta-, kappa- and mu-selective antagonists. *Life Sci* **2003,** *73*, 691-698.

39.   Sole, N. A. B., G. Optimization of Solid-Phase Synthesis of [Ala^8]-Dynorphin A. *J. Org. Chem.* **1992,** *57*, 5399-5403.

40.   Turcotte, A.; Lalonde, J. M.; St-Pierre, S.; Lemaire, S. Dynorphin-(1-13). I. Structure-function relationships of Ala-containing analogs. *Int J Pept Protein Res* **1984,** *23*, 361-367.

41.   Gillan, M. G.; Kosterlitz, H. W. Spectrum of the mu, delta- and kappa-binding sites in homogenates of rat brain. *Br J Pharmacol* **1982,** *77*, 461-469.

42.   Arttamangkul, S.; Ishmael, J. E.; Murray, T. F.; Grandy, D. K.; DeLander, G. E.; Kieffer, B. L.; Aldrich, J. V. Synthesis and opioid activity of conformationally constrained dynorphin A

analogues. 2. Conformational constraint in the "address" sequence. *J Med Chem* **1997,** *40*, 1211-1218.

43.   Cheng, Y.; Prusoff, W. H. Relationship between the inhibition constant (K1) and the concentration of inhibitor which causes 50 per cent inhibition (I50) of an enzymatic reaction. *Biochem Pharmacol* **1973,** *22*, 3099-3108.

44.   Ross, N. C.; Reilley, K. J.; Murray, T. F.; Aldrich, J. V.; McLaughlin, J. P. Novel opioid cyclic tetrapeptides: Trp isomers of CJ-15,208 exhibit distinct opioid receptor agonism and short-acting kappa opioid receptor antagonism. *Br J Pharmacol* **2012,** *165*, 1097-1108.

Chapter 4 - Structure-activity relationships of Zyklophin – A systemically active, selective kappa opioid receptor antagonist.

*Compound numbers in this chapter are applicable only to this chapter

4.1 Introduction

Kappa (κ) opioid receptors (KOR) are one of the three types of opioid receptors.[1] KOR agonists can produce analgesia with less addiction liability and respiratory depression than mu (μ) opioid receptor (MOR) agonists,[2, 3] but they can also produce dysphoria.[4] KOR antagonists were initially used only as pharmacological tools, but recently their potential therapeutic uses in the treatment of depression,[5-8] anxiety[8-10] and opiate and cocaine addiction [6, 8, 11, 12] have been recognized.

Previously different [N-alkyl-Tyr[1],D-Pro[10]]Dyn A(1-11)NH$_2$ analogs were explored in our laboratory.[13, 14] The monoalkylated analogs showed comparable affinities and higher KOR selectivities vs. MOR and δ opioid receptor (DOR) as compared to the parent peptide [D-Pro[10]]Dyn A(1-11)NH$_2$. In the guinea pig ileum (GPI) assay the N-benzyl analog displayed lower agonist potency than other N-alkyl derivatives, despite its high affinity for KOR. While the monosubstituted analogs displayed full agonism in the GPI assay, the N-benzyl analog displayed partial agonism in the adenylyl cyclase (AC) assay (>70%).[15] A series of (5,8) cyclic Dyn A(1-13)NH$_2$ analogs with varying ring sizes were previously synthesized in our laboratory and all of them displayed very low agonist potencies in the GPI assay.[16] Based on these studies, the dynorphin (Dyn) A(1-11)NH$_2$ based KOR selective peptide antagonist zyklophin (Figure 4.1) was designed and synthesized in our laboratory.[17] Zyklophin is a cyclic Dyn A analog with a lactam bridge between D-Asp and 2,3-diaminopropionic acid (Dap) in positions 5 and 8, respectively, and a benzyl group on the N-terminal Tyr.

Tyr-Gly-Gly-Phe-Leu-Arg-Arg-Ile-Arg-Pro-Lys-NH$_2$
Dyn A(1-11)NH$_2$

*N*Benzyl-Tyr-Gly-Gly-Phe-D-Asp-Arg-Arg-Dap-Arg-Pro-Lys-NH$_2$

‖   —NH

O
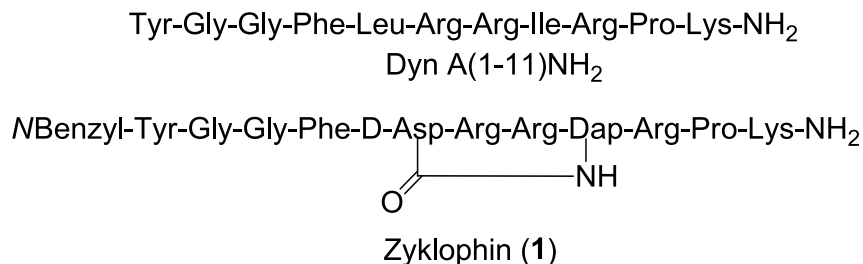
Zyklophin (**1**)

Figure 4.1 Structures of Dyn A(1-11)NH$_2$ and zyklophin (**1**)

Zyklophin displayed negligible efficacy (<10% maximum inhibition relative to Dyn A-(1-13)NH$_2$) in the AC assay and was found to be an antagonist at KOR in this assay.[17] It was subsequently found to be a selective KOR antagonist *in vivo*, with a finite duration of activity (12-18 h).[18] Following peripheral subcutaneous administration, zyklophin antagonized the antinociceptive activity of the centrally administered KOR agonist U50,488, suggesting that this peptide crossed the blood-brain barrier (BBB) to act on KOR in the CNS.[18] This peptide also suppressed stress-induced reinstatement of cocaine seeking behavior in mice following systemic administration, suggesting its potential as a lead compound for the development of therapeutics for the treatment of cocaine addiction.[18]

We are interested in exploring the structure-activity relationships (SAR) of zyklophin in order to examine its potential interactions with KOR and enhance its antagonist potency. We explored the effect of different alkyl substituents at the N-terminus Tyr on the receptor affinity and activity of zyklophin (Figure 4.2). We hypothesized that the N-terminal alkyl group might affect the interactions of the rest of the peptide with KOR, and therefore the ability of zyklophin to bind to the receptor without activating it.

Initial pharmacological findings from the AC assay suggested that modifications in the C-terminus, except those in positions 5 and 8, did not affect the efficacy of [*N*-benzyl]Dyn A(1-11)NH$_2$[19] and the modifications in positions 5 and 8 along with the *N*-terminal alkylation are

responsible for the lack of efficacy of zyklophin.[17] Hence we explored which of these residue(s) were responsible for the lack of efficacy of zyklophin (Figure 4.2). Based on the "message-address" concept[20] we expected that the residue in position 5 would play a major role in contributing to the lack of efficacy of zyklophin. In addition, we explored the role of ring size and residues involved in the cyclic constraint on the KOR interactions and the antagonist activity of zyklophin. We synthesized several cyclic analogs including ring variants analogs (Figure 4.2). We also investigated the role of different residues on the KOR affinity and activity of zyklophin. Hence, we performed an Ala scan of the non-glycine residues, excluding residues 5 and 8, up through residue 9 of zyklophin. In addition, to explore the importance of the phenolic group of Tyr[1] on the activity of zyklophin we synthesized the Phe[1] analog of zyklophin (Figure 4.2).

4.1.1 Analogs of zyklophin

A) Linear analogs

   2   *N*Benzyl-Tyr^1-Gly-Gly-Phe-**DAsn^5**-Arg-Arg-**Ile**-Arg-Pro-Lys-NH$_2$

   3   *N*Benzyl-Tyr^1-Gly-Gly-Phe-**Leu**-Arg-Arg-**Dap(Ac)^8**-Arg-Pro-Lys-NH$_2$

B) Cyclic analogs

$$\overset{R^1}{\underset{R^2}{}}\!\!\text{—Tyr}^1\text{-Gly-Gly-Phe}^4\text{-}\mathbf{X}^5\text{-Arg}^6\text{-Arg}^7\text{-}\mathbf{Y}^8\text{-Arg}^9\text{-Pro-Lys-NH}_2$$

with ring closure: $O=C$ —— NH
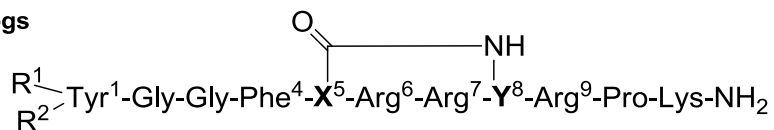
	R^1	R^2	X^5	Y^8	Other substitutions
1 (Zyklophin)	Benzyl	H	D-Asp	Dap	
N-terminal modifications					
4	**Ph-CH$_2$-CH$_2$**	H	D-Asp	Dap	
5	**CH$_2$=CH-CH$_2$**	H	D-Asp	Dap	
6	**Me**	H	D-Asp	Dap	
7	**CPM**	H	D-Asp	Dap	
8	**Benzyl**	**Me**	D-Asp	Dap	
9	**Benzoyl**	H	D-Asp	Dap	
Amino acid substitutions					
10	Benzyl	H	D-Asp	Dap	**Ala^1**
11	Benzyl	H	D-Asp	Dap	**Ala^4**
12	Benzyl	H	D-Asp	Dap	**Ala^6**
13	Benzyl	H	D-Asp	Dap	**Ala^7**
14	Benzyl	H	D-Asp	Dap	**Ala^9**
15	Benzyl	H	D-Asp	Dap	**Phe^1**
Ring variants					
16	Benzyl	H	D-Asp	**Dab**	
17	Benzyl	H	D-Asp	**Orn**	
18	Benzyl	H	**L-Asp**	Dap	

Figure 4.2 Analogs of zyklophin; changes from zyklophin are bolded.

4.2 Results and discussion

    The synthesis of the analogs of zyklophin involved synthesis of the N-terminal *N*-alkyl amino acid derivatives in solution and solid phase assembly of the (2-11) peptide fragments. Finally the appropriate *N*-alkyl amino acid derivatives were coupled to the (2-11) peptide fragments followed by cleavage of the peptides from the resin.

4.2.1 Amino acid syntheses

The *N*-alkyl amino acid derivatives were generally synthesized by subjecting the amino acid *t*-butyl ester to reductive amination with the appropriate aldehyde and sodium triacetoxyborohydride to yield the *N*-alkyl amino acid *t*-butyl ester, which was subsequently cleaved with 90% trifluoroacetic acid (TFA) and 10% water to yield the *N*-alkyl amino acid. Almost all of the *N*-alkyl-Tyr derivatives (Scheme 4.1a) and *N*-benzyl-Ala (Scheme 4.1d) were synthesized according to this procedure. The one exception was *N*-allyl-Tyr (Scheme 4.1b) which was prepared by alkylating H-Tyr-O*t*Bu with 1 equivalent of allyl bromide (to minimize diallylation) in the presence of *N,N*-diisopropylethylamine (DIEA) in *N,N*-dimethylformamide (DMF) followed by subsequent cleavage of the *t*-butyl ester with 90% TFA and 10% water. For the synthesis of *N*-benzyl,*N*-methyl-Tyr (Scheme 4.1e), H-Tyr(*t*Bu)-O*t*Bu was subjected to reductive amination with benzaldehyde and sodium triacetoxyborohydride to yield *N*-benzyl-Tyr(*t*Bu)-O*t*Bu, which was subsequently treated with triphenylphosphine (TPP), iodomethane and diisopropyl azodicarboxylate (DIAD) in tetrahydrofuran (THF)[21] to obtain *N*-benzyl-*N*-methyl-Tyr(*t*Bu)-O*t*Bu. The *t*-butyl ester and ether of the dialkylated product were cleaved with 90% TFA and 10% water to obtain *N*-benzyl-*N*-methyl-Tyr-OH.

N-Benzyl-Tyr exhibited low solubility in DMF at RT and required heating to 85°C for solubilization. While microwave couplings are routinely performed at ≥ 75°C, racemization at elevated temperatures could be a potential issue during coupling of *N*-alkyl amino acids to the (2-11) peptide. To prevent this potential problem, selected *N*-alkyl-amino acid derivatives, namely *N*-CPM-Tyr-O*t*Bu and *N*-benzyl-Phe-O*t*Bu, were treated with allyl chloroformate and DIEA in methylene chloride (DCM) to afford the Alloc (allyloxycarbonyl) protected *N*-alkyl amino acid esters (Scheme 1c). In the case of *N*-CPM-Tyr-O*t*Bu the *bis*-Alloc derivative was

obtained. The ester derivatives were subsequently cleaved with 90% TFA/10% DCM to afford the Alloc-protected amino acids (Scheme 4.1c). Unlike the unprotected *N*-alkyl amino acids, the Alloc-protected amino acids were readily soluble in DMF at RT. This avoided heating and potential racemization of the amino acids during coupling (see section 4.2.3 below)

Scheme 4.1 Synthesis of amino acid derivatives:

a) Synthesis of *N*-alkyl-Tyr derivatives by reductive amination:

L-Tyr, R = Ph, **20a** (80%)
D-Tyr, R = Ph, **20b** (55%)
L-Tyr, R = PhCH$_2$, **21** (66%)

L-Tyr, R = Ph, **22a** (68%)
D-Tyr, R = Ph, **22b** (49%)
L-Tyr, R = PhCH$_2$, **23** (65%)
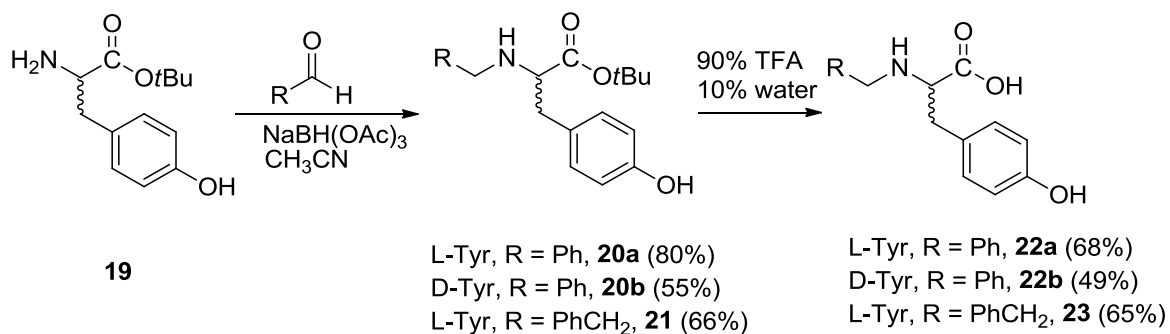
b) Synthesis of *N*-allyl-Tyr:
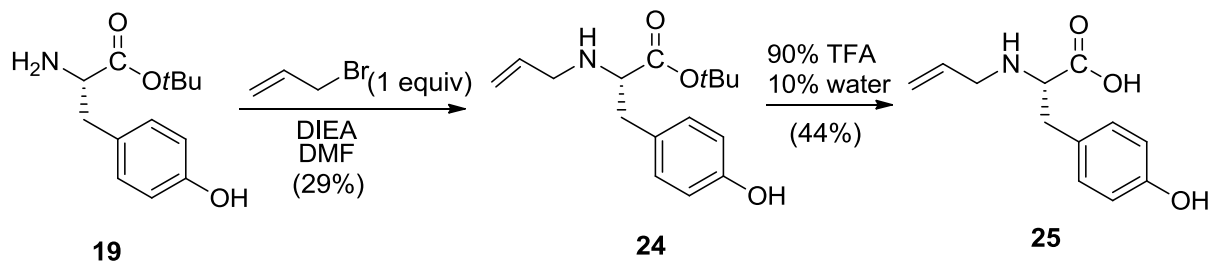
c) Synthesis of Alloc-*N*-cyclopropylmethyl-Tyr(Alloc)-OH and Alloc-*N*-benzyl-Phe-OH:

X = OH, **19**
X = H, **26**

X = OH, R = CPM, **27** (55%)
X = H, R = benzyl, **28** (44%)

X = OAlloc, R = CPM, **29** (73%)
X = H, R = benzyl, **30** (65%)

X = OAlloc, R = CPM, **31** (94%)
X = H, R = benzyl, **32** (98%)
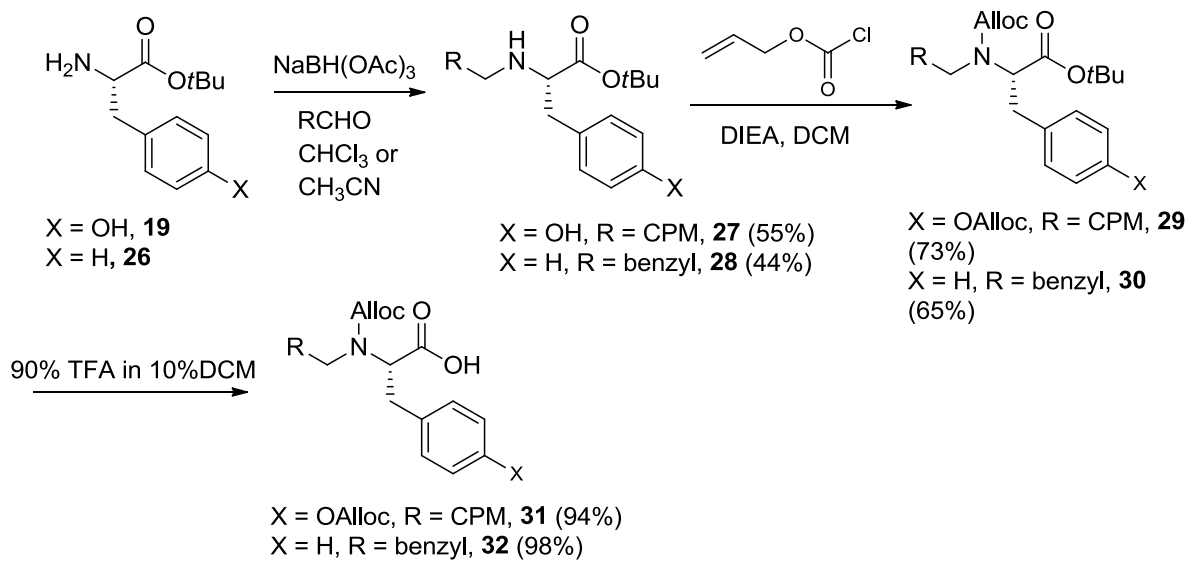
d) Synthesis of *N*-benzyl-Ala:

33 (39%)

34

R = Ph
35

e) Synthesis of *N*-benzyl-*N*-methyl-Tyr:

36

37

38

39
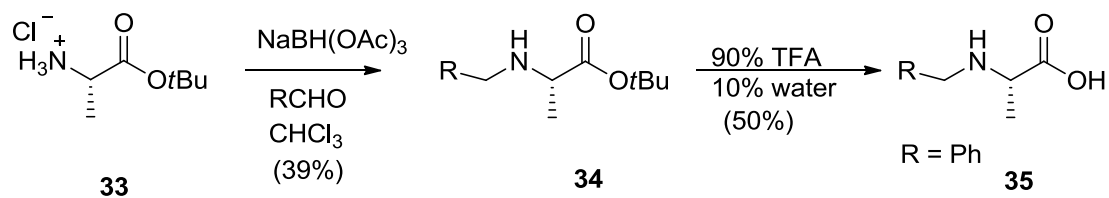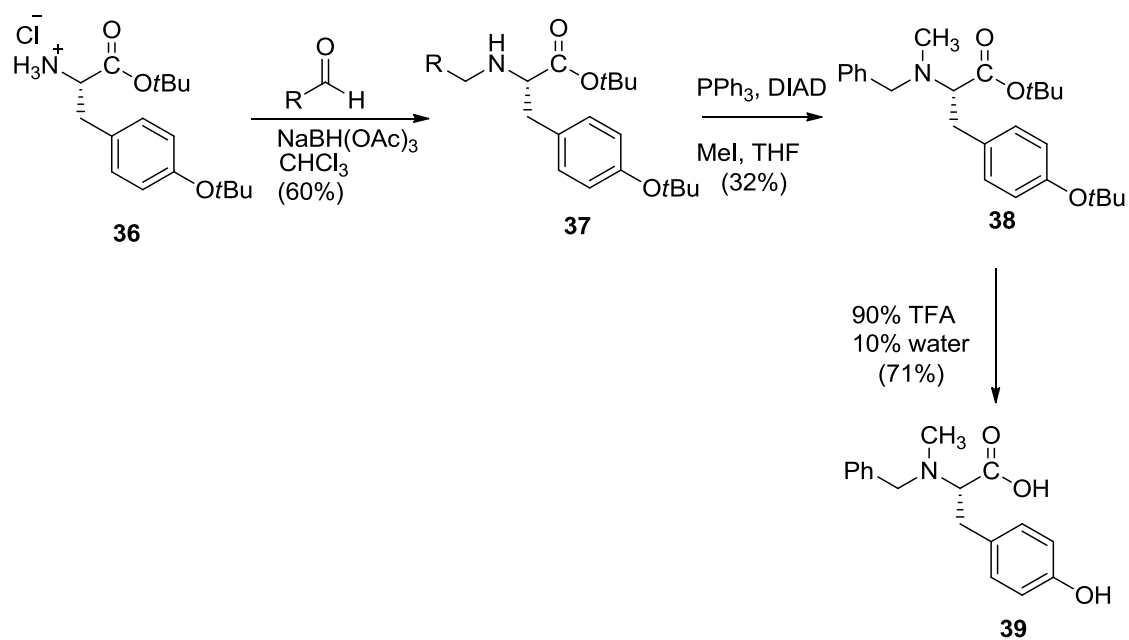
4.2.2 Peptide synthesis

The peptides were synthesized using the Fmoc (9-fluorenylmethoxycarbonyl) solid phase synthetic strategy. The (2-11) peptide fragments were assembled on a low load poly(ethylene glycol)-polystyrene (PEG-PS) resin containing the peptide amide linker [PAL, 5-(4-aminomethyl-3,5-dimethoxyphenoxy)valeric acid linker] using benzotriazol-1-yl-oxytripyrrolidinophosphonium hexafluorophosphate (PyBOP), 1-hydroxybenzotriazole (HOBt) (4 equiv. each) and DIEA (10 equiv.) in DCM:DMF (1:1) to couple the Fmoc-amino acids (4 equiv) to the growing peptide chain on a manual peptide synthesizer (CHOIR).[22] The side chain protecting groups used were Pbf (2,2,4,6,7-pentamethyl dihydrobenzofurane-5-sufonyl) and Boc (*tert*-butyloxycarbonyl) for Arg and Lys, respectively.

For the synthesis of selected linear analogs, the (2-11) linear peptide precursors of the peptides **2** and **3** were synthesized similar to the above procedure (Scheme 4.2a). The side chains of D-Asn in peptide **2** and Dap (Dap = 2,3-diaminopropionic acid) in peptide **3** were protected by trityl (Trt) and 4-methyltrityl (Mtt), respectively. For peptide **3**, following the synthesis of the (2-11) linear fragment, the Mtt protecting group on Dap was selectively deprotected by 3% TFA and 5% triisopropylsilane (TIS) in DCM, and the resulting amine was acetylated using acetyl imidazole in DMF (Scheme 4.2a).

The (2-11) fragments of the cyclic peptides **4-10** and **15-18** were synthesized by a similar approach (see Scheme 4.2b). The D-Asp and Dap residues in positions 5 and 8 were protected with the hyperacid labile 2-phenylisopropyl (Pip) and Mtt groups, respectively. Following the synthesis of the (5-11) fragments, the Pip and Mtt groups were deprotected by 3% TFA and 5% TIPS in DCM. Subsequently, the carboxyl group of D-Asp^5 and the amine of Dap^8 were cyclized using 6-chloro-benzotriazole-1-yl-oxy-tris-pyrrolidino-phosphonium hexafluorophosphate

(PyClocK) and 1-hydroxy-7-azabenzotriazole (HOAt) (4 equiv. each) with DIEA (10 equiv) in a mixture of DCM:DMF (1:1), generally for 20-24 h. The cyclizations were monitored using the qualitative ninhydrin test. Any remaining unreacted free amine of Dap was acetylated by treatment with acetyl imidazole and DIEA in DMF. Further extension of the peptide up to Gly^2 afforded the (2-11) fragments of the cyclic peptides.

For the synthesis of peptides **16** and **17,** Dab(Mtt) and Orn(Mtt) were incorporated in position 8, respectively and for peptide **18** L-Asp(OPip) was incorporated in position 5. In the case of these three peptides the cyclizations required longer reaction times (~ 36 h) to go to completion.

Scheme 4.2 Solid phase synthesis of (2-11) peptide fragments:

a) Synthesis of the 2-11 fragment of peptide **3 :**

b) Synthesis of the 2-11 fragments of the cyclic peptides **4-10** and **15-18**.

Fmoc-NH-PAL-PEG-PS

Fmoc deprotection and coupling cycles

OPip   Mtt

Fmoc--X-Arg-Arg-Y-Arg-Pro-Lys-NH-PAL-PEG-PS

         Pbf Pbf   Pbf   Boc

X = D-Asp, L-Asp
Y = Dap, Orn, Dab

1) 3% TFA, 5% TIPS in DCM
2) PyClocK, HOAt and
    DIEA, DMF:DCM (1:1)
3) acetyl imidazole, DIEA, DMF

O   —NH

Fmoc-X-Arg-Arg-Y-Arg-Pro-Lys- NH-PAL-PEG-PS

        Pbf Pbf   Pbf   Boc

Fmoc deprotection and coupling cycles

O   —NH

H-Gly-Gly-Phe-X-Arg-Arg-Y-Arg-Pro-Lys-NH-PAL-PEG-PS

              Pbf Pbf   Pbf   Boc
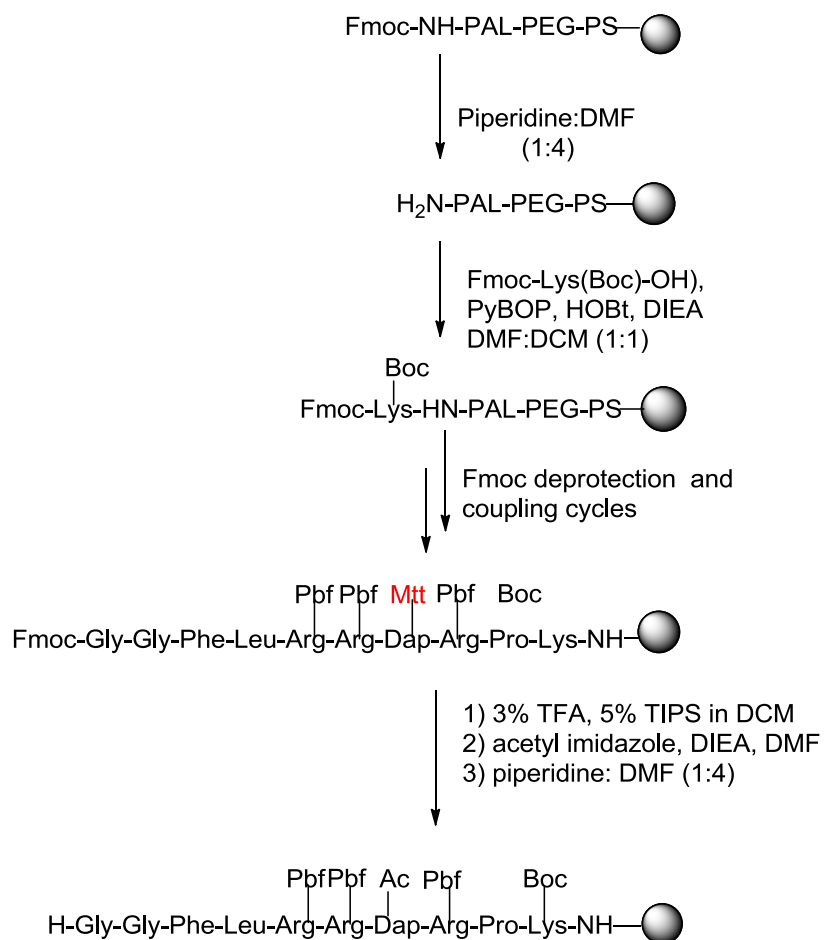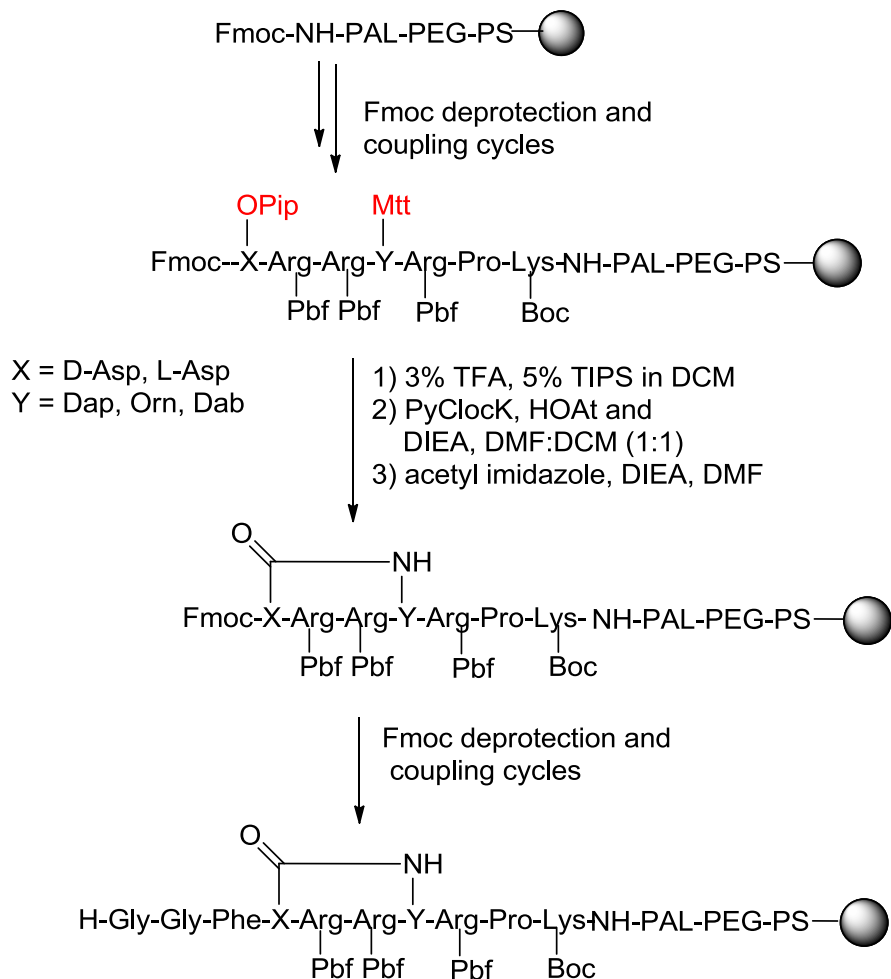
4.2.3   Coupling of *N*-alkyl amino acid derivatives to the (2-11) peptide fragment

The coupling of the N-terminal amino acid derivatives to the resin-bound (2-11) peptide sequences was carried out using PyClocK, HOAt and DIEA in DMF. *N*-Benzyl-Tyr required heating to 80-85°C to solubilize in DMF prior to coupling. *N*-Benzyl-Tyr/Ala solutions were allowed to cool, followed by addition of the coupling reagents and base, and then the activated amino acid was coupled to the (2-11) peptide fragment. The peptides having an N-terminal benzyl group, except for peptide **15,** were prepared by this procedure.

Scheme 4.3 Scheme for coupling of *N*-alkyl-Tyr to the (2-11) peptide fragment and cleavage from the resin
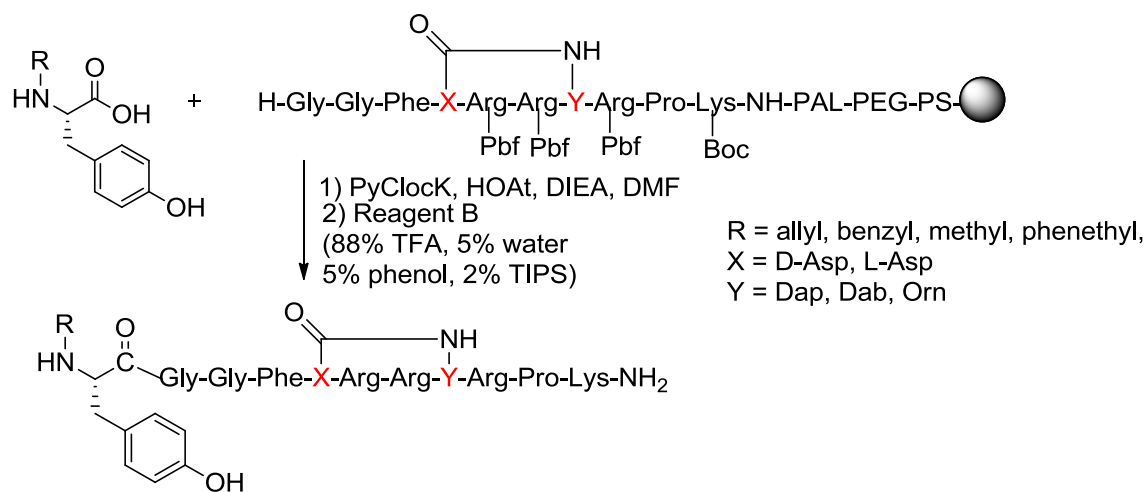
The *N*-allyl and *N*-phenethyl Tyr derivatives required higher temperatures (above ~100°C) to obtain complete dissolution. After allowing the solutions to cool they became turbid and hence the coupling agents were added to solutions while they were still hot with subsequent cooling and addition of the base, followed by coupling to the (2-11) fragment. In the case of peptide **7**, *N*-CPM-Tyr-OH did not couple to the (2-11) fragment, potentially due to its minimal solubility in DMF. In the case of peptide **15**, following coupling of *N*-benzyl-Phe-OH to the (2-11) fragment the final peptide showed a potential epimerization product (Figure 4.6 (a) below), suggesting *N*-benzyl-Phe-OH underwent racemization during heating or subsequent coupling to the (2-11) fragment (Figure 4.6 (a)). To avoid this potential side reaction and enhance the solubility of these *N*-alkyl amino acid derivatives, the Alloc-protected derivatives of *N*-CPM-Tyr-OH and *N*-benzyl-Phe-OH were prepared which were soluble in DMF at RT. Following coupling of the Alloc derivatives to the (2-11) peptide fragment on the resin, the Alloc group was removed by Pd(0) and phenylsilane.[23] In the case of peptide **6**, Fmoc-MeTyr(O*t*Bu)-OH, which

is soluble in DMF at RT, was coupled to the (2-11) peptide fragment for 12 h, followed by Fmoc deprotection. In the case of peptide **9**, Fmoc-Tyr(O*t*Bu)-OH was coupled to the (2-11) peptide fragment at RT by the standard coupling procedure, followed by Fmoc deprotection and subsequent acylation of the N-terminal of Tyr with benzoic anhydride in the presence of DIEA in DMF.

4.2.4   Investigation of racemization of N-terminal residue of zyklophin and analog 15 by HPLC analysis

Because dissolution of the *N*-alkyl amino acids required elevated temperature, potential racemization was a concern. We identified an HPLC solvent system that could separate the diastereomers of zyklophin. *N*-Benzyl-D-Tyr-OH was then synthesized as described above under the general procedure for amino acid synthesis. The *N*-benzyl-D-Tyr analog of zyklophin was synthesized by the procedure described for the zyklophin analogs. While a reversed phase high performance liquid chromatography (RP-HPLC) system using a gradient of 10-25% aqueous MeCN containing TFA over 30 min did not adequately resolve the diastereomeric mixture of zyklophin and [*N*-benzyl-D-Tyr[1]]zyklophin (Figure 4.3 (a)), a solvent system using a 1-21% gradient of aqueous 0.09M triethyammonium phosphate (pH = 2.5)[24] in MeCN over 40 min did successfully resolved the diastereomers of zyklophin (Figure 4.3 (b)). In addition, by increasing the concentration of one of the diastereomers in the co-injection mixture, we were able to verify the identities of the peaks for the individual diastereomers, with the D-Tyr analog of zyklophin eluting before the parent peptide zyklophin (Figure 4.4). Zyklophin synthesized by the above procedure that involved solubilization of *N*-benzyl Tyr at 85°C did not show detectable racemization when analyzed using the TEAP solvent system (Figure 4.5). This HPLC solvent

system served as a tool to detect potential racemization of the N-terminal residue during the synthesis of zyklophin and its analogs.
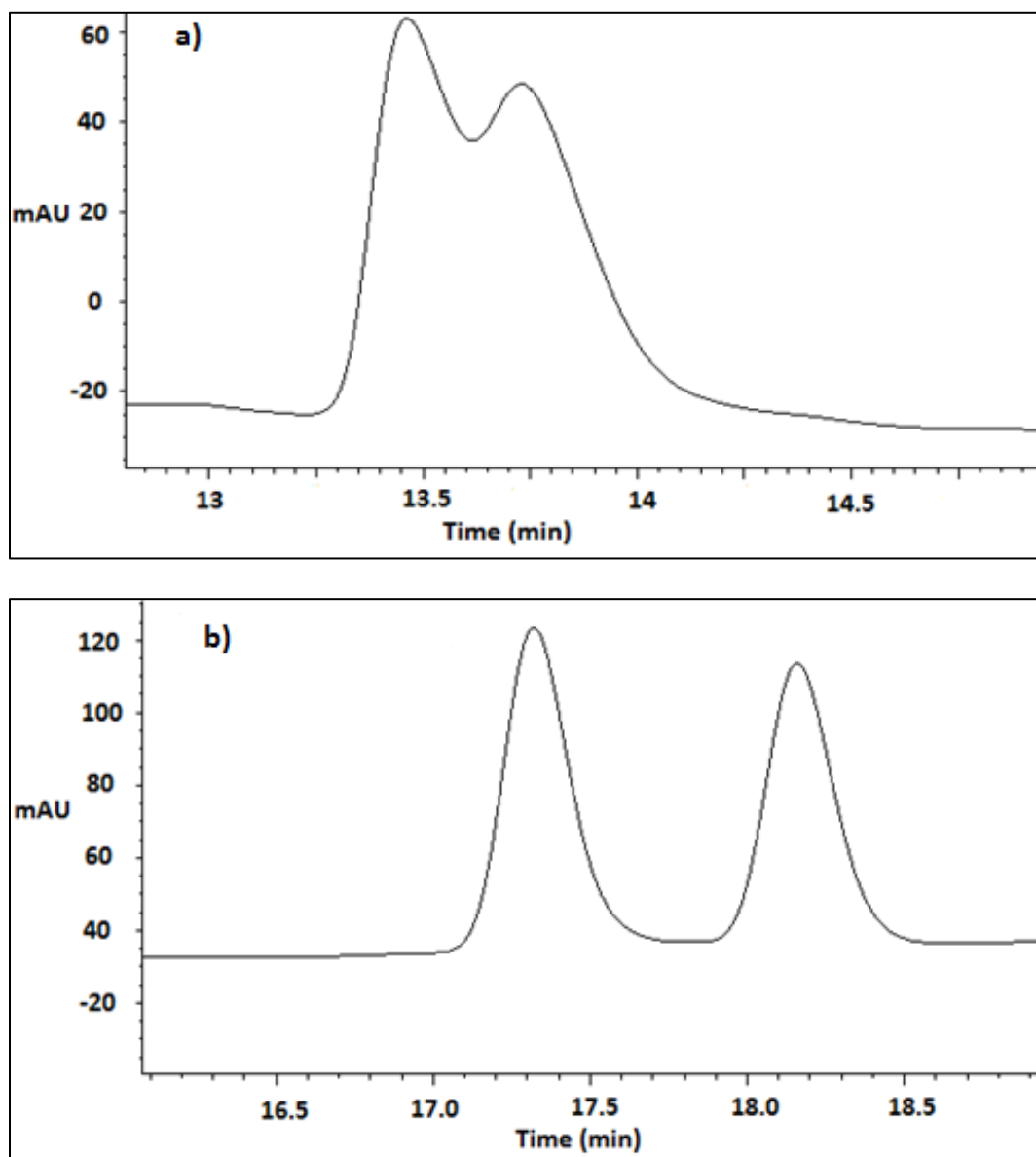
Figure 4.3 Coinjection of a diastereomeric mixture containing [*N*-benzyl D-Tyr[1]]zyklophin and zyklophin. a) a linear gradient of 10-25% solvent B (solvent A = aqueous 0.1% TFA and solvent B = MeCN containing 0.1% TFA) over 30 min. b) a linear gradient of 1-21% solvent B (solvent A = aqueous 0.09 M TEAP and solvent B= MeCN) over 40 min.
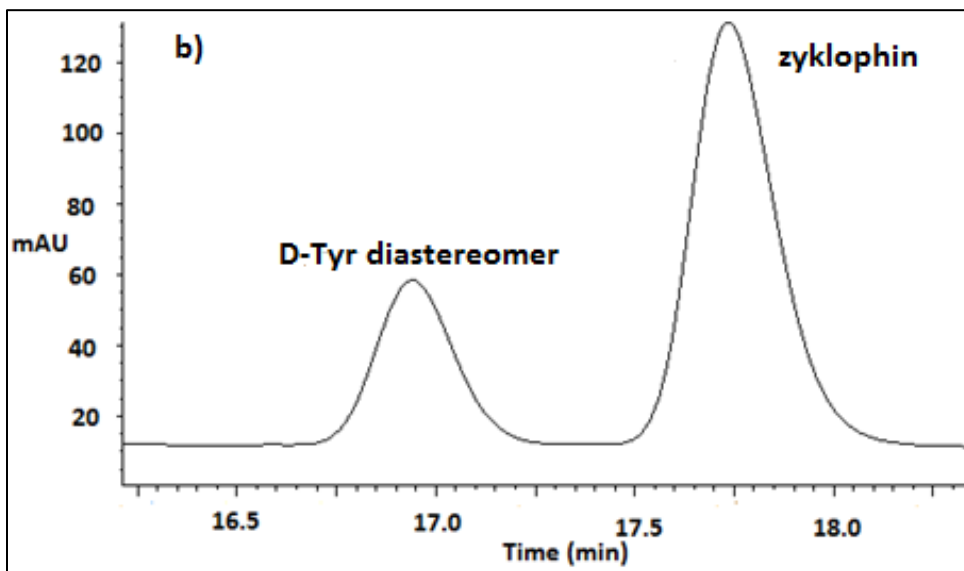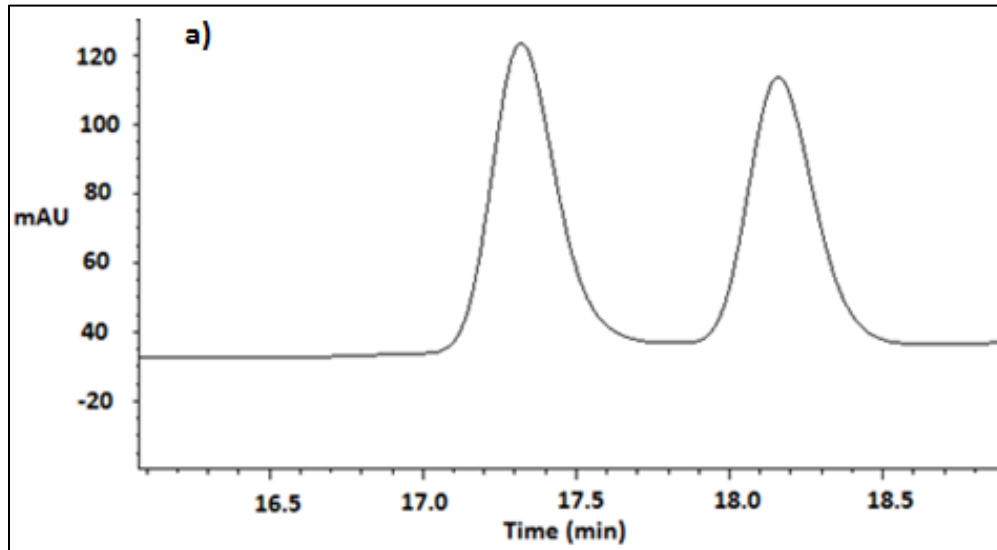
Figure 4.4 Coinjection of a diastereomeric mixture of [*N*-benzyl-D-Tyr[1]]zyklophin and zyklophin. a) a 1:1 mixture of the diastereomers, b) a mixture with a higher concentration of zyklophin. The coinjections were analyzed using a linear gradient of 1-21% solvent B (solvent A = aqueous 0.09 M TEAP and solvent B = MeCN) over 40 min. t_R for the D-Tyr diastereomer of zyklophin = 16.9 min and for parent zyklophin = 17.7 min

The Phe[1] analog of zyklophin, peptide **15**, however, displayed racemization of the N-terminal residue when synthesized by the general procedure that involved solubilization of *N*-

benzyl-Phe in DMF and subsequent coupling to the (2-11) peptide fragment. Figure 4.6 (a) shows that a mixture of two peaks A (17.5%) and B (82.5%) was obtained for the peptide synthesized by the standard method. However, when synthesized using Alloc-protected *N*-benzyl-Phe (Scheme 4.1c), peptide **15** did not show detectable epimerization of the N-terminal residue (Figure 6 (b)); only peak B was observed. In order to verify the identity of the peaks in Figure 4.6 (a), samples obtained by both the procedures were co-injected. The AUC ratio of peak B:peak A was higher in the co-injection chromatogram compared to that in Figure 6 (a), verifying that peak B was the desired product.
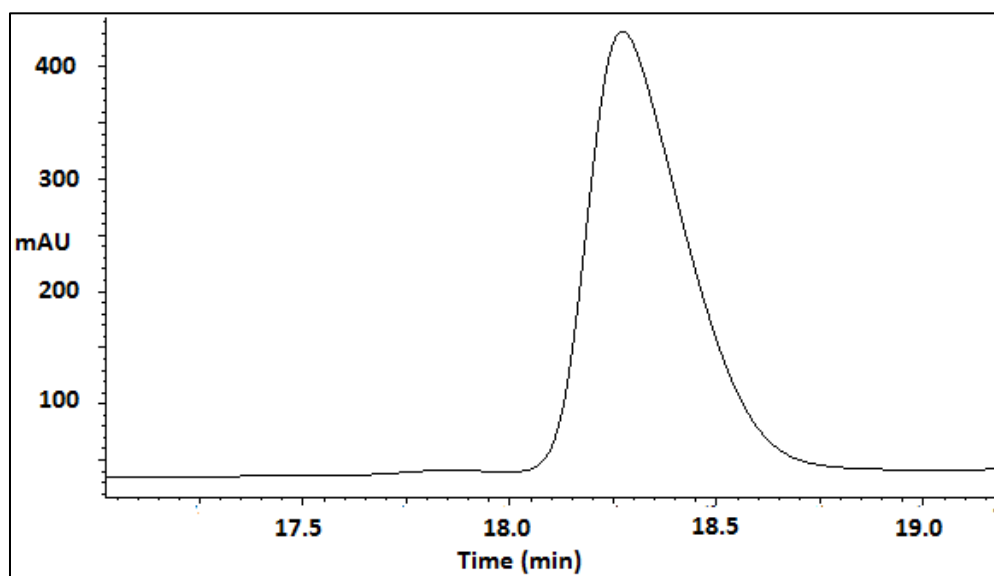
Figure 4.5 Zyklophin synthesized by standard procedure and analyzed using a linear gradient of 1-21% solvent B (solvent A = aqueous 0.09 M TEAP and solvent B = MeCN) over 40 min.

None of the peptides analyzed by system 3 (Table 4.1), except for peptide **15** showed racemization of the N-terminal residue. All of the peptides were purified by preparative RP-HPLC and analyzed by electrospray ionization mass spectroscopy (ESI-MS) and analytical RP-HPLC. The final purity of all of the peptides by all methods was ≥ 98%.
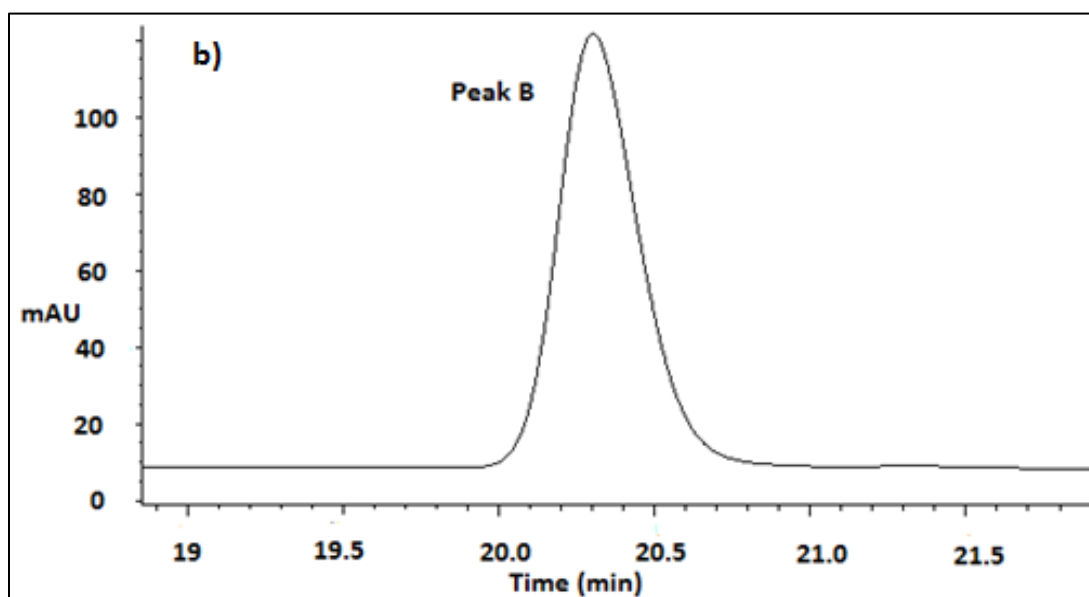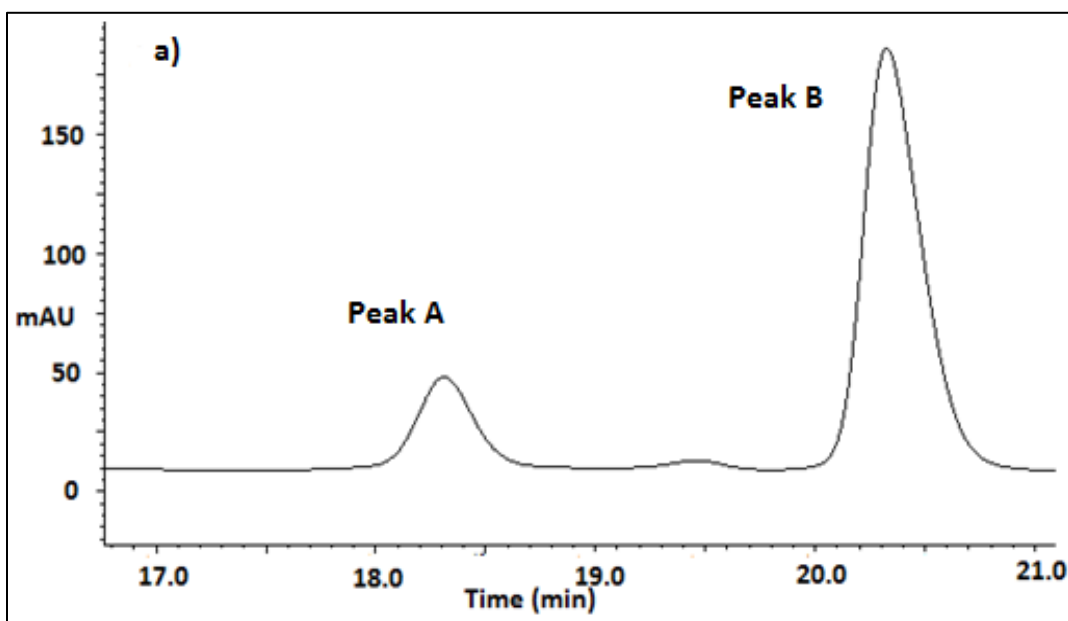
Figure 4.6 a) Peptide **15** synthesized by the general procedure. b) Peptide **15** synthesized using Alloc(benzyl)Phe. t_R for peak A = 18.3 min and peak B = 20.3 min.

Table 4.1 Analytical data for the peptides

Peptides	HPLC t_R (min)			ESI-MS(m/z)	
	System 1[a] (% Purity)	System 2[b] (% Purity)	System 3[c] (% Purity)	Calcd	obsd
2	15.4 (100)	18.0 (100)		$[M + 3H]^{3+} = 484.9$	$[M + 3H]^{3+} = 484.9$
				$[M + 2H]^{2+} = 726.9$	$[M + 2H]^{2+} = 726.9$
3	17.7 (99.4)	23.1 (100)		$[M + 3H]^{3+} = 489.6$	$[M + 3H]^{3+} = 489.6$
				$[M + 2H]^{2+} = 733.9$	$[M + 2H]^{2+} = 733.9$
4	17.0 (100)	15.3 (100)	21.52 (98.9)	$[M + 3H]^{3+} = 474.9$	$[M + 3H]^{3+} = 474.9$
5	12.1 (100)	14.2 (100)	11.9 (100)	$[M + 3H]^{3+} = 453.5$	$[M + 3H]^{3+} = 453.6$
				$[M + 2H]^{2+} = 679.8$	$[M + 2H]^{2+} = 679.9$
6	11.3 (100)	13.1 (99.4)		$[M + 3H]^{3+} = 444.9$	$[M + 3H]^{3+} = 444.9$
				$[M + 2H]^{2+} = 666.8$	$[M + 2H]^{2+} = 666.9$
7	13.1 (100)	14.4 (100)	13.5 (99.0)	$[M + 3H]^{3+} = 458.2$	$[M + 3H]^{3+} = 458.2$
				$[M + 2H]^{2+} = 686.8$	$[M + 2H]^{2+} = 686.8$
8	20.04 (99.6)	17.9 (100)	21.3 (100)	$[M + 3H]^{3+} = 474.9$	$[M + 3H]^{3+} = 474.9$
				$[M + 2H]^{2+} = 711.8$	$[M + 2H]^{2+} = 711.9$
9	18.1 (100)	23.3 (100)		$[M + 3H]^{3+} = 474.9$	$[M + 3H]^{3+} = 474.9$
				$[M + 2H]^{2+} = 711.8$	$[M + 2H]^{2+} = 711.9$
10	13.3 (100)	13.3 (100)	11.58 (100)	$[M + 3H]^{3+} = 439.5$	$[M + 3H]^{3+} = 439.6$
11	10.1 (100)	8.0 (100)		$[M + 3H]^{3+} = 444.9$	$[M + 3H]^{3+} = 444.9$
				$[M + 2H]^{2+} = 666.8$	$[M + 2H]^{2+} = 666.9$
12	15.1 (100)	18.4 (100)		$[M + 3H]^{3+} = 441.9$	$[M + 3H]^{3+} = 441.9$
				$[M + 2H]^{2+} = 662.3$	$[M + 2H]^{2+} = 662.4$
13	14.8 (100)	15.2 (98.9)		$[M + 3H]^{3+} = 441.9$	$[M + 3H]^{3+} = 441.9$
				$[M + 2H]^{2+} = 662.3$	$[M + 2H]^{2+} = 662.4$
14	14.8 (99.7)	14.6 (100)		$[M + 3H]^{3+} = 441.9$	$[M + 3H]^{3+} = 441.9$
				$[M + 2H]^{2+} = 662.3$	$[M + 2H]^{2+} = 662.3$
15	17.0 (98.1)	15.6 (100)	20.1 (98.7)	$[M + 3H]^{3+} = 464.9$	$[M + 3H]^{3+} = 464.9$
16	15.3 (100)	18.5 (100)		$[M + 3H]^{3+} = 474.9$	$[M + 3H]^{3+} = 474.9$
				$[M + 2H]^{2+} = 711.9$	$[M + 2H]^{2+} = 711.9$
17	15.1 (100)	18.1 (100)		$[M + 3H]^{3+} = 479.6$	$[M + 3H]^{3+} = 479.6$
				$[M + 2H]^{2+} = 718.9$	$[M + 2H]^{2+} = 718.9$
18	13.2 (99.1)	15.2 (99.0)		$[M + 3H]^{3+} = 470.2$	$[M + 3H]^{3+} = 470.2$
				$[M + 2H]^{2+} = 704.8$	$[M + 2H]^{2+} = 704.8$
1 (zyklophin)	13.32 (99.8)	16.9 (100)	18.3 (100)	$[M + 3H]^{3+} = 470.2$	$[M + 3H]^{3+} = 470.2$
				$[M + 2H]^{2+} = 704.8$	$[M + 2H]^{2+} = 704.8$

[a] Aqueous MeCN containing 0.1 % TFA; [b] aqueous MeOH containing 0.1 % TFA; [c] aqueous MeCN containing 0.09M triethyl ammonium phosphate (TEAP). See the experimental section for details.

4.3 Pharmacological results

The peptides were evaluated for affinity in radioligand binding assays using Chinese hamster ovary (CHO) cells stably expressing opioid receptors (Table 4.2). While peptide **2** had 2-fold lower KOR affinity, peptide **3** had 8-fold higher KOR affinity compared to zyklophin. This suggested that the residue in position 5 had a much larger influence on the KOR binding affinity of zyklophin than position 8. While zyklophin has a D-Asp involved in the lactam linkage at position 5, peptide **3** has L-Leu at position 5 as found in the endogenous Dyn A. Hence, the side chain of the residue at position 5 and/or changes in the backbone conformation of the peptide due to the difference in configuration at residue 5 are likely influencing the KOR affinity of the zyklophin analogs. While peptide **2** had low MOR affinity, peptide **3** had 30-fold higher MOR affinity compared to zyklophin thereby decreasing its KOR vs. MOR selectivity. Both linear analogs **2** and **3** displayed lower selectivity for KOR vs. MOR compared to zyklophin.

Sterically diverse alkyl groups ranging from methyl to phenethyl were incorporated at the N-terminus to examine their effect on the affinity, efficacy and potency of the zyklophin analogs. Peptides **4**-**7** had KOR affinities similar to or higher than zyklophin, suggesting that these *N*-alkyl modifications are tolerated by KOR. The *N*-CPM analog **7** had the highest KOR affinity, while the *N*-allyl analog **5** had the lowest KOR affinity among the *N*-alkylated analogs examined. Peptide **9** showed only slightly (<2-fold) lower KOR affinity compared to zyklophin, suggesting that a basic secondary amine at the N-terminus is not necessary for maintaining the affinity of zyklophin analogs at KOR. All of the analogs displayed low MOR affinity (K_i = >1000 nM). Thus while the MOR affinity of all the *N*-alkyl analogs did not vary much compared to zyklophin (except peptide **6** that displayed 4-fold increase in MOR affinity compared to

zyklophin) the increased KOR affinity of some analogs (**4** and **7**) resulted in an increase in their KOR vs. MOR selectivity.

Changes in the ring size of zyklophin were also well tolerated by KOR. Peptides **16** and **17** showed affinity within 2-fold that of zyklophin. Peptide **18** showed less than a 2-fold change in affinity, suggesting that a change in configuration at position 5 was also tolerated by KOR. Analogs **16-18** all displayed low affinity for MOR. The KOR vs. MOR selectivity of analogs **16** and **18** was lower while analog **17** showed slightly higher KOR vs. MOR selectivity compared to zyklophin. Hence, the KOR vs. MOR selectivity varied somewhat depending on the analog.

An alanine scan of zyklophin that included non-glycine residues from position 1 up through position 9, excluding residues in position 5 and 8, was also performed to identify residues important for the KOR binding of zyklophin. Peptide **10** displayed a 2.5-fold decrease in the KOR affinity compared to zyklophin, suggesting that Tyr in position 1 contributes to, but is not critical for, zyklophin's KOR affinity. Alanine substituted analogs **11** (Ala^4) and **12** (Ala^6) showed the largest decreases, 18- and 8-fold in KOR affinity, respectively, as compared to zyklophin, indicating that the residues in positions 4 and 6 are important for maintaining the binding affinity of zyklophin at KOR. Peptide **13** (Ala^7) showed a 3-fold increase in KOR affinity, while **14** (Ala^9) displayed KOR affinity comparable to zyklophin. This suggested that the positively charged residues in positions 7 and 9 are not important for the KOR binding affinity of zyklophin. The *N*-benzyl-Phe^1 analog **15** displayed a 2-fold increase in KOR affinity compared to zyklophin, indicating that the phenol of N-terminal Tyr^1 is not necessary to maintain the affinity of zyklophin for KOR.

Recently obtained KOR affinity values for zyklophin (K_i = 207 ± 12 nM) have been 7-fold higher compared to those earlier obtained originally (K_i = 30.3 ± 1.9 nM)[17] in the

radioligand binding assay. Similarly, the KOR binding affinity value obtained for Dyn A(1-11)NH$_2$ (K_i = 2.6 ± 0.3 nM) was 5 fold higher than those earlier obtained(K_i = 0.57 ± 0.01 nM).[19] These differences in the K_i values appear to be related to the CHO cells expressing the cloned KOR since aliquots of previously prepared peptides showed higher K_i values than those reported earlier.

Table 4.2 Opioid receptor binding affinities of the zyklophin analogs

Peptide	K_i (nM ± SEM)[a]		
	KOR	MOR	KOR/MOR
2 [D-Asn^5]	424 ± 52	2440 ± 570	1/6
3 [Dap(Ac)^8]	28.6 ± 0.6	189 ± 40	1/7
4 [*N*-Phenethyl]	118 ± 6	8470 ± 560	1/72
5 [*N*-Allyl]	336 ± 69	> 10000	1/26
6 [*N*-Me]	159 ± 18	1490 ± 410	1/9
7 [*N*-CPM]	88.8 ± 11.0	8570 ± 2220 (n=2)	1/96
8 [*N*-Benzyl, *N*-Me]		3520 ± 370	
9 [*N*-Benzoyl]	346 ± 21		
10 [Ala^1]	515 ± 82		
11 [Ala^4]	4010 ± 350	< 10000 (n=2)	1/>2.5
12 [Ala^6]	1750 ± 530		
13 [Ala^7]	66.5 ± 3.7		
14 [Ala^9]	172 ± 80	2550 ± 640	1/15
15 [Phe^1]	107 ± 10.0		
16 [Dab^8]	403 ± 91	3200 ± 850	1/8
17 [Orn^8]	222 ± 5	8180 ± 2640	1/37
18 [L-Asp^5]	409 ± 16	2610 ± 790	1/6
1 (zyklophin)	207 ± 12	5880 ± 1420[b]	1/28

[a] values are mean ± SEM for n ≥3 except where noted, [b] ref. 17

The alanine scan of Dyn A(1-13) performed previously[25] revealed that within the Leu-enkephalin core of the peptide Ala^1 and Ala^4 substitution caused dramatic decreases in the opioid receptor binding affinities, indicating that Tyr^1 and Phe^4 residues were critical for opioid receptor binding affinity. Kawasaki *et al.* synthesized [Phe^1]Dyn A(1-11)NH$_2$ and it displayed 23-fold lower KOR affinity compared to Dyn A(1-11)NH$_2$ in guinea pig brain homogenates assay

indicating that the phenol of Tyr is critical for the KOR affinity of Dyn A(1-11)NH$_2$.[26] Outside the Leu-Enk core of Dyn A(1-13), the Ala[6] and Ala[7] analogs showed the largest decreases (3- to 7-fold) in binding affinities, suggesting that Arg[6] and Arg[7] contributed to the opioid receptor binding affinity of Dyn A(1-13). Ala[9] and Ala[11] analogs showed small decreases (2- to 3-fold) in opioid receptor binding affinity suggesting that these residues had minor contributions to the opioid receptor binding affinity of Dyn A(1-13).[25]

Comparison of the alanine scan data of Dyn A(1-13) and zyklophin reveals that while residue 1 was critical in maintaining the opioid receptor binding affinity for Dyn A(1-13), it appeared to make a relatively minor contribution to the KOR binding affinity of zyklophin. Comparing the data from [Phe[1]] Dyn A(1-11)NH$_2$[26] to Phe[1] analog of zyklophin indicated that while the phenol of Tyr was important for maintaining the KOR binding affinity of Dyn A(1-11)NH$_2$, the Tyr phenol of zyklophin was not important. Residue 4 was critical for the opioid receptor binding affinity of Dyn A(1-13) and the KOR binding affinity of zyklophin. Residue 6 contributed to both the opioid binding affinity of Dyn A(1-13) and for the KOR binding affinity of zyklophin. In addition, while residue 7 contributed to the opioid receptor binding affinity of Dyn A(1-13), it did not in the case of zyklophin. The Arg residue in position 9 did not appear to contribute to the binding affinity of either of the peptides. The differences in the alanine scan of the two peptides suggest that there could be differences in the binding interactions of the two peptides with the receptor. This is not surprising as one of them is a KOR agonist (Dyn A(1-13)) while the other is a KOR antagonist (zyklophin). However, in comparing the data obtained from the alanine substituted analogs of Dyn A(1-13) and zyklophin, it should be noted that there exists several differences in the radioligand binding assays used to evaluate the Ala-substituted analogs of the two peptides. Radioligand binding assays for Dyn A(1-13) analogs were performed in rat

brain homogenates as the tissue preparation and using the non-selective radioligand [^{3}H]etorphine, while Chinese hamster ovary (CHO) cell membranes expressing cloned KOR with [^{3}H]diprenorphine as the radioligand was used in the case of the zyklophin analogs. While the CHO membranes exclusively express KOR, rat brain homogenates contain MOR and DOR along with lower levels of KOR.[27]

The analogs were also screened against cloned DOR at 10 μM, and all of them exhibited minimal DOR affinity (< 20% inhibition of binding).

The efficacies of the zyklophin analogs were evaluated in the GTPγS assay (Table 4.3). All of the peptides displayed negligible efficacy (<15%) in the GTPγS assay, except peptide **3** which showed partial agonist activity (26% efficacy for peptide **3** compared to the full agonist Dyn A(1-13)NH$_2$, Table 4.3).

It was hypothesized that the N-terminal alkyl group might shift the peptide in the binding site thereby changing the interactions of the rest of the peptide with the receptor and its ability to activate the receptor. Among the *N*-alkyl analogs, peptide **6** with an *N*-methyl substitution was expected to cause minimal shift of the peptide in its binding site. The negligible efficacy of peptides **4-7** and **16-18** suggested that changes in the N-terminal alkyl group, ring size or configuration of the residue at position 5 did not alter the negligible efficacy of zyklophin as measured in the GTPγS assay.

Although peptides **11** and **12** displayed negligible efficacy, given the low KOR affinity of these peptides, it is difficult to evaluate the contributions of residues in position 4 and 6 to the lack of efficacy of zyklophin. The GTPγS results for peptides **14** suggested that the residue in position 9 does not contribute to the lack of efficacy of zyklophin. The GTPγS results for peptide

15 suggested that removal of the phenol of Tyr[1] does not contribute to the inability of zyklophin to activate the receptor.

Schild analysis[28] of selected analogs is being performed at KOR in the GTPγS assay (Table 4.4), to evaluate the antagonist potency of these analogs. The preliminary results for peptide **3** suggested that although it was partial agonist it retained the KOR antagonist potency comparable to zyklophin. The results from peptide **7** suggested that the *N*-CPM modification could be the most appropriate N-terminal modification to yield a potent KOR antagonist. In addition, preliminary results of peptide **15** suggested that the Tyr phenol may not be required for the KOR antagonist potency of zyklophin.

Table 4.3 Efficacies of the zyklophin analogs at KOR in the GTPγS assay

Peptide	% efficacy[a]
2 [D-Asn⁵]	0
3 [Dap(Ac)⁸][b]	26 ± 6 (n=5)
4 [*N*-Phenethyl]	6.5 (n=1)
5 [*N*-Allyl]	< 10
6 [*N*-Me]	<15
7 [*N*-CPM]	0
8 [*N*-Benzyl, *N*-Me]	ND
9 [*N*-Benzoyl]	0
10 [Ala¹]	0 (n=1)
11 [Ala⁴]	< 10
12 [Ala⁶]	0
13 [Ala⁷]	0 (n=1)
14 [Ala⁹]	0
15 [Phe¹]	0
16 [Dab⁸]	0
17 [Orn⁸]	< 10
18 [L-Asp⁵]	0
1 (zyklophin)	< 10

[a] Compared to Dyn A(1-13)NH$_2$ (efficacy = 100%); values are for n = 2 except where noted.
[b] EC$_{50}$ = 39.5 ± 17 nM; ND = not determined

Table 4.4. Preliminary antagonist potencies of selected zyklophin analogs in the GTPγS assay at KOR

Peptide	K_B (nM)[a]
3 [Dap(Ac)[8]]	791
7 [*N*-CPM]	43.7
15 [Phe[1]]	175
1(zyklophin)[b]	985 ± 110 (n=2)

[a]Obtained from Schild analysis in a GTPγS assay. Values obtained from (n = 1) unless otherwise stated. [b]K_B for zyklophin in AC assay previously found to be 83.9 nM (8.81-313 nM, 95% confidence interval).

4.4 Conclusions

Various linear and cyclic analogs of zyklophin were synthesized. In order to detect potential racemization of the N-terminal residue, an HPLC solvent system that could resolve the diastereomers was also identified. To avoid potential racemization a modified synthetic strategy involving preparation of the Alloc derivatives of *N*-alkyl amino acids was devised. These derivatives were readily soluble at RT in the solvents used for the coupling reaction, thereby minimizing the potential for racemization.

The *in vitro* pharmacological evaluation of the linear and the cyclic zyklophin analogs provided initial information about the SAR of the lead peptide zyklophin. The results from radioligand binding assay for the linear analogs **2** and **3** suggested that the residue at position 5 has a greater influence on the affinity of zyklophin as compared to residue 8. The L-configuration and/or the hydrophobic side chain of Leu in position 5 of peptide **3** likely contributes to the higher KOR affinity of this peptide. However, the KOR binding affinity data for cyclic analog **18** which has an L-Asp at position 5, suggested that the configuration of residue 5 might have a minor influence on the KOR affinity of cyclic zyklophin analogs. While all of the N-terminal modifications and ring variations were reasonably well tolerated in zyklophin, among

the *N*-alkyl analogs the analog with the *N*-CPM substitution displayed the highest affinity for KOR. It also appears that the basic secondary amine at the N-terminus of zyklophin is not necessary for maintaining the KOR affinity of zyklophin, given the similar KOR affinity of **9** and zyklophin. The pharmacological results for alanine substituted analogs suggested that the residues at positions 4 and 6 are important for zyklophin's KOR affinity. Substitution of Ala at postion 7 surprisingly increased the KOR affinity, while the Ala[9] analog displayed affinity comparable to zyklophin. This suggested that not only are the basic residues 7 and 9 not important for the maintaining the KOR affinity of zyklophin, but that Ala substitution in position 7 could be either causing favorable interactions or eliminating unfavorable interactions with the receptor that are responsible for the analog's increased affinity. In addition, the results suggested that the phenolic moiety of Tyr is not important for the KOR affinity of zyklophin. The results from the GTPγS assay indicated that all of the zyklophin analogs, except peptide **3**, synthesized in the present study exhibited negligible efficacy (< 15% compared to full agonist Dyn A(1-11)NH$_2$) similar to zyklophin. The Schild analysis of selected analogs found that the *N*-CPM analog and the Phe[1] analog were more potent KOR antagonists than zyklophin in this assay. These two analogs appear to be promising analogs for *in vivo* studies towards the development of potent peptide KOR antagonists. Further studies of selected zyklophin analogs are underway in our laboratory.

4.5   Experimental section

Materials

Fmoc-protected PAL-PEG-PS resin was purchased from Applied Biosystems (Foster City, CA). Standard Fmoc-protected amino acids were obtained from EMD Biosciences (Gibbstown, NJ) and Peptides International (Louisville, KY), Fmoc-D-Asp(OPip)OH was

obtained from Bachem (King of Prussia, PA), and Fmoc-Dap(Mtt)OH, Fmoc-Dab(Mtt)-OH and Fmoc-Orn(Mtt)-OH were obtained from EMD Biosciences. Fmoc-NMe-Tyr(OtBu)-OH was obtained from APPTec (Louisville, KY), and Tyr-OtBu was obtained from EMD Biosciences. PyBOP and PyClocK were purchased from EMD Biosciences. HOBt was purchased from Peptides International, and DIEA was from Fisher Scientific (Fair Lawn, NJ). Piperidine was purchased from Sigma-Aldrich (St. Louis, MO). All HPLC-grade solvents (MeCN, DMF, DCM, EtOAc, hexane and MeOH) used for amino acid and peptide synthesis or HPLC analysis were obtained from Fisher Scientific. TFA for HPLC analysis was purchased from Pierce (Rockford, IL); benzaldehyde, sodium cyanoborohydride, iodomethane, DIAD and triphenylphosphine (TPP) were from Sigma-Aldrich; and phenylacetaldehyde, allyl bromide, allyl chloroformate and TIS were from Acros Organics (Fairlawn, NJ).

Amino acid synthesis

General procedure for N-alkyl-Tyr-OH synthesis

The amino acid t-butyl ester (1 equiv.) and NaBH(OAc)$_3$ (1 equiv.) were dissolved in anhydrous acetonitrile (SureSeal, 5-10 mL/mmol) followed by the addition of the corresponding aldehyde (1.5 equiv.) and a catalytic amount of glacial acetic acid (0.2 mL). The reaction was performed under N$_2$ for 12-16 h at RT with continuous stirring. The reaction was monitored by TLC (1:2 EtOAc:hexane plus 1 drop NEt$_3$). After completion of the reaction the acetonitrile was evaporated *in vacuo* the pH adjusted to 7.0 with saturated NaHCO$_3$ and the aqueous layer extracted with EtOAc (3 x 10 mL). The combined EtOAc extracts were washed with water, and the organic layer was dried (MgSO$_4$) and evaporated under reduced pressure to obtain crude N-alkyl-Tyr-OtBu that was purified by flash silica gel column chromatography (20-30% EtOAc in hexane). The N-alkyl-Tyr-OtBu was analyzed by HPLC for purity using a gradient of 5-50%

aqueous MeCN with 0.1% TFA over 45 min at a flow rate of 1 mL/min. The *t*-butyl ester on the purified *N*-alkyl-Tyr-O*t*Bu was cleaved by 90% TFA plus 10% water (8-10 mL/mmol) for 12 h. The reaction mixture was concentrated *in vacuo*, and the desired product was obtained by precipitation with diethyl ether.

N-Benzyl-Tyr-OH (22a)

Tyr-O*t*Bu (0.474 g, 2.0 mmol, 1 equiv.) and NaBH(OAc)$_3$ (0.422 g, 2.0 mmol, 1 equiv.) were dissolved in anhydrous acetonitrile (12 mL), followed by the addition of benzaldehyde (0.32 mL, 3.0 mmol, 1.5 equiv.) and 7 drops of glacial acetic acid, and the reaction stirring for 18 h. The crude product was isolated as described above, and pure *N*-benzyl-Tyr-O*t*Bu was obtained following flash silica gel column chromatography (25% EtOAc/hexane) as an off-white amorphous solid: 520 mg (80%); ESI-MS *m/z* [M+H]$^+$ 328.1913 (calcd), 328.1784 (observed); HPLC: t_R 24.3 min (purity 100%); ^{1}H NMR (500 MHz, d_6-acetone) δ 8.14 (s, 1H), 7.35 − 7.15 (m, 5H), 7.04 (d, J = 8.2 Hz, 2H), 6.74 (d, J = 8.7 Hz, 2H), 3.82 (d, J = 13.3 Hz, 1H), 3.64 (d, J = 13.3 Hz, 1H), 3.30 (t, J = 6.8 Hz, 1H), 2.88 − 2.71 (m, 2H), 1.38 (s, 9H); ^{13}C NMR (126 MHz, CDCl$_3$) δ 171.90, 153.14, 136.83, 128.38, 126.42, 126.38, 125.96, 125.20, 113.40, 79.60, 60.52, 49.84, 36.56, 25.98.

N-Benzyl-Tyr-O*t*Bu (200 mg) was cleaved to the corresponding acid using TFA as described above to yield *N*-benzyl-Tyr-OH as a white amorphous powder: 160 mg (68%); ESI-MS *m/z* [M+H]$^+$ 272.1287 (calcd), 272.1227 (observed).

N-Phenethyl-Tyr-OH (23)

Tyr-O*t*Bu (0.474 g, 2.0 mmol, 1 equiv.) and NaBH(OAc)$_3$ (0.422 g, 2.0 mmol, 1 equiv.) were dissolved in anhydrous acetonitrile (10 mL), followed by the addition of phenyl acetaldehyde (0.35 mL, 1.5 mmol, 1.5 equiv.) and 4 drops of glacial acetic acid, and the reaction stirred for 16 h. The crude product was isolated as described above under the general procedure.

Pure *N*-phenethyl-Tyr-O*t*Bu was obtained by flash silica gel column chromatography (25% EtOAc in hexane) as an off-white oil: 452 mg (66%); ESI-MS *m/z* [M+H]$^+$ 342.2069 (calcd), 342.2004 (observed); HPLC: t_R 27.9 min (purity 100%); ^{1}H NMR (500 MHz, d_6-acetone) δ 8.13 (s, 1H), 7.32 – 7.11 (m, 5H), 7.04 (d, *J* = 8.5 Hz, 2H), 6.74 (d, *J* = 8.5 Hz, 2H), 3.31 (dd, *J* = 6.4 and 7.6 Hz, 1H), 2.83 – 2.68 (m, 6H), 1.34 (s, 9H); ^{13}C NMR (126 MHz, d_6-acetone) δ 174.49, 156.89, 141.43, 131.36, 129.64, 129.18, 126.82, 115.77, 80.84, 64.77, 50.22, 39.67, 37.42, 28.25.

N-Phenethyl-Tyr-O*t*Bu (165 mg) was cleaved to afford the corresponding acid as a yellowish-white solid: 125 mg (65%); ESI-MS *m/z* [M+H]$^+$ 286.1443 (calcd), 286.1432 (observed).

N-Benzyl Ala-O*t*Bu (35)

Ala-O*t*Bu HCl (0.43 g, 2.4 mmol, 1.2 equiv.) and benzaldehyde (0.2 mL, 2.0 mmol, 1 equiv.) were dissolved in CHCl$_3$ (10 mL) and a solution of NaBH(OAc)$_3$ (0.63 g, 3 mmol, 1.5 equiv) in CHCl$_3$ (5 mL) was added to the Ala-O*t*Bu solution. The reaction mixture was allowed to stir at RT for 12 h and water (20 mL) was added to the CHCl$_3$ solution. The water layer was separated and extracted with CHCl$_3$ (2 x 20 mL). The combined CHCl$_3$ layers were washed with water (20 mL), dried over MgSO$_4$ and the solvent evaporated to obtain *N*-benzyl-Ala-O*t*Bu. The product was purified by flash silica gel column chromatography (15% EtOAc /hexane) to give a white semisolid: 220 mg (39%); ESI-MS *m/z* [M+H]$^+$ 236.1651 (calcd), 236.1628 (observed); HPLC: t_R 13.08 min (purity 95.8%) ;^{1}H NMR (500 MHz, CDCl$_3$) δ 7.39 – 7.23 (m, 5H), 3.82 (d, *J* = 12.7 Hz, 1H), 3.68 (d, *J* = 12.7 Hz, 1H), 3.27 (q, *J* = 7.0 Hz, 1H), 1.86 (s, 1H), 1.51 (s, 9H), 1.30 (d, *J* = 7.0 Hz, 3H); ^{13}C NMR (126 MHz, CDCl$_3$) δ 175.37, 140.14, 128.59, 128.45, 127.19, 81.07, 56.86, 52.15, 28.29, 19.35.

N-Benzyl-Ala-O*t*Bu (120 mg) was cleaved to afford the corresponding acid as a yellowish-white solid: 75 mg (50%); ESI-MS *m/z* [M+H]$^+$ 180.1025 (calcd), 180.1009 (observed).

N-Benzyl-D-Tyr-OH (22b)

D-Tyr-O*t*Bu (0.118 g, 0.5 mmol, 1 equiv.) and NaBH(OAc)$_3$ (0.105 g, 0.5 mmol, 1 equiv.) were dissolved in anhydrous acetonitrile (5 mL), followed by the addition of benzaldehyde (0.083 mL, 0.75 mmol, 1.5 equiv.) and 3 drops of glacial acetic acid, and the reaction stirred for 18 h. The crude product was isolated as described above, and pure *N*-benzyl-D-Tyr-O*t*Bu was obtained following flash silica gel column chromatography (20% EtOAc/hexane) as an off-white amorphous solid: 90 mg (55%); ESI-MS *m/z* [M+H]$^+$ 328.1913 (calcd), 328.1890 (observed); ^{1}H NMR (500 MHz, CDCl$_3$) δ 7.35 – 7.17 (m, 5H), 6.97 (d, *J* = 8.4 Hz, 2H), 6.62 (d, *J* = 8.5 Hz, 2H), 3.80 (d, *J* = 12.8 Hz, 1H), 3.66 (d, *J* = 12.8 Hz, 1H), 3.42 (t, *J* = 6.9 Hz, 1H), 2.95 – 2.77 (m, 2H), 1.39 (s, 1H); ^{13}C NMR (126 MHz, CDCl$_3$) δ 172.36, 153.37, 137.44, 128.83, 126.84, 126.74, 126.67, 125.59, 113.75, 79.98, 60.98, 50.29, 37.03, 26.43.

N-Benzyl-D-Tyr-O*t*Bu (90 mg) was cleaved to the corresponding acid using TFA as described above to yield *N*-benzyl-D-Tyr-OH as a white amorphous powder: 51 mg (49%); ESI-MS *m/z* [M+H]$^+$ 272.1287 (calcd), 272.1251 (observed).

N-Cyclopropylmethyl-Tyr-O*t*Bu (27)

Tyr-O*t*Bu (0.237 g, 1.0 mmol, 1 equiv.) and NaBH(OAc)$_3$ (0.211 g, 1.0 mmol, 1 equiv.) were dissolved in anhydrous acetonitrile (7 mL), followed by addition of cyclopropylcarboxaldehyde (0.066 mL, 0.95 mmol, 0.95 equiv.) and 2 drops of glacial acetic acid, and the reaction allowed to proceed for 12 h. The crude product was isolated as described under the general procedure. The product was purified by flash silica gel column

chromatography (30% EtOAc in hexane) to give a white solid powder: 160 mg (55%); ESI-MS *m/z* [M+H]$^+$ 292.1913 (calcd), 292.1819 (observed); HPLC: t_R 19.10 min (purity 97.4%); ^{1}H NMR (500 MHz, acetone) 8.05 (s, 1H), 6.97 (dd, *J* = 6.5, 2.0 Hz, 2H), 6.65 (dd, *J* = 6.5, 2.1 Hz, 2H), 3.22 (dd, *J* = 7.6, 6.3 Hz, 1H), 2.79 – 2.67 (m, 1H), 2.66 – 2.59 (m, 1H), 2.38 (dd, *J* = 11.7, 6.1 Hz, 1H), 2.21 (dd, *J* = 11.7, 7.2 Hz, 1H), 1.26 (s, 9H), 0.82 – 0.72 (m, 1H), 0.35 – 0.27 (m, 2H), 0.05-0.01 (dd, *J* = 4.8, 1.8 Hz, 2H); ^{13}C NMR (126 MHz, CDCl$_3$) δ 174.11, 155.11, 130.60, 128.73, 115.55, 81.53, 63.38, 53.28, 38.99, 28.23, 11.10, 3.86, 3.46.

Alloc-*N*-cyclopropylmethyl-Tyr(Alloc)-OH (31)

N-Cyclopropylmethyl-Tyr-O*t*Bu (0.08 g, 0.27 mmol, 1 equiv.) was dissolved in anhydrous DCM (2.5 mL), then allyl chloroformate (0.117 mL, 1.08 mmol, 4 equiv.) followed by DIEA (0.189 mL, 1.08 mmol, 4 equiv.) were added, and the reaction was allowed to proceed at RT for 12 h. DCM was evaporated *in vacuo,* and EtOAc (10 mL) was added, and the solution washed with water (10 mL). The water layer was back-extracted with additional EtOAc (10 mL). The EtOAc fractions were finally washed with water (10 mL) dried (MgSO$_4$) and evaporated *in vacuo* to afford the product as a yellowish white semisolid: 91 mg (73%); ESI-MS *m/z* [M+Na]$^+$ 482.2155 (calcd), 482.2087 (observed); HPLC t_R 18.51 min (25-95% of aqueous acetonitrile with 0.1 %TFA over 35 min, purity 95.4%); ^{1}H NMR (500 MHz, CDCl$_3$, 50 ^{o}C) δ 7.22 – 7.14 (m, 2H), 7.07 (d, *J* = 8.5 Hz, 2H), 6.03 – 5.87 (m, 2H), 5.46 – 5.18 (m, 4H), 4.74 – 4.48 (m, 4H), 4.08 (m, 1H), 3.23 (m, 3H), 2.56 (m, 1H), 1.44 (s, 9H), 0.69 (m, 2H), 0.35 (m, 2H), 0.05 (m, 1H); ^{13}C NMR (126 MHz, CDCl$_3$) δ 169.97, 155.99, 153.61, 150.25, 136.79, 131.57, 130.48, 121.02, 119.34, 81.73, 69.17, 66.30, 63.35, 53.64, 29.86, 28.24, 10.34, 4.19, 3.83.

The ester was cleaved with 90% TFA in DCM for 12 h at RT. TFA was evaporated and EtOAc (10 mL) and water (10 mL) was added. The water layer was extracted with EtOAc (10 mL). The organic extracts were finally washed with water (10 mL), dried with MgSO$_4$ and the

solution was evaporated under *vacuo* to yield the product as a yellowish white semisolid: 75 mg (94%); ESI-MS *m/z* (M+K)$^+$ 442.1268. (calcd), 442.1250 (observed); HPLC: t_R 12.05 min (25-95% aqueous acetonitrile with 0.1 % TFA over 35 min, purity 94.5%).

N-Benzyl Phe-OtBu (28)

H-Phe-O*t*Bu HCl (0.618 g, 2.4 mmol, 1.2 equiv.) and benzaldehyde (0.2 mL, 2.0 mmol, 1 equiv.) were dissolved CHCl$_3$ (5 mL). A solution of NaBH(OAc)$_3$ (0.31 g, 3.0 mmol, 1.5 equiv.) in CHCl$_3$ (2 mL) was then added to the Phe-O*t*Bu solution, and the reaction mixture allowed to stir at RT for 12 h. Water (20 mL) was added to CHCl$_3$ solution. The water layer was separated from CHCl$_3$ layer and again extracted with CHCl$_3$ (3 x 20 mL). The combined CHCl$_3$ extracts were washed with water (20 mL) and dried over MgSO$_4$, and the crude product was purified by flash silica gel column chromatography (5-10% EtOAc in hexane) to obtain a white semisolid: 335 mg (44%); ESI-MS *m/z* [M+H]$^+$ 312.1964 (calcd), 312.1853 (observed); HPLC: t_R 28.96 min (purity 99.1%); ^{1}H NMR (500 MHz, CDCl$_3$) δ 7.31 − 7.18 (m, 10H), 3.86 (d, *J* = 13.0 Hz, 1H), 3.73 (d, *J* = 13.0 Hz, 1H), 3.51 (dd, *J* = 7.6 and 6.6 Hz, 1H), 3.00 (dd, *J* = 13.6 and 6.5 Hz, 1H), 2.91 (dd, *J* = 13.6 and 7.7 Hz, 1H), 1.35 (s, 9H); ^{13}C NMR (126 MHz, CDCl$_3$) δ 172.82, 138.19, 136.99, 129.47, 128.53, 128.49, 128.31, 127.45, 126.70, 81.65, 62.23, 51.65, 39.21, 27.97.

Alloc-N-benzyl-Phe-OH (32)

N-Benzyl-Phe-O*t*Bu (0.25 g, 0.8 mmol, 1 equiv.) was dissolved in anhydrous DCM (2 mL), then allyl chloroformate (0.169 mL, 1.6 mmol, 2 equiv.) followed by DIEA (0.278 mL, 1.6 mmol, 2 equiv.) were added, and the reaction was allowed to proceed for 12 h. DCM was evaporated *in vacuo*, EtOAc (20 mL) was added and the solution washed with water (20 mL). The water layer was extracted with additional EtOAc (20 mL), and the combined EtOAc extracts were washed with additional water (20 mL). The EtOAc fractions were dried (MgSO$_4$) and

evaporated *in vacuo* to obtain the product as a yellowish semisolid: 208 mg (65%); ESI-MS *(m/z)* [M+Na]$^+$ 418.1994 (calcd), 418.2047; HPLC: t_R 18.68 min (25-95% aqueous acetonitrile with 0.1 % TFA over 35 min, purity 96.5%); ^{1}H NMR (500 MHz, CDCl$_3$, 50^{0}C) δ 7.32 – 7.21 (m, *J* = 7.0 Hz, 6H), 7.21 – 7.05 (m, 4H), 6.05 – 5.89 (m, 1H), 5.28 (m, 2H), 4.82 – 4.52 (m, 3H), 4.16 (m, 1H), 3.99 – 3.82 (m, *J* = 13.4 Hz, 1H), 3.32 (dd, *J* = 14.0, 5.8 Hz, 1H), 3.16 (dd, *J* = 14.0, 5.8 Hz, 1H), 1.39 (s, 9H); ^{13}C NMR (126 MHz, CDCl$_3$) δ 169.47, 156.03, 138.33, 137.51, 132.81, 129.21, 128.33, 128.13, 127.07, 126.36, 117.50, 81.49, 66.26, 62.40, 51.77, 36.24, 27.86.

The ester (120 mg) was cleaved with 90% TFA/10% water for 12 h at RT. The work up was done as described under TFA cleavage of **31** to yield the product as a yellowish white semisolid: 100 mg (98%); ESI-MS *m/z* (M+Na)$^+$ 362.1368 (calcd), 362.1347 (observed); HPLC: t_R 12.14 min (25-95% aqueous acetonitrile with 0.1 % TFA over 35 min, purity 100%).

N-Allyl-Tyr-OH (25)

Tyr-O*t*Bu (0.237 g, 1.0 mmol, 1 equiv.) was dissolved in DMF (2 mL) and the temperature maintained at 0-4 ^{0}C. DIEA (0.174 mL, 1.0 mmol, 1 equiv.) was added to the solution, followed by slow addition of allyl bromide (0.086 mL, 1 mmol, 1 equiv.). The reaction mixture was stirred at room temperature under N$_2$ and the progress of the reaction was monitored by TLC (1:3 EtOAc:hexane plus 2 drops NEt$_3$). After 45 h, the DMF was removed *in vacuo.* A negligible amount of diallyl product was visible on TLC while a substantial amount of residual starting material was present. The crude product was purified by flash silica gel column chromatography (22% EtOAc/hexane) as a white solid powder: 80 mg (29%); ESI-MS *(m/z)* [M-*t*Bu]$^+$ 222.1130 (calcd), 222.1083 (observed); HPLC: t_R 15.91 min (purity 100%); ^{1}H NMR (500 MHz, d$_6$-acetone) δ 8.19 (s, 1H), 7.05 (d, *J* = 8.1 Hz, 2H), 6.75 (d, *J* = 8.3 Hz, 2H), 5.82 (m, 1H),

5.15 (dd, *J* = 17.2 and 1.3 Hz, 1H), 5.01 (d, *J* = 10.2 Hz, 1H), 3.31 (t, *J* = 6.9 Hz, 1H), 3.19 (ddd, *J* = 77.8, 14.2, 5.9 Hz, 2H), 2.79 (ddd, *J* = 21.1, 13.5, 6.9 Hz, 2H), 1.37 (s, 9H); ^{13}C NMR (126 MHz, d_6-acetone) δ 174.52, 156.89, 138.10, 131.35, 129.53, 115.85, 115.76, 80.94, 63.75, 51.09, 39.67, 28.26.

Pure *N*-allyl-Tyr-O*t*Bu (80 mg) was deprotected as described above as to obtain *N*-allyl-Tyr-OH as a white solid powder: 43 mg (44%); ESI-MS *(m/z)* [M+H]+ 222.1130 (calcd), 222.1060 (observed).

Synthesis of *N*-benzyl, *N*-methyl Tyr(*t*Bu)-O*t*Bu

N-Benzyl-Tyr(*t*Bu)-O*t*Bu (37)

H-Tyr(*t*Bu)-O*t*Bu HCl (0.79 g, 2.4 mmol, 1.2 equiv.) and benzaldehyde (0.2 mL, 2 mmol, 1 equiv.) were dissolved in CHCl$_3$ (10 mL), solution of NaBH(OAc)$_3$ (0.63 g, 3 mmol, 1.5 equiv.) in CHCl$_3$ (3 mL) was added to the Tyr-O*t*Bu solution, and the reaction mixture was allowed to stir for 16 h. The crude product was isolated according to the procedure described for *N*-benzyl-Phe-O*t*Bu and purified by flash silica gel column chromatography (25% EtOAc/hexane) to obtain a white powder: 550 mg (60%); ESI-MS *m/z* [M+H]+ 384.2539 (calcd), 384.2461 (observed); HPLC: t_R 37.0 min (purity 100%); ^{1}H NMR (500 MHz, d$_6$-acetone) ^{1}H NMR (500 MHz, CDCl$_3$) δ 7.34 − 7.19 (m, 5H), 7.13 − 7.03 (m, 2H), 6.94 − 6.85 (m, 2H), 3.82 (d, *J* = 13.1 Hz, 1H), 3.64 (d, *J* = 13.1 Hz, 1H), 3.39 (t, *J* = 7.2 Hz, 1H), 2.95 − 2.89 (m, 1H), 2.86 − 2.80 (m, 1H), 1.35 (s, 9H), 1.32 (s, 9H); ^{13}C NMR (126 MHz, d_6-acetone) δ 174.51, 155.02, 141.47, 133.84, 130.83, 129.05, 128.92, 127.62, 124.64, 81.09, 78.40, 63.64, 52.32, 39.87, 29.19, 28.29.

N-Benzyl,N-methyl Tyr(*t*Bu)-OH (39)

N-Benzyl-Tyr(*t*Bu)-O*t*Bu (0.550 g, 1.43 mmol, 1 equiv.), DIAD (424 μL, 2.14 mmol, 1.5 equiv.) and TPP (374 mg, 1.43 mmol, 1 equiv.) were dissolved in dry THF (SureSeal, 6 mL) and allowed to stir for 2-3 min at RT. Iodomethane (274 μL, 4.28 mmol, 3 equiv.) was added, and the reaction was allowed to proceed for 12 h, at which time TLC system (1:4 EtOAC:hexane plus 2 drops TEA) and ESI-MS showed that the reaction was incomplete. As iodomethane is volatile, the reaction mixture was evaporated, fresh reagents were added and the reaction was continued for an additional 30 h. At the end of a total of 42 h, the reaction appeared to be complete by TLC and ESI-MS. The reaction mixture was evaporated, and EtOAc (25 mL) was added followed by filtration to remove precipitate. The EtOAc solution was washed twice with water (15 mL) and the combined aqueous extracts were again extracted with EtOAc (15 mL). The combined EtOAc extracts were dried (MgSO$_4$) and evaporated in *vacuo*. Along with the desired product formation of a quaternary amine product was also observed. The desired product was purified by silica flash column chromatography and the product eluted in 5% EtOAc in hexane to give *N*-benzyl,*N*-methyl Tyr(*t*Bu)-O*t*Bu as a yellowish white semisolid: 180 mg (32%); ESI-MS *(m/z)* [M+H]$^+$ 398.2695 (calcd), 398.2490 (observed); HPLC: t_R 37.04 min (purity 99.1%); ^{1}H NMR (500 MHz, CDCl$_3$) ^{1}H NMR (500 MHz, CDCl$_3$) δ 7.27 − 7.16 (m, 5H), 7.07 (dd, *J* = 6.6, 1.8 Hz, 2H), 6.91 − 6.87 (m, 2H), 3.83 (d, *J* = 13.6 Hz, 1H), 3.63 (d, *J* = 13.6 Hz, 1H), 3.50 − 3.43 (m, 1H), 3.02 (dd, *J* = 13.7, 8.4 Hz, 1H), 2.94 − 2.86 (m, 1H), 2.33 (s, 1H), 1.41 (s, 9H), 1.33 (s, 9H); ^{13}C NMR (126 MHz, CDCl$_3$) δ 170.18, 152.50, 138.47, 132.48, 128.70, 127.65, 127.09, 125.81, 122.99, 79.92, 77.14, 66.83, 57.67, 36.86, 34.35, 27.79, 27.27.

The pure *N*-benzyl, *N*-methyl-Tyr-O*t*Bu (105 mg) was deprotected as described above to obtain *N*-benzyl, *N*-methyl-Tyr-OH as a white powder: 75 mg (71%), ESI-MS *(m/z)* [M+H]$^+$ 286.1443 (calcd), 286.1023 (observed)

General procedures for solid phase peptide synthesis

Synthesis of (2-11) peptide fragments

The peptides were assembled on a low load Fmoc-PAL-PEG-PS resin (0.19 mmol/g). Following removal of the Fmoc group from the resin (200 mg, 0.038 mmol) using 20% piperidine in DMF (2 x 20 min) the Fmoc-protected amino acids (4 equiv., 0.152 mmol) were coupled using PyBOP and HOBt (4 equiv. each, 0.152 mmol) as the coupling reagents and DIEA (10 equiv., 0.38 mmol) as the base in DCM:DMF (1:1, 3-4 mL) for 2 h (unless otherwise noted) on a manual peptide synthesizer (CHOIR)[22] to afford the linear fragments. The side chains of Lys and Arg were protected by Boc and 2,2,4,6,7-pentamethyldihydrobenzofuran-5-sulfonyl (Pbf), respectively; those of Dap, Dab and Orn were protected by Mtt, and those of D-Asp and L-Asp were protected by OPip.

The (5-11) linear precursors of the cyclic peptides were synthesized by these standard procedures. Selective deprotection of the Pip and Mtt protecting groups on D-Asp and Dap, respectively, was performed using 3% TFA and 5% TIS in DCM (3 x 10-15 min). The cyclizations were performed using PyClocK and HOAt (4 equiv. each) with DIEA (10 equiv.) as the base in DCM:DMF (1:1) (4 mL for 200 mg peptide-resin) for 24 h, with the coupling reagents refreshed after every 8-12 h unless otherwise noted. The cyclizations were monitored using the qualitative ninhydrin test. Any remaining unreacted free amine of Dap was capped by treatment with acetyl imidazole (16 equiv., 0.61 mmol) with DIEA (8 equiv.) as the base in

DMF(~ 3 mL) for 30 min. Further extension of the peptide assembly up to Gly^2 afforded the cyclic (2-11) peptide fragments.

Coupling of the N-terminal amino acid to the (2-11) peptide

Prior to coupling, complete dissolution of the *N*-alkyl-Tyr-OH (2 equiv.) was achieved by heating to 80-120 ^{o}C in DMF (1 mL/0.02 mmol of N-alkyl amino acid) followed by cooling to RT (unless otherwise indicated), and subsequent addition to PyClock and HOAt (2 equiv. each) as the coupling agents plus DIEA (6 equiv). The coupling reactions were generally complete after 12 h, as indicated by the qualitative ninhydrin test.

Final deprotection of the peptides

The peptides were cleaved from the resin using Reagent B[29] (88% TFA containing 5% water, 5% phenol and 2.5% TIS, 4-5 mL/200 mg resin). The solutions were filtered, diluted with 10% aqueous acetic acid (10-15 mL), and extracted with diethyl ether (3 x 10 mL). The ether extracts were back extracted with 10% acetic acid (10 mL). The combined aqueous solutions were pooled and lyophilized to give the crude peptides.

Synthesis of peptides 2 and 3

The linear (2-11) fragments were synthesized as described above under the general procedure except that Fmoc-DAsn(Trt)OH and Fmoc-Dap(Mtt)OH were used in a 2-fold excess for the synthesis of peptides **2** and **3,** respectively. In addition, for peptide **3** the coupling of Fmoc-Dap(Mtt)-OH to the peptide resin was performed using PyClocK and HOAt (2 equiv each) in the presence of DIEA (6 equiv) and DCM:DMF (1:1, 4 mL). For peptide **3**, the Mtt on Dap was selectively deprotected by 3% TFA and 5% TIPS in DCM (3 x 10 min, 3-4 mL each time) followed by acetylating with acetyl imidazole (16 equiv., 0.61 mmol) in the presence of DIEA (8

equiv.) in DMF (3 mL) for 1 h. The coupling of *N*-benzyl-Tyr-OH (2 equiv) to the (2-11) fragment was performed according to the general procedure described above.

Synthesis of peptides 4-10 and 15.

The (2-11) cyclic peptide fragment was synthesized according to the general procedure described above.

For peptide **4,** complete dissolution of *N*-phenethyl-Tyr-OH (33 mg, 0.114 mmol, 2 equiv.) was achieved by heating to 115 $^{\circ}$C in DMF (10 mL). The solution was cooled to ~70 $^{\circ}$C, followed by the addition to PyClocK and HOAt (2 equiv. each). Subsequently, the solution was cooled to RT followed by the addition of DIEA (6 equiv.). The amino acid was reacted with the (2-11) peptide fragment for 24 h with reagents replaced after 12 h. In the case of peptide **5**, *N*-allyl-Tyr-OH (20 mg, 0.076 mmol, 2 equiv.) was dissolved in DMF (6 mL) by heating to 105 $^{\circ}$C. When the solution was cooled to ~70 $^{\circ}$C it became turbid. Therefore, the coupling reagents were added to the amino acid solution at 105 $^{\circ}$C. When the solution was cooled to RT, DIEA (6 equiv.) was added and the solution was reacted with the (2-11) peptide fragment for 12 h to obtain peptide **5**. For peptide **6,** Fmoc-*N*Me-Tyr(O*t*Bu)-OH (54 mg, 0.114 mmol, 2 equiv.) was dissolved in DMF (5 mL) at RT and coupled to the (2-11) cyclic peptide using PyBOP (60 mg, 0.114 mmol, 2 equiv.) and HOBt (16 mg, 0.114 mmol, 2 equiv.) in the presence of DIEA (6 equiv.) followed by subsequent removal of Fmoc to afford peptide **6**. For peptide **7,** Alloc-*N*-cyclopropylmethyl-Tyr(Alloc)-OH (23 mg, 0.057 mmol, 2 equiv.) was dissolved in DMF (3 mL) at RT, and the coupling reaction to the (2-11) peptide was performed with PyClocK (31 mg, 0.057 mmol, 2 equiv.) and HOAt (8 mg, 0.057 mmol, 2 equiv.) in the presence of DIEA (6 equiv) for 1 h, followed by the subsequent removal of the Alloc group (see below) to afford protected peptide **7** on the resin. For peptide **8**, *N*-benzyl,*N*-methyl-Tyr (21 mg, 0.076 mmol, 2

equiv.) in DMF (4 mL) was heated to 65-70 ^{o}C and then cooled, followed by the addition of PyClocK and HOAt (2 equiv. each) and DIEA (6 equiv.). The amino acid solution was then reacted with the (2-11) peptide for 4 h to obtain peptide **8**. For peptide **9,** Fmoc-Tyr(*t*Bu)-OH (52 mg, 0.114 mmol, 4 equiv.) was coupled to the (2-11) peptide fragment in the presence of PyBOP (60 mg, 0.114 mmol, 4 equiv), HOBt (15 mg, 0.114 mmol, 4 equiv. each) and DIEA (10 equiv.) in DCM:DMF (1:1, 3mL) for 2 h. Following Fmoc deprotection of Tyr, the N-terminus of the Tyr was reacted with benzoic anhydride (0.025 mg, 0.114 mmol, 4 equiv.) and DIEA (8 equiv.) in DMF (2-3 mL) overnight. In the case of the synthesis of peptide **10,** *N*-benzyl-Ala (2 equiv.) was heated to 85 ^{o}C in DMF (3.5 mL) followed by cooling the solution to 60 ^{o}C before adding PyClocK and HOAt (2 equiv each) and DIEA (6 equiv.). The coupling was performed for 24 h with the amino acid and coupling reagents replaced after 12 h. For peptide **15** Alloc-*N*-benzyl-Phe-OH (20 mg, 0.057 mmol, 2 equiv.) was dissolved in DMF (3 mL) at RT with PyClocK and HOAt (2 equiv. each) and DIEA (6 equiv.) and coupled to the (2-11) peptide-resin. The coupling reaction was performed for 1 h followed by subsequent removal of the Alloc group (see below) to afford the peptide **15** on resin. For the D-Tyr derivative of zyklophin, *N*-benzyl-D-Tyr (5.16 mg, 0.019 mmol, 2 equiv.) was dissolved in DMF (2 mL) by heating to 85 ^{o}C. The solution was allowed to cool at RT followed by addition of PyClocK and HOAt (2 equiv. each) and DIEA (6 equiv.) and coupled to the (2-11) peptide for 12 h.

Alloc deprotection of peptides 7 and 15

The resin was swollen in DCM (2 x 5 min), phenylsilane (24 equiv./ g of resin) was added, and the mixture was bubbled with N$_2$ for 5 min. *Tetrakis*-(triphenylphosphine) palladium (0.3 equiv.) was added, and a septum with a needle was fixed onto the reaction vessel to allow the evolved carbon dioxide to escape. The reaction was allowed to proceed on the rocking arm

shaker for 12 h. The solution was drained and the resin was subsequently subjected to a series of washes as follows: DCM (4 x 1 min), THF (4 x 1 min), DCM (3 x 1 min), DMF (3 x 1 min), 0.5 % DIEA in DMF (3 x 2 min), 0.2 M sodium diethyldithiocarbamate in DMF (3 x 15 min), DMF (3 x 2 min), DCM (3 x 1 min), and MeOH (3 x 1 min), followed by drying of the resin.[23, 30]

Synthesis of cyclic peptides 11-14

The synthesis of peptide **11** was performed according to the general procedure described above with Ala incorporated in position 4.

In the case of peptides **12-14** the (5-11) linear peptide fragments with Ala incorporated in the indicated position were synthesized as described under the general procedure. Following selective deprotection by 3% TFA and 5% TIPS (3 x 10 min) in DCM, the cyclization reactions were performed for 24 h using PyClocK and HOAt (4 equiv. each) in the presence of DIEA (6 equiv) in DCM:DMF (1:1, 4 mL) with the reagents replaced after 12 h. Following capping with acetyl imidazole the peptides were extended up through Gly^2 as described under the general procedure. The coupling of *N*-benzyl-Tyr-OH to the (2-11) fragments followed the general procedure as described above to obtain peptides **12-14**.

Synthesis of cyclic peptides 16-18

For peptide **16** [D-Asp(OPip)^5,Dab(Mtt)^8]Dyn A-(5-11)-NH$_2$ was synthesized according to the general procedure described above, except that Fmoc-Dab(Mtt)OH (2 equiv.) was coupling three times for 2 h each during the initial two couplings and overnight for the third coupling. Subsequently, the Pip and Mtt protecting groups on D-Asp and Dab, respectively, were selectively deprotected, and the peptide was cyclized for 36 h as described above, with coupling agents replaced every 8 h. Any unreacted free amine of Dab was acetylated as described above

for Dap. Further extension of the peptide chain up through Gly^2 was performed as described above under the general procedure.

For peptides **17** and **18** the (5-11) linear peptide fragment was synthesized by the general procedure as described above. The Pip and Mtt protecting groups on D-Asp and Orn, respectively (peptide **17**) and L-Asp and Dap, respectively (peptide **18**), were selectively deprotected using 3% TFA and 5% TIS in DCM (3 x 10 min). The peptides were cyclized for 36 h using PyClocK and HOAt (4 equiv. each) in the presence of DIEA (6 equiv.) in DCM:DMF (1:1, 4 mL) with the reagents replace after every 12 h. Following capping with acetyl imidazole the peptide was extended up through Gly^2 as described under the general procedure. Subsequent coupling of *N*-benzyl-Tyr-OH to the corresponding (2-11) fragments was done as described for the general procedure to afford peptides **16-18.**

Purification and analysis of the peptides

The crude peptides were purified by preparative reversed phased HPLC on an LC-AD Shimadzu liquid chromatograph system equipped with an SPD-10A VP system controller and SPD-10A VP UV-Vis detector on a Vydac C18 column (10 μ, 300 Å, 22 x 250 mm) equipped with a Vydac C18 guard cartridge. For purification, a linear gradient of 5-50% aqueous MeCN containing 0.1% TFA over 45 min, at a flow rate of 18 mL/min, was used. The purifications were monitored at 214 nm. The purity of the final peptides was verified on a Vydac 218-TP column (5 μ, 300 Å, 4.6 mm x 50 mm) equipped with a Vydac guard cartridge on a Shimadzu LC-10AT VP analytical HPLC liquid chromatograph (equipped with SCL-10A VP system controller and SPD-10A VP UV-Vis detector) or on an Agilent 1200 series liquid chromatograph system equipped with a multiple wavelength UV-Vis detector. Two systems, a linear gradient of 5-50% solvent B (solvent A = aqueous 0.1% TFA and solvent B = MeCN containing 0.1% TFA)

over 45 min at a flow rate of 1 mL/min (system 1), and a linear gradient of 15-60% solvent B (solvent A = aqueous 0.1% TFA and solvent B = MeOH containing 0.1% TFA) over 45 min at a flow rate of 1.0 mL/min (system 2), were used for the analyses. A third system utilized a linear gradient of 1-21% solvent B (solvent A = aqueous 0.09 M TEAP, pH = 2.5 and solvent B = MeCN) over 40 min. The final purity of all peptides by both analytical systems was ≥ 98% (see Table 4.1). Molecular weights of the compounds were determined by ESI-MS using a time of flight mass spectrometer analyzer (LCT premier, Waters, Milford, MA).

Pharmacological assays

Radioligand binding assays

Radioligand binding assays were performed as previously described[16] using cloned rat KOR and MOR and mouse DOR stably expressed on CHO cells. [^{3}H]Diprenorphine (K_d=0.45 nM), [^{3}H]DAMGO ([D-Ala^2,NMePhe^4,glyol]encephalin, K_d = 0.49 nM), and [^{3}H]DPDPE (*cyclo*[D-Pen^2,D-Pen^5]encephalin, K_d = 1.76 nM) were used as radioligands in assays for KOR, MOR, and DOR, respectively.

GTPγS assay

The binding of the GTP analog [^{35}S]GTPγS to membranes containing KOR was assayed as described previously.[31] Binding of the test compound was determined in a volume of 500 μL. The assay mixture contained 50 mM HEPES, pH 7.4, 1 mM EDTA, 5 mM magnesium acetate, 1 μM GDP, 1 mM dithiothreitol, 100 mM NaCl, 10 μM bestatin, 30 μM captopril, 50 μM Leu-Leu, 1 mg/mL bovine serum albumin, and approximately 100,000 disintegrations per min (dpm) [^{35}S]GTPγS (0.08 - 0.15 nM). Approximately 10 μg of KOR expressing CHO cell membrane protein was used per tube. Following 90 min incubation at 22 °C, the assay was terminated by filtration under vacuum on a Brandel (Gaithersburg, MD) model M-48R cell harvester using

Schleicher and Schuell Inc. (Keene, NH) number 32 glass fiber filters. The filters were rinsed five times (4 mL for each wash) with ice-cold (5 $^{\circ}$C) 50 mM Tris HCl, pH 7.4, containing 5 mM MgCl to remove unbound [^{35}S]GTPγS. Filter disks were then placed into counting vials to which 8 mL of Biocount scintillation fluid (Research Products International Corp., Mount Prospect, IL) was added. Filter-bound radioactivity was determined by liquid scintillation spectrometry (Beckman Instruments, Fullerton, CA) following overnight extraction at room temperature. The amount of radioligand bound was less than 10% of the total added in all experiments. Specific binding was defined as total binding minus that occurring in the presence of 3 μM unlabeled GTPγS. Nonspecific binding was approximately 1% of the total binding at 0.1 nM [^{35}S]GTPγS.

4.6   References

1.   Aldrich, J. V.; Vigil-Cruz, S. C., Narcotic Analgesics. In *Burger's Medicinal Chemistry & Drug Discovery*, Abraham, D. J., Ed. John Wiley & Sons, Inc. New York, 2003; Vol. 6, pp 329-481.

2.   Millan, M. J. Kappa-opioid receptors and analgesia. *Trends Pharmacol Sci* **1990,** *11*, 70-76.

3.   Park, H. S.; Lee, H. Y.; Kim, Y. H.; Park, J. K.; Zvartau, E. E.; Lee, H. A highly selective kappa-opioid receptor agonist with low addictive potential and dependence liability. *Bioorg Med Chem Lett* **2006,** *16*, 3609-3613.

4.   Pfeiffer, A.; Brantl, V.; Herz, A.; Emrich, H. M. Psychotomimesis mediated by kappa opiate receptors. *Science* **1986,** *233*, 774-776.

5.   Mague, S. D.; Pliakas, A. M.; Todtenkopf, M. S.; Tomasiewicz, H. C.; Zhang, Y.; Stevens, W. C., Jr.; Jones, R. M.; Portoghese, P. S.; Carlezon, W. A., Jr. Antidepressant-like

effects of kappa-opioid receptor antagonists in the forced swim test in rats. *J Pharmacol Exp Ther* **2003,** *305*, 323-330.

6.	Beardsley, P. M.; Howard, J. L.; Shelton, K. L.; Carroll, F. I. Differential effects of the novel kappa opioid receptor antagonist, JDTic, on reinstatement of cocaine-seeking induced by footshock stressors vs cocaine primes and its antidepressant-like effects in rats. *Psychopharmacology (Berl)* **2005,** *183*, 118-126.

7.	Zhang, H.; Shi, Y. G.; Woods, J. H.; Watson, S. J.; Ko, M. C. Central kappa-opioid receptor-mediated antidepressant-like effects of nor-Binaltorphimine: behavioral and BDNF mRNA expression studies. *Eur J Pharmacol* **2007,** *570*, 89-96.

8.	Aldrich, J. V.; McLaughlin, J. P. Peptide kappa opioid receptor ligands: potential for drug development. *AAPS J* **2009,** *11*, 312-322.

9.	Knoll, A. T.; Meloni, E. G.; Thomas, J. B.; Carroll, F. I.; Carlezon, W. A., Jr. Anxiolytic-like effects of kappa-opioid receptor antagonists in models of unlearned and learned fear in rats. *J Pharmacol Exp Ther* **2007,** *323*, 838-845.

10.	Wittmann, W.; Schunk, E.; Rosskothen, I.; Gaburro, S.; Singewald, N.; Herzog, H.; Schwarzer, C. Prodynorphin-derived peptides are critical modulators of anxiety and regulate neurochemistry and corticosterone. *Neuropsychopharmacology* **2009,** *34*, 775-785.

11.	Rothman, R. B.; Gorelick, D. A.; Heishman, S. J.; Eichmiller, P. R.; Hill, B. H.; Norbeck, J.; Liberto, J. G. An open-label study of a functional opioid kappa antagonist in the treatment of opioid dependence. *J Subst Abuse Treat* **2000,** *18*, 277-281.

12.	Carey, A. N.; Borozny, K.; Aldrich, J. V.; McLaughlin, J. P. Reinstatement of cocaine place-conditioning prevented by the peptide kappa-opioid receptor antagonist arodyn. *Eur J Pharmacol* **2007,** *569*, 84-89.

13.   Choi, H.; Murray, T. F.; DeLander, G. E.; Caldwell, V.; Aldrich, J. V. N-terminal alkylated derivatives of [D-Pro[10]]dynorphin A-(1-11) are highly selective for kappa-opioid receptors. *J Med Chem* **1992,** *35*, 4638-4639.

14.   Choi, H.; Murray, T. F.; DeLander, G. E.; Schmidt, W. K.; Aldrich, J. V. Synthesis and opioid activity of [D-Pro[10]]dynorphin A-(1-11) analogues with N-terminal alkyl substitution. *J Med Chem* **1997,** *40*, 2733-2739.

15.   Soderstrom, K.; Choi, H.; Berman, F. W.; Aldrich, J. V.; Murray, T. F. *N*-alkylated derivatives of [D-Pro[10]]dynorphin A-(1-11) are high affinity partial agonists at the cloned rat kappa-opioid receptor. *Eur J Pharmacol* **1997,** *338*, 191-197.

16.   Arttamangkul, S.; Ishmael, J. E.; Murray, T. F.; Grandy, D. K.; DeLander, G. E.; Kieffer, B. L.; Aldrich, J. V. Synthesis and opioid activity of conformationally constrained dynorphin A analogues. 2. Conformational constraint in the "address" sequence. *J Med Chem* **1997,** *40*, 1211-1218.

17.   Patkar, K. A.; Yan, X.; Murray, T. F.; Aldrich, J. V. [N^a-benzylTyr[1],*cyclo*(D-Asp[5],Dap[8])]- dynorphin A-(1-11)NH$_2$ cyclized in the "address" domain is a novel kappa-opioid receptor antagonist. *J Med Chem* **2005,** *48*, 4500-4503.

18.   Aldrich, J. V.; Patkar, K. A.; McLaughlin, J. P. Zyklophin, a systemically active selective kappa opioid receptor peptide antagonist with short duration of action. *Proc Natl Acad Sci U S A* **2009,** *106*, 18396-18401.

19.   Patkar, K. A.; Murray, T. F.; Aldrich, J. V. The effects of C-terminal modifications on the opioid activity of [*N*-benzylTyr(1)]dynorphin A-(1-11) analogues. *J Med Chem* **2009,** *52*, 6814-6821.

20.   Chavkin, C.; Goldstein, A. Specific receptor for the opioid peptide dynorphin: structure--activity relationships. *Proc Natl Acad Sci U S A* **1981,** *78*, 6543-6547.

21.   Kurosu, M. D., S. S.; and Crick, D. C. Efficient synthesis of tertiary amines from secondary amines. *Tetrahedron Letters* **2006,** *47*, 4871-4875.

22.   Vig, B. S. A., J. V. An Inexpensive, Manually Operated, Solid-Phase, Parallel Synthesizer. *Aldrichimica Acta* **2004,** *37*, 2.

23.   Leelasvatanakij, L.; Aldrich, J. V. A solid-phase synthetic strategy for the preparation of peptide-based affinity labels: synthesis of dynorphin A analogs. *J Pept Res* **2000,** *56*, 80-87.

24.   Corran, P. H., Reverse-phase chromatography of proteins. In *HPLC of Macromolecules*, second ed.; Oliver, R. W. A., Ed. Oxford University Press: New York, 1998; pp 122.

25.   Turcotte, A.; Lalonde, J. M.; St-Pierre, S.; Lemaire, S. Dynorphin-(1-13). I. Structure-function relationships of Ala-containing analogs. *Int J Pept Protein Res* **1984,** *23*, 361-367.

26.   Kawasaki, A. M.; Knapp, R. J.; Walton, A.; Wire, W. S.; Zalewska, T.; Yamamura, H. I.; Porreca, F.; Burks, T. F.; Hruby, V. J. Syntheses, opioid binding affinities and potencies of dynorphin A analogues substituted in positions 1, 6, 7, 8 and 10. *Int J Pept Protein Res* **1993,** *42*, 411-419.

27.   Gillan, M. G.; Kosterlitz, H. W. Spectrum of the mu, delta- and kappa-binding sites in homogenates of rat brain. *Br J Pharmacol* **1982,** *77*, 461-469.

28.   Schild, H. O. A New Scale for the Measurement of Drug Antagonism. *Br J Pharmacol* **1947,** *2*, 189-206.

29.   Sole, N. A. B., G. Optimization of Solid-Phase Synthesis of [Ala[8]]-Dynorphin A. *J. Org. Chem.* **1992,** *57*, 5399-5403.

30.   Kates, S. A.; Daniels, S. B.; Albericio, F. Automated allyl cleavage for continuous-flow synthesis of cyclic and branched peptides. *Anal Biochem* **1993,** *212*, 303-310.

31.   Ross, N. C.; Reilley, K. J.; Murray, T. F.; Aldrich, J. V.; McLaughlin, J. P. Novel opioid cyclic tetrapeptides: Trp isomers of CJ-15,208 exhibit distinct opioid receptor agonism and short-acting kappa opioid receptor antagonism. *Br J Pharmacol* **2012,** *165*, 1097-1108.

Chapter 5 - Literature review – Intestinal transport of peptides

5.1   Anatomy and physiology of the intestine

The human small intestine is 2-6 m in length and is divided into three sections, namely the duodenum, jejunum and ileum. The duodenum comprises about 5% of the total length of the intestine, whereas the jejunum and ileum comprise about 50 and 45%, respectively.[1] Out of the total absorption of the ingested material in the gastrointestinal tract, approximately 90% occurs in the small intestine. The surface of the intestine has numerous surface projections called villi that dramatically increase the surface area. While villi increase the surface area by 30-fold, the microvilli increase it by a factor of 600.[1]

The intestinal surface is made up of epithelial cells and is covered by a hydrated gel consisting of heavily glycosylated peptides known as mucins. The mucins are secreted by gastric faveolar cells and intestinal goblet cells and create a barrier that restricts large particles and bacteria from directly coming in contact with the intestinal epithelial cells.[2] The mucous layer is in turn covered by an unstirred water layer that slows down the nutrient absorption by reducing the rate at which nutrients reach the microvilli, but also contributes to the absorption by limiting the diffusional loss of small nutrients that are released from their larger precursors by the brush border digestive enzymes.[3]

The epithelial cells in the intestine include populations of different cell types including enterocytes or absorptive cells, goblet cells, endocrine cells, paneth cells, M cells, tuft cells and cup cells.[4, 5] The epithelial cell layer is sealed by an apical junctional complex which is composed of the tight junction and subadjacent adherens junction. Both tight and subadjacent adherens junctions are supported by a ring of actin and myosin that regulate barrier function.[3] The adherens junctions are composed of cadherins, a family of transmembrane proteins that form strong adhesive interactions between the cells. The adherens junctions are required for the

assembly of tight junctions which seal the paracellular space. Several transmembrane proteins that define tight junctions include claudins, occludins and the peripheral membrane proteins like zona occludens 1 and 2.[3] The tight junction is rate determining in transepithelial transport and a major determinant of mucosal permeability.[3]

5.2   Different routes of intestinal drug absorption

Drug molecules can cross cellular barriers either by diffusion between the cells (paracellular route) or diffusion across the cells (transcellular route, Figure 5.1). Low molecular weight hydrophilic molecules are likely to cross the cellular barriers by the paracellular route while highly lipophilic molecules generally diffuse through the barrier by the transcellular route.[6]

5.2.1   Transcellular route

5.2.1.1 Passive absorption

Passive absorption occurs through the epithelial cells membranes from a region of high concentration to that of low concentration.[7, 8] Passive absorption is not saturable and usually exhibits minimal sensitivity to stereochemical changes in the drug. Passive permeability depends on the uncharged fraction of the drug (in other words the pK_a of the drug), its octanol partition coefficient, hydrogen bonding potential and its molecular size.[8] The solubility of the drug in the aqueous phase of the gut lumen at the site of absorption is also an important requirement for passive intestinal drug absorption.[9]

5.2.1.2 Active transport

While some hydrophilic compounds are transported through the paracellular route others are likely to use a specific transporter system(s) for absorption from the intestine.[8] Active transporters have the capacity to generate concentration gradients across the barriers with the help of various energy coupling mechanisms. While some active transporters directly use ATP as

a source of energy during the transport cycle, other transporters indirectly couple to ATP through the Na^+ electrochemical gradient generated by the ubiquitous Na^+/K^+ ATPase.[7] Unlike passive absorption where increasing the drug dose will cause an increase in the drug absorption, in active absorption increasing the drug dose can cause saturation of the carrier resulting in a plateau for the amount of drug absorbed.[10] Absorption of compounds which are substrates of apical active efflux transporters such as P-glycoprotein (Pgp) may be limited by active secretion back to the apical (luminal) side of the intestinal cells.[10]
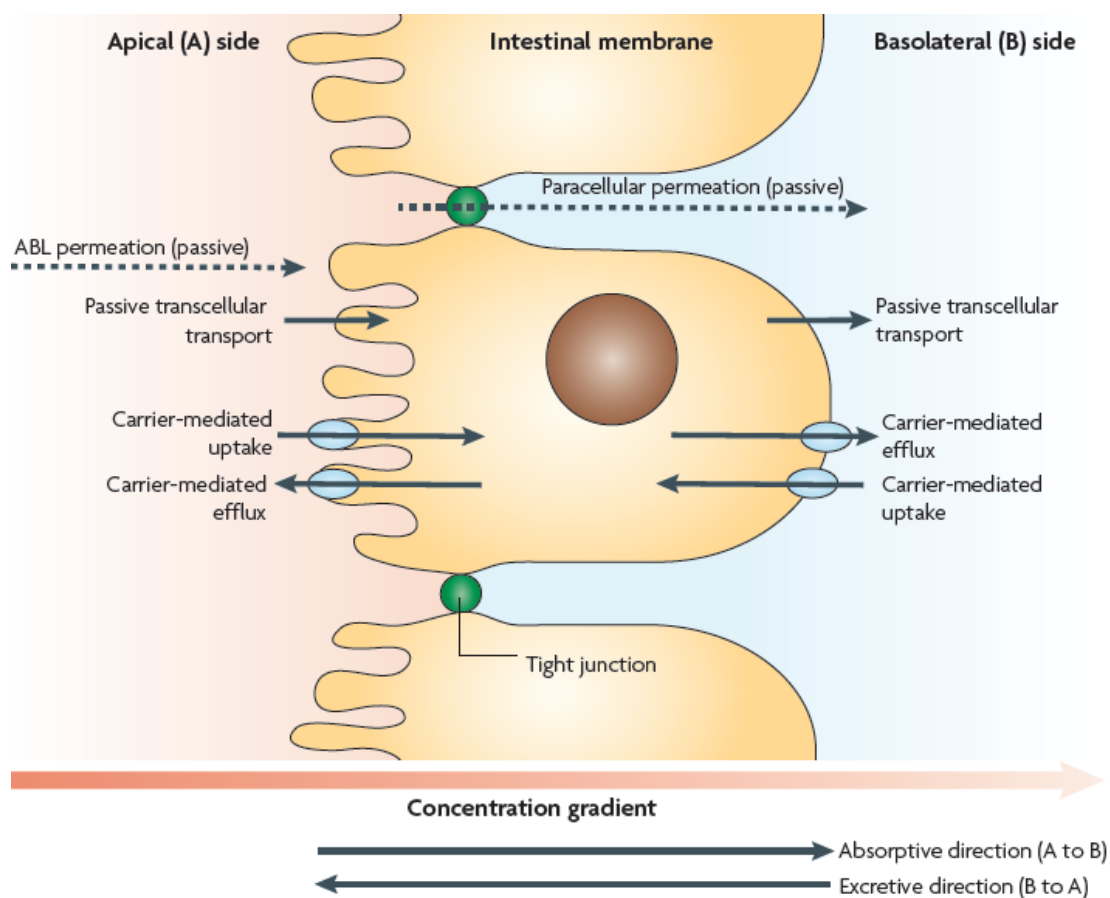
Figure 5.1. A schematic representation of different routes of drug permeation through intestinal cells.[8] (Reprinted with permission from Nature Publishing group)

5.2.1.2.1 Influx transporters in the small intestine

Various transporters are present in the intestine that transport drug molecules across the intestinal wall into blood. The peptide transporter 1 (PEPT-1) oligopeptide transporter that

belongs to the family of solute carrier (SLC) family of transporters is present in the small intestine.[11] The PEPT-1 transporter is mainly present on the brush border membranes of intestinal cells. PEPT-1 transports di- and tripeptides with different charges, but not free amino acids or tetrapeptides.[11]

Organic anion transporting polypeptides (OATPs) are another group of SLC transporters that possess a wide spectrum of amphipathic transport substrates.[12] Amongst the various OATPs, OATP-B is present in the human small intestine.[12] In general, OATP substrates are mainly anionic or amphipathic molecules with a higher molecular weight (>450) and are mostly albumin bound under physiological conditions.[12]

Ganapathy *et al.* recently provided evidence of two novel transporters, namely sodium dependent oligopeptide transporters (SOPT)-1 and 2, in the human ARPE-19 retinal pigment epithelial cell line,[13] the rabbit CJVE conjunctival cell line,[14] and the human SK-N-SH neuronal cell line cell line.[15] Subsequently, the same group showed the presence of these transporters in the Caco-2 cell line.[16] Unlike PEPT-1, these transporters do not transport dipeptides and tripeptides but transport peptides consisting of 5 or more amino acids. These transporters transport various endogenous opioid peptides[14, 17] and synthetic opioid peptides[13, 14] including deltorphin II, DADLE ([D-Ala^2, D-Leu^5]-enkephalin), DAMGO ([D-Ala^2,*N*-MePhe^4,Gly-ol]enkephalin), DSLET ([D-Ser^2,Leu^5,Thr^6]-enkephalin) and other peptides including Tat$_{47-57}$.[13]

Other groups of transporters including the organic cation transporters (OCT); OCT-1, OCT-2 and OCT-3 are expressed in Caco-2 cells and the human intestine.[18-21] This group of transporters is involved in the absorption, distribution and elimination of endogenous compounds (e.g. amines) as well as drugs and other xenobiotics that are positively charged.[18]

5.2.1.2.2   Efflux transporters in the small intestine

Three efflux transporters belong to the ATP binding cassette (ABC) superfamily of transporters, namely multidrug resistant transporter 1 (MDR1) or P-glycoprotein (Pgp), multidrug resistance associated protein (MRP) which includes MRP 1, 2 and 3 and breast cancer related protein (BCRP).[22] These efflux proteins are abundant on the apical side of the cells which is exposed to various xenobiotics and function as gatekeepers against foreign substances in the gut. However, they are not selective for toxic substances and thereby decrease the bioavailability of a number of drugs. The ABC family of transporters consists of a highly conserved ATP-binding cassette consisting of two nucleotide binding domains.[23, 24] The general structure consists of 12 transmembrane (TM) regions; however, the number of transmembrane segments varies with different sub-families.[22] Expression of MDR1 and MRP3 in the human intestine increases from proximal to distal regions, resulting in the highest expression levels in the colon.[25, 26] Expression of MRP2 is highest in the duodenum and decreases in the direction of the ileum and colon where it is minimal.[27]

Intestinal Pgp is localized at the villus tip enterocytes.[28, 29] This is the major site for absorption of orally administered drugs, and hence Pgp is ideally positioned to restrict the absorption by driving efflux back into the lumen.[22] A broad range of molecules that are lipophilic, basic or uncharged and ranging from 300 to 2000 Da can be substrates for Pgp.[22] One of the modes through which Pgp interacts with substrates includes an induced fit mechanism where Pgp is able to accommodate different substrates by altering the packing of its TM domains.[30] For example, while cyclosporine A can be accommodated in the binding site, another Pgp substrate such as colchicine can cause rearrangement in the packing of the TM domain to fit

into the drug binding site.[30] The expression of the other transporters in the MDR subfamily, namely MDR3, is reported to be low in the small intestine and even lower in Caco-2 cells.[31]

While Pgp shares some degree of substrate similarity with MRP2, MRP2 transports organic anions, especially conjugated compounds. It also transports amphipathic compounds.[22] Like Pgp, MRP2 is also localized on the apical side of intestinal cells. There have been reports of the efflux of the fluoroquinolone antibiotic grepafloxacin in Caco-2 cells by both Pgp and MRP2[32-34] and of the dietary flavonoids by MRP2.[35]

BCRP appears to plays a similar role as Pgp and regulates the absorption and disposition of drugs along the intestinal border. Anticancer drugs such as topotecan, irinotecan, mitoxantrone are substrates for BCRP.[22, 36] In addition HIV-1 nucleoside reverse transcriptase inhibitors including zidovudine also act as substrates for BCRP.[37]

5.2.1.2.3   Endocytosis

Endocytosis is characterized by internalization of molecules from the surface of the cell into endosomes/vesicles. Bio-macromolecules such as peptide antigens which are not transported by other pathways due to their size are transported by endocytosis.[10, 38] However, the membrane vesicles formed during the transport process contain proteolytic enzymes that can cause extensive degradation of macromolecular drugs.[10] Endocytosis can be of two types, the highly specific receptor mediated endocytosis or adsorptive mediated endocytosis. Macromolecules such as immunoglobulins and growth factors are transported by receptor mediated endocytosis.[39] Along with macromolecules; smaller peptides are also transported by endocytosis. Sai *et al.* showed that the basic peptide H-Me-Tyr-Arg-MeArg-D-Leu-NH(CH$_2$)$_8$NH$_2$ was internalized by adsorptive mediated endocytosis into Caco-2 cells.[40] Terasaki *et al.* have shown that the dynorphin (Dyn) analog E-2078 is transported into brain capillaries by adsorptive mediated

endocytosis.[41, 42] Uptake of Big Dyn, Dyn A and Dyn B has been studied across neuronal and non-neuronal cells.[43] Preliminary data suggested that while both energy dependent (caveolar endocytosis) and energy independent mechanisms facilitated Big Dyn and Dyn A translocation across the plasma membrane into the cells, Dyn B did not translocate.[43]

5.2.2 Paracellular route

Low molecular weight hydrophilic molecules generally are transported across the cellular barrier by the paracellular route. However, the ability of the drug to cross the cellular barrier by this route is limited by the presence of tight junctions between the cells. The main structural features that affect the paracellular permeability of drug molecules include the molecular size, charge and hydrophilicity. The tight junctions contain narrow pores or gates which open or close and hence create a sieving effect which regulates the molecular diffusion of drug molecules.[6] The tight junctions are impermeable to molecules with molecular radii larger than 11-15 Å.[44] In terms of molecular weight, molecules lower than 200 Da can be absorbed by the paracellular route. Borchardt *et al.* studied the effect of size and charge of peptides on paracellular transport in the Caco-2 intestinal model and observed that as the molecular weight increased (e.g. hexapeptides) the size played an important role while the effect of charge became negligible.[45]

5.3   Intestinal absorption of peptides

Intestinal absorption of peptides is generally limited because of poor biopharmaceutical properties which include metabolic liability and poor cellular permeation. Intestinal permeation of peptides can occur via both paracellular and transcellular pathways. Hydrophilic peptides are generally restricted to the paracellular pathway[44] which depends on the size and the charge of the peptide.[45, 46] Hydrophobic peptides that lack charge and exhibit low hydrogen bonding potential can traverse through the transcellular route.[6, 47] While some peptides that permeate through the

transcellular route diffusely passively, others cross the intestinal barrier with the aid of various transporters located on the apical side of the enterocytes.

5.3.1   Transporters involved in peptide absorption

5.3.1.1 PEPT-1 and PEPT-2 transporters

Both PEPT-1 and PEPT-2 transport di- and tripeptides with different charges, but not free amino acids and tetrapeptides.[11] PEPT-1[48] is present on the brush border membranes of intestinal and renal epithelial cells while the PEPT-2[49] transporter is located on the brush border membranes of renal epithelial cells. While the presence of peptide bond(s) was considered the most important factor in recognition of substrates by these transporters, some studies showed that even compounds without peptide bond(s) can be accepted as substrates.[11] Subsequent studies suggested that the α− or β−amino carbonyl structure of substrates is the key determinant of substrate affinity for PEPT-2 as opposed to PEPT-1.[50, 51] After permeating through the apical side di- or tripeptides are either hydrolyzed by intracellular peptidases in the cytoplasm to amino acids, which then cross the basolateral membrane and are absorbed into the blood, or escape hydrolysis and are absorbed as intact peptides into the blood.[52] Ganapathy *et al.* showed the presence of the PEPT-1 transporter in Caco-2 cells.[53] Similarly, there are reports about an oligopeptide transporter on the basolateral side of Caco-2 cells.[54, 55] However, the characteristics of the apical and basolateral transporters appear to be different in terms of pH requirements of the extracellular media for transport of substrates.[55]

Very recently, Dr. Newstead's group has determined the crystal structure of PEPT-1 from *Shewanella oneises*[56] and from the bacterium *Streptococcus thermophilus*.[57] While the crystal structure obtained from the latter reveals an inward facing conformation, the overall crystal structure of the transporters from both organisms is similar.[57]

5.3.1.2 SOPT-1 and SOPT-2

Ganapathy *et al*. showed the existence of SOPT-1 and 2 in Caco-2 cells.[16] Unlike PEPT-1 and 2, these transporters do not transport dipeptides and tripeptides but instead transport peptides consisting of 5 or more amino acids. SOPT-1 is almost entirely sodium dependent, while SOPT-2 is partially Na^+ dependent. H^+ and Cl^- also significantly influence these transport systems. SOPT-1 and 2 can be differentiated on the basis of the modulating effects of di- and tripeptides on these transporters.[16] While the di- and tripeptides stimulate SOPT-1, SOPT-2 is inhibited by these peptides. This inhibition is not due to competition for the transport site, as these peptides do not appear to be substrates for SOPT-2. Instead, they appear to function as allosteric modulators of SOPT-1 and 2.[16] The model peptide substrates used to characterize these transporters included the opioid peptide deltorphin II for SOPT-1 and DADLE, a metabolically stable analog of enkephalin, for SOPT-2. Although these peptides are known substrates for OATP's, Ganapathy *et al.* showed that these substrates were transported by SOPT-1 and SOPT-2, respectively, and not *via* OATP's in Caco-2 cells. While the discovery of these transporters is encouraging, it is not known whether these systems are expressed in the normal intestinal tract. The physiological role of these transporters remains unknown.[16]

5.3.1.3 Other transporters

Members of the OATP family of transporters have been shown to be involved in transporting opioid peptides across the blood-brain barrier (BBB) and blood cerebrospinal fluid barrier in c-RNA injected *Xenopus* oocytes.[58] While the human OATP-A, which is expressed at the human BBB was shown to transport the linear peptide deltorphin II and to a lesser extent the cyclic peptide DPDPE (*cyclo*[D-Pen^2,D-Pen^5]enkephalin), rat OAPT1 which is expressed on the apical membrane of choroid plexus epithelial cells exhibited high transport activity for both

deltorphin II and DPDPE. DPDPE was also transported by rat OATP2 which is expressed at rat BBB and the basolateral plasma membrane of choroid plexus epithelial cells. [58] Furthermore, Pollack *et al.* demonstrated *in vivo* in the murine brain perfusion model that DPDPE could be transported into the brain by OATP's, although it was also a Pgp substrate.[59] Recently, OATP 4A1 and OATP3A1 have been shown to exist in Caco-2 cell membranes.[60-62]

The microcystins (MC) (Figure 5.2) are a group of non-ribosomal macrocyclic peptides that display hepatotoxicity.[63] MC variants namely MC-LR and MC-RR display varying levels of hepatotoxicity which is partly attributed to their uptake by heaptic OATPs.[64, 65] In order to investigate the intestinal absorption of these peptides uptake studies of variants of microcystins were performed in Caco-2 cells. These studies suggested that these molecules have a fast; non-ATP dependent mechanism of uptake.[62] The MC variants also displayed a temperature dependent mechanism of efflux from the Caco-2 cells. The low lipid permeability of MC's, the presence of OATP transporters and the non-ATP dependent uptake of MCs into Caco-2 cells suggested that the uptake of MC variants likely involved OATP transporters. There also existed a likely active mechanism of excretion through efflux pumps.[62]

Microcystin-LR
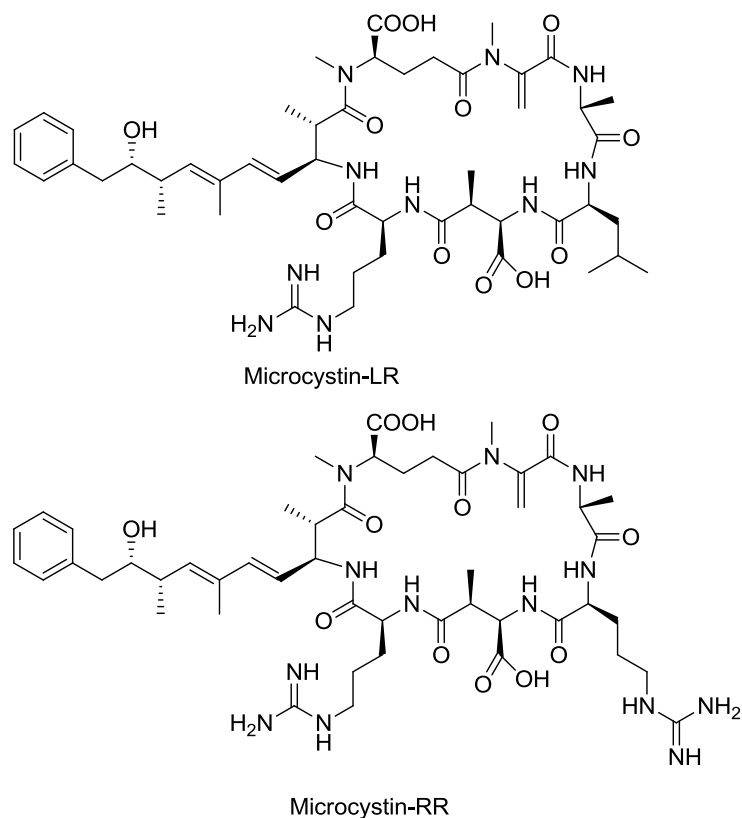
Microcystin-RR

Figure 5.2 Microcystins

5.3.2   Peptides exhibiting intestinal absorption

A few orally active non-opioid and opioid peptides have been studied previously. The orally active octapeptide analog of somatostatin octreotide (oral bioavalability $\leq 0.3\%$), was shown to be at least partially absorbed by a membrane transport system.[66-68] The orally administered leutinizing-hormone-releasing hormone (LHRH) analog (D-Ala[6]-desGly[10]-NH$_2$)LHRH-ethylamide, dose = 10 µg in rats) was shown to be orally active.[69, 70] One of the early examples of opioid peptides absorbed through the rat intestine is the synthetic pentapeptide metkephamid (Tyr-D-Ala-Gly-Phe-NMe-Met-NH$_2$) which displayed an oral bioavalability of 0.22%.[71] A dermorphin analog, ADAMB (N^{α}-amidino-Tyr-D-Arg-Phe-Meβ-Ala-OH, Figure 5.3) that contains N-terminal guanidylation, exhibited oral analgesic activity in mice with an ED$_{50}$ of 5.5 mg/kg[72] and was 4-fold more potent as an analgesic than morphine following oral

administration. Another tetrapeptide analog containing D-Arg at position 2, Dmt[1]-DALDA (Dmt = 2', 6'-dimethyltyrosine, DALDA = Tyr-D-Arg-Phe-Lys-NH$_2$), was transported across Caco-2 monolayers (P$_{app}$ = 1.24 x 10^{-5} cm/s), suggesting that it could be absorbed orally.[73] The Dmt-Tic (Tic = tetrahydroisoquinoline-3-carboxylic acid) derivative Dmt-Tic-Lys-NH-CH$_2$-Ph (MZ-2, Figure 5.3) displayed antagonism at both MOR and DOR and blocked centrally administered morphine after oral administration in mice with an AD$_{50}$ of 1.64 mg/kg.[74] Oral administration of this peptidomimetic caused reduction in weight gain and improvement in obesity related factors in obese mice.[75]

Certain orally active macrocyclic peptides have also been studied. The most significant example of an orally active peptide is that of the immunosuppressive undecapeptide cyclosporine A (Figure 5.3). The permeability of cyclosporine A (Caco-2 P$_{app}$ (A-B) = 1 x 10^{-6} cm/s at a concentration of 0.5 μM) is thought to occur through passive diffusion, but there also exists evidence for carrier mediated efflux, presumably by Pgp.[76] Cyclosporine A has several unusual physicochemical properties that affect its absorption. Nine of the eleven peptide bonds in cyclosporine are methylated, reducing the number of hydrogen bonding positions. The *N*-methyl groups, lack of charged groups and the partial β-sheet conformation result in high lipophilicity and low aqueous solubility, and hence the peptide requires emulsifying formulations for drug delivery.[77, 78] The L- and D-Trp isomers of the opioid macrocyclic natural product CJ-15,208 have been shown to exhibit opioid activity after oral administration[79, 80] (see chapter 6 for more information). Lokey and coworkers have identified a membrane permeating orally bioavailable peptide scaffold. The macrocyclic hexapeptide (*cyclo*[Leu-*N*Me-D-Leu-*N*Me-Leu-Leu-D-Pro-*N*Me-Tyr]) possessed an impressive oral bioavailability of 28% in rat.[81] Kessler and coworkers synthesized *N*-methyl analogs of the somatostatin receptor agonist *cyclo*(-Pro-Phe-D-Trp-Lys-

Thr-Phe-) (Figure 5.3), also known as the Veber-Hirschmann peptide, and studied their permeability in the Caco-2 intestinal model. Among the various *N*-methyl analogs synthesized, an analog with three methyl substituents displayed an absolute oral bioavailability of 9.9% in rats and had 8- to 10-fold higher apparent permeability (P_{app}) as compared to the parent peptide (P_{app} = 0.5 x 10^{-6} cm/sec).[82] In order to evaluate the effect of multiple methyl groups on the bioavalability of peptides, Kessler and coworkers also synthesized a polyalanine cyclic hexapeptide library (Figure 5.3) varying in the number and position of the *N*-methyl groups. The peptides were evaluated for intestinal permeability in the Caco-2 model, and selected peptides displayed P_{app} > 1 x 10^{-5} cm/sec. A methyl group placed adjacent to the D-Ala residue was a common structural feature in most of the analogs that displayed high P_{app} values. While the exact transport route was not characterized, the peptides did not appear to be transported by passive or active transcellular route and were likely transported by facilitated diffusion.[83]
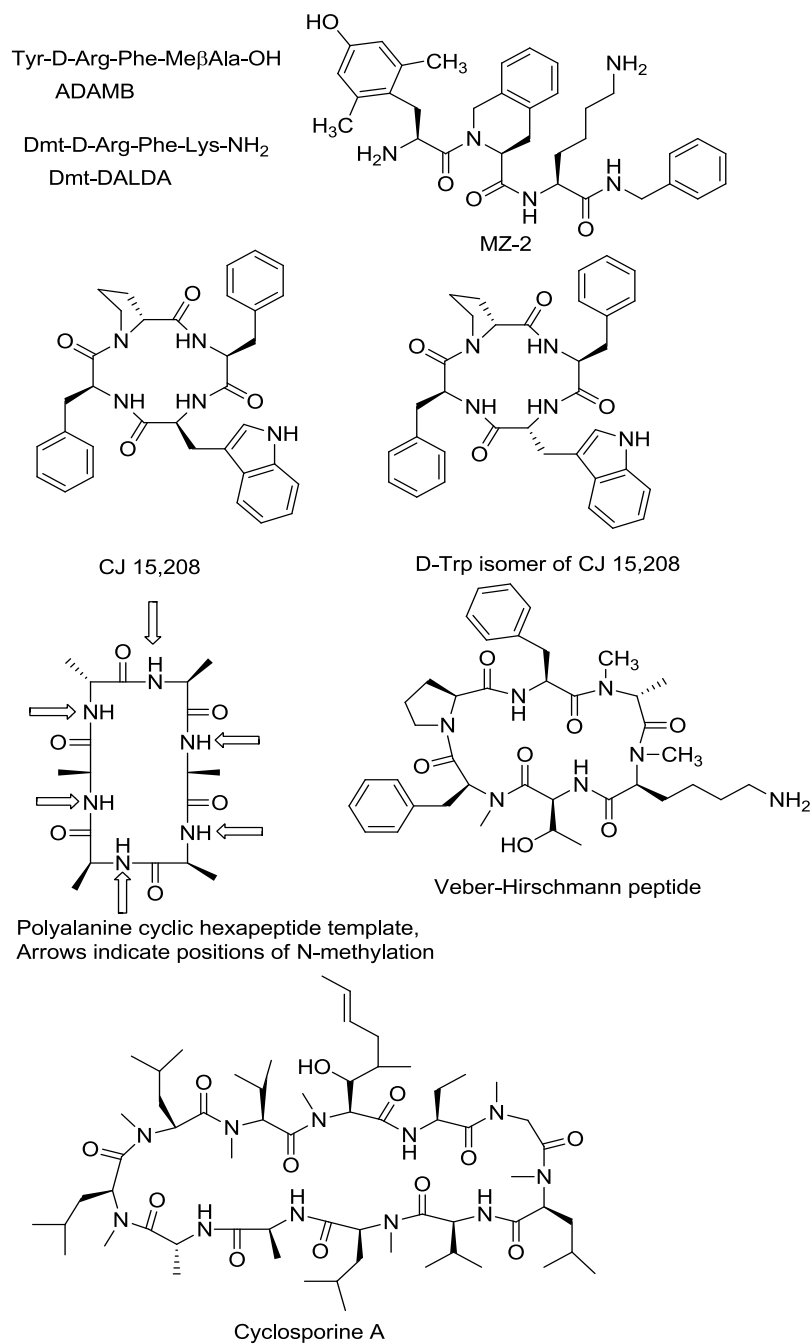
Figure 5.3. Peptides exhibiting intestinal absorption

Borchardt and coworkers developed the concept of using cyclic peptide prodrugs to modify the physicochemical properties of peptides to increase intestinal permeability and thereby enhance oral bioavalability.[84] The acyloxyalkoxy (ACA),[85] phenylpropionic acid (PPA)[86] and

174

coumarinic acid (CA)[87] based cyclic prodrugs of DADLE were synthesized (Figure 5.4) and evaluated for their permeation characteristics in the Caco-2cell monolayer model. As expected the P_{app} of DADLE was very low ($7.8 \pm 0.7 \times 10^{-8}$ cm/sec). While the CA[87] and PPA[86] prodrugs showed 31- and 72-fold increased Caco-2 permeability, respectively, the the ACA[85] prodrugs displayed 4-fold lower transport as compared to DADLE. While the CA[87] and PPA[86] prodrugs did not appear to be substrates for efflux transporters, the low permeability of ACA[85] prodrug suggested that it might be acting as a substrate for at least one of the efflux transporters present in Caco-2 cells. However, subsequent studies with the CA prodrugs suggested that it was a substrate for P-glycoprotein and MRP-2 efflux transporters present in Caco-2 cells.[88] In addition, a modified CA prodrug (Figure 5.4) was also found to be a substrate for both Pgp and MRP2.[89] This difference with the previous results was attributed to the different lots of Caco-2 cells used.[88] Borchardt and coworkers also studied the effects of Pgp inhibitors on the blood-brain barrier (BBB) permeation of cyclic prodrugs of DADLE in MDR1-MDCK cells and showed that Pgp is the major determinant affecting the permeability of these prodrugs across this model of the BBB.[90] They also performed transport studies of cyclic prodrugs of DADLE in the *in situ* perfused rat ileum model.[91] In these studies the cyclic prodrugs exhibited low permeation and were also found to be substrates for Pgp. In addition, efflux by other transporters and/or drug metabolizing enzymes were likely to play a role in their low permeation.
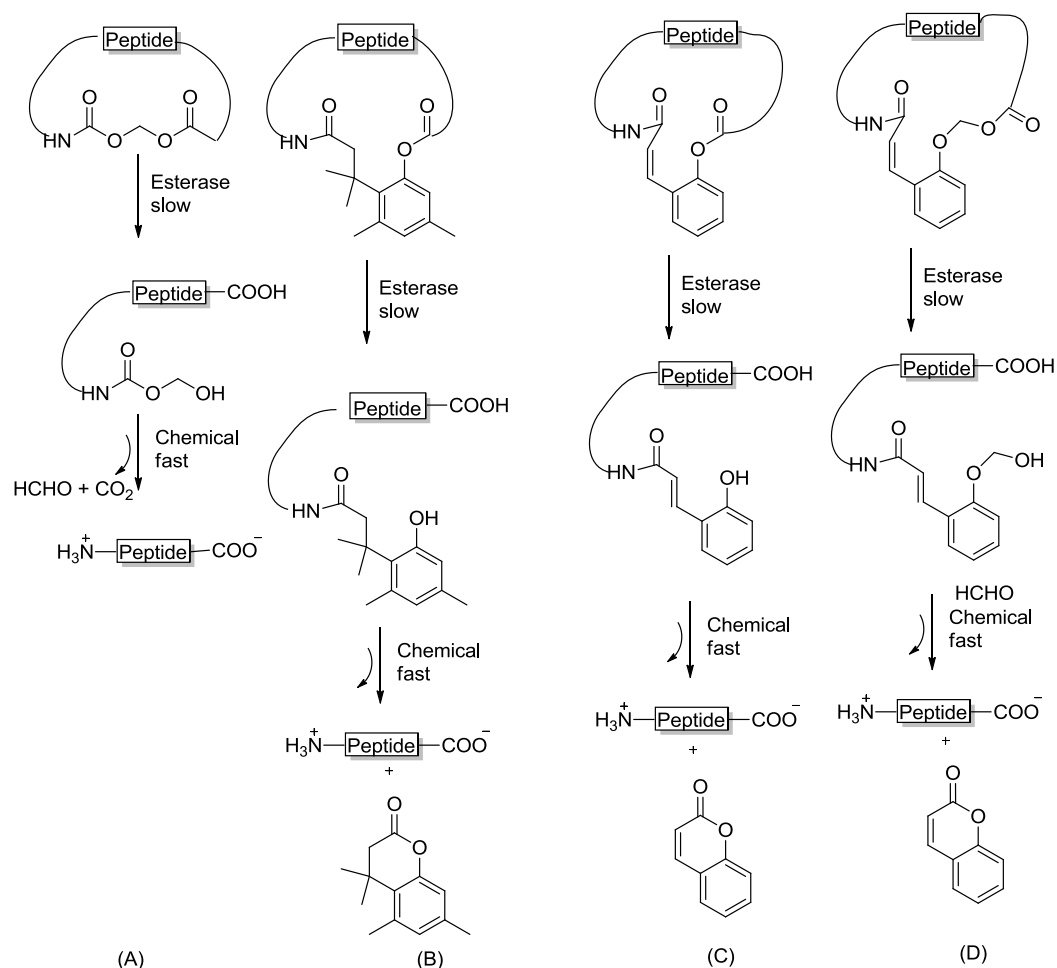
Figure 5.4. Bioconversion of peptide cyclic prodrugs to peptides. (a) ACA,[85] (b) PPA,[86] (c) CA,[87] and (d) modified CA[89] cyclic prodrugs.

5.4   Methods for evaluation of intestinal permeability

5.4.1   Physicochemical methods

Lipophilicity is one of the most important physicochemical parameters for predicting intestinal absorption of drugs. Historically, the octanol-water partition coefficient (log *P*) was used for predicting absorption. While there is generally a correlation between log *P* and absorption that appears to hold true for passively transported drugs that are not subject to efflux, the correlation may not hold true for drugs that are transported by active transport.[92]

Immobilized artificial membrane chromatography (IAMC) is a technique which consists of phospholipid molecules covalently attached to the silica particles of the column. IAMC is efficient, cost effective and can predict permeability of passively permeable compounds.[93] However, the permeability of actively transported compounds cannot be predicted by this method.[93] IAMC has also been used to predict solute partitioning into liposomes, brain uptake and human skin permeability.[1] Giralt and coworkers used IAMC to evaluate NMe-Phe rich peptides as BBB shuttles for carrying drug cargoes into the CNS.[94, 95] The permeability of the peptides correlated well with the phospholipophilicity (k_{IAM}) obtained by IAMC until the number of NMe-Phe residues was increased to four in the peptides. However, with further increase in the number of NMe Phe residues, the phospholipophilicity obtained by IAMC was too high for the peptide to permeate through the artificial membrane in the parallel artificial membrane permeability (PAMPA) assay.[94]

PAMPA[96] method consists of a hydrophobic filter material that is impregnated with a solution of lecithin in an inert organic solvent such as dodecane or hexadecane. The lecithin solution is adsorbed on to a porous frit that mimics a membrane and the permeability of drugs through this membrane is studied. The results obtained from this assay show an excellent correlation with the extent of absorption of a diverse set of well characterized drugs in humans.[96] Although it has high throughput capability, it suffers from similar limitations as the IAMC technique. Giralt and coworkers studied NMe-Phe rich peptides as BBB shuttles for carrying drug cargoes into the CNS in the PAMPA model. Among the various NMe-Phe rich peptides studied, the peptides containing NMe-Phe as the N-terminal amino acid showed high permeability in PAMPA and were the best shuttles for carrying drug cargoes into the CNS.[95] Kessler and coworkers studied permeability of macrocyclic hexapeptides with multiple N-methyl

groups in different positions in the PAMPA model. While N-methylation was shown to increase permeability as compared to the non-methylated peptides in the Caco-2 model, none of them permeated through the PAMPA artificial membranes, suggesting that N-methylation does not facilitate transcellular permeability of the cyclic hexapeptides.[83]

5.4.2   *In vitro* methods

The *in vitro* techniques used for assessment of intestinal absorption are less laborious and cost intensive compared to *in vivo* analyses. However, the effects of physiological factors during absorption such as gastric emptying, gastrointestinal pH, etc. are not taken into account in these methods.

5.4.2.1 Animal tissue based methods

The everted gut technique[97] involves incubation of the everted sacs of the rodent intestinal region of interest in appropriate media which contains the drug solution. The drug transport is monitored by measuring concentration of drug inside the sacs. It is an ideal model for studying intestinal absorption as it can be applied for drugs transported by both active and passive transport. However, the gut lacks active blood supply and hence this can lead to rapid loss of viability. Additionally, everting the gut can cause morphological changes leading to erroneous results.[1]

The Ussing method[98] involves isolation of intestinal tissue, which is cut into strips of appropriate size and clamped it to a suitable device for measurement of drug transport across the tissue. The method is ideal for studying the regional differences on the absorption of drugs by mounting tissues from different intestinal areas. However, it also suffers from the same limitations as mentioned above for the everted gut technique.[1]

5.4.2.2 Cell based methods

5.4.2.2.1   Caco-2 model of intestinal permeability

The Caco-2 cell monolayer model is the most extensively used model for evaluating intestinal drug permeability and absorption. Caco-2 cells were obtained from a human colon adenocarcinoma.[99-102] They undergo spontaneous enterocytic differentiation and grow to confluency on semipermeable porous filters in 21 days. This model is used for mechanistic studies and as an *in vitro* screening tool for assessing the permeability of drugs. However, there remains variability in the absolute permeability coefficients of the individual compounds due to differences in the source of Caco-2 cells, differences in the cell culture conditions, the composition of cell subpopulations, procedures for transport experiments and calculation methods. This model can be used to measure both active and passive transport. The Caco-2 model can give false negative results as the cell monolayer appears to be exhibit tighter junctions than the human small intestine due to its colonic origin.[103] For example, ranitidine and atenolol showed poor permeability in this model despite adequate absorption in humans.[1] Furthermore, there is also a limit to the amount of organic solvent that can be used in the Caco-2 assay. Hence, a significant percentage of new lipophilic drug entities cannot be evaluated in this model.[1]

I.   Factors that affect Caco-2 monolayer permeability
a.   Factors related to the Caco-2 cells

Caco-2 cells are a heterogeneous cell population with different morphologies[104] and with varying levels of Pgp expression and function.[105, 106] Differences have been noted in the transepithelial electric resistance (TEER) and in the permeability values of low and high permeability standards in Caco-2 cells from different sources.[107] Differences were also noted in the cell shape and size, multilayer formation, expression levels of influx and efflux transporters and actin staining.[108]

It has been shown that differences in passage number can cause variations in TEER, cell growth and mannitol flux.[109] The passaging procedure affects the biological and the barrier properties of Caco-2 monolayers with a selection for faster growing subpopulations.[110] The passage number affects efflux mediated by the Caco-2 cells because of variations in the expression of efflux pumps including Pgp.[111]

The cell seeding density on the semi-porous filters affects the time taken for the cells to proliferate and subsequently differentiate. A lower seeding density can cause incomplete formation of a monolayer, while higher seeding density can cause formation of multilayers. Also the expression levels of Pgp were found to decrease with increasing cell density.[112]

The age of the monolayer influences the morphology, barrier properties and expression of transporters. The cells exhibit different morphologies at different monolayer ages.[101] On polycarbonate (PC) filters initial cell migration occurs on day 2 followed by subconfluency on day 4 and apparent confluency on day 6.[113] Using phalladoin for visualizing cell morphology, it was found that a thin monolayer was formed on day 7, a well-established brush border was formed on day 21 and multi-layer formation was observed on day 28.[112] Hence, differences can occur in the permeability values depending on the day the transport experiments are performed. It was also found that the TEER values are higher and permeability values for mannitol, a low permeability standard, were lower with an increase in the age of the monolayers.[114] There are different findings reported concerning whether the expression levels of Pgp are affected by monolayer age.[111, 115]

The cell source also causes significant variations in the levels of transporter expression[106] (see the next section for a detailed discussion).

b.   Factors related to the media

Different components of the cell culture media and frequency of cell feeding can also influence Caco-2 cell monolayer integrity, expression levels of transporters and permeability values. The concentrations of both glucose and glutamine in the culture media can affect the tight junctions and the barrier properties of Caco-2 monolayers.[116, 117] The frequency of changing the culture media affects the activity of the enzymes present in the cell membranes and the expression of various transporters in Caco-2 cells.[118] Consequently, this can affect the permeability of substrates transported by active transport. The presence of serum in the media can also influence tight junction formation, and monolayers nourished with serum-containing media displayed higher TEER values than those without serum.[119] Knipp and coworkers showed that the source of Caco-2 cells and the media composition caused significant variations in transporter expression.[106] For example, Pgp was expressed approximately 7-fold higher in cells obtained from ATCC as compared to cells obtained from Dr. Thomas Cook's laboratory (Rutger's University) cultured in minimum essential medium alpha (AMEM) and approximately 3-fold higher in cells obtained from ATCC as compared to cells from Dr Cook's laboratory cultured in Dulbecco's modified Eagle's medium (DMEM). Further, the differences in the expression levels of Pgp were decreased when cells from both the sources were cultured in DMEM as compared to those cultured in AMEM. Similar differences were obtained in the case of several other SLC transporter family members.[106]

The pH of the transport buffer determines the ionization state of drugs which can affect drug permeability. While the permeability of acidic drugs was greater in a buffer with pH 5.4, the permeability of basic drugs was greater in buffer with pH 7.2.[120]

c.   Factors related to other experimental conditions

The characteristics of the semi-porous filter, including its composition, diameter, and pore size can also affect cell proliferation and differentiation. The type of filter material can affect the thickness of the monolayer and the morphology of the cells. It was also found that Caco-2 monolayers were more prevalent on PC filters as compared to polyethylene terephthalate (PET) filters where multilayers were observed.[121] Filters with pores greater than 1 μM resulted in cell migration and subsequent loss of polarity.[113] The TEER values increased with an increase in the filter diameter from 6.5 to 12 to 24 mm.[122] It was also noted that Pgp expression decreased with increased cell culture time if cells were grown in plastic flasks, whereas growing the cells on PC filters led to an increase in the expression of Pgp.[111]

Collagen coating can accelerate cell proliferation and development of cell monolayers and also influences drug adsorption.[123] The presence of a collagen coating was found to increase the expression levels of transporters.[112]

Variation in agitation can result in variability in the transport of drugs by passive diffusion. Passive diffusion across the barrier is a combination of diffusion through the unstirred water layer (UWL) and the cell monolayer.[114] It has been shown that the absorption of highly permeable lipophilic, poorly water soluble drugs is significantly affected by the UWL.[124] Agitation or stirring during the transport experiments reduces the thickness of the UWL.[125] An increase in agitation increases the permeability of poorly water soluble, passively transported compounds.[126]

Variations can arise in the P_{app} values depending on whether permeability is analyzed using a single time point or multiple time points and also whether the calculations are performed using a fixed donor compartment concentration for all time points or by adjusting the donor

concentration for drug loss over time. In the case of high permeability drugs, P_{app} values can be higher for multiple time points rather than a single time point.[127] Varying permeability values can also be obtained through calculations depending on whether they take into account cellular retention and filter adsorption.[128, 129]

II.   Comparison of the transporter expression levels in the human small intestine and the Caco-2 cells

Seithel *et al*. determined a general ranking of the mRNA expression levels of the transporters in Caco-2 cells and human jejunal tissue (Table 5.1).[21] In Caco-2 cells it was: MRP2 > OATPB > PEPT1 >> MDR1 > monocarboxylate transporter (MCT1) ~ MRP3 ~ BCRP ~ OCT-N2 ~ OCT3 ~ OCT1 > organic anion transporter (OAT)-2. The general rank order of the transporters in human jejunal tissues was found to be PEPT1 >> MRP2 ~ MDR1 ~ BCRP > MRP3 > OCTN2 > MCT1 > OATP-B > OCT1 > OAT2 ~ OCT3. Quantitatively, PEPT1 was 10-fold, MDR1 7-fold and MRP2 2-fold lower in Caco-2 cells compared to human jejunum. Similarly, the genes with intermediate expression levels in human jejunum were also expressed 2- to 7-fold lower in Caco-2 cells. An exception was OATP-B, which was expressed at 13-fold higher levels in Caco-2 cells as compared to the human jejunum. However, there is some uncertainty in data for OATP-B due to the low amplification efficiency of this transporter. However, in contrast to the above finding, Yee and coworkers reported that Pgp is overexpressed in the Caco-2 cells as compared to the human intestine.[130] The significant difference in the expression levels of the transporter is an important factor to be considered when analyzing the permeability data obtained from the Caco-2 cell based model.

Table 5.1 Transporter ranking according to their relative gene expression in Caco-2 cells and human jejunum[21]

Transporter	Caco-2 cells[a]	Human Jejunum[a]
MRP2	1	2
OATP-B	2	8
PEPT1	3	1
MDR1	4	3
MCT1	5	7
MRP3	6	5
BCRP	7	4
OCTN2	8	6
OCT3	9	11
OCT1	10	10
OAT2	11	9

[a] 1 corresponds to the transporter with the highest expression and 11 corresponds to the transporter with the lowest transporter expression.

TC-7 and 2/4/A1 are alternative cell-based models to the Caco-2 model. However, they display certain limitations and hence they have not replaced the Caco-2 model for evaluating intestinal permeability. TC-7 is a subclone isolated from the Caco-2 cells that has similar morphology as the Caco-2 cells and gives higher TEER values after 21 days as compared to the Caco-2 cell line.[131] However, the TC-7 has been shown to be unsuitable for predicting permeability of highly lipophilic drugs, drugs that have low-moderate intestinal absorption and drugs that are actively transported.[132] The 2/4/A1 cells originate from fetal rat intestine.[133] However, they do not display the morphological properties of a fully differentiated human intestine. This is because the 2/4/A1 cell line is obtained from a fetal rat intestine at 18 day gestation, when the rat intestine is not well differentiated. However, the human fetal intestine is well differentiated at this time point. While the2/4/A1 cells express intestinal brush border enzymes, efflux transporters such as Pgp, MRP and BCRP are not functional in these cells.[133, 134] In addition these cells do not express the dipeptide transporter PEPT1.[134] Hence the 2/4/A1 cells

are also considered unsuitable for evaluating actively transported compounds or identifying potential Pgp substrates.

5.4.2.2.2 MDCK cell based model

The Madin Darby canine kidney (MDCK) cells differentiate into columnar epithelial cells and form tight junctions, and hence are used as a model to assess permeability of drug molecules.[135] A good correlation has been obtained between the permeability values obtained from MDCK cell and Caco-2 cell monolayers for passively transported drugs;[136] however, more extensive studies are required to confirm this for actively transported drugs. MDCK cells have been transfected with various transporter genes to produce MDCK cell lines that express selected transporters. For example, the MDCK cells are transfected with the *mdr1* gene responsible for expressing Pgp to produce MDR1-MDCK cells. The shorter culture time (3 days vs. 3 weeks) give the MDCK cells a major advantage over the Caco-2 cell model.[136] However, the difference in species and organ is a disadvantage of the MDCK cell line compared to the Caco-2 cell line which was obtained from human colon. The tendencies of transfected MDCK cells to form multi-layers and loss of polarization in the lower layers of cells are also disadvantages for permeability studies.[137] Borchardt and coworkers showed that the apparent kinetic constants and affinities of substrates determined in MDR1-MDCK and MRP2-MDCK cell monolayers may be different from those obtained in Caco-2 cell monolayers.[138, 139] These differences were suggested to result from differences in the relative expression levels of total Pgp and MRP in Caco-2 and transfected MDCK cells, different orientations of the Pgp or MRP in the two cell lines and/or the different partitioning of substrates into the cell membranes.[138, 139]

Recently, MDCK cells have been used as an intestinal model to study the transport of exedin-4, a 39 amino acid anti-diabetic peptide. To improve patient compliance efforts are being

made towards development of its oral administration. It displayed low permeability (0.10 ± 0.06 $\times$ 10^{-6} cm/s) and showed time dependence and, energy independence transport indicative of passive transport.[140] The effect of a self nano-emulsifying drug delivery system (SNEDDS) on the transport of insulin phospholipid complex (IPC) was evaluated in the MDCK cell monolayers and shown to enhance the transport of IPC.[141]

5.4.3   *In situ* method

This method utilizes *in situ* perfusion of intestinal segments to study the permeability of drugs.[142-145] The cannulated intestinal segments are perfused with the drug solution prepared in physiological buffer, and the absorption of the drug is assessed on the basis of the disappearance of the drug from the intestinal lumen. The major advantage of this technique as compared to other techniques is the intact blood and nerve supply to the tissue in the experimental animals. The method is highly accurate for predicting permeability by passive diffusion.[146] Although this method accurately predicts drug absorption, it is costly as it requires a large number of animals to get statistically significant results and also requires large amounts of compound. Administration of anesthesia and surgery can also cause significant changes in blood flow to the intestine which can affect the rate of compound absorption. Another major disadvantage of this method involves its dependence on the disappearance of the compound from the luminal side as an indication of absorption, since the decrease in the concentration in the perfusate may not always represent the rate of absorption, especially in cases where intestinal or presystemic metabolism occurs.[1]

5.4.4   *In vivo* methods

Bioavailability studies are performed in laboratory animal models to predict the rate and extent of drug absorption in humans. The conventional method of estimating oral bioavailability

is through administration of systemic intravenous (IV) and oral doses with a washout period between administrations. The order of IV and oral doses can be randomized. The drug concentration is plotted vs. time and the oral bioavailability is defined as the area under the curve (AUC) of the drug administered by the oral route divided by the AUC obtained following IV administration. The underlying assumption in this setting is that the clearance of the drug from one dose to the next remains constant. However, some drugs are able to modify their absorption, distribution, metabolism and excretion by induction or inhibition of cytochrome P450s which can affect the time course of the subsequent dose.

5.5   Common challenges pertaining to analysis of poorly water soluble drugs

Drug transport experiments of poorly water soluble drugs involve various challenges. For poorly water soluble compounds the stock solution of the drug, generally in DMSO, when added to the aqueous transport buffer can result in immediate precipitation. Filtration of the drug solution prior to the experiment removes the insoluble drug particles, but may result in a low concentration of drug that is below the limit of analytical detection.[147] Without filtration, the drug solutions may be heterogeneous suspensions which can result in variations in the drug concentration and low reproducibility.[124] Lipophilic drugs can adsorb to plastic and the filter support, and accumulation within the barrier can cause loss of compound, poor recovery and low mass balance, which in turn can also result in erroneous permeability values. [124]

For *in vitro* models one technique to improve the ability to measure permeability is to establish sink conditions throughout the course of the experiment. Passive diffusion is driven by a concentration gradient. If sink conditions aren't maintained passive diffusion may not occur because of loss of a concentration gradient. Practically for sink conditions to be maintained the concentration of the receiver compartment should not exceed 10% of the concentration in the

donor compartment.[124] Maintaining sink conditions can be problematic in the case of poorly soluble drugs[124] and can have a major impact while studying transport of low solubility and high permeability compounds.[148] Maintaining sink conditions in the case of low solubility compounds avoids saturation in the receiver compartment, and in the case of high permeability compounds inhibits the back diffusion to the donor compartment.[148]

5.6   Experimental modifications for poorly water soluble compounds

5.6.1   Modifications in the media composition

Several excipients can be used for solubilizing poorly soluble drugs, but the effect of the excipient on drug solubility and drug permeability can vary in a compound dependent manner.[149] Different excipients also have variable effects on the monolayer integrity of Caco-2 cells. Solubilizing agents that have been used in Caco-2 studies include organic cosolvents such as dimethylsulfoxide (DMSO), *N,N*-dimethylacetamide (DMA), *N*-methylpyrrolidone (NMP), and cyclic polysaccharide cyclodextrins.[150, 151]

Solubilizing agents, especially surfactants such Cremaphor EL and Tween 80, appear to diminish the activity of efflux transporters, [152, 153] and hence the permeability values obtained for drugs differ with changes in the concentration of excipient used.[154] The use of solubilizing agents such as surfactants in transport studies can compromise the free drug concentration due to micellization. Hence, to avoid erroneous conclusions the data must be corrected for the free concentration of the drug. The data can be corrected by a method called the reciprocal permeability approach.[155] It enables the calculation of true P_{app} *via* extrapolation of the P_{app} measured at three surfactant concentrations above the critical micellar concentration.

Highly lipophilic compounds tend to adsorb to cell membranes. Inclusion of bovine serum albumin (BSA) appears to minimize the binding of compounds to cell membranes and

also reduces non-specific binding of the drug to experimental apparatus.[156] Recovery values of the compounds can be increased with inclusion of BSA in the medium.[157, 158] BSA also appears to mimic the *in vivo* sink conditions.[124] Although inclusion of BSA appears to be beneficial in many respects, it increases the cost and the complexity of the study as an additional step of sample preparation is often involved.[158]

Most permeability studies are performed in Hanks balanced salt solution (HBSS) without a pH gradient across the monolayers and without physiologically important molecules umsuch as phospholipids and bile salts. Utilizing a biologically relevant medium such as fasted state intestinal simulated fluid (FaSSIF)[159] which contains both bile salts and phospholipids helps to mimic *in vivo* conditions and reduces non-specific adsorption of drugs. This biorelevant medium can also assist in solubilizing the poorly soluble drugs through micellization.[124] However, the effects of these micelle forming agents on drug permeability studies are controversial and appear to be dependent on the transport mechanism of the drug.[124] In addition, inclusion of biologically relevant macromolecules increases the complexity of sample preparation. For example, for non-radioactive analytical methods, prior to analysis samples containing biologically relevant molecules like BSA must be treated with an organic solvent such as MeCN to precipitate proteins.[158]

5.7   References

1.   Balimane, P. V.; Chong, S.; Morrison, R. A. Current methodologies used for evaluation of intestinal permeability and absorption. *J Pharmacol Toxicol Methods* **2000,** *44*, 301-312.

2.   Johansson, M. E.; Phillipson, M.; Petersson, J.; Velcich, A.; Holm, L.; Hansson, G. C. The inner of the two Muc2 mucin-dependent mucus layers in colon is devoid of bacteria. *Proc Natl Acad Sci U S A* **2008,** *105*, 15064-15069.

3.   Turner, J. R. Intestinal mucosal barrier function in health and disease. *Nat Rev Immunol* **2009,** *9*, 799-809.

4.   Carr, K., and Toner, P., Morphology of the intestine. In *Pharmacology of the intestine*, Csaky, T., Ed. Springer and Verlag: New York, 1984; pp 1-50.

5.   Madara, J., and Trier, J., Functional morphology of the mucosa of the small intestine. In *Physiology of the gastrointestinal tract*, Johnson, L., Ed. Raven press: New York, 1987; pp 1209-1249.

6.   Conardi, R. A.; Burton, R. T.; Borchardt, R. T., Physicochemical and biochemical factors that influence a drug's cellular permeability by passive diffusion. In *Lipophilicity in Drug action and Toxicity*, Plisaki, V.; Testa, B.; Waterbeend, H. V., Eds. VCH: Weinheim, 1996; pp 233-252.

7.   Sarmento, B.; Andrade, F.; da Silva, S. B.; Rodrigues, F.; das Neves, J.; Ferreira, D. Cell-based in vitro models for predicting drug permeability. *Expert Opin Drug Metab Toxicol* **2012,** *8*, 607-621.

8.   Sugano, K.; Kansy, M.; Artursson, P.; Avdeef, A.; Bendels, S.; Di, L.; Ecker, G. F.; Faller, B.; Fischer, H.; Gerebtzoff, G.; Lennernaes, H.; Senner, F. Coexistence of passive and carrier-mediated processes in drug transport. *Nat Rev Drug Discov* **2010,** *9*, 597-614.

9.   Martinez, M. N.; Amidon, G. L. A mechanistic approach to understanding the factors affecting drug absorption: a review of fundamentals. *J Clin Pharmacol* **2002,** *42*, 620-643.

10.   Artursson, P.; Palm, K.; Luthman, K. Caco-2 monolayers in experimental and theoretical predictions of drug transport. *Adv Drug Deliv Rev* **2001,** *46*, 27-43.

11.   Terada, T.; Inui, K. Recent advances in structural biology of Peptide transporters. *Curr Top Membr* **2012,** *70*, 257-274.

12.   Hagenbuch, B.; Meier, P. J. The superfamily of organic anion transporting polypeptides. *Biochim Biophys Acta* **2003,** *1609*, 1-18.

13.   Chothe, P. P.; Thakkar, S. V.; Gnana-Prakasam, J. P.; Ananth, S.; Hinton, D. R.; Kannan, R.; Smith, S. B.; Martin, P. M.; Ganapathy, V. Identification of a novel sodium-coupled oligopeptide transporter (SOPT2) in mouse and human retinal pigment epithelial cells. *Invest Ophthalmol Vis Sci* **2010,** *51*, 413-420.

14.   Ananth, S.; Karunakaran, S.; Martin, P. M.; Nagineni, C. N.; Hooks, J. J.; Smith, S. B.; Prasad, P. D.; Ganapathy, V. Functional identification of a novel transport system for endogenous and synthetic opioid peptides in the rabbit conjunctival epithelial cell line CJVE. *Pharm Res* **2009,** *26*, 1226-1235.

15.   Thakkar, S. V.; Miyauchi, S.; Prasad, P. D.; Ganapathy, V. Stimulation of Na+/Cl--coupled opioid peptide transport system in SK-N-SH cells by L-kyotorphin, an endogenous substrate for H+-coupled peptide transporter PEPT2. *Drug Metab Pharmacokinet* **2008,** *23*, 254-262.

16.   Chothe, P.; Singh, N.; Ganapathy, V. Evidence for two different broad-specificity oligopeptide transporters in intestinal cell line Caco-2 and colonic cell line CCD841. *Am J Physiol Cell Physiol* **2011,** *300*, C1260-1269.

17.   Hu, H.; Miyauchi, S.; Bridges, C. C.; Smith, S. B.; Ganapathy, V. Identification of a novel Na+- and Cl--coupled transport system for endogenous opioid peptides in retinal pigment epithelium and induction of the transport system by HIV-1 Tat. *Biochem J* **2003,** *375*, 17-22.

18.   Hayer-Zillgen, M.; Bruss, M.; Bonisch, H. Expression and pharmacological profile of the human organic cation transporters hOCT1, hOCT2 and hOCT3. *Br J Pharmacol* **2002,** *136*, 829-836.

19.   Bleasby, K.; Chauhan, S.; Brown, C. D. Characterization of MPP+ secretion across human intestinal Caco-2 cell monolayers: role of P-glycoprotein and a novel Na(+)-dependent organic cation transport mechanism. *Br J Pharmacol* **2000,** *129*, 619-625.

20.   Martel, F.; Grundemann, D.; Calhau, C.; Schomig, E. Apical uptake of organic cations by human intestinal Caco-2 cells: putative involvement of ASF transporters. *Naunyn Schmiedebergs Arch Pharmacol* **2001,** *363*, 40-49.

21.   Seithel, A.; Karlsson, J.; Hilgendorf, C.; Bjorquist, A.; Ungell, A. L. Variability in mRNA expression of ABC- and SLC-transporters in human intestinal cells: comparison between human segments and Caco-2 cells. *Eur J Pharm Sci* **2006,** *28*, 291-299.

22.   Chan, L. M.; Lowes, S.; Hirst, B. H. The ABCs of drug transport in intestine and liver: efflux proteins limiting drug absorption and bioavailability. *Eur J Pharm Sci* **2004,** *21*, 25-51.

23.   Higgins, C. F.; Hiles, I. D.; Salmond, G. P.; Gill, D. R.; Downie, J. A.; Evans, I. J.; Holland, I. B.; Gray, L.; Buckel, S. D.; Bell, A. W.; et al. A family of related ATP-binding subunits coupled to many distinct biological processes in bacteria. *Nature* **1986,** *323*, 448-450.

24.   Hyde, S. C.; Emsley, P.; Hartshorn, M. J.; Mimmack, M. M.; Gileadi, U.; Pearce, S. R.; Gallagher, M. P.; Gill, D. R.; Hubbard, R. E.; Higgins, C. F. Structural model of ATP-binding proteins associated with cystic fibrosis, multidrug resistance and bacterial transport. *Nature* **1990,** *346*, 362-365.

25.   Suzuki, H.; Sugiyama, Y. Role of metabolic enzymes and efflux transporters in the absorption of drugs from the small intestine. *Eur J Pharm Sci* **2000,** *12*, 3-12.

26.   Fricker, G.; Drewe, J.; Huwyler, J.; Gutmann, H.; Beglinger, C. Relevance of p-glycoprotein for the enteral absorption of cyclosporin A: in vitro-in vivo correlation. *Br J Pharmacol* **1996,** *118*, 1841-1847.

27.   Rost, D.; Mahner, S.; Sugiyama, Y.; Stremmel, W. Expression and localization of the multidrug resistance-associated protein 3 in rat small and large intestine. *Am J Physiol Gastrointest Liver Physiol* **2002,** *282*, G720-726.

28.   Hunter, J.; Jepson, M. A.; Tsuruo, T.; Simmons, N. L.; Hirst, B. H. Functional expression of P-glycoprotein in apical membranes of human intestinal Caco-2 cells. Kinetics of vinblastine secretion and interaction with modulators. *J Biol Chem* **1993,** *268*, 14991-14997.

29.   Terao, T.; Hisanaga, E.; Sai, Y.; Tamai, I.; Tsuji, A. Active secretion of drugs from the small intestinal epithelium in rats by P-glycoprotein functioning as an absorption barrier. *J Pharm Pharmacol* **1996,** *48*, 1083-1089.

30.   Loo, T. W.; Bartlett, M. C.; Clarke, D. M. Substrate-induced conformational changes in the transmembrane segments of human P-glycoprotein. Direct evidence for the substrate-induced fit mechanism for drug binding. *J Biol Chem* **2003,** *278*, 13603-13606.

31.   Taipalensuu, J.; Tornblom, H.; Lindberg, G.; Einarsson, C.; Sjoqvist, F.; Melhus, H.; Garberg, P.; Sjostrom, B.; Lundgren, B.; Artursson, P. Correlation of gene expression of ten drug efflux proteins of the ATP-binding cassette transporter family in normal human jejunum and in human intestinal epithelial Caco-2 cell monolayers. *J Pharmacol Exp Ther* **2001,** *299*, 164-170.

32.   Naruhashi, K.; Tamai, I.; Inoue, N.; Muraoka, H.; Sai, Y.; Suzuki, N.; Tsuji, A. Active intestinal secretion of new quinolone antimicrobials and the partial contribution of P-glycoprotein. *J Pharm Pharmacol* **2001,** *53*, 699-709.

33.   Naruhashi, K.; Tamai, I.; Inoue, N.; Muraoka, H.; Sai, Y.; Suzuki, N.; Tsuji, A. Involvement of multidrug resistance-associated protein 2 in intestinal secretion of grepafloxacin in rats. *Antimicrob Agents Chemother* **2002,** *46*, 344-349.

34.   Lowes, S.; Cavet, M. E.; Simmons, N. L. Evidence for a non-MDR1 component in digoxin secretion by human intestinal Caco-2 epithelial layers. *Eur J Pharmacol* **2003,** *458*, 49-56.

35.   Walgren, R. A.; Karnaky, K. J., Jr.; Lindenmayer, G. E.; Walle, T. Efflux of dietary flavonoid quercetin 4'-beta-glucoside across human intestinal Caco-2 cell monolayers by apical multidrug resistance-associated protein-2. *J Pharmacol Exp Ther* **2000,** *294*, 830-836.

36.   Dietrich, C. G.; Geier, A.; Oude Elferink, R. P. ABC of oral bioavailability: transporters as gatekeepers in the gut. *Gut* **2003,** *52*, 1788-1795.

37.   Wang, X.; Furukawa, T.; Nitanda, T.; Okamoto, M.; Sugimoto, Y.; Akiyama, S.; Baba, M. Breast cancer resistance protein (BCRP/ABCG2) induces cellular resistance to HIV-1 nucleoside reverse transcriptase inhibitors. *Mol Pharmacol* **2003,** *63*, 65-72.

38.   de Aizpurua, H. J.; Russell-Jones, G. J. Oral vaccination. Identification of classes of proteins that provoke an immune response upon oral feeding. *J Exp Med* **1988,** *167*, 440-451.

39.   Sanderson, I. R.; Walker, W. A. Uptake and transport of macromolecules by the intestine: possible role in clinical disorders (an update). *Gastroenterology* **1993,** *104*, 622-639.

40.   Sai, Y.; Kajita, M.; Tamai, I.; Wakama, J.; Wakamiya, T.; Tsuji, A. Adsorptive-mediated endocytosis of a basic peptide in enterocyte-like Caco-2 cells. *Am J Physiol* **1998,** *275*, G514-520.

41.   Terasaki, T.; Hirai, K.; Sato, H.; Kang, Y. S.; Tsuji, A. Absorptive-mediated endocytosis of a dynorphin-like analgesic peptide, E-2078 into the blood-brain barrier. *J Pharmacol Exp Ther* **1989,** *251*, 351-357.

42.   Terasaki, T.; Deguchi, Y.; Sato, H.; Hirai, K.; Tsuji, A. In vivo transport of a dynorphin-like analgesic peptide, E-2078, through the blood-brain barrier: an application of brain microdialysis. *Pharm Res* **1991,** *8*, 815-820.

43.   Marinova, Z.; Vukojevic, V.; Surcheva, S.; Yakovleva, T.; Cebers, G.; Pasikova, N.; Usynin, I.; Hugonin, L.; Fang, W.; Hallberg, M.; Hirschberg, D.; Bergman, T.; Langel, U.; Hauser, K. F.; Pramanik, A.; Aldrich, J. V.; Graslund, A.; Terenius, L.; Bakalkin, G. Translocation of dynorphin neuropeptides across the plasma membrane. A putative mechanism of signal transmission. *J Biol Chem* **2005,** *280*, 26360-26370.

44.   Pauletti, G. M. G., S.; Knipp, G. T.; Nerurkar, M. M.; Okumu, F. W.; Tamura, K.; Siahaan, T. J.; Borchardt, R. T. Structural requirements for intestinal absorption of peptide drugs. *J Control Release* **1996,** *41*, 3-17.

45.   Pauletti, G. M.; Okumu, F. W.; Borchardt, R. T. Effect of size and charge on the passive diffusion of peptides across Caco-2 cell monolayers via the paracellular pathway. *Pharm Res* **1997,** *14*, 164-168.

46.   Borchardt, R. T.; Jeffrey, A.; Siahaan, T. J.; Gangwar, S.; Pauletti, G. M. Improvement of oral peptide bioavailability: Peptidomimetics and prodrug strategies. *Adv Drug Deliv Rev* **1997,** *27*, 235-256.

47.   Burton, P. S.; Conradi, R. A.; Ho, N. F.; Hilgers, A. R.; Borchardt, R. T. How structural features influence the biomembrane permeability of peptides. *J Pharm Sci* **1996,** *85*, 1336-1340.

48.   Ogihara, H.; Saito, H.; Shin, B. C.; Terado, T.; Takenoshita, S.; Nagamachi, Y.; Inui, K.; Takata, K. Immuno-localization of H+/peptide cotransporter in rat digestive tract. *Biochem Biophys Res Commun* **1996,** *220*, 848-852.

49.   Shen, H.; Smith, D. E.; Yang, T.; Huang, Y. G.; Schnermann, J. B.; Brosius, F. C., 3rd. Localization of PEPT1 and PEPT2 proton-coupled oligopeptide transporter mRNA and protein in rat kidney. *Am J Physiol* **1999,** *276*, F658-665.

50.   Terada, T.; Sawada, K.; Irie, M.; Saito, H.; Hashimoto, Y.; Inui, K. Structural requirements for determining the substrate affinity of peptide transporters PEPT1 and PEPT2. *Pflugers Arch* **2000,** *440*, 679-684.

51.   Theis, S.; Hartrodt, B.; Kottra, G.; Neubert, K.; Daniel, H. Defining minimal structural features in substrates of the H(+)/peptide cotransporter PEPT2 using novel amino acid and dipeptide derivatives. *Mol Pharmacol* **2002,** *61*, 214-221.

52.   Adibi, S. A. The oligopeptide transporter (Pept-1) in human intestine: biology and function. *Gastroenterology* **1997,** *113*, 332-340.

53.   Liang, R.; Fei, Y. J.; Prasad, P. D.; Ramamoorthy, S.; Han, H.; Yang-Feng, T. L.; Hediger, M. A.; Ganapathy, V.; Leibach, F. H. Human intestinal H+/peptide cotransporter. Cloning, functional expression, and chromosomal localization. *J Biol Chem* **1995,** *270*, 6456-6463.

54.   Saito, H.; Inui, K. Dipeptide transporters in apical and basolateral membranes of the human intestinal cell line Caco-2. *Am J Physiol* **1993,** *265*, G289-294.

55.   Thwaites, D. T.; Brown, C. D.; Hirst, B. H.; Simmons, N. L. H(+)-coupled dipeptide (glycylsarcosine) transport across apical and basal borders of human intestinal Caco-2 cell monolayers display distinctive characteristics. *Biochim Biophys Acta* **1993,** *1151*, 237-245.

56.   Newstead, S.; Drew, D.; Cameron, A. D.; Postis, V. L.; Xia, X.; Fowler, P. W.; Ingram, J. C.; Carpenter, E. P.; Sansom, M. S.; McPherson, M. J.; Baldwin, S. A.; Iwata, S. Crystal

structure of a prokaryotic homologue of the mammalian oligopeptide-proton symporters, PepT1 and PepT2. *EMBO J* **2011,** *30*, 417-426.

57. Solcan, N.; Kwok, J.; Fowler, P. W.; Cameron, A. D.; Drew, D.; Iwata, S.; Newstead, S. Alternating access mechanism in the POT family of oligopeptide transporters. *EMBO J* **2012,** *31*, 3411-3421.

58. Gao, B.; Hagenbuch, B.; Kullak-Ublick, G. A.; Benke, D.; Aguzzi, A.; Meier, P. J. Organic anion-transporting polypeptides mediate transport of opioid peptides across blood-brain barrier. *J Pharmacol Exp Ther* **2000,** *294*, 73-79.

59. Dagenais, C.; Ducharme, J.; Pollack, G. M. Uptake and efflux of the peptidic delta-opioid receptor agonist. *Neurosci Lett* **2001,** *301*, 155-158.

60. Hayeshi, R.; Hilgendorf, C.; Artursson, P.; Augustijns, P.; Brodin, B.; Dehertogh, P.; Fisher, K.; Fossati, L.; Hovenkamp, E.; Korjamo, T.; Masungi, C.; Maubon, N.; Mols, R.; Mullertz, A.; Monkkonen, J.; O'Driscoll, C.; Oppers-Tiemissen, H. M.; Ragnarsson, E. G.; Rooseboom, M.; Ungell, A. L. Comparison of drug transporter gene expression and functionality in Caco-2 cells from 10 different laboratories. *Eur J Pharm Sci* **2008,** *35*, 383-396.

61. Hilgendorf, C.; Ahlin, G.; Seithel, A.; Artursson, P.; Ungell, A. L.; Karlsson, J. Expression of thirty-six drug transporter genes in human intestine, liver, kidney, and organotypic cell lines. *Drug Metab Dispos* **2007,** *35*, 1333-1340.

62. Zeller, P.; Clement, M.; Fessard, V. Similar uptake profiles of microcystin-LR and -RR in an in vitro human intestinal model. *Toxicology* **2011,** *290*, 7-13.

63. Fastner, J.; Erhard, M.; von Dohren, H. Determination of oligopeptide diversity within a natural population of Microcystis spp. (cyanobacteria) by typing single colonies by matrix-

assisted laser desorption ionization-time of flight mass spectrometry. *Appl Environ Microbiol* **2001,** *67*, 5069-5076.

64.   Fischer, W. J.; Altheimer, S.; Cattori, V.; Meier, P. J.; Dietrich, D. R.; Hagenbuch, B. Organic anion transporting polypeptides expressed in liver and brain mediate uptake of microcystin. *Toxicol Appl Pharmacol* **2005,** *203*, 257-263.

65.   Hermansky, S. J.; Markin, R. S.; Fowler, E. H.; Stohs, S. J. Hepatic ultrastructural changes induced by the toxin microcystin-LR (MCLR) in mice. *J Environ Pathol Toxicol Oncol* **1993,** *12*, 101-106.

66.   Fricker, G.; Drewe, J.; Vonderscher, J.; Kissel, T.; Beglinger, C. Enteral absorption of octreotide. *Br J Pharmacol* **1992,** *105*, 783-786.

67.   Kohler, E.; Duberow-Drewe, M.; Drewe, J.; Ribes, G.; Loubatieres-Mariani, M. M.; Mazer, N.; Gyr, K.; Beglinger, C. Absorption of an aqueous solution of a new synthetic somatostatin analogue administered to man by gavage. *Eur J Clin Pharmacol* **1987,** *33*, 167-171.

68.   Fricker, G.; Bruns, C.; Munzer, J.; Briner, U.; Albert, R.; Kissel, T.; Vonderscher, J. Intestinal absorption of the octapeptide SMS 201-995 visualized by fluorescence derivatization. *Gastroenterology* **1991,** *100*, 1544-1552.

69.   Amoss, M.; Rivier, J.; Guillemin, R. Release of gonadotropins by oral administration of synthetic LRF or a tripeptide fragment of LRF. *J Clin Endocrinol Metab* **1972,** *35*, 175-177.

70.   Nishi, N.; Arimura, A.; Coy, D.; Vilchez-Martinez, J. A.; Schally, A. V. The effect of oral and vaginal administration of synthetic LH-RH and [D-ALA-6, DES GLY-10-NH2]-LH-RH ethylamide on serum LH levels in ovariectomized, steroid blocked rats. *Proc Soc Exp Biol Med* **1975,** *148*, 1009-1012.

71.   Langguth, P.; Bohner, V.; Biber, J.; Merkle, H. P. Metabolism and transport of the pentapeptide metkephamid by brush-border membrane vesicles of rat intestine. *J Pharm Pharmacol* **1994,** *46*, 34-40.

72.   Ogawa, T.; Miyamae, T.; Murayama, K.; Okuyama, K.; Okayama, T.; Hagiwara, M.; Sakurada, S.; Morikawa, T. Synthesis and structure-activity relationships of an orally available and long-acting analgesic peptide, N(alpha)-amidino-Tyr-D-Arg-Phe-MebetaAla-OH (ADAMB). *J Med Chem* **2002,** *45*, 5081-5089.

73.   Zhao, K.; Luo, G.; Zhao, G. M.; Schiller, P. W.; Szeto, H. H. Transcellular transport of a highly polar 3+ net charge opioid tetrapeptide. *J Pharmacol Exp Ther* **2003,** *304*, 425-432.

74.   Jinsmaa, Y.; Marczak, E. D.; Balboni, G.; Salvadori, S.; Lazarus, L. H. Inhibition of the development of morphine tolerance by a potent dual mu-delta-opioid antagonist, H-Dmt-Tic-Lys-NH-CH$_2$-Ph. *Pharmacol Biochem Behav* **2008,** *90*, 651-657.

75.   Marczak, E. D.; Jinsmaa, Y.; Myers, P. H.; Blankenship, T.; Wilson, R.; Balboni, G.; Salvadori, S.; Lazarus, L. H. Orally administered H-Dmt-Tic-Lys-NH-CH$_2$-Ph (MZ-2), a potent mu/delta-opioid receptor antagonist, regulates obese-related factors in mice. *Eur J Pharmacol* **2009,** *616*, 115-121.

76.   Augustijns, P. F.; Bradshaw, T. P.; Gan, L. S.; Hendren, R. W.; Thakker, D. R. Evidence for a polarized efflux system in CACO-2 cells capable of modulating cyclosporin A transport. *Biochem Biophys Res Commun* **1993,** *197*, 360-365.

77.   Tarr, B. D.; Yalkowsky, S. H. Enhanced intestinal absorption of cyclosporine in rats through the reduction of emulsion droplet size. *Pharm Res* **1989,** *6*, 40-43.

78.   Fahr, A. Cyclosporin clinical pharmacokinetics. *Clin Pharmacokinet* **1993,** *24*, 472-495.

79.   Aldrich, J. V.; Senadheera, S. N.; Ross, N. C.; Ganno, M. L.; Eans, S. O.; McLaughlin, J. P. The Macrocyclic Peptide Natural Product CJ-15,208 Is Orally Active and Prevents Reinstatement of Extinguished Cocaine-Seeking Behavior. *J Nat Prod* **2013,** *76*, 433-438.

80.   Eans, S. O.; Ganno, M. L.; Reilley, K. J.; Patkar, K. A.; Senadheera, S. N.; Aldrich, J. V.; McLaughlin, J. P. The macrocyclic tetrapeptide [D-Trp]CJ-15,208 produces short-acting kappa opioid receptor antagonism in the CNS after oral administration. *Br J Pharmacol* **2013,** *169*, 426-436.

81.   White, T. R.; Renzelman, C. M.; Rand, A. C.; Rezai, T.; McEwen, C. M.; Gelev, V. M.; Turner, R. A.; Linington, R. G.; Leung, S. S.; Kalgutkar, A. S.; Bauman, J. N.; Zhang, Y.; Liras, S.; Price, D. A.; Mathiowetz, A. M.; Jacobson, M. P.; Lokey, R. S. On-resin N-methylation of cyclic peptides for discovery of orally bioavailable scaffolds. *Nat Chem Biol* **2011,** *7*, 810-817.

82.   Chatterjee, J.; Gilon, C.; Hoffman, A.; Kessler, H. N-methylation of peptides: a new perspective in medicinal chemistry. *Acc Chem Res* **2008,** *41*, 1331-1342.

83.   Ovadia, O.; Greenberg, S.; Chatterjee, J.; Laufer, B.; Opperer, F.; Kessler, H.; Gilon, C.; Hoffman, A. The effect of multiple N-methylation on intestinal permeability of cyclic hexapeptides. *Mol Pharm* **2011,** *8*, 479-487.

84.   Borchardt, R. T. Optimizing oral absorption of peptides using prodrug strategies. *J Control Release* **1999,** *62*, 231-238.

85.   Bak, A.; Gudmundsson, O. S.; Friis, G. J.; Siahaan, T. J.; Borchardt, R. T. Acyloxyalkoxy-based cyclic prodrugs of opioid peptides: evaluation of the chemical and enzymatic stability as well as their transport properties across Caco-2 cell monolayers. *Pharm Res* **1999,** *16*, 24-29.

86.   Gudmundsson, O. S.; Nimkar, K.; Gangwar, S.; Siahaan, T.; Borchardt, R. T. Phenylpropionic acid-based cyclic prodrugs of opioid peptides that exhibit metabolic stability to peptidases and excellent cellular permeation. *Pharm Res* **1999,** *16*, 16-23.

87.   Gudmundsson, O. S.; Pauletti, G. M.; Wang, W.; Shan, D.; Zhang, H.; Wang, B.; Borchardt, R. T. Coumarinic acid-based cyclic prodrugs of opioid peptides that exhibit metabolic stability to peptidases and excellent cellular permeability. *Pharm Res* **1999,** *16*, 7-15.

88.   Tang, F.; Borchardt, R. T. Characterization of the efflux transporter(s) responsible for restricting intestinal mucosa permeation of the coumarinic acid-based cyclic prodrug of the opioid peptide DADLE. *Pharm Res* **2002,** *19*, 787-793.

89.   Ouyang, H.; Tang, F.; Siahaan, T. J.; Borchardt, R. T. A modified coumarinic acid-based cyclic prodrug of an opioid peptide: its enzymatic and chemical stability and cell permeation characteristics. *Pharm Res* **2002,** *19*, 794-801.

90.   Ouyang, H.; Andersen, T. E.; Chen, W.; Nofsinger, R.; Steffansen, B.; Borchardt, R. T. A comparison of the effects of p-glycoprotein inhibitors on the blood-brain barrier permeation of cyclic prodrugs of an opioid peptide (DADLE). *J Pharm Sci* **2009,** *98*, 2227-2236.

91.   Ouyang, H.; Chen, W.; Andersen, T. E.; Steffansen, B.; Borchardt, R. T. Factors that restrict the intestinal cell permeation of cyclic prodrugs of an opioid peptide (DADLE): Part I. Role of efflux transporters in the intestinal mucosa. *J Pharm Sci* **2009,** *98*, 337-348.

92.   Ho, N., Park, J., Morozowich, W., & Higuchi, W., Physical model approach to the design with improved intestinal absorption. In *Design of biopharmaceutical properties through prodrugs and analogues*, Roche, E., Ed. APhA/APS: Washington D.C., 1977; pp 136-277.

93.   Pidgeon, C. Solid phase membrane mimetics: immobilized artificial membranes. *Enzyme Microb Technol* **1990,** *12*, 149-150.

94.   Malakoutikhah, M.; Teixido, M.; Giralt, E. Toward an optimal blood-brain barrier shuttle by synthesis and evaluation of peptide libraries. *J Med Chem* **2008,** *51*, 4881-4889.

95.   Malakoutikhah, M.; Prades, R.; Teixido, M.; Giralt, E. N-methyl phenylalanine-rich peptides as highly versatile blood-brain barrier shuttles. *J Med Chem* **2010,** *53*, 2354-2363.

96.   Kansy, M.; Senner, F.; Gubernator, K. Physicochemical high throughput screening: parallel artificial membrane permeation assay in the description of passive absorption processes. *J Med Chem* **1998,** *41*, 1007-1010.

97.   Wilson, T. H.; Wiseman, G. The use of sacs of everted small intestine for the study of the transference of substances from the mucosal to the serosal surface. *J Physiol* **1954,** *123*, 116-125.

98.   Ussing, H. H.; Zerahn, K. Active transport of sodium as the source of electric current in the short-circuited isolated frog skin. *Acta Physiol Scand* **1951,** *23*, 110-127.

99.   Artursson, P. Cell cultures as models for drug absorption across the intestinal mucosa. *Crit Rev Ther Drug Carrier Syst* **1991,** *8*, 305-330.

100.   Artursson, P.; Lindmark, T.; Davis, S. S.; Illum, L. Effect of chitosan on the permeability of monolayers of intestinal epithelial cells (Caco-2). *Pharm Res* **1994,** *11*, 1358-1361.

101.   Hidalgo, I. J.; Raub, T. J.; Borchardt, R. T. Characterization of the human colon carcinoma cell line (Caco-2) as a model system for intestinal epithelial permeability. *Gastroenterology* **1989,** *96*, 736-749.

102.   Borchardt, R. The application of cell culture systems in drug discovery and development. *J Drug Target* **1995,** *3*, 179-182.

103.   Matsson, P.; Bergstrom, C. A.; Nagahara, N.; Tavelin, S.; Norinder, U.; Artursson, P. Exploring the role of different drug transport routes in permeability screening. *J Med Chem* **2005,** *48*, 604-613.

104.   Vachon, P. H.; Beaulieu, J. F. Transient mosaic patterns of morphological and functional differentiation in the Caco-2 cell line. *Gastroenterology* **1992,** *103*, 414-423.

105.   Kumpf, S. L., Ribabeneira, M. D., Sharpe., D, Link, J., Huber, R., Burton, C., Aungst, B Isolation and characterization of Caco-2 cells expressing high and low levels of P-glycoprotein. *AAPS PharmSci* 3: 2001; abstract, pp 1383.

106.   Roth, W. J.; Lindley, D. J.; Carl, S. M.; Knipp, G. T. The effects of intralaboratory modifications to media composition and cell source on the expression of pharmaceutically relevant transporters and metabolizing genes in the Caco-2 cell line. *J Pharm Sci* **2012,** *101*, 3962-3978.

107.   Walter E., K., T. . Heterogeneity in human intestinal cell line Caco-2 leads to differences in transepithelial transport. *European journal of pharmaceutical sciences* **1995,** *3*, 215-230.

108.   Behrens, I.; Kamm, W.; Dantzig, A. H.; Kissel, T. Variation of peptide transporter (PepT1 and HPT1) expression in Caco-2 cells as a function of cell origin. *J Pharm Sci* **2004,** *93*, 1743-1754.

109.   Briske-Anderson, M. J.; Finley, J. W.; Newman, S. M. The influence of culture time and passage number on the morphological and physiological development of Caco-2 cells. *Proc Soc Exp Biol Med* **1997,** *214*, 248-257.

110.   Yu, H.; Cook, T. J.; Sinko, P. J. Evidence for diminished functional expression of intestinal transporters in Caco-2 cell monolayers at high passages. *Pharm Res* **1997,** *14*, 757-762.

111.   Anderle, P.; Niederer, E.; Rubas, W.; Hilgendorf, C.; Spahn-Langguth, H.; Wunderli-Allenspach, H.; Merkle, H. P.; Langguth, P. P-Glycoprotein (P-gp) mediated efflux in Caco-2 cell monolayers: the influence of culturing conditions and drug exposure on P-gp expression levels. *J Pharm Sci* **1998,** *87*, 757-762.

112.   Behrens, I.; Kissel, T. Do cell culture conditions influence the carrier-mediated transport of peptides in Caco-2 cell monolayers? *Eur J Pharm Sci* **2003,** *19*, 433-442.

113.   Tucker, S. P.; Melsen, L. R.; Compans, R. W. Migration of polarized epithelial cells through permeable membrane substrates of defined pore size. *Eur J Cell Biol* **1992,** *58*, 280-290.

114.   Volpe, D. A. Variability in Caco-2 and MDCK cell-based intestinal permeability assays. *J Pharm Sci* **2008,** *97*, 712-725.

115.   Hosoya, K. I.; Kim, K. J.; Lee, V. H. Age-dependent expression of P-glycoprotein gp170 in Caco-2 cell monolayers. *Pharm Res* **1996,** *13*, 885-890.

116.   DeMarco, V. G.; Li, N.; Thomas, J.; West, C. M.; Neu, J. Glutamine and barrier function in cultured Caco-2 epithelial cell monolayers. *J Nutr* **2003,** *133*, 2176-2179.

117.   D'Souza, V. M., Shertzer, H. G., Menon, A. G., Pauletti, G. M. High glucose concentration in isotonic media alters Caco-2 cell permeability. *AAPS PharmSci 5* **2003,** *article 24*.

118.   Bestwick, C. S.; Milne, L. Alteration of culture regime modifies antioxidant defenses independent of intracellular reactive oxygen levels and resistance to severe oxidative stress within confluent Caco-2 "intestinal cells". *Dig Dis Sci* **2001,** *46*, 417-423.

119.   Ranaldi, G.; Consalvo, R.; Sambuy, Y.; Scarino, M. L. Permeability characteristics of parental and clonal human intestinal Caco-2 cell lines differentiated in serum-supplemented and serum-free media. *Toxicol In Vitro* **2003,** *17*, 761-767.

120.   Pade, V.; Stavchansky, S. Estimation of the relative contribution of the transcellular and paracellular pathway to the transport of passively absorbed drugs in the Caco-2 cell culture model. *Pharm Res* **1997,** *14*, 1210-1215.

121.   Rothen-Rutishauser, B.; Braun, A.; Gunthert, M.; Wunderli-Allenspach, H. Formation of multilayers in the caco-2 cell culture model: a confocal laser scanning microscopy study. *Pharm Res* **2000,** *17*, 460-465.

122.   Markowska, M.; Oberle, R.; Juzwin, S.; Hsu, C. P.; Gryszkiewicz, M.; Streeter, A. J. Optimizing Caco-2 cell monolayers to increase throughput in drug intestinal absorption analysis. *J Pharmacol Toxicol Methods* **2001,** *46*, 51-55.

123.   Delie, F.; Rubas, W. A human colonic cell line sharing similarities with enterocytes as a model to examine oral absorption: advantages and limitations of the Caco-2 model. *Crit Rev Ther Drug Carrier Syst* **1997,** *14*, 221-286.

124.   Buckley, S. T.; Fischer, S. M.; Fricker, G.; Brandl, M. In vitro models to evaluate the permeability of poorly soluble drug entities: challenges and perspectives. *Eur J Pharm Sci* **2012,** *45*, 235-250.

125.   Karlsson, J.; Artursson, P. A new diffusion chamber system for the determination of drug permeability coefficients across the human intestinal epithelium that are independent of the unstirred water layer. *Biochim Biophys Acta* **1992,** *1111*, 204-210.

126.   Hidalgo, I. J.; Hillgren, K. M.; Grass, G. M.; Borchardt, R. T. Characterization of the unstirred water layer in Caco-2 cell monolayers using a novel diffusion apparatus. *Pharm Res* **1991,** *8*, 222-227.

127.   Bourdage, J. S., Burton, P. S., Cole, C. J., Conardi, R. A., Day, J. S., Hilgers, A. R., Pfund, W. P. Characterization of Caco-2 permeability model and rat intestinal perfusion model for use with the BCS. *AAPS PharmSci 1* **1999**.

128.   Palmgren, J. J.; Monkkonen, J.; Korjamo, T.; Hassinen, A.; Auriola, S. Drug adsorption to plastic containers and retention of drugs in cultured cells under in vitro conditions. *Eur J Pharm Biopharm* **2006,** *64*, 369-378.

129.   Ingels, F.; Deferme, S.; Delbar, N.; Oth, M.; Augustijns, P. Implementation of the caco-2 cell culture model as a predictive tool for the oral absorption of drugs. In-house evaluation procedures. *J Pharm Belg* **2002,** *57*, 153-158.

130.   Yee, S. In vitro permeability across Caco-2 cells (colonic) can predict in vivo (small intestinal) absorption in man--fact or myth. *Pharm Res* **1997,** *14*, 763-766.

131.   Gres, M. C.; Julian, B.; Bourrie, M.; Meunier, V.; Roques, C.; Berger, M.; Boulenc, X.; Berger, Y.; Fabre, G. Correlation between oral drug absorption in humans, and apparent drug permeability in TC-7 cells, a human epithelial intestinal cell line: comparison with the parental Caco-2 cell line. *Pharm Res* **1998,** *15*, 726-733.

132.   Turco, L.; Catone, T.; Caloni, F.; Di Consiglio, E.; Testai, E.; Stammati, A. Caco-2/TC7 cell line characterization for intestinal absorption: how reliable is this in vitro model for the prediction of the oral dose fraction absorbed in human? *Toxicol In Vitro* **2011,** *25*, 13-20.

133.   Tavelin, S.; Milovic, V.; Ocklind, G.; Olsson, S.; Artursson, P. A conditionally immortalized epithelial cell line for studies of intestinal drug transport. *J Pharmacol Exp Ther* **1999,** *290*, 1212-1221.

134.   Tavelin, S.; Taipalensuu, J.; Hallbook, F.; Vellonen, K. S.; Moore, V.; Artursson, P. An improved cell culture model based on 2/4/A1 cell monolayers for studies of intestinal drug transport: characterization of transport routes. *Pharm Res* **2003,** *20*, 373-381.

135. Cho, M. J.; Thompson, D. P.; Cramer, C. T.; Vidmar, T. J.; Scieszka, J. F. The Madin Darby canine kidney (MDCK) epithelial cell monolayer as a model cellular transport barrier. *Pharm Res* **1989,** *6*, 71-77.

136. Irvine, J. D.; Takahashi, L.; Lockhart, K.; Cheong, J.; Tolan, J. W.; Selick, H. E.; Grove, J. R. MDCK (Madin-Darby canine kidney) cells: A tool for membrane permeability screening. *J Pharm Sci* **1999,** *88*, 28-33.

137. Braun, A.; Hammerle, S.; Suda, K.; Rothen-Rutishauser, B.; Gunthert, M.; Kramer, S. D.; Wunderli-Allenspach, H. Cell cultures as tools in biopharmacy. *Eur J Pharm Sci* **2000,** *11 Suppl 2*, S51-60.

138. Tang, F.; Horie, K.; Borchardt, R. T. Are MDCK cells transfected with the human MRP2 gene a good model of the human intestinal mucosa? *Pharm Res* **2002,** *19*, 773-779.

139. Tang, F.; Horie, K.; Borchardt, R. T. Are MDCK cells transfected with the human MDR1 gene a good model of the human intestinal mucosa? *Pharm Res* **2002,** *19*, 765-772.

140. Wang, M.; Sun, B.; Feng, J.; Zhang, H.; Liu, B.; Li, C.; Chen, Y.; Zhang, Y.; Kong, W. Investigation of transport mechanism of exendin-4 across Madin Darby canine kidney cell monolayers. *Biol Pharm Bull* **2012,** *35*, 745-752.

141. Zhang, Q.; He, N.; Zhang, L.; Zhu, F.; Chen, Q.; Qin, Y.; Zhang, Z.; Wang, S.; He, Q. The in vitro and in vivo study on self-nanoemulsifying drug delivery system (SNEDDS) based on insulin-phospholipid complex. *J Biomed Nanotechnol* **2012,** *8*, 90-97.

142. Amidon, G. E.; Ho, N. F.; French, A. B.; Higuchi, W. I. Predicted absorption rates with simultaneous bulk fluid flow in the intestinal tract. *J Theor Biol* **1981,** *89*, 195-210.

143.   Tsuji, A.; Miyamoto, E.; Hashimoto, N.; Yamana, T. GI absorption of beta-lactam antibiotics II: deviation from pH--partition hypothesis in penicillin absorption through in situ and in vitro lipoidal barriers. *J Pharm Sci* **1978,** *67*, 1705-1711.

144.   van Rees, H.; de Wolff, F. A.; Noach, E. L. The influence of diphenylhydantoin on intestinal glucose absorption in the rat. *Eur J Pharmacol* **1974,** *28*, 310-315.

145.   Doluisio, J. T.; Billups, N. F.; Dittert, L. W.; Sugita, E. T.; Swintosky, J. V. Drug absorption. I. An in situ rat gut technique yielding realistic absorption rates. *J Pharm Sci* **1969,** *58*, 1196-1200.

146.   Lennernas, H. Human intestinal permeability. *J Pharm Sci* **1998,** *87*, 403-410.

147.   Liu, H.; Sabus, C.; Carter, G. T.; Du, C.; Avdeef, A.; Tischler, M. In vitro permeability of poorly aqueous soluble compounds using different solubilizers in the PAMPA assay with liquid chromatography/mass spectrometry detection. *Pharm Res* **2003,** *20*, 1820-1826.

148.   Ingels, F. M.; Augustijns, P. F. Biological, pharmaceutical, and analytical considerations with respect to the transport media used in the absorption screening system, Caco-2. *J Pharm Sci* **2003,** *92*, 1545-1558.

149.   Saha, P.; Kou, J. H. Effect of solubilizing excipients on permeation of poorly water-soluble compounds across Caco-2 cell monolayers. *Eur J Pharm Biopharm* **2000,** *50*, 403-411.

150.   Takahashi, Y.; Kondo, H.; Yasuda, T.; Watanabe, T.; Kobayashi, S.; Yokohama, S. Common solubilizers to estimate the Caco-2 transport of poorly water-soluble drugs. *Int J Pharm* **2002,** *246*, 85-94.

151.   Ginski, M. J., Gadre, N., Vatsaraj, N., Grover, N., and Rhodes, C. Evaluation of cosolvents systems to facilitate caco-2 permeability screening of poorly water soluble drug candidates. *AAPS. PharmSciTech.* **2000,** *2*, 3247-.

152.   Hanke, U.; May, K.; Rozehnal, V.; Nagel, S.; Siegmund, W.; Weitschies, W. Commonly used nonionic surfactants interact differently with the human efflux transporters ABCB1 (p-glycoprotein) and ABCC2 (MRP2). *Eur J Pharm Biopharm* **2010,** *76*, 260-268.

153.   Rege, B. D.; Kao, J. P.; Polli, J. E. Effects of nonionic surfactants on membrane transporters in Caco-2 cell monolayers. *Eur J Pharm Sci* **2002,** *16*, 237-246.

154.   Brouwers, J.; Tack, J.; Lammert, F.; Augustijns, P. Intraluminal drug and formulation behavior and integration in in vitro permeability estimation: a case study with amprenavir. *J Pharm Sci* **2006,** *95*, 372-383.

155.   Katneni, K.; Charman, S. A.; Porter, C. J. Permeability assessment of poorly water-soluble compounds under solubilizing conditions: the reciprocal permeability approach. *J Pharm Sci* **2006,** *95*, 2170-2185.

156.   Aungst, B. J.; Nguyen, N. H.; Bulgarelli, J. P.; Oates-Lenz, K. The influence of donor and reservoir additives on Caco-2 permeability and secretory transport of HIV protease inhibitors and other lipophilic compounds. *Pharm Res* **2000,** *17*, 1175-1180.

157.   Krishna, G.; Chen, K.; Lin, C.; Nomeir, A. A. Permeability of lipophilic compounds in drug discovery using in-vitro human absorption model, Caco-2. *Int J Pharm* **2001,** *222*, 77-89.

158.   Hubatsch, I.; Ragnarsson, E. G.; Artursson, P. Determination of drug permeability and prediction of drug absorption in Caco-2 monolayers. *Nat Protoc* **2007,** *2*, 2111-2119.

159.   Galia, E.; Nicolaides, E.; Horter, D.; Lobenberg, R.; Reppas, C.; Dressman, J. B. Evaluation of various dissolution media for predicting in vivo performance of class I and II drugs. *Pharm Res* **1998,** *15*, 698-705.

Chapter 6 - Caco-2 permeability and solubility analysis of opioid macrocyclic tetrapeptides

6.1 Introduction

We are interested in metabolically stable peptidic ligands for kappa opioid receptors (KOR) as potential treatments for drug abuse and pain. The natural product CJ 15,208 is a macrocyclic tetrapeptide (*cyclo*[Phe-D-Pro-Phe-Trp]) that was reported to exhibit KOR antagonism *in vitro*.[1] While the L-Trp isomer of CJ 15,208, which appears to be the natural product, exhibited mixed agonist activity mediated by KOR and mu opioid receptors (MOR) *in vivo* as well as selective KOR antagonism, the D-Trp isomer exhibited minimal agonist activity and dose dependent KOR selective antagonism that lasted less than 18 h *in vivo*.[2] Following oral administration, the L-Trp isomer displayed both KOR agonism and antagonism and prevented stress- and cocaine-induced extinguished cocaine seeking behavior in a dose and time-dependent manner.[3] The D-Trp isomer, which exhibited weak KOR agonism, displayed KOR antagonism and prevented stress-induced, but not cocaine-induced extinguished cocaine seeking behavior in a dose-dependent manner following oral administration.[4] These peptides serve as lead compounds for further exploration.

In order to enhance their oral activity we are exploring the physicochemical and pharmacokinetic properties of these lead peptides. Because of their hydrophobicity, we have examined various solubilizing agents, including organic cosolvents, cyclodextrins and surfactants that are compatible with *in vivo* studies, to solubilize these compounds. To investigate the intestinal absorption of the macrocyclic tetrapeptides, we performed bidirectional Caco-2 permeability studies.
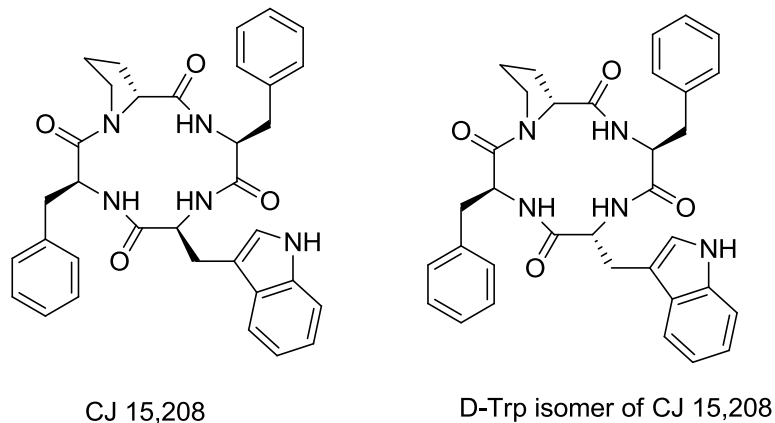
CJ 15,208   D-Trp isomer of CJ 15,208

Figure 6.1 Structures of the lead peptides

6.2   Results and Discussion

6.2.1   Permeability studies

The Caco-2 cells were seeded on polycarbonate filters, and monolayers were allowed to develop for 21 days. On the 21st day the monolayer integrity was assessed by measuring transepithelial electrical resistance (TEER) and lucifer yellow permeability. A TEER value of >200 Ω/cm^2 and a P$_{app}$ value of $\leq$1 x 10^{-6} cm/sec for lucifer yellow were the criteria to use the cell monolayers for transport studies. All of the cell monolayers used in the present study met the required TEER and P$_{app}$ values.

The cyclic tetrapeptides are hydrophobic and require organic cosolvents for solubilization. *N,N*-Dimethylacetamide (DMA, 3%) or *N*-methylpyrrolidone (NMP, 2.5%) have been used as organic cosolvents to solubilize hydrophobic compounds in the Caco-2 cell permeability assay.[5] The L-Trp and the D-Trp isomers were soluble in 0.25% DMSO + 2.25% DMA in Hank's balanced salt solution (HBSS) (vehicle 1) and 0.25% DMSO + 2.25% NMP in HBSS (vehicle 2), respectively, at a concentration of 50 μM. These were the working solutions

used for the Caco-2 transport studies and the concentrations of these solutions were verified by RP-UPLC.

Due to the high organic content in the vehicles, it was necessary to examine the effect of the vehicles on the integrity of the cell monolayers. On the 21st day, the transwells containing Caco-2 monolayers were incubated with the vehicles for 2 h, followed by examining transport of lucifer yellow in the apical to basolateral direction. Lucifer yellow permeability in monolayers exposed to vehicle 1 was 4.2 ± 0.7 x 10^{-7} cm/sec, while for the monolayers exposed to vehicle 2 lucifer yellow permeability was 5.4 ± 0.2 x 10^{-7} cm/sec compared to 1.8 ± 0.4 x 10^{-7} cm/sec displayed by control wells exposed exclusively to HBSS, pH 7.4 (Figure 6.2). Hence, these vehicles appeared to be acceptable for Caco-2 permeability studies.
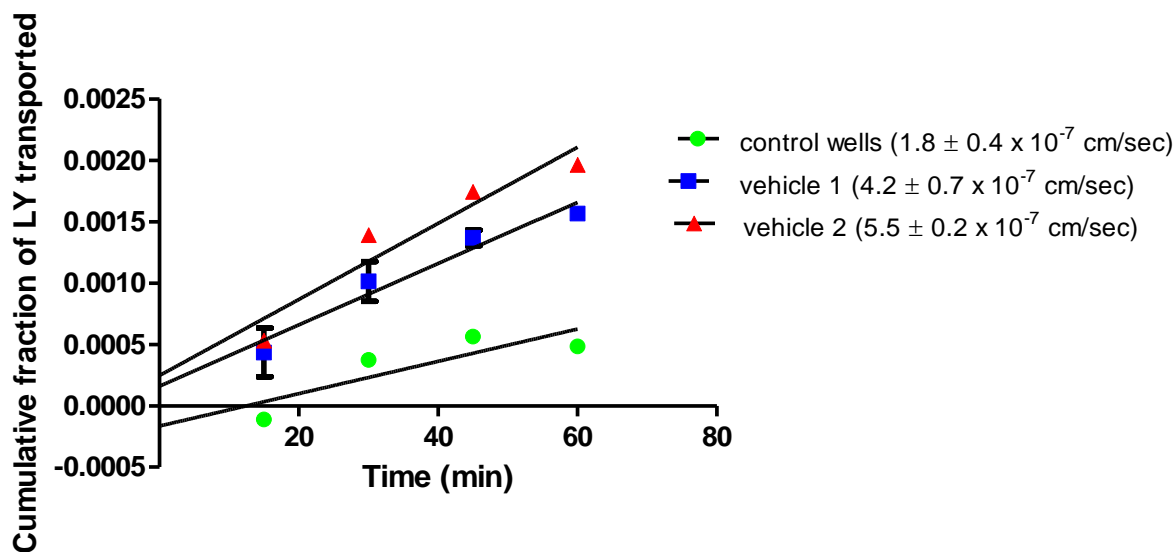

Figure 6.2 Effect of the vehicles on Caco-2 monolayer integrity (n=2). The control wells were incubated with HBSS, pH 7.4, and vehicle treated wells with the respective vehicles for the initial 2 h and lucifer yellow (LY) transport was carried out during the 3rd h.

The peptide permeability experiments were performed similar to the lucifer yellow transport experiment except in both the apical to basolateral (A-B) and basolateral to apical (B-

A) directions. Liquid chromatography electrospray ionization tandem mass spectroscopy (LC-ESI-MS/MS) in positive ion mode coupled to reversed phase ultra-high performance liquid chromatography (RP-UPLC) was employed for quantifying both the L-Trp and D-Trp isomers. Following fragmentation, the fragment ions were quantified by multiple reaction monitoring (MRM).

The L-Trp isomer showed a permeability of $3.2 \pm 0.6 \times 10^{-6}$ cm/sec in the A-B direction and $18.9 \pm 0.5 \times 10^{-6}$ cm/sec in the B-A direction (Figure 6.3 and Table 6.1). The value for B-A transport was almost 6 times the value for A-B transport which implies that L-Trp isomer is a substrate for P-glycoprotein (Pgp) or other efflux transporter, although this needs to be confirmed by experiments in the presence of known efflux protein inhibitors. The mass balance ($\pm$ SEM) was $82 \pm 3\%$ for the A-B permeability studies and $71 \pm 6\%$ for B-A permeability studies for the L-Trp isomer (Table 6.1). Because of a lower mass balance value in the B-A direction a study investigating possible adsorption of the peptide to the transwells was also performed. However, in this study recoveries were >94%, indicating that the peptide may not be adsorbing significantly to the transwells.

The D-Trp isomer showed permeability of $25.5 \pm 6.3 \times 10^{-6}$ cm/sec in the A-B direction and $22.7 \pm 0.9 \times 10^{-6}$ cm/sec in the B-A direction (Figure 6.4 and Table 6.1). Mass balance values ($\pm$ SEM) of $76 \pm 3\%$ for the A-B direction and $82 \pm 1\%$ for B-A direction were obtained for the D-Trp isomer (Table 6.1). Both the L- and D-Trp isomers displayed an initial short lag phase (10 min) which is suggestive of carrier mediated transport.[6]

The difference in the permeabilities of the isomers may be attributed to differences in their conformations. The two isomers may exhibit differences in intramolecular hydrogen bonding which could affect the permeability of the two peptides. Lokey *et al.* showed that changes in the

intramolecular hydrogen bonding of peptides can affect their permeability.[7] A detailed conformational analysis of the two isomers is currently being performed.

Subsequent to the peptide transport experiments lucifer yellow transport was performed for 1 h to monitor the effect of peptide on the integrity of cell monolayers. The lucifer yellow transport experiment in the peptide-incubated wells was performed in the A-B direction regardless of the direction of the peptide transport. The lucifer yellow permeability values post L-Trp isomer transport were 0.8×10^{-6} cm/sec and 0.9×10^{-6} cm/sec for the wells in which peptide transport in the A-B and B-A directions, respectively, was performed compared to 0.9×10^{-6} cm/sec for the wells incubated with vehicle 1 and 1.1×10^{-6} cm/sec for control wells (Figure 6.5). These values indicated that neither vehicle 1 nor the L-Trp isomer compromised the integrity of the cell monolayers.

The lucifer yellow permeability values post D-Trp isomer transport were 5.7×10^{-6} cm/sec and 13×10^{-6} cm/sec for the wells in which peptide transport in the A-B and B-A directions was performed, respectively, compared to 8.2×10^{-6} cm/sec displayed by wells incubated with vehicle 2 and 1.4×10^{-6} cm/sec displayed by the control wells (Figure 6.6). These values indicated that while vehicle 2 compromised the integrity of the monolayers the D-Trp isomer did not appear to have an effect on monolayer integrity.

Table 6.1. Results obtained from Caco-2 monolayer permeability experiments for the L- and D-Trp isomers.

Peptide	Peptide transport[a] P_{app} cm/sec (x 10^{-6})		Post-peptide LY transport[b] P_{app} cm/sec (x 10^{-6})		Mass balance (%)[a]	
	A-B	B-A	Peptide (A-B) treated wells (cm/sec)	Peptide (B-A) treated wells (cm/sec)	A-B	B-A
CJ-15,208 (L-Trp isomer)	3.2 ± 0.6	18.9 ± 0.5	0.8[c]	0.9[c]	82 ± 3	71 ± 6
D-Trp isomer	25.5 ± 6.3	22.7 ± 0.9	5.7[d]	13[d]	76 ± 3	82 ± 1

[a] Results presented are average ± SEM from duplicate determinations.
[b] Results presented are from a single determinations.
[c] Lucifer yellow (LY) transport in the wells incubated with vehicle 1 only was 0.9 x 10^{-6} cm/sec.
[d] LY transport in the wells incubated with vehicle 2 only was 8.2 x 10^{-6} cm/sec.
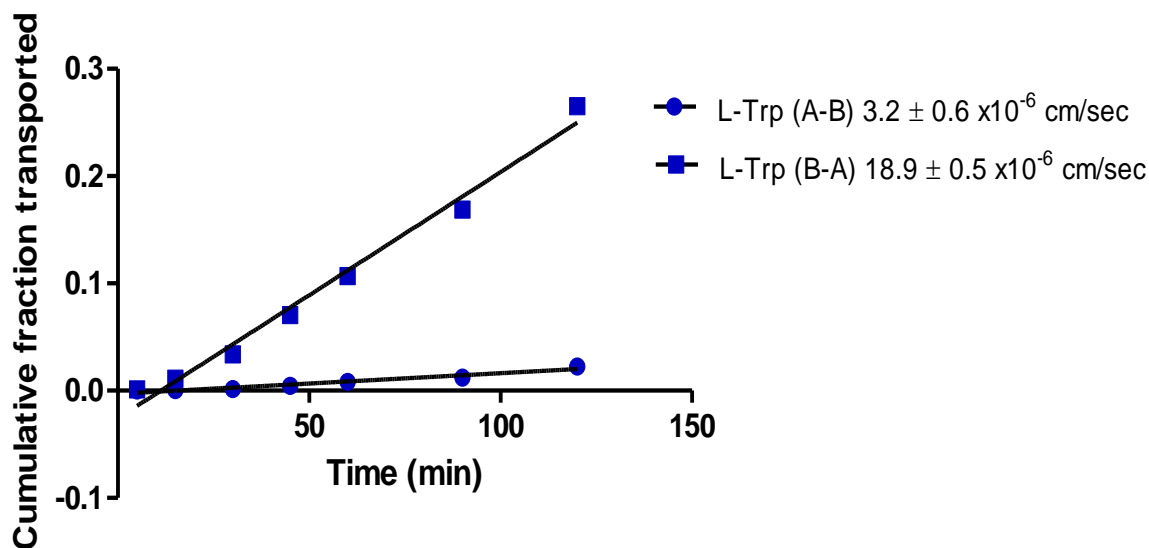

Figure 6.3 Caco-2 monolayer permeability of the L-Trp isomer (n = 2); error bars are too small to be visible.
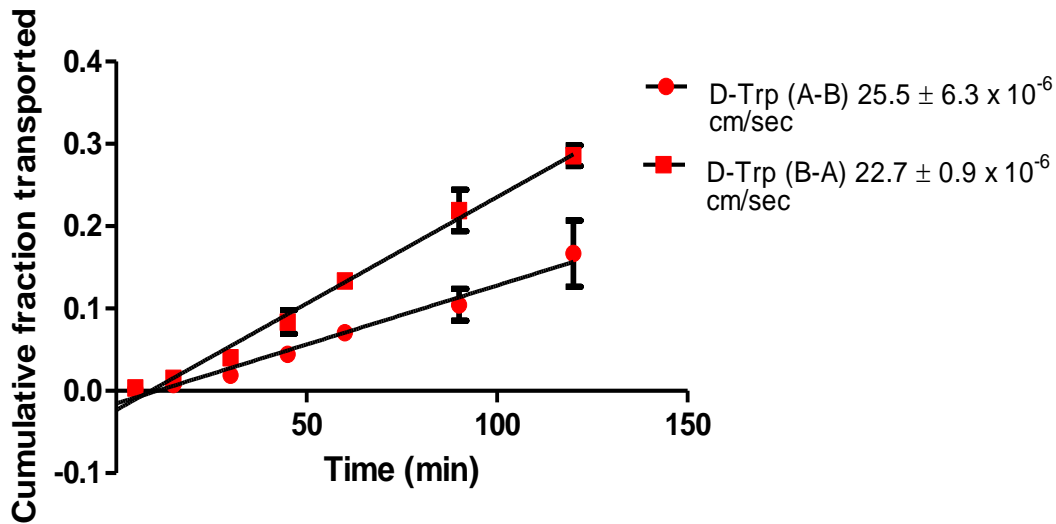
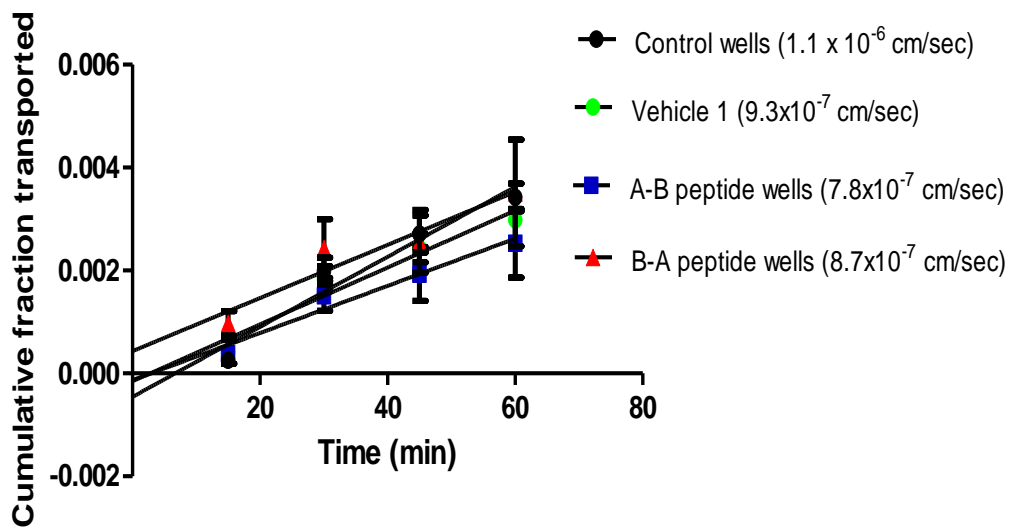Figure 6.4. Caco-2 monolayer permeability of the D-Trp isomer (n = 2).

Figure 6.5. Post L-Trp isomer lucifer yellow (LY) transport through Caco-2 monolayers (n = 1). Control wells were incubated with HBSS, vehicle treated wells with vehicle 1 and the peptide treated wells with L-Trp isomer solution for the initial 2 h, and LY transport was carried out in the wells during the 3rd h.
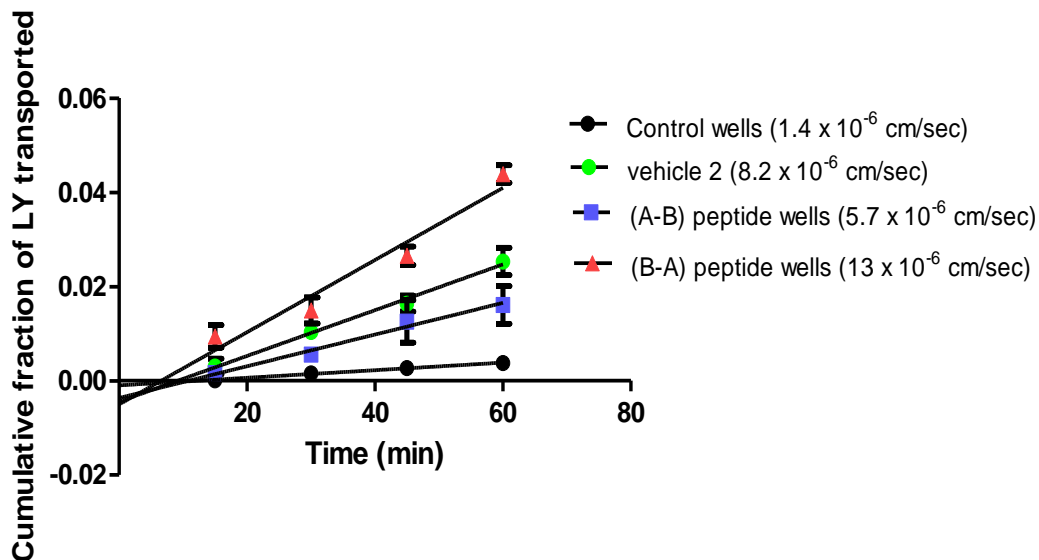
Figure 6.6. Post D-Trp isomer lucifer yellow (LY) transport through Caco-2 monolayers (n = 1). Control wells were incubated with HBSS, vehicle treated wells with vehicle 1 and the peptide treated wells with D-Trp isomer solution for the initial 2 h, and LY transport was carried out in the wells during the 3rd h.

Transport of caffeine, a high permeability standard was also evaluated through the Caco-2 monolayers (previously reported P_{app} values for caffeine in Caco-2 cells are 3.1×10^{-5} cm/sec[8] and 5.1×10^{-5} cm/sec[9]). Caffeine samples were analyzed by HPLC-UV with analysis at 280 nm; it displayed a permeability of 4.9×10^{-5} cm/sec in the A-B direction (Figure 6.7).
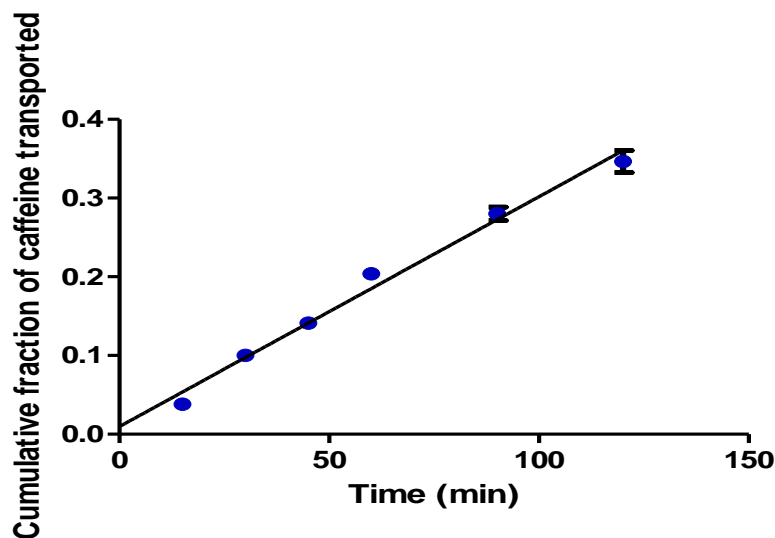
Figure 6.7. A-B Caco-2 monolayer permeability of caffeine (n=1).

Permeability of other molecules, including the macrocyclic peptides cyclosporine,[10] opioids such as morphine and known Pgp substrates including paclitaxel,[11] have been studied previously in Caco-2 monolayers. Cyclosporine displayed permeability values of 1 x 10^{-6} cm/sec in the A-B direction and 10 x 10^{-6} cm/sec in the B-A direction when the permeability was studied at a concentration of 0.5 µM. Thus it showed an efflux ratio of 10, suggesting that it was a substrate for an efflux transporter(s). However, at a concentration of 5 µM it displayed an efflux ratio of 2, suggesting saturation of the efflux transporter. The involvement of Pgp efflux was confirmed by the use of known Pgp inhibitors.[10] Cyclosporine also displayed an initial short lag phase indicative of carrier mediated transport.[10] Studies of the prototypical opioid morphine in Caco-2 cells showed a permeability of 2 x 10^{-6} cm/sec in the A-B direction and 4 x 10^{-6} cm/sec in B-A direction when the transport studies were carried out at concentrations ranging from 10-75 µM.[11] The anticancer agent paclitaxel showed a permeability of <0.1 x 10^{-6} cm/sec in the A-B direction and 18 x 10^{-6} cm/sec in the B-A direction when the transport studies were carried out from 10-75 µM; thus the ratio of transport in the B-A to A-B direction was over 100.[11] The efflux ratio for

paclitaxel was approximately 1 when the transport study was done in the presence of a known Pgp inhibitor. Hence, while morphine appeared to be at best a weak efflux substrate, Pgp caused extensive efflux of paclitaxel. Efflux by Pgp could be a likely explanation for the higher B-A transport of the L-Trp isomer.

6.2.2 Solubility studies for *in vivo* administration

In addition to the *in vitro* permeability studies, the macrocyclic tetrapeptides are currently being tested *in vivo* for various potential therapeutic applications including analgesia and drug abuse treatment following systemic, including oral administration.[3, 4] Depending on the route of administration, *in vivo* studies often require higher concentrations of compound be administered but can also tolerate a higher concentration of the organic component to solubilize the compounds. Hence, we attempted to enhance the solubility of the L- and D-Trp isomers using organic cosolvents such as ethanol and DMSO, the β-cyclodextrin derivative Captisol and the surfactants Solutol HS 15 and Tween-80 (TW-80). Solutions of the L- and D-Trp isomers (10 mM) were prepared in 5, 10 and 20% of each of the solubilizing enhancer in normal saline. The solutions were filtered and analyzed by RP-HPLC, to determine their peptide concentrations. At either 20% EtOH or 20% TW-80 in normal saline, the L-Trp isomer displayed approximately ~ 5- and 17-fold lower solubility, respectively, than the D-Trp isomer. At concentrations of either 20% Captisol or Solutol HS 15 in normal saline, the L-Trp isomer also displayed approximately 9- to 11-fold lower solubility, respectively, than the D-Trp isomer (Figures 6.8 and 6.9). The L-Trp absorbance in varying concentrations of DMSO in saline was below the limits of quantification by RP-HPLC indicating that the L-Trp peptide CJ-15,208 had very low solubility in 5-20% DMSO in normal saline. Initially, a cocktail of 10% EtOH or DMSO + 10% TW-80 in normal saline (80%) was used for solubilizing the L- and D-Trp isomers for *in vivo* studies.[3, 4]

Solutions of both peptides (10 mM) were also prepared in the above cocktail, filtered and the peptide concentrations subsequently determined by RP-HPLC (Figures 6.10 a and b). The L-Trp isomer displayed 40-fold lower solubility than the D-Trp isomer in 10% EtOH + 10% TW-80 in normal saline. The L-Trp solution containing 10% DMSO + 10% TW-80 in normal saline formed a gel and could not be filtered and analyzed.
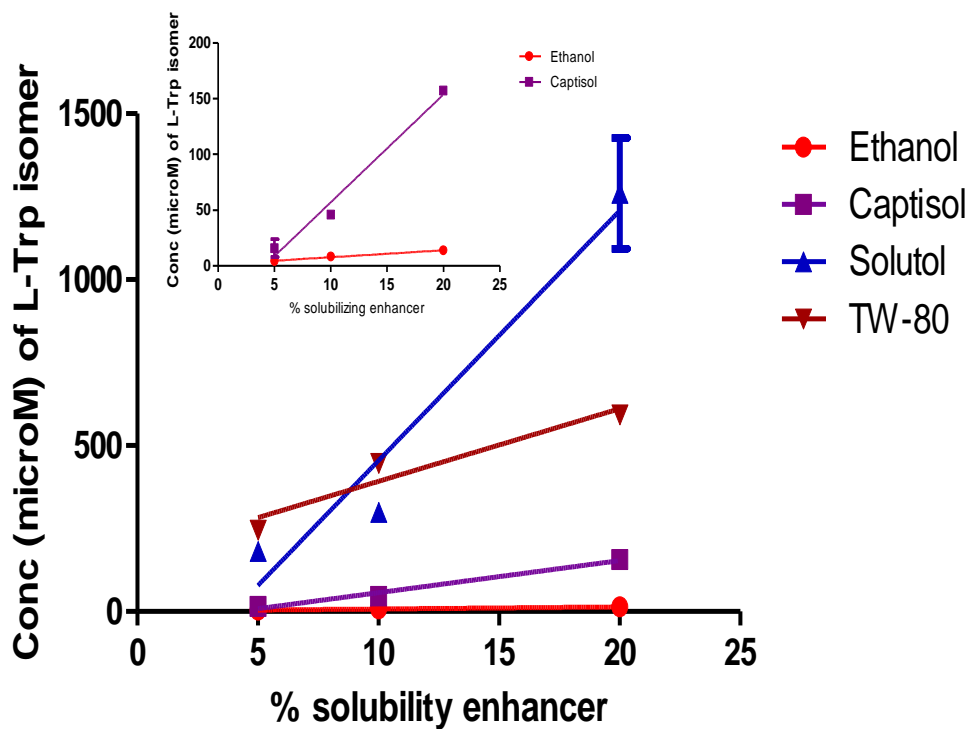

Figure 6.8. Solubility analysis of the L-Trp peptide; error bars are too small to be visible. The concentrations of peptide with DMSO as a cosolvent were below the limits of quantitation.
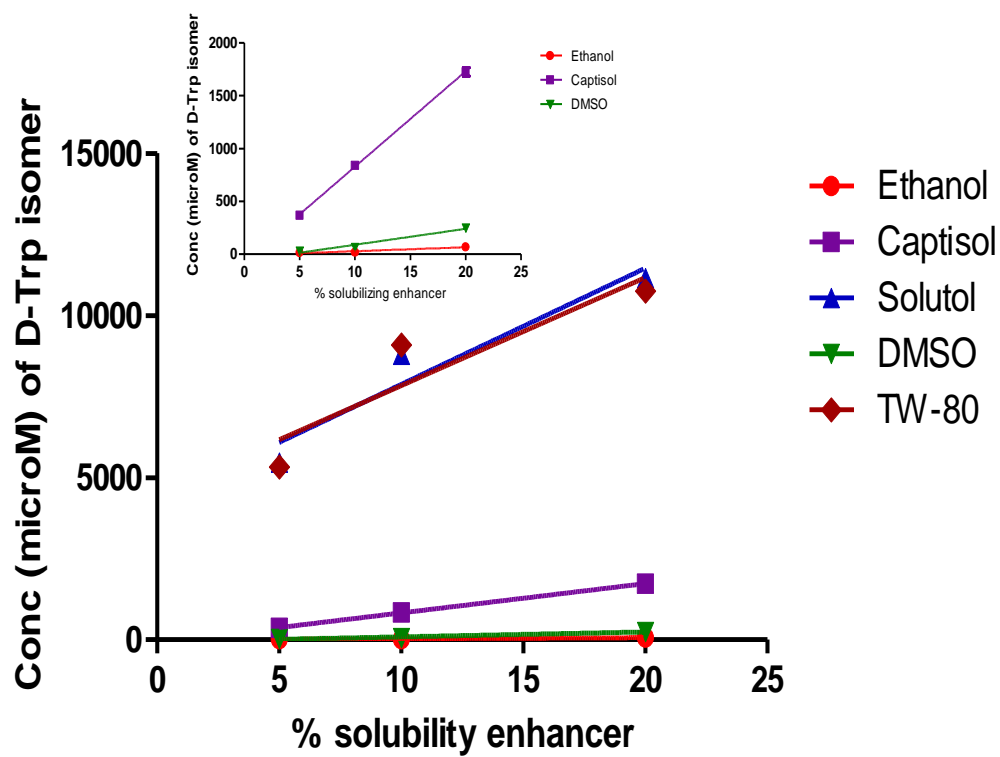
Figure 6.9. Solubility analysis of the D-Trp peptide; error bars are too small to visualize.
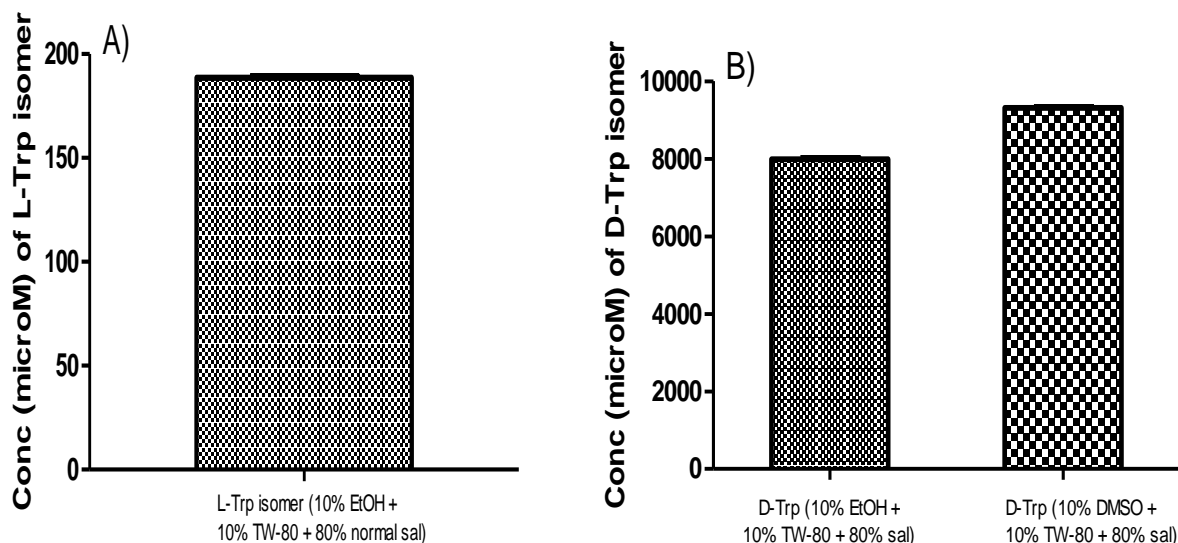
Figure 6.10. a) Solubility of the L-Trp isomer in the solvent mixture containing 10% EtOH + 10% TW-80 in normal saline (sal); error bars are too small to visualize. The solution of the L-Trp peptide containing 10% DMSO and 10% TW-80 in normal saline formed a gel and could not be analyzed. a) Solubility of the D-Trp isomers in solvent mixtures containing 10% EtOH or DMSO, 10% TW-80 in normal saline (sal), error bars too small to visualize.

6.3   Conclusions and future directions

The Caco-2 monolayer studies of the L- and D-Trp peptides indicate that the D-Trp isomer has 7-fold higher permeability compared to CJ-15,208. Based on the ratio of the permeabilities in the B-A and A-B directions, the L-Trp isomer appears to be a substrate for one or more of the efflux proteins expressed by Caco-2 cells. While in the initial studies neither vehicle appeared to significantly affect the integrity of the Caco-2 monolayers, in the post peptide lucifer yellow transport studies wells exposed to vehicle 2 exhibited values $> 1 \times 10^{-6}$ cm/sec, suggesting vehicle 2 may affect the monolayer integrity of the cells. A different batch of Caco-2 cells from the N_2 freezer was used to perform the experiment in Figure 6.2 from those performed in Figures 6.5 and 6.6 which could be one reason for the differences in the results.

While the permeability studies suggest that the L-Trp isomer CJ-15,208 is a substrate for an efflux transporter protein(s), it will be necessary to study the permeability of the L-Trp isomer in the presence of known efflux protein inhibitors to identify the specific efflux protein(s) involved. In addition, examination of the transport of both peptides, especially the D-Trp isomer, at lower concentrations (< 5 μM) could potentially identify involvement of efflux transporters which might not be apparent at 50 μM. Additional future studies could use alternate models such as MDCK cells transfected with the appropriate efflux transporter gene to corroborate the results obtained from the Caco-2 studies. Transfected MDCK cells are considered a model for the blood-brain barrier (BBB), and hence can also be used to study the relative ability of these peptides to permeate the BBB.

The solubility studies indicate that the D-Trp isomer has much higher (5- to 40-fold) solubility than the L-Trp isomer irrespective of the type of solubilizing enhancer or combination used.

6.4   Experimental section

Materials

Dulbecco's modified Eagle's medium (DMEM) was obtained from Gibco (Grand Island, NY, USA), and fetal bovine serum (FBS) was obtained from Atlanta Biologics (Lawrenceville, GA, USA). Non-essential amino acids, penicillin and streptomycin were purchased from Cellgro (Manassas, VA, USA). HBSS pH 7.4, lucifer yellow, and TW-80 were purchased from Sigma-Aldrich (St. Louis, MO, USA), and polycarbonate transwell filters and polystyrene plates were obtained from Costar (Corning, NY, USA). Captisol was a gift from Dr. Valentino Stella, University of Kansas, Lawrence and Solutol HS 15 (BASF Lot# 19602536W0) was a gift from BASF, NJ, USA. A SpectraMax M3 microplate fluorometer (Molecular Devices, Sunnyvale,

CA) was used for analysis of lucifer yellow transport, while LC-MS/MS analysis for peptide transport was performed on an Acquity Ultra Performance Liquid Chromatography system coupled to a Quattro mass spectrometer (Waters, Milford, MA, USA). Quantification of caffeine and solubility analysis of peptides for *in vivo* administration was performed on an Agilent 1200 series liquid chromatograph system equipped with a multiple wavelength UV-Vis detector.

Cell culture

Caco-2 cells (American Type Culture Collection, Manassas, VA, USA) (passage 10-16) were grown in a humidified incubator at 37 $^{\circ}$C under 5% CO_2 in air in Dulbecco's modified Eagle's medium (DMEM) containing 10% heat inactivated FBS, 0.1 mM nonessential amino acids, 2 mM L-glutamine, 100 U/ml penicillin, and 100 µg/ml streptomycin. Caco-2 cells were seeded on polycarbonate transwells (0.4 µM pore size, 12 mm diameter, Costar #3401) at a density of 3 x 10^5 cells/cm^2 and grown for 21 days. Cell culture media was replaced within 12 h of seeding, and thereafter every other day for the initial 7 days, and subsequently every day until the 21st day.

Standard curves of the L- and D-Trp peptides for the working solutions for the Caco-2 transport experiments

The concentrations of the working solutions of both peptides used for Caco-2 permeability studies were determined from standard curves (Figures 6.11 and 6.12) obtained by RP-UPLC with UV detection at varying concentrations (ranging from 12.5-75 µM) in 75% MeOH in HBSS. The LC method was from 25-75% of aqueous MeCN with 0.03% formic acid over 3min at a flow rate of 0.6 mL/min and at a wavelength of 214 nm. The solutions were analyzed on a Acquity UPLC HSS T3 column (1.8 μm, 100 Å, 2.1 x 50 mm).
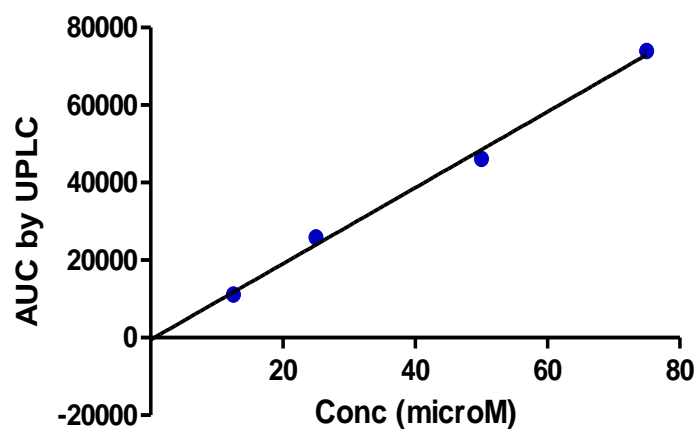
Figure 6.11 Standard curve of the L-Trp peptide CJ-15,208 by RP-UPLC used for determining the concentration of working solutions used in the Caco-2 permeability experiments.
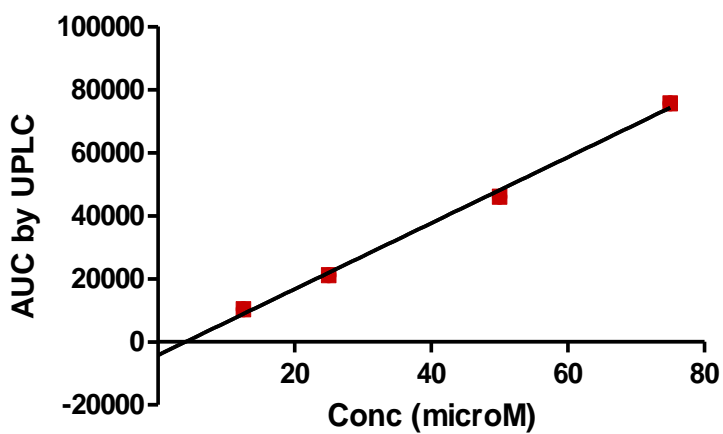
Figure 6.12 Standard curve of the D-Trp isomer by RP-UPLC used for determining the concentration of working solutions used in the Caco-2 permeability experiments.

Standard curves of low (Lucifer yellow) and high (caffeine) permeability standards

The standard curve of Lucifer yellow and caffeine were obtained in HBSS ranging over a range of concentrations from 1-100 μM. The solutions of Lucifer yellow (200 μL) were analyzed using a 96 well fluorescence plate reader with an excitation wavelength of 485 nm and emission wavelength of 538 nm and displayed linearity from 1-100 μM. (r^2 = 0.9957, Figure 6.13). Solutions of caffeine were analyzed on a Vydac C18 column (5 μm, 300 Å, 4.6 x 50 mm) equipped with a Vydac C18 guard cartridge and a gradient of 6-13% aqueous MeCN containing 0.1% TFA over 7 min with UV detection at 280 nm at a flow rate (1 mL/min) and displayed linearity from 1-100 μM (r^2 = 0.9999, Figure 6.14).

Figure 6.13 Representative standard curve of lucifer yellow
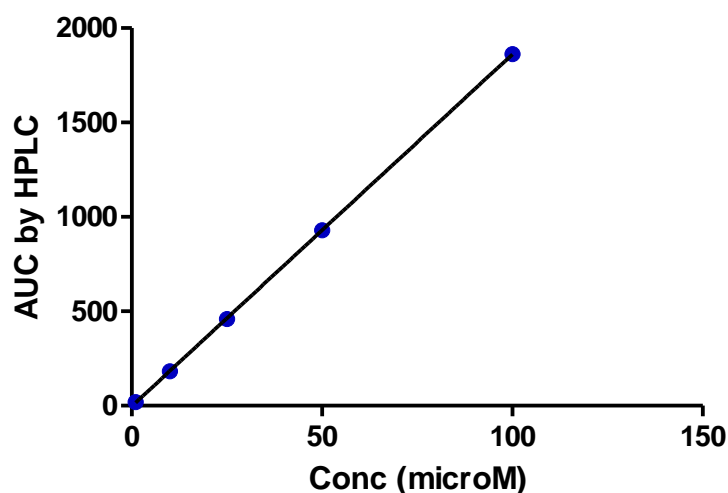
Figure 6.14 Standard curve of caffeine.

Transport experiments

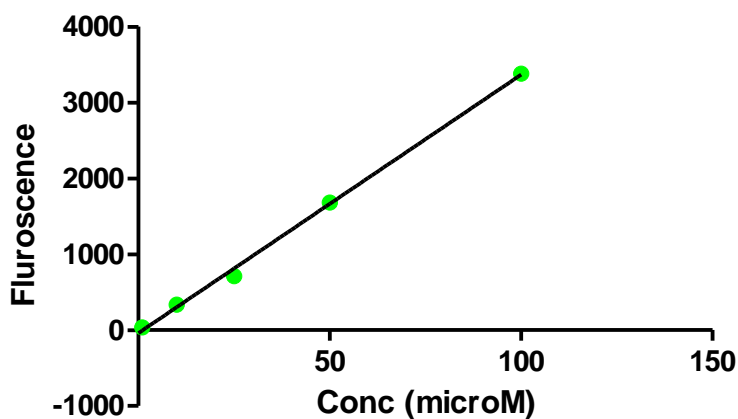The integrity of the cell monolayers was examined by the measurement of TEER values and the transport of the low paracellular permeability standard lucifer yellow. The TEER values were corrected by subtracting background values for the filters. The monolayers exhibiting TEER values, monitored in HBSS pH 7.4 at 37 ^{o}C, above 200 Ω cm^2 and apparent permeability (P_{app}) values for lucifer yellow of $\leq$ 1 x 10^{-6} cm/sec were used for the transport experiments 21–25 days after seeding. The filters containing cell monolayers were incubated in HBSS pH 7.4 (apical side volume 0.5 mL and basolateral side volume 1.0 mL) and allowed to equilibrate for 10 min in a bench top incubator-shaker at 37 ^{o}C and 100 rpm. For assessment of monolayer integrity of the cells, HBSS on the apical side was replaced with lucifer yellow (0.5 mL of 100 µM solution in HBSS). The experiment was performed in triplicate for 120 min with aliquots (200 µL) taken at 15, 30, 45, 60, 90 and 120 min from the basolateral side. At every time point an aliquot was removed it was replaced by an equal amount of HBSS to maintain constant volume. Aliquots were taken prior to the start of the experiment to serve as blanks and at the end

of the experiments from the apical side for estimating mass balance and recovery. The samples were analyzed using a 96 well fluorescence plate reader (see materials). The lucifer yellow transport to evaluate cell monolayer integrity was performed simultaneously with the peptide transport experiment during the initial 2 h, as opposed to the post-peptide lucifer yellow transport experiments which were performed only in the 3rd h.

Transport experiments for the peptides were performed by the same procedure as described for lucifer yellow, except that for transport in the B-A direction the donor solution of the peptide was placed on the basolateral side and the aliquots were taken from the apical side with an additional 5 min time point. The additional time point was taken to monitor an initial lag in the transport of the two peptides. The working concentrations used for both the L- and D-Trp isomers were 50 μM in vehicle 1 and vehicle 2, respectively. Aliquots of the donor compartment were taken at the beginning and the end of the experiments to monitor mass balance and were diluted 10 times with the respective vehicle immediately after the experiment. The peptide concentrations were determined by LC-MS/MS (see below). Transport experiments involving the high permeability standard caffeine were analyzed by RP-HPLC with a gradient of 6-13% aqueous MeCN containing 0.1% TFA over 7 min with UV detection at 280 nm and at flow rate of 1 mL/min.

LC-ESI-MS/MS analysis

Sample preparation for the L- and D-Trp macrocyclic peptides

The samples from the transport studies of the L- and D-Trp macrocyclic peptides were stored at -20 ^{o}C immediately after the experiments. Following thawing of the Caco-2 samples, the internal standard *cyclo*[L-Phe-*N*Me-D-Ala-L-Phe-Trp] (20 μL of a 12.5 μM solution in MeCN) was added to 80 μL of the sample from the transport studies. The samples were

vortexed and injected into the LC-ESI-MS/MS for quantification. As the peptides are hydrophobic they can adsorb to plastic, and hence all of the samples were prepared and stored in glass vials.

LC-MS/MS method for the L- and D-Trp isomers

The LC method used a Hypersil BDS C8 column (3 μm, 2.1 x 50 mm) with a flow rate of 200 µL/min and a gradient of solvent A (99% H_2O, 1% MeCN, 0.08% formic acid) and solvent B (99% MeCN, 1% H_2O, 0.08% formic acid). The initial conditions were 20% B for the first 2 min, followed by a rapid increase to 50% over one minute and then increasing from 50 to 80% over 3 min. The same LC method was used for both macrocyclic tetrapeptides. The retention times for the L- and D-Trp isomers were 4.4 min and 5.7 min, respectively. The retention time of the IS was 5.0 min. Ions between *m/z* 70 to 600 were captured after electrospray ionization.
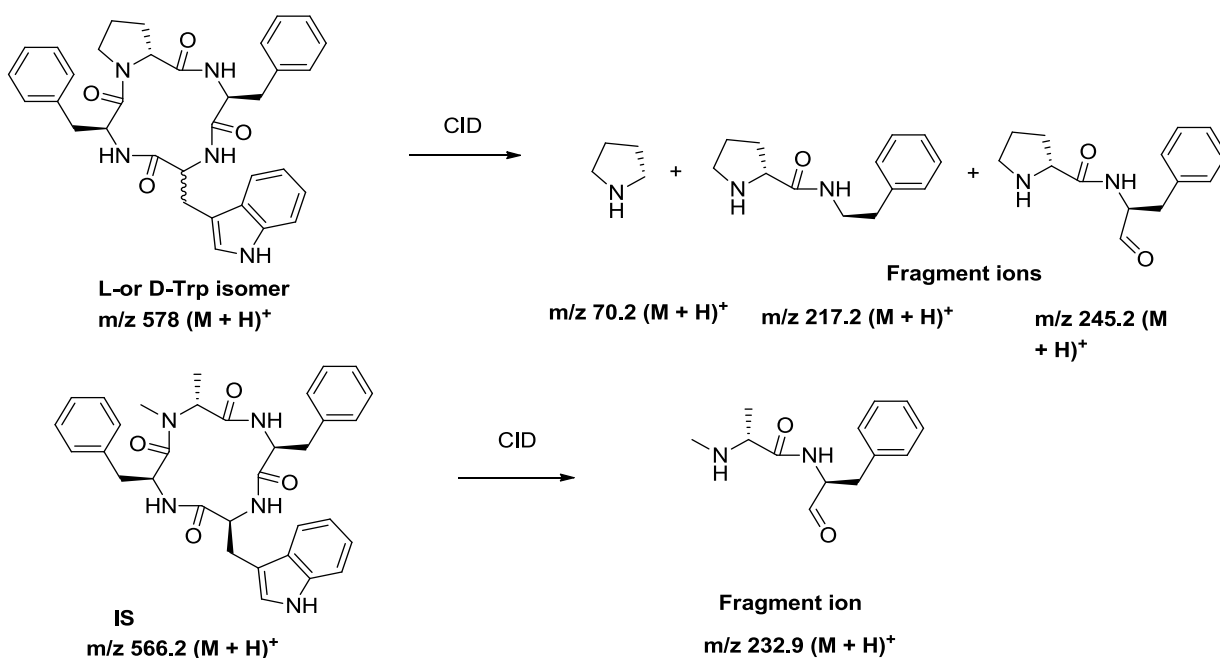
Figure 6.15 Mass spectral fragmentation of the cyclic tetrapeptides

The following mass spectrometer settings were used during sample quantification: capillary voltage 3.8 kV, cone voltage 80 V, source temperature 100 $^{\circ}$C, desolvation temperature 150 $^{\circ}$C. The collision energy (CE) varied with the transitions; the ion transitions used were 600.1 > 572.2 (CE 35 eV), 578 > 245.2 (CE 35 eV), 578 > 217.2 (CE 35 eV), 578 > 159 (CE 35 eV), 578 > 120.1 (60 eV), and 578 > 70.2 (CE 60 eV) for the L-Trp and D-Trp isomers, and 588 > 559.8 (CE 35 eV) and 566.2 > 232.9 (CE 22 eV) for the IS. The standard curve for the L-Trp isomer was obtained from 25 nM to 25 μM and displayed linearity (r^2 = 0.9976, Figure 6.16). The standard curve for the D-Trp isomer was obtained from 100 nM to 10 μM and also displayed linearity (r^2 = 0.9867, Figure 6.17). The Caco-2 samples were analyzed using the same conditions as the standards.
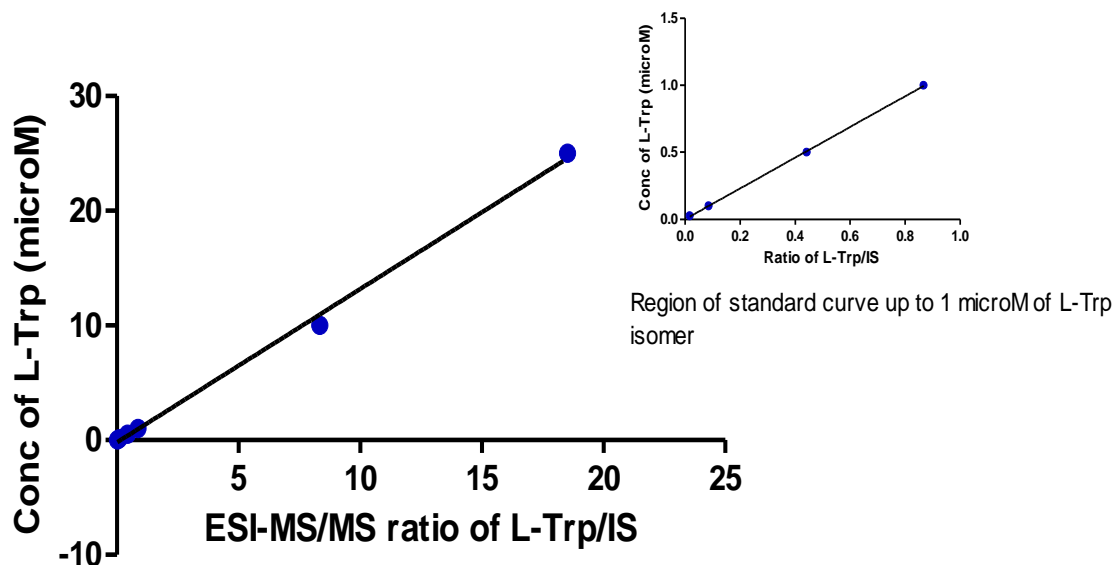
Figure 6.16 Representative standard curve of the L-Trp isomer by LC-MS/MS used for determining Caco-2 monolayer permeability.
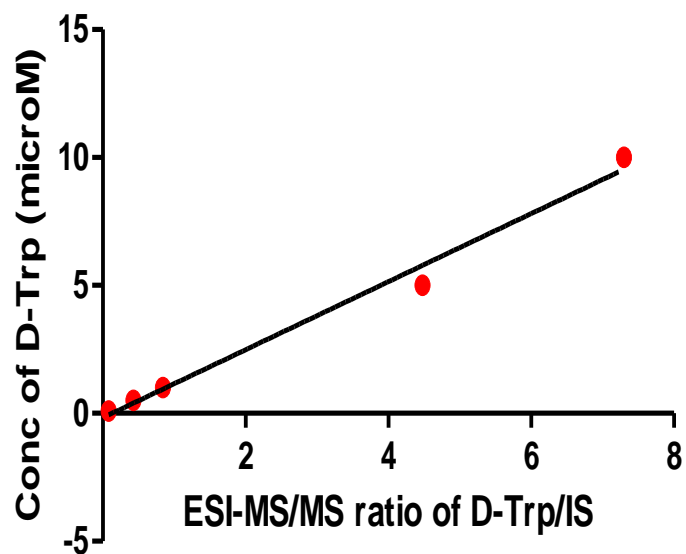
Figure 6.17 Representative standard curve of the D-Trp isomer by LC-MS/MS used for determining Caco-2 monolayer permeability.

P_{app} calculations

The cumulative fraction of the drug transported for each time point was calculated by dividing the concentration in the receiver at each time point following correction for aliquot removal (by addition of an equal volume of HBSS) by the donor concentration (concentration of the drug at time = 0). The cumulative fraction transported was plotted vs. time to obtain the slope of the line (flux). The P_{app} value was then calculated from the following formula:

P_{app} = slope x volume of receiver chamber (cm^3)/Area of the filter (cm^2) x 60 (sec)

Solubility analysis for *in vivo* applications

Solutions of the L-Trp and D-Trp peptides (10 mM) were prepared by initially adding EtOH, DMSO or TW-80 to the preweighed drug powder followed by vortexing (30 sec) and sonication (2 min). Subsequently, normal saline was added to the drug solutions. The drug solutions involving Captisol and Solutol HS 15 were prepared by adding solutions containing 5, 10 and 20% Captisol or Solutol HS 15 in normal saline to the drug powder. The peptide solutions containing Captisol and Solutol HS 15 were also vortexed (30 sec) and sonicated (2 min). All the peptide solutions were incubated in a water bath at 25 °C for 24 h with simultaneous shaking at 25 rpm. The solutions were centrifuged at 13,000 rpm for 30 min followed by filtration using nylon syringe filters. The solutions were diluted to a concentration range of 50-500 μM with the corresponding vehicles containing mixtures of solubilizing enhancers in normal saline and then analyzed by RP-HPLC-UV analysis using a gradient of 20-80% aqueous MeCN with 0.1% TFA over 10 min at 280 nm and at a flow rate (1 mL/min).

Standard curves for the L-Trp and D-Trp peptides for solubility studies were analyzed by RP-HPLC-UV analysis at 280 nm. The standard curve samples were prepared over a concentration range of 50-500 μM in 2% DMSO in MeOH and analyzed using the same HPLC conditions as above (Figures 6.18 and 6.19).
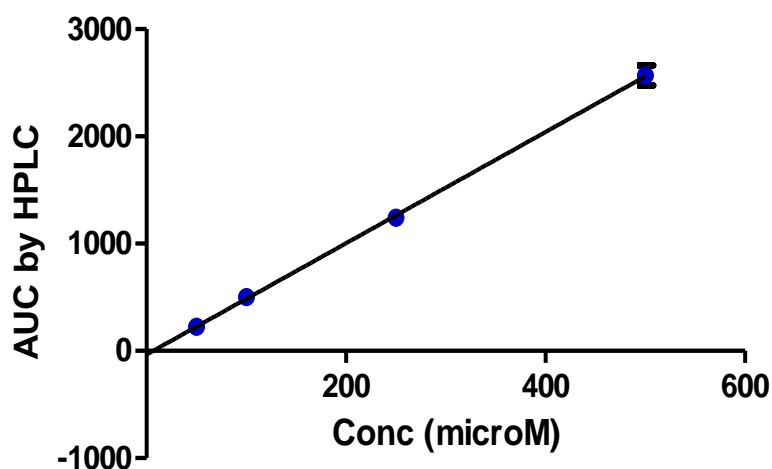
Figure 6.18 Standard curve of the L-Trp isomer for solubility studies
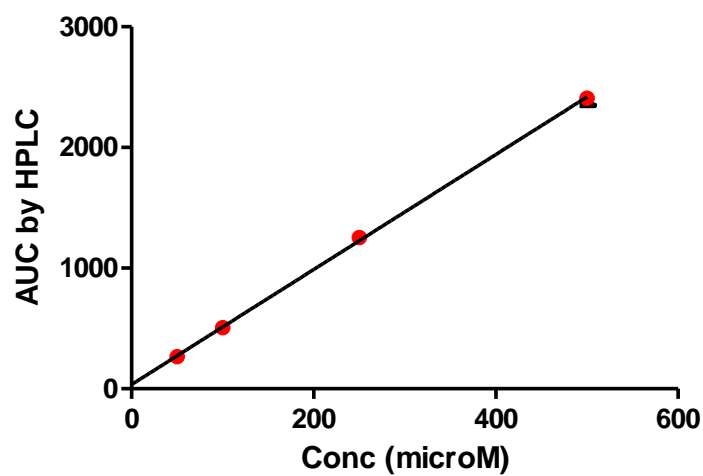

Figure 6.19 Standard curve of the D-Trp isomer for solubility studies

6.5   References

1.   Saito, T.; Hirai, H.; Kim, Y. J.; Kojima, Y.; Matsunaga, Y.; Nishida, H.; Sakakibara, T.; Suga, O.; Sujaku, T.; Kojima, N. CJ-15,208, a novel kappa opioid receptor antagonist from a fungus, Ctenomyces serratus ATCC15502. *J Antibiot (Tokyo)* **2002,** *55*, 847-854.

2.   Ross, N. C.; Reilley, K. J.; Murray, T. F.; Aldrich, J. V.; McLaughlin, J. P. Novel opioid cyclic tetrapeptides: Trp isomers of CJ-15,208 exhibit distinct opioid receptor agonism and short-acting kappa opioid receptor antagonism. *Br J Pharmacol* **2012,** *165*, 1097-1108.

3.   Aldrich, J. V.; Senadheera, S. N.; Ross, N. C.; Ganno, M. L.; Eans, S. O.; McLaughlin, J. P. The Macrocyclic Peptide Natural Product CJ-15,208 Is Orally Active and Prevents Reinstatement of Extinguished Cocaine-Seeking Behavior. *J Nat Prod* **2013,** *76*, 433-438.

4.   Eans, S. O.; Ganno, M. L.; Reilley, K. J.; Patkar, K. A.; Senadheera, S. N.; Aldrich, J. V.; McLaughlin, J. P. The macrocyclic tetrapeptide [D-Trp]CJ-15,208 produces short-acting kappa opioid receptor antagonism in the CNS after oral administration. *Br J Pharmacol* **2013,** *169*, 426-436.

5.   Ingels, F. M.; Augustijns, P. F. Biological, pharmaceutical, and analytical considerations with respect to the transport media used in the absorption screening system, Caco-2. *J Pharm Sci* **2003,** *92*, 1545-1558.

6.   Christoffel, J. J.; de Jong, F.; Reinhoudt, D. N. Mechanistic studies of carrier mediated transport through supported liquid media. *In Chemical Separation with Liquid Membranes*, ACS Symposium, Washington D.C., Bartsch R.A.; Way, J. D., Ed. American Chemical Society: Washington D.C., 1996; pp 19-56.

7.   White, T. R.; Renzelman, C. M.; Rand, A. C.; Rezai, T.; McEwen, C. M.; Gelev, V. M.; Turner, R. A.; Linington, R. G.; Leung, S. S.; Kalgutkar, A. S.; Bauman, J. N.; Zhang, Y.; Liras, S.; Price, D. A.; Mathiowetz, A. M.; Jacobson, M. P.; Lokey, R. S. On-resin N-methylation of cyclic peptides for discovery of orally bioavailable scaffolds. *Nat Chem Biol* **2011,** *7*, 810-817.

8.   Yee, S. In vitro permeability across Caco-2 cells (colonic) can predict in vivo (small intestinal) absorption in man--fact or myth. *Pharm Res* **1997,** *14*, 763-766.

9.   Yazdanian, M.; Glynn, S. L.; Wright, J. L.; Hawi, A. Correlating partitioning and caco-2 cell permeability of structurally diverse small molecular weight compounds. *Pharm Res* **1998,** *15*, 1490-1494.

10.   Augustijns, P. F.; Bradshaw, T. P.; Gan, L. S.; Hendren, R. W.; Thakker, D. R. Evidence for a polarized efflux system in CACO-2 cells capable of modulating cyclosporin A transport. *Biochem Biophys Res Commun* **1993,** *197*, 360-365.

11.   Crowe, A. The influence of P-glycoprotein on morphine transport in Caco-2 cells. Comparison with paclitaxel. *Eur J Pharmacol* **2002,** *440*, 7-16.

Chapter 7 - Conclusions and future directions

7.1   Introduction

One of the objectives of this dissertation was to study structure-activity relationships (SAR) of dynorphin (Dyn) analogs. The SAR of two Dyn analogs, Dyn B amide and the selective kappa opioid receptor (KOR) antagonist [N^α-benzylTyr[1],*cyclo*(D-Asp[5],Dap[8])]Dyn A(1–11)NH$_2$ (now called zyklophin),[1] were studied. The information obtained from the SAR studies of Dyn B amide is useful to explore the contributions of different residues of Dyn B amide to its opioid activity. The SAR of zyklophin provided information about the role of different modifications to zyklophin's KOR activity and hence will aid in designing novel zyklophin analogs with improved affinity, selectivity and antagonist potency at KOR.

Another objective of this dissertation was to explore the pharmacokinetic and physicochemical properties of the opioid macrocyclic natural product CJ 15,208 (*cyclo*[L-Phe-D-Pro-L-Phe-L-Trp]) and its D-Trp isomer. We studied their bidirectional permeability in the Caco-2 cell monolayer model for intestinal absorption and solubility of these peptides in various solubilizing enhancers. The results from the Caco-2 permeability studies may reflect the intestinal permeability of these peptides, while those from the solubility studies provided us with information about possible vehicles that can be used for *in vivo* studies.

7.2   Conclusions and future work for research projects

Project 1: Structure-activity relationships of Dynorphin B amide (Chapter 3).

Dyn A and Dyn B have identical N-terminal sequences but their C-terminal sequences differ. Although Dyn B exhibits lower affinity, potency and selectivity for KOR (see chapter 3, section 3.2), it has been reported to be devoid of the cytotoxic non-opioid effects exhibited by Dyn A.[2] Hence, the differences in the C-terminal sequence results in the differences in their pharmacological actions.

Tyr^1-Gly-Gly-Phe^4-Leu^5-Arg^6-Arg^7-Ile^8-Arg^9-Pro^{10}-Lys^{11}-Leu-Lys

Dyn A(1-13)

Tyr^1-Gly-Gly-Phe^4-Leu^5-Arg^6-Arg^7-Gln^8-Phe^9-Lys^{10}-Val^{11}-Val-Thr-NH$_2$

Dyn B amide

Figure 7.1 Dyn A(1-13) and Dyn B amide

In this project, alanine substituted analogs of Dyn B amide were synthesized. All of the non-glycine residues up to residue 11 were substituted with Ala in order to explore the importance of these residues to the activity of Dyn B. The alanine scan of Dyn B amide revealed that Tyr^1 and Phe^4 in the N-terminal region of the peptide are critical for opioid receptor binding affinity. These residues also contribute to the KOR vs. mu opioid receptor (MOR) selectivity of Dyn B amide. While the basic residue Arg^7 appears to be important, Arg^6 and Lys^{10} also contribute to the KOR binding affinity of Dyn B amide. While the basic residues Arg^6 and Arg^7 contribute to KOR selectivity by both increasing KOR affinity and decreasing MOR affinity, the Lys^{10} residue contributes to the KOR selectivity primarily by increasing the KOR affinity of Dyn B amide. In the case of Dyn A(1-13), along with Arg^6 and Arg^7, basic residues Arg^9 and Lys^{11} also make minor contributions to the opioid receptor binding affinity.[3] Hence it appears that the basic residues in the C-terminus of both peptides contribute to opioid receptor binding; however, the differences in their relative positions in positions 8-11 might be one of the reasons contributing to their different pharmacological profiles.

The pharmacological information obtained from the Ala substituted analogs could be used to design newer analogs of Dyn B amide that could provide additional information about the SAR of Dyn B amide and aid in the development of peptidic opioid ligands as pharmacological tools.

Project 2: Structure-activity relationships of the KOR selective antagonist zyklophin (Chapter 4).

The cyclic Dyn A derivative zyklophin is a selective KOR antagonist *in vitro*[1] and is active *in vivo* after systemic administration.[4] However, there is minimal SAR information available for zyklophin. The objectives of this project were to study the SAR of zyklophin, identify structural features of zyklophin responsible for its high selectivity and antagonist activity, and to enhance its antagonist potency.

*N*Benzyl-Tyr-Gly-Gly-Phe-D-Asp-Arg-Arg-Dap-Arg-Pro-Lys-NH$_2$

Zyklophin

Figure 7.2 Zyklophin

The synthesis of the zyklophin analogs involved dissolution of the N-terminal *N*-alkyl amino acid in DMF at elevated temperature because of its low solubility, followed by cooling and coupling with the (2-11) peptide fragment on resin.[1] This could potentially lead to racemization of the N-terminal residue of zyklophin or its analogs. While we did not observe racemization with *N*-benzyl-Tyr-OH in the synthesis of zyklophin, *N*-benzyl-Phe-OH appeared to undergo racemization. Also the *N*-CPM-Tyr-OH had minimal solubility in DMF and did not couple with the peptide fragment on resin. Therefore, we devised a modified synthetic strategy to prepare *N*-alkyl amino acids that would be readily soluble in DMF at room temperature (RT) and hence would not require use of an elevated temperature for solubilization. This involved preparing Alloc derivatives of the *N*-alkyl amino acids which were readily soluble at RT in the solvents used for the coupling reaction, thereby minimizing potential for racemization of the N-terminal residue of the zyklophin analogs.

To study the SAR of zyklophin, both linear analogs containing modifications in positions 5 and 8 and cyclic analogs including N-terminal *N*-alkyl analogs, ring variants and alanine substituted analogs were synthesized. The results from the radioligand binding assays for the linear analogs suggested that the residue at position 5 has a greater influence on the affinity of zyklophin as compared to residue 8. The L-configuration and/or the hydrophobic side chain of Leu in position 5 of [*N*-benzylTyr[1],Dap(Ac)[8]]Dyn A(1-11)NH$_2$ could be responsible for its high KOR affinity. However, the KOR binding affinity for the ring variant analog with L-Asp at position 5 suggested that changing the configuration of residue 5 does not have a significant influence on the affinity of cyclic zyklophin analogs. While all of the N-terminal modifications and ring variations were well tolerated in zyklophin, to date the analog with the *N*-CPM modification on the N-terminal residue displayed the highest KOR affinity. It was also shown that the basic secondary amine and the phenol of the N-terminal Tyr were not necessary for maintaining the KOR affinity of zyklophin. The pharmacological results for the alanine substituted analogs suggested that residues at positions 4 and 6, but not Tyr[1], are important for zyklophin's KOR affinity, while the basic residues 7 and 9 did not appear to be important for the maintaining the KOR affinity of zyklophin. Surprisingly, the Ala substitution at position 7 displayed a 3-fold increase in KOR affinity, suggesting that the Ala residue might result in favorable interactions or eliminate unfavorable interactions with the receptor that are responsible for its increased affinity.

The results from the GTPγS assay indicated that none of the structural changes to the cyclic zyklophin analogs altered the low efficacy of zyklophin. Preliminary results from Schild analysis suggested that among the analogs evaluated the *N*-CPM modification at the N-terminal resulted in the most potent analog. The results for the Phe[1] analog of zyklophin suggested that

the Tyr phenol is not required for KOR antagonist potency of zyklophin. Thus, the *N*-CPM-Tyr[1]

and *N*-benzyl-Phe[1] analogs of zyklophin appear to promising analogs for *in vivo* studies towards

the development of potent Dyn A based KOR antagonists.

Future studies include performing molecular modeling studies of zyklophin with the aid

of the reported crystal structure of KOR.[5] The crystal structure provides a starting framework for

analysis of potential interactions of zyklophin with the receptor. The docking studies with

zyklophin analogs could provide insight into which analogs would have better affinity and

activity at KOR. However, due to the variety of conformations exhibited by zyklophin it is

challenging to perform molecular docking studies using the reported crystal structure. The

crystal structure of JDTic with KOR is a single snap shot and does not take into account the

dynamic nature of the receptor and the conformational flexibility of JDTic. It is also reported that

the peptides and non-peptides may interact differently with the receptor,[6, 7] hence interactions of

zyklophin with the receptor may be significantly different compared to JDTic. The SAR of

zyklophin suggests that neither the phenol of Tyr[1] nor a basic N-terminus is required for

maintaining the KOR activity of zyklophin. However, in the case of JDTic the basic amines of

piperidine and tetrahydrisoquinoline (Tic) groups make key salt-bridge interactions with Asp 138

in KOR. Further, the removal of the hydroxyl groups on the piperidine and Tic causes a 100-fold

loss in KOR affinity.[5] Other KOR antagonists like norbinaltorphimine (norBNI) and 5-

guanidinonaltrindole (5'-GNTI) have been docked with the KOR crystal structure, and those

studies suggest that while the amino group of *N*-cyclopropylmethyl (CPM) moiety interacts with

Asp 138, the second amine moiety (the second amino group in norBNI and the guanidine group

in GNTI) in these antagonists interacts with Glu 297 residue which is thought to be responsible

for their KOR selectivity. The *N*-CPM group in norBNI and GNTI appears to be in the same

position in the crystal structure as that of the isopropyl group of JDTic. The discovery of norBNI and GNTI was based on the "message-address" concept (see chapter 2, section 2.7) for opioid ligands, and can be related to the endogenous ligands dynorphins.[8] Thus, incorporating an isopropyl group or other hydrophobic alkyl group instead of a benzyl group in zyklophin may produce an analog(s) with potent KOR antagonism. Hence, although the discovery of the KOR crystal structure is ground breaking, the information obtained from this structure should be applied with caution while designing second-generation zyklophin analogs. In addition, while docking to the crystal structure can be used to suggest modifications to incorporate into zyklophin, experimental evidence will be needed to evaluate the proposed docking structures.

Project 3: Caco-2 permeability and solubility analysis of opioid macrocyclic tetrapeptides (chapter 6)

The natural product CJ 15,208, a macrocyclic tetrapeptide (*cyclo*[L-Phe-D-Pro-L-Phe-L-Trp]), was reported to exhibit KOR antagonism *in vitro*.[9] The L- and D-Trp isomers of this peptide exhibit different pharmacological profiles *in vivo* after intracerebroventricular administration to mice,[10] and both exhibit opioid activity following oral administration.[11, 12] Because of the promise of these lead compounds we wanted to explore their pharmacokinetic properties such as bidirectional Caco-2 permeability and physicochemical properties such as solubility.

The aim of this project was to study the bidirectional permeability of the peptides in the Caco-2 monolayer model for intestinal permeability and examine the solubility of these peptides in various solubilizing agents, including organic cosolvents such as ethanol and *N,N*-dimethylsulfoxide (DMSO), the cyclodextrin Captisol and the surfactants Solutol HS 15 and Tween-80.

CJ 15,208   D-Trp isomer of CJ 15,208

Figure 7.3 CJ-15,208 and its D-Trp isomer.

The Caco-2 permeability studies indicated that the D-Trp isomer ($25.5 \pm 6.3 \times 10^{-6}$ cm/sec) has 7-fold higher permeability in the A-B direction compared to the L-Trp isomer ($3.2 \pm 0.6 \times 10^{-6}$ cm/sec). CJ-15,208 displayed a P_{app} ratio (P_{app} (B-A)/P_{app} (A-B)) ratio of 6, suggesting it is a substrate for one or more of the efflux proteins expressed by Caco-2 cells. The ratio of D-Trp isomer was close to 1, suggesting that it was not an efflux substrate.

The solubility studies showed that the D-Trp isomer has much higher (5- to 40-fold) solubility than the L-Trp isomer irrespective of the type of solubilizing enhancer or combination used.

In order to identify the protein involved in the efflux of CJ-15,208 we need to study the Caco-2 permeability of this peptide in the presence of known efflux inhibitors. In addition, the examination of the transport of both peptides, especially the D-Trp isomer, at lower concentrations (< 5 µM) could potentially detect involvement of efflux transporters that might not be apparent at 50 µM. Additional future studies could also use alternate models such as Madin-Darby canine kidney (MDCK) cells transfected with the appropriate efflux transporter gene to corroborate the results obtained from the Caco-2 studies. The MDCK permeability could also give an estimation of the blood-brain barrier (BBB) permeability of these peptides.

7.3   References

1.   Patkar, K. A.; Yan, X.; Murray, T. F.; Aldrich, J. V. [N^a-benzylTyr^1,*cyclo*(D-Asp^5,Dap^8)]- dynorphin A-(1-11)NH$_2$ cyclized in the "address" domain is a novel kappa-opioid receptor antagonist. *J Med Chem* **2005,** *48*, 4500-4503.

2.   Tan-No, K.; Cebers, G.; Yakovleva, T.; Hoon Goh, B.; Gileva, I.; Reznikov, K.; Aguilar-Santelises, M.; Hauser, K. F.; Terenius, L.; Bakalkin, G. Cytotoxic effects of dynorphins through nonopioid intracellular mechanisms. *Exp Cell Res* **2001,** *269*, 54-63.

3.   Turcotte, A.; Lalonde, J. M.; St-Pierre, S.; Lemaire, S. Dynorphin-(1-13). I. Structure-function relationships of Ala-containing analogs. *Int J Pept Protein Res* **1984,** *23*, 361-367.

4.   Aldrich, J. V.; Patkar, K. A.; McLaughlin, J. P. Zyklophin, a systemically active selective kappa opioid receptor peptide antagonist with short duration of action. *Proc Natl Acad Sci U S A* **2009,** *106*, 18396-18401.

5.   Wu, H.; Wacker, D.; Mileni, M.; Katritch, V.; Han, G. W.; Vardy, E.; Liu, W.; Thompson, A. A.; Huang, X. P.; Carroll, F. I.; Mascarella, S. W.; Westkaemper, R. B.; Mosier, P. D.; Roth, B. L.; Cherezov, V.; Stevens, R. C. Structure of the human kappa-opioid receptor in complex with JDTic. *Nature* **2012,** *485*, 327-332.

6.   Hjorth, S. A.; Thirstrup, K.; Grandy, D. K.; Schwartz, T. W. Analysis of selective binding epitopes for the kappa-opioid receptor antagonist nor-binaltorphimine. *Mol Pharmacol* **1995,** *47*, 1089-1094.

7.   Paterlini, G.; Portoghese, P. S.; Ferguson, D. M. Molecular simulation of dynorphin A-(1-10) binding to extracellular loop 2 of the kappa-opioid receptor. A model for receptor activation. *J Med Chem* **1997,** *40*, 3254-3262.

8.   Metzger, T. G.; Paterlini, M. G.; Portoghese, P. S.; Ferguson, D. M. Application of the message-address concept to the docking of naltrexone and selective naltrexone-derived opioid antagonists into opioid receptor models. *Neurochem Res* **1996,** *21*, 1287-1294.

9.   Saito, T.; Hirai, H.; Kim, Y. J.; Kojima, Y.; Matsunaga, Y.; Nishida, H.; Sakakibara, T.; Suga, O.; Sujaku, T.; Kojima, N. CJ-15,208, a novel kappa opioid receptor antagonist from a fungus, Ctenomyces serratus ATCC15502. *J Antibiot (Tokyo)* **2002,** *55*, 847-854.

10.   Ross, N. C.; Reilley, K. J.; Murray, T. F.; Aldrich, J. V.; McLaughlin, J. P. Novel opioid cyclic tetrapeptides: Trp isomers of CJ-15,208 exhibit distinct opioid receptor agonism and short-acting kappa opioid receptor antagonism. *Br J Pharmacol* **2012,** *165*, 1097-1108.

11.   Aldrich, J. V.; Senadheera, S. N.; Ross, N. C.; Ganno, M. L.; Eans, S. O.; McLaughlin, J. P. The Macrocyclic Peptide Natural Product CJ-15,208 Is Orally Active and Prevents Reinstatement of Extinguished Cocaine-Seeking Behavior. *J Nat Prod* **2013,** *76*, 433-438.

12.   Eans, S. O.; Ganno, M. L.; Reilley, K. J.; Patkar, K. A.; Senadheera, S. N.; Aldrich, J. V.; McLaughlin, J. P. The macrocyclic tetrapeptide [D-Trp]CJ-15,208 produces short-acting kappa opioid receptor antagonism in the CNS after oral administration. *Br J Pharmacol* **2013,** *169*, 426-436.